Regular and chaotic dynamics in scalar field cosmology

A dissertation presented

by

Orest Hrycyna

to

Faculty of Physics, Astronomy and Applied Computer Science

in partial fulfillment of the requirements

for the degree of

Doctor of Philosophy

in the subject of

Physics

Jagiellonian University

UNIVERSITAS
IAGELLONICA
CRACOVIENSIS

Kraków, Poland

February 2011

to my first science teacher

Acknowledgments

Many people have their contribution in this dissertation on various levels. First and foremost, I would like to thank my advisor Marek Szydłowski for comments, suggestions and our collaboration. It is always a graeat pleasure to work with him.

I thank my colleagues and collaborators Jacek Golbiak, Monika Hereć, Adam Krawiec, Aleksandra Kurek, Jakub Mielczarek, Tomasz Stachowiak and Paweł Tambor, for all the hard work dedicated to our common projects and many conversations, not only but mostly, about science.

Finally, I wish to thank my family, especially my wife Natalia, for constant support and inspiration during the preparation of this dissertation.

Thesis advisor
Marek Szydłowski

Author
Orest Hrycyna

Regular and chaotic dynamics in scalar field cosmology

Abstract

This dissertation is devoted to investigations of dynamics of Friedmann–Robertson–Walker cosmological models with a non-minimally coupled scalar field and a barotropic matter content. Using dynamical systems methods two types of evolution: the complex behaviour and the regular expansion of the universe were studied in details. Different manifestations of the coexistence of chaotic and regular behaviour in the conformally coupled scalar field cosmology were demonstrated. Also, the fragility of cosmological evolution with respect to the value of non-minimal coupling parameter was presented. The full characteristic of the dynamical evolution of a non-minimally coupled scalar field cosmological models was performed. It was shown that the inclusion of both types of matter opens an enormous dynamical complexity of possible evolutional paths of the universe, which are not present in standard cosmological models or in the models filled with a scalar field only. The generic evolutional path, which does not depend on the form of the scalar field potential function, was found. It leads to new and natural possibility of unified description of the cosmological evolution. Within one framework of a non-minimally coupled scalar field cosmology all the major epochs in the history of the universe emerge as critical points of the corresponding dynamical system (a finite scale factor singularity, an inflation (slow-roll and fast-roll), a radiation era, a barotropic matter domination era and finally the present accelerated expansion epoch).

Contents

Chapter 1

Introduction

Scalar fields, the simplest physical fields, play a very important role in modern cosmology. In an inflationary scenario they generate an exponential rate of expansion of the universe as well as density fluctuations due to vacuum energy [1, 2]. The discovery of accelerated cosmic expansion [3, 4] gave a motivation to study the dynamics of dark energy models (see [5] for review). In the context of the quintessence idea [6, 7] the simplest dynamical models involving the scalar field ϕ with a potential function $U(\phi)$ are used to model a time dependent equation of state parameter w_ϕ. While the simplest candidate for dark energy seems to be a positive cosmological constant, the ΛCDM model is favoured by observational data [8, 9, 10], such an explanation of the cosmic acceleration suffers from the fine tuning problem [11] and the coincidence problem [12]. In order to alleviate those problems many alternatives have been proposed, like for example phantom dark energy [13, 14] or extended quintessence [15, 16, 17, 18].

Scalar fields are also very important in the description of dynamics in the loop quantum cosmology, which is based on the background independent theory without the canonical notion of time. In this theory one scalar field is chosen as an internal clock for other fields [19]. The scalar fields with a potential function are also very important in modelling of inflation. For example a scalar field with the simplest quadratic potential function was assumed in Linde's conception of chaotic inflation [2]. The 5 years of WMAP observations [20] rejected many inflationary scenarios (potential functions $U(\phi)$), while models with a simple quadratic potential are admitted at the 1σ confidence level.

If we are going to generalise the scalar field cosmology minimally coupled to gravity, then the inclusion of the non-minimal coupling term of type $\xi R\phi^2$ [21, 22, 23] seems to

be natural and the simplest generalisation of the Lagrangian for scalar field dynamics in the background of cosmological models with maximal symmetry of space-like slices. Of course the value of this additional parameter should be estimated from observational data [24, 25, 26] or given from some theoretical arguments [16]. The nonzero ξ arises from quantum corrections [27] and it is required by the renormalization [22]. While the simplest minimally coupled scalar field with a quadratic potential function has strong motivations in observations [20, 28] its generalisations with a non-minimal coupling term was studied [29] in the context of the origin of the canonical inflaton itself. The role of the non-minimal coupling in evolution of the universe in the context of inflation and quintessence was studied previously by many authors [30, 31, 32, 33, 34, 35, 36, 37, 38, 39, 40, 41, 42, 43, 44, 45, 46, 47, 48, 49, 50, 51] and in connection with the development of the Standard Model with a non-minimally coupled Higgs field [52, 53, 54, 55]. Moreover, recently there were great wave of interest in generalisations of supergravity to the case with scalar fields non-minimally coupled to gravity [56, 57, 58].

The Einstein field equations for spatially homogeneous cosmological models can be reduced to the form of an autonomous dynamical system. This enables us to study the evolution of cosmological models in the terms of dynamical systems theory [59, 60, 61].

The theory of dynamical systems give us the possibility of study all the evolutional paths admissible for all initial conditions. It is especially important in cosmology where there is the problem of initial conditions. Using the dynamical systems methods one hopes to answer the question of what is the range of initial conditions and parameters of the system for which the subsequent evolution is compatible with current observations of the universe [61]. The observational cosmology can be dedicated to distinguish solutions obvious for our universe.

The main aim of this dissertation is to study dynamical complexity of the dynamical systems of cosmological origin. My investigations show that in the phase space both, regular and chaotic, behaviour coexist. I characterise different manifestations of complex chaotic behaviour in the class of model under consideration (chaotic and non-chaotic scattering). Using the dynamical systems methods one is able to reveal all degree of complexity of dynamical evolution of the cosmological models with a scalar field. One can distinguish the generic and non-generic cases, study their stability, etc.

The organisation of this dissertation is as follows: Chapter 2 is devoted to investigations of the spatially closed FRW cosmological model with the conformally coupled

scalar field and quadratic potential function. Complexity of dynamics is investigated in a geometrical way by means of geodesics of the Jacobi metric, the Poincaré sections and complex behaviour of trajectories in terms of symbolic dynamics. Dynamics of conformally coupled phantom scalar field is investigated in Chapter 3. We demonstrate that this type of cosmological model can be treated as a scattering process of two types: multiple chaotic and classical non-chaotic and its character depends on whether the spontaneous symmetry breaking takes place. In Chapter 4 we show that the dynamics of spatially flat FRW models where there is no other form of matter except the non-minimally coupled scalar field can be reduced to a two dimensional dynamical system on the phase plane. All evolutional paths are visualised and classified on the phase plane and the parameter of non-minimal coupling plays the role of a control parameter. The fragility of global dynamics with respect to changes of the coupling constant is carefully studied. Dynamics of a flat FRW cosmological model with a non-minimally coupled scalar field (both canonical and phantom) and a barotropic matter is investigated in Chapters 5 and 6. We show that the dynamics of the models can be reduced to a three dimensional dynamical system. We have found the stationary solutions of the system and discussed their stability. In Chapter 5 we formulate the notion of "twister solution" travelling between three critical points representing the radiation dominated universe, the barotropic matter dominating state and finally the de Sitter attractor. The extension of these results to the arbitrary form of the potential function of the scalar field is formulated in Chapter 6. We have found the set of fixed points representing all important epochs in evolution of the universe: a finite scale factor singularity, an inflation (slow–roll and rapid–roll), a radiation and matter domination and finally a quintessence era. The discovered evolutional paths are realized only if the nonzero coupling constant is present. The final and concluding remarks are given in Chapter 7. We also discuss there possible future developments and projects in non-minimally coupled scalar field cosmology.

Citations to Previously Published Work

The content of this dissertation is solely based on the following research papers published in refereed journals

Chapter 2 Orest Hrycyna, Marek Szydłowski, *Different faces of chaos in FRW models with scalar fields – geometrical point of view*,
Chaos, Solitons and Fractals **28**, 1252 (2006), `arXiv:gr-qc/0505155`

Chapter 3 Marek Szydłowski, Orest Hrycyna, Adam Krawiec, *Phantom cosmology as a scattering process*,
JCAP06(2007)010, `arXiv:hep-th/0608219`

Chapter 4 Orest Hrycyna, Marek Szydłowski, *Non-minimally coupled scalar field cosmology on the phase plane*,
JCAP04(2009)026, `arXiv:0812.5096 [hep-th]`

Chapter 5 Orest Hrycyna, Marek Szydłowski, *Twister quintessence scenario*,
Phys. Lett. B **694**, 191 (2010), `arXiv:0906.0335 [astro-ph.CO]`

Chapter 6 Orest Hrycyna, Marek Szydłowski, *Uniting cosmological epochs through the twister solution in cosmology with non-minimal coupling*,
JCAP12(2010)016, `arXiv:1008.1432 [astro-ph.CO]`

The complete list of publications of the author is given at the end of this dissertation.

Notations and conventions

In this dissertation the following notations and conventions are used. The metric signature is $(-,+,+,+)$. The fundamental constants: the speed of light c and the reduced Planck constant $\hbar$ assume the value unity. The Planck mass is $m_{Pl} = G^{-1/2}$, where G is Newton's constant, and $\kappa^2 \equiv 8\pi G$. The Greek indices assume the values 0, 1, 2, 3. A comma after the terms denotes ordinary differentiation and also $\frac{\partial A}{\partial x^\mu} = \partial_\mu A = A_{,\mu}$, ∇_μ is the covariant derivative operator and g denotes the determinant of the metric tensor $g_{\mu\nu}$.
In terms of the Christoffel symbols

$$\Gamma^\alpha_{\mu\nu} = \frac{1}{2}\, g^{\alpha\sigma}\big(\, g_{\nu\sigma,\mu} + g_{\sigma\mu,\nu} - g_{\mu\nu,\sigma}\big) \tag{1.1}$$

the Ricci tensor is given by

$$R_{\mu\nu} = \Gamma^{\alpha}_{\mu\nu,\alpha} - \Gamma^{\alpha}_{\alpha\nu,\mu} + \Gamma^{\alpha}_{\mu\nu}\,\Gamma^{\beta}_{\beta\alpha} - \Gamma^{\alpha}_{\beta\nu}\,\Gamma^{\beta}_{\alpha\mu} \tag{1.2}$$

and the Ricci scalar is

$$R = g^{\mu\nu}\,R_{\mu\nu}. \tag{1.3}$$

$R > 0$ for the standard metric on a sphere.
The d'Alembert's operator is

$$\Box \equiv g^{\mu\nu}\,\nabla_\mu\nabla_\nu = \frac{1}{\sqrt{-g}}\,\partial_\mu\big(\sqrt{-g}\,g^{\mu\nu}\partial_\nu\big) \tag{1.4}$$

Basic equations of standard cosmology

The Friedmann–Robertson–Walker metric (from now on "FRW") can be presented as

$$\mathrm{d}s^2 = -\mathrm{d}t^2 + a^2(t)\Big[\frac{\mathrm{d}r^2}{1-k\,r^2} + r^2\big(\mathrm{d}\theta^2 + \sin^2\theta\,\mathrm{d}\varphi^2\big)\Big] \tag{1.5}$$

or

$$\mathrm{d}s^2 = -\mathrm{d}t^2 + a^2(t)\Big[\mathrm{d}\chi^2 + f^2(\chi)\,\big(\mathrm{d}\theta^2 + \sin^2\theta\,\mathrm{d}\varphi^2\big)\Big] \tag{1.6}$$

where

$$f(\chi) = \begin{cases} \sin\chi, & 0 \le \chi \le \pi \quad k = +1 \\ \chi, & 0 \le \chi \le \infty \quad k = 0 \\ \sinh\chi, & 0 \le \chi \le \infty \quad k = -1 \end{cases} \tag{1.7}$$

$k = 0, \pm 1$ is the normalised curvature index, $0 \le \varphi \le 2\pi$ and $0 \le \theta \le \pi$ are comoving coordinates, t stands for the cosmological time.

In order to find the form of the equations which describe the evolution of the universe we need to find the form of the Einstein tensor as well as the form of the energy–momentum tensor of the matter component. The Einstein field equations are

$$R_{\mu\nu} - \frac{1}{2}g_{\mu\nu}\,R + \Lambda\,g_{\mu\nu} = \kappa^2 T_{\mu\nu} \tag{1.8}$$

where $R_{\mu\nu}$ and R are the Ricci tensor and the Ricci scalar, respectively, and $T_{\mu\nu}$ is the energy-momentum tensor of the cosmic fluid.

In the homogeneous and isotropic universe the Einstein field equations reduce to the ordinary differential equation in the following form

$$H^2 = \frac{\kappa^2}{3}\rho - \frac{k}{a^2}, \tag{1.9}$$

$$\dot{H} = \frac{\ddot{a}}{a} - H^2 = -\frac{\kappa^2}{2}(\rho + p) + \frac{k}{a^2} \tag{1.10}$$

where $H \equiv \dot{a}/a$, an over dot denotes differentiation with respect to the cosmological time t, ρ and p are the energy density and pressure of the cosmic fluid, respectively. From the covariant conservation condition of the energy-momentum tensor

$$\nabla^\mu T_{\mu\nu} = 0, \tag{1.11}$$

we have the conservation equation for the energy density and pressure

$$\dot{\rho} = -3H(\rho + p). \tag{1.12}$$

1.1 Scalar fields in cosmology

The action of the phantom or canonical scalar field minimally coupled to gravity is of the form

$$S = S_g + S_\phi = \frac{1}{2\kappa^2}\int \mathrm{d}^4x\sqrt{-g}\,R - \frac{1}{2}\int \mathrm{d}^4x\sqrt{-g}\Big\{\varepsilon\, g^{\mu\nu}\nabla_\mu\phi\nabla_\nu\phi + 2U(\phi)\Big\} \tag{1.13}$$

where $U(\phi)$ is the potential function of the scalar field and $\varepsilon = \pm 1$ corresponds to the canonical and phantom scalar field, respectively. The energy–momentum tensor of ϕ assumes the following form

$$T_{\mu\nu} = \varepsilon\,\nabla_\mu\phi\nabla_\nu\phi - \varepsilon\,\frac{1}{2}g_{\mu\nu}\nabla^\alpha\phi\nabla_\alpha\phi - U(\phi)g_{\mu\nu} \tag{1.14}$$

In the special case of a homogeneous scalar field which depends only on the cosmological time $\phi = \phi(t)$ we have the energy density and the pressure of a scalar field in the following forms

$$p_\phi = \varepsilon\frac{1}{2}\dot{\phi}^2 - U(\phi), \qquad \rho_\phi = \varepsilon\frac{1}{2}\dot{\phi}^2 + U(\phi)\,. \tag{1.15}$$

The equation of motion for the scalar field ϕ reads

$$\Box\phi - \varepsilon\frac{\partial U(\phi)}{\partial\phi} = 0 \tag{1.16}$$

where $\Box = \frac{1}{\sqrt{-g}}\partial_\mu(\sqrt{-g}g^{\mu\nu}\partial_\nu)$ which for the FRW cosmology simply reduces to

$$\ddot{\phi} + 3H\dot{\phi} + \varepsilon U'(\phi) = 0. \tag{1.17}$$

The phantom scalar field (with $\varepsilon = -1$) was introduced by Caldwell [62], who proposed it as a possible explanation of the observed acceleration of the current Universe when $\Omega_{\mathrm{m},0} \gtrsim 0.2$. Note that a coupling to gravity in the quintessence models was also explored [40]. For example in the Friedmann–Robertson–Walker (FRW) model the phantom field minimally coupled to a gravity field leads to $\rho + p = -\dot{\phi}^2$ which is always a negative quantity, and $p < -\rho$ corresponds to a fluid with a super-negative pressure. Phantom fields lead to the super-accelerated expansion of the Universe, i.e. $\mathrm{d}H/\mathrm{d}t > 0$. The simplest models describe this field in terms of minimally coupled real scalar field with the negative kinetic energy term $-\frac{1}{2}\dot{\phi}^2$ [62, 13, 63]. It is interesting that phantom fields are also present in string theories [64, 65, 66] and arise as a phenomenological description of quantum effects of particle production in terms of bulk viscosity [67]. Because the phantom fields violate the Lorentz invariance condition most physicists believe that the phantoms open the doors to new physics [68]. The investigation of the theoretical possibility to describe dark energy in terms of phantom field was the subject of many papers [69, 46, 70, 71, 72, 73, 74, 75, 76, 77, 14, 78, 79, 80, 81, 82, 83, 84, 47]. In the paper by Dabrowski et al. [85] it is considered the quantisation of phantom field via the Wheeler-DeWitt equation in quantum cosmology. They showed that quantum effects give rise to avoiding the big-rip singularity. Also some other basic problems in cosmology like the problem of direction of time can be solved.

1.2 Scalar–tensor theories of gravitation

The introductory material presented below follows the book V. Faraoni, *Cosmology in Scalar–Tensor Gravity* [86].

1.2.1 Brans–Dicke theory

The Brans–Dicke theory [87] referred as the prototype of gravitational theories alternative to general relativity is described by the basic action

$$S_{\mathrm{BD}} = \frac{1}{16\pi}\int \mathrm{d}^4x\sqrt{-g}\Big\{\varphi\, R - \frac{\omega}{\varphi}\, g^{\mu\nu}\nabla_\mu\varphi\nabla_\nu\varphi - V(\varphi)\Big\} + S_{\mathrm{m}} \tag{1.18}$$

where S_{m} is the action describing ordinary matter (any form of matter different from the scalar field φ) and the dimensionless constant ω is the only parameter of the theory. The factor φ in the denominator of the second term in brackets in (1.18) is introduced to make ω dimensionless. The adjective "prototype" emphasises the unique features that characterise the original model compared with many others extended versions. The dynamics of the model is described by the gravitational field, which is described by the metric tensor $g_{\mu\nu}$ and by the BD scalar field φ, and the matter S_{m} which does not depend on φ.

The search for a theory of gravity containing Mach's principle, which is not completely embodied in general relativity, was the original motivation for the introduction of the Brans–Dicke theory [87].

Lets take a better look at the first term on the right-hand side of (1.18), the non-minimal coupling term. This replaces the Einstein–Hilbert action

$$S_{\mathrm{EH}} = \frac{1}{16\pi G}\int \mathrm{d}^4x\sqrt{-g}\,R \tag{1.19}$$

in the standard theory of gravitation. We find that the Brans–Dicke model has no gravitational "constant" but is characterised by the effective gravitational constant G_{eff} defined by

$$G_{\mathrm{eff}}(\phi) = \frac{1}{\varphi} \tag{1.20}$$

as long as the dynamical field φ varies slowly enough. Thus the effective gravitational coupling becomes a function of the spacetime point. The values of $\varphi > 0$ are usually chosen which corresponds to attractive gravity.

From the theoretical point of view, a value of the DB parameter ω of order unity would be natural [86], and it does appear in the low-energy limit of string theories. However, the larger the value of ω is, the closer BD theory is to general relativity. The bound from the VLBI experiments, concerning the light-deflection phenomenon involving light from extragalactic radio sources places the constraint $\omega > 3300$ [88, 89, 86].

The BD theory reduces to general relativity in the limit of large ω, this is why many physicists believe that the large value of ω required to satisfy the experimental bounds on this parameter amounts to a fine-tuning that makes BD theory unattractive from the physical point of view. Currently, the growing interest in the scalar-tensor theories, which the BD theory is a special case, comes from the discovery that BD theory is related to the Kaluza–Klein compactification of extra spatial dimensions and that the low energy limit of the gravitational sector of bosonic string theory yields a BD theory with $\omega = -1$ [86].

1.2.2 Kaluza–Klein theory

Growing interest in BD theory is motivated by the fact that in the Kaluza–Klein theory the BD scalar has a geometrical origin in the determinant of the metric defined on the submanifold of the extra dimensions [86]. In the classical Kaluza–Klein theory [90] the spacetime is $(M \otimes K, \hat{g}_{AB})$, where M is a 4-dimensional manifold with one timelike dimension and K is a submanifold with d spatial dimensions ($d \geq 1$). The $D = 4 + d$–dimensional metric with d–dimensional compactified space is:

$$\hat{g}_{AB} = \begin{pmatrix} \hat{g}_{\mu\nu} & 0 \\ 0 & \hat{\phi}_{ab} \end{pmatrix}. \tag{1.21}$$

where $A, B, \cdots = 0, 1, \ldots, (3 + d)$, $\mu, \nu, \cdots = 0, 1, 2, 3$ and $a, b, \cdots = 4, 5, \ldots, (3 + d)$

It is assumed that the metric (1.21) is diagonal, i.e. there are no off-diagonal terms which where present in the original formulation of Kaluza–Klein theory, introduced in order to unify electromagnetism and gravity [90].

The Kaluza–Klein cosmology in vacuum is described by the general relativity action in $D = 4 + d$ dimensions

$$S = \int \mathrm{d}^{(4+d)}x\sqrt{-\hat{g}}\,\mathcal{L}^{(4+d)} = \frac{1}{16\pi\hat{G}}\int \mathrm{d}^{(4+d)}x\sqrt{-\hat{g}}\Big\{\hat{R} - 2\hat{\Lambda}\Big\} \tag{1.22}$$

where $\hat{g} = \det(\hat{g}_{AB})$, $\hat{R}$ is the Ricci curvature for the metric $\hat{g}_{AB}$, $\hat{\Lambda}$ and $\hat{G}$ are the $4 + d$-dimensional cosmological and gravitational constant. We assume that there is no other form of matter different from $\hat{\Lambda}$ in order to consider a regime in which the dynamics of the universe is dominated by a single scalar field.

Introducing the determinant of the metric of the extra dimensions,

$$\varphi \equiv \big|\det\hat{\phi}_{ab}\big| \tag{1.23}$$

and the symmetric tensor $\rho_{ab} \equiv \varphi^{-1/d}\phi_{ab}$ it is, by definition, $|\det(\rho_{ab})| = 1$. It is also assumed that the extra dimensions are compactified to a scale of size l. Then, the integral over the $(4+d)$ dimensions in (1.22) can be separated into an integral over the four spacetime dimensions $\int \mathrm{d}^4x$ and an integral over the remaining d dimensions $\int \mathrm{d}^dx$. The action reduces to

$$S = \frac{V^{(l)}}{16\pi\hat{G}}\int \mathrm{d}^4x\sqrt{-g}\,\sqrt{\varphi}\left\{\Big(R + R_K - 2\hat{\Lambda}\Big) + \frac{(d-1)}{4d}\frac{g^{\mu\nu}\nabla_\mu\varphi\nabla_\nu\varphi}{\varphi^2}\right\} \tag{1.24}$$

where $V^{(l)}$ is the volume of the compact manifold K of the extra dimensions and R_K is the Ricci curvature of K.

Introducing the scalar field variable

$$\phi \equiv \sqrt{\varphi}$$

and defining $G = \hat{G}/V^{(l)}$, the action is

$$S = \frac{1}{16\pi G}\int \mathrm{d}^4x\sqrt{-g}\Big\{\phi\Big(R + R_K - 2\hat{\Lambda}\Big) + \frac{d-1}{d}\frac{g^{\mu\nu}\nabla_\mu\phi\nabla_\nu\phi}{\phi}\Big\} \tag{1.25}$$

which describes a Brans–Dicke theory (1.18)with

$$\omega = -\frac{d-1}{d}.$$

In most investigations of inflation or quintessence, a cosmological scalar field is required. Usually it is done by introducing this field by hand. Due to the presence of extra spatial dimensions in vacuum, higher dimensional, general relativity, the Kaluza–Klein theory give us an aesthetic derivation of the cosmological scalar field.

1.2.3 The dilaton from string theory

At tree level, the low energy action of the bosonic string theory in the string frame is [91]

$$S = \frac{1}{2k_D^2}\int \mathrm{d}^Dx\sqrt{-g}\,e^{-2\Phi}\left\{R + 4g^{\mu\nu}\partial_\mu\Phi\partial_\nu\Phi - \frac{1}{12}H_{\alpha\beta\gamma}H^{\alpha\beta\gamma} - \frac{D-26}{l_S^2}\right\} \tag{1.26}$$

where Φ is the dimensionless string dilaton, the 3-form $H_{\alpha\beta\gamma} = \partial_{[\alpha}b_{\beta\gamma]}$ is the strength of the Kalb–Ramond field $b_{\alpha\beta}$, k_D is the D-dimensional gravitational constant, and l_s is the string scale. In a spatially homogeneous and isotropic cosmology the 3-form field reduces to $H_{0\beta\gamma} = 0$, $H_{123} = h(t)$ and can be modelled by a perfect fluid [92, 86]. This is why one usually sets $H_{\alpha\beta\gamma}H^{\alpha\beta\gamma} = 0$ and preserves only the strong dilaton.

In four dimensions, the redefinition of the dilaton

$$\varphi = e^{-2\Phi}$$

transforms (1.26) into the BD action (1.18) with $\omega = -1$

$$S = \frac{1}{2k^2}\int \mathrm{d}^4x\sqrt{-g}\left\{\varphi\,R + \frac{1}{\varphi}\,g^{\mu\nu}\partial_\mu\varphi\partial_\nu\varphi\right\}. \tag{1.27}$$

1.3 Non-minimal coupling

This dissertation is devoted to investigations of dynamical evolution of the Friedmann–Robertson–Walker cosmological models, where a scalar field is explicitly coupled to the Ricci curvature of spacetime. The gravitational part of the action is given by

$$S_g = \frac{1}{2\kappa^2}\int \mathrm{d}^4x\sqrt{-g}\big(R-2\Lambda\big) \tag{1.28}$$

where $\kappa^2 = 8\pi G$, the action of a non-minimally coupled scalar field is

$$S_\phi = -\frac{1}{2}\int \mathrm{d}^4x\sqrt{-g}\Big\{\varepsilon\Big(g^{\mu\nu}\nabla_\mu\phi\nabla_\nu\phi + \xi R\phi^2\Big) + 2U(\phi)\Big\} \tag{1.29}$$

where $\varepsilon = \pm 1$ corresponds to the canonical and the phantom scalar field, respectively, and the action

$$S_m = \int \mathrm{d}^4x\sqrt{-g}\mathcal{L}_m \tag{1.30}$$

describes barotropic matter content in the model.

The Einstein field equations we obtained from variation of the full action

$$\frac{\delta}{\delta g^{\mu\nu}}\big(S_g + S_\phi + S_m\big) = 0 \tag{1.31}$$

are

$$R_{\mu\nu} - \frac{1}{2}g_{\mu\nu}R + \Lambda g_{\mu\nu} = \kappa^2\Big(T^{(\phi)}_{\mu\nu} + T^{(m)}_{\mu\nu}\Big), \tag{1.32}$$

where the energy-momentum tensor of a non-minimally coupled scalar field is

$$\begin{aligned} T^{(\phi)}_{\mu\nu} &= \varepsilon\nabla_\mu\phi\nabla_\nu\phi - \varepsilon\frac{1}{2}g_{\mu\nu}\nabla^\alpha\phi\nabla_\alpha\phi - U(\phi)g_{\mu\nu} \\ &\quad +\varepsilon\xi\left(R_{\mu\nu} - \frac{1}{2}g_{\mu\nu}R\right)\phi^2 + \varepsilon\xi\left(g_{\mu\nu}g^{\alpha\beta}\nabla_\alpha\nabla_\beta - \nabla_\mu\nabla_\nu\right)\phi^2 \end{aligned} \tag{1.33}$$

and

$$T^{(m)}_{\mu\nu} = \frac{-2}{\sqrt{-g}}\frac{\delta}{\delta g^{\mu\nu}}\Big(\sqrt{-g}\mathcal{L}_m\Big) \tag{1.34}$$

is the energy–momentum tensor for a barotropic matter. In Appendix A we have presented a pedagogical derivation of these equations. The dynamical equation for the scalar field we can obtain from the variation $\delta S/\delta\phi = 0$

$$\Box\phi - \xi R\phi - \varepsilon U'(\phi) = 0, \tag{1.35}$$

where $\Box = g^{\alpha\beta}\nabla_\alpha\nabla_\beta$. In Appendix B we show that this equation is conformally invariant in four spacetime dimensions for $\xi = 1/6$ and $U(\phi) = 0$ or $U(\psi) = \lambda\phi^4$. This is the main

reason to include ε parameter in equation (1.29) that the conformal coupling value $\xi = 1/6$ is valid for canonical and phantom scalar fields.

Now one should answer the question why non-minimally coupled scalar field? The non-minimal coupling of the scalar ϕ in equation (1.35) is commonly known from the work of Callan, Coleman and Jackiw [22], but it was earlier introduced by Chernikov and Tagirov [21]. The main motivation for introduction of non-minimal coupling in Ref. [22] was that $\xi \neq 0$ is generated by first loop corrections even if it is absent in the classical action and is required by renormalizability of the theory. For any value of ξ different from the conformal coupling 1/6 the Einstein equivalence principle is violated, therefore if we study cases with $\xi \neq 1/6$ we are probing cosmological implications of violation of this principle. From a pragmatic point of view [86], since non-minimal coupling is usually crucial for inflation, it is better to take it into account and then decide whether or not its effects can be verified through the observational astronomical data.

It is easy to notice that the theory of a non-minimally coupled scalar field is formally equivalent to a scalar–tensor theory. The redefinition of the scalar field

$$\varphi = \frac{1}{\kappa^2} - \varepsilon\xi\phi^2 \tag{1.36}$$

transforms the actions (1.28) and (1.29) into

$$S = \frac{1}{2}\int \mathrm{d}^4x\sqrt{-g}\Big\{\varphi\, R - \frac{\omega(\varphi)}{\varphi}\, g^{\mu\nu}\nabla_\mu\varphi\nabla_\nu\varphi - V(\varphi)\Big\} \tag{1.37}$$

where

$$\omega(\varphi) = \frac{\kappa^2\varphi}{4\xi(1-\kappa^2\varphi)} \tag{1.38}$$

and

$$V(\varphi) = U(\phi(\varphi)) = U\left(\pm\sqrt{\frac{1-\kappa^2\varphi}{\varepsilon\xi\kappa^2}}\right). \tag{1.39}$$

On the other hand using an appropriate conformal transformation (see Appendix B) and redefined scalar field [86] one can relate a cosmological scenario in the Jordan frame, in which the scalar field is non-minimally coupled to the Ricci curvature, with an evolution in an Einstein frame, in which the transformed scalar field is minimally coupled. At present there is no satisfactory answer which frame is physical [93, 86], this is why we work in the original formulation of the theory in the Jordan frame.

Note, that when a non-minimal coupling constant is present the Einstein field equations can be written in three possible inequivalent ways, resulting in different ways

of defining of the energy density ρ_ϕ and the pressure p_ϕ of the scalar field. In the case adopted in this dissertation, called the Callan–Coleman–Jackiw approach [86], the energy-momentum tensor (1.33)

$$\begin{aligned} T^{(\phi)}_{\mu\nu} &= \varepsilon\nabla_\mu\phi\nabla_\nu\phi - \varepsilon\frac{1}{2}g_{\mu\nu}\nabla^\alpha\phi\nabla_\alpha\phi - U(\phi)g_{\mu\nu} \\ &\quad +\varepsilon\xi\left(R_{\mu\nu} - \frac{1}{2}g_{\mu\nu}R\right)\phi^2 + \varepsilon\xi\left(g_{\mu\nu}g^{\alpha\beta}\nabla_\alpha\nabla_\beta - \nabla_\mu\nabla_\nu\right)\phi^2 \end{aligned} \tag{1.40}$$

in the fourth term contains a contribution proportional to the Einstein tensor. The contracted Bianchi identities

$$\nabla^\mu\left(R_{\mu\nu} - \frac{1}{2}g_{\mu\nu}R\right) = 0 \tag{1.41}$$

(for clarity we have omitted the Λ term in (1.32) because it always can be put in the right hand side of this equation together with the redefinition of the potential function $\widetilde{U}(\phi) = U(\phi) + \Lambda/\kappa^2$) yield

$$\nabla^\mu T^{(\phi)}_{\mu\nu} + \nabla^\mu T^{(m)}_{\mu\nu} = 0. \tag{1.42}$$

Since $T^{(m)}_{\mu\nu}$ does not depend on ϕ and $\nabla^\mu T^{(m)}_{\mu\nu}$ vanishes when the action is varied with respect to the matter variables, $T^{(m)}_{\mu\nu}$ and $T^{(\phi)}_{\mu\nu}$ are conserved separately,

$$\nabla^\mu T^{(m)}_{\mu\nu} = 0, \tag{1.43}$$

$$\nabla^\mu T^{(\phi)}_{\mu\nu} = 0. \tag{1.44}$$

This is the reason of choosing the energy-momentum tensor for a non-minimally coupled scalar field in the form (1.33). As we will see below it is not always true for other forms [94].

In the second way, called the effective coupling approach [86], one proceeds by writing the field equations (1.32) and (1.33) taking the term proportional to the Einstein tensor from right side to the left hand side of equation, then

$$(1 - \varepsilon\xi\kappa^2\phi^2)\left(R_{\mu\nu} - \frac{1}{2}g_{\mu\nu}R\right) = \kappa^2\left(T^{(II)}_{\mu\nu} + T^{(m)}_{\mu\nu}\right) \tag{1.45}$$

where now the energy-momentum tensor of a non-minimally coupled scalar field is

$$\begin{aligned} T^{(II)}_{\mu\nu} &= \varepsilon\nabla_\mu\phi\nabla_\nu\phi - \varepsilon\frac{1}{2}g_{\mu\nu}\nabla^\alpha\phi\nabla_\alpha\phi - U(\phi)g_{\mu\nu} \\ &\quad +\varepsilon\xi\left(g_{\mu\nu}g^{\alpha\beta}\nabla_\alpha\nabla_\beta - \nabla_\mu\nabla_\nu\right)\phi^2 = T^{(\phi)}_{\mu\nu} - \varepsilon\xi\left(R_{\mu\nu} - \frac{1}{2}g_{\mu\nu}R\right)\phi^2 \end{aligned} \tag{1.46}$$

Next, dividing equation (1.45) by the factor $(1-\varepsilon\xi\kappa^2\phi^2)$, we get

$$R_{\mu\nu}-\frac{1}{2}g_{\mu\nu}R=\kappa^2_{\text{eff}}\left(T^{(II)}_{\mu\nu}+T^{(m)}_{\mu\nu}\right) \tag{1.47}$$

where

$$\kappa^2_{\text{eff}}(\phi)=\frac{\kappa^2}{1-\varepsilon\xi\kappa^2\phi^2} \tag{1.48}$$

is an effective time dependent gravitational coupling for both $T^{(\phi)}_{\mu\nu}$ and $T^{(m)}_{\mu\nu}$. From the contracted Bianchi identities we have

$$\nabla^\mu\left(\kappa^2_{\text{eff}}\left(T^{(II)}_{\mu\nu}+T^{(m)}_{\mu\nu}\right)\right)=0 \tag{1.49}$$

which leads to

$$\nabla^\mu\left(T^{(II)}_{\mu\nu}+T^{(m)}_{\mu\nu}\right)=-\frac{\varepsilon 2\xi\kappa^2\phi}{1-\varepsilon\xi\kappa^2\phi^2}\left(\nabla^\mu\phi\right)\left(T^{(II)}_{\mu\nu}+T^{(m)}_{\mu\nu}\right). \tag{1.50}$$

The third and last possible way to write the Einstein field equations of the non-minimally coupled scalar field theory, called a mixed approach [86],

$$R_{\mu\nu}-\frac{1}{2}g_{\mu\nu}R=\kappa^2\left(T^{(III)}_{\mu\nu}+\frac{T^{(m)}_{\mu\nu}}{1-\varepsilon\xi\kappa^2\phi^2}\right) \tag{1.51}$$

where

$$\begin{aligned} T^{(III)}_{\mu\nu} &= \frac{1}{1-\varepsilon\xi\kappa^2\phi}\Big[\varepsilon\nabla_\mu\phi\nabla_\nu\phi-\varepsilon\frac{1}{2}g_{\mu\nu}\nabla^\alpha\phi\nabla_\alpha\phi-U(\phi)g_{\mu\nu} \\ &\quad +\varepsilon\xi\left(g_{\mu\nu}g^{\alpha\beta}\nabla_\alpha\nabla_\beta-\nabla_\mu\nabla_\nu\right)\phi^2\Big]=\frac{T^{(II)}_{\mu\nu}}{1-\varepsilon\xi\kappa^2\phi^2}. \end{aligned} \tag{1.52}$$

We clearly see that there is again the limitation due to presence of the factor $1/(1-\varepsilon\xi\kappa^2\phi^2)$ in the energy-momentum tensor. Note that

$$\kappa^2T^{(III)}_{\mu\nu}=\kappa^2_{\text{eff}}T^{(II)}_{\mu\nu}. \tag{1.53}$$

In this case the contracted Bianchi identities yield conservation of the total energy-momentum tensor

$$\nabla^\mu\left(T^{(III)}_{\mu\nu}+\frac{T^{(m)}_{\mu\nu}}{1-\varepsilon\xi\kappa^2\phi^2}\right)=0. \tag{1.54}$$

One can easy note that in the absence of ordinary matter, $T^{(III)}_{\mu\nu}$ is covariantly conserved, i.e., $\nabla^\mu T^{(III)}_{\mu\nu}=0$. In general case $T^{(III)}_{\mu\nu}$ alone

$$\nabla^\mu T^{(III)}_{\mu\nu}=-\frac{\varepsilon 2\xi\kappa^2\phi}{(1-\varepsilon\xi\kappa^2\phi^2)^2}\left(\nabla^\mu\phi\right)T^{(m)}_{\mu\nu} \tag{1.55}$$

is not covariantly conserved.

Let us consider the flat FRW cosmology with a non-minimally coupled scalar field and barotropic matter content. Then from (1.35) we have

$$\ddot{\phi} + 3H\dot{\phi} + \xi R\phi + \varepsilon U'(\phi) = 0, \tag{1.56}$$

and energy conservation condition from the variation $\delta S/\delta g^{\mu\nu} = 0$

$$\mathcal{E} = \varepsilon\frac{1}{2}\dot{\phi}^2 + \varepsilon 3\xi H^2\phi^2 + \varepsilon 3\xi H(\phi^2)^{\cdot} + U(\phi) + \rho_m - \frac{3}{\kappa^2}H^2. \tag{1.57}$$

Then conservation conditions read

$$\frac{3}{\kappa^2}H^2 = \rho_\phi + \rho_m, \tag{1.58}$$

$$\dot{H} = -\frac{\kappa^2}{2}\Big[(\rho_\phi + p_\phi) + \rho_m(1 + w_m)\Big] \tag{1.59}$$

where the energy density and the pressure of the scalar field are

$$\rho_\phi = \varepsilon\frac{1}{2}\dot{\phi}^2 + U(\phi) + \varepsilon 3\xi H^2\phi^2 + \varepsilon 3\xi H(\phi^2)^{\cdot}, \tag{1.60}$$

$$p_\phi = \varepsilon\frac{1}{2}(1 - 4\xi)\dot{\phi}^2 - U(\phi) + \varepsilon\xi H(\phi^2)^{\cdot} - \varepsilon 2\xi(1 - 6\xi)\dot{H}\phi^2 - \varepsilon 3\xi(1 - 8\xi)H^2\phi^2 + 2\xi\phi U'(\phi). \tag{1.61}$$

These expressions are very complicated and it is very hard to make any conclusions by inspecting their form. Therefore, the dynamical systems methods seem to be an appropriate tool to investigate evolution of the cosmological models with a non-minimally coupled scalar field.

Chapter 2

Geometry of chaos in scalar field FRW models

FRW cosmologies with conformally coupled scalar fields are investigated in a geometrical way by the means of geodesics of the Jacobi metric. In this model of dynamics, trajectories in the configuration space are represented by geodesics. Because of the singular nature of the Jacobi metric on the boundary set $\partial\mathcal{D}$ of the domain of admissible motion, the geodesics change the cone sectors several times (or an infinite number of times) in the neighbourhood of the singular set $\partial\mathcal{D}$.

We show that this singular set contains interesting information about the dynamical complexity of the model. Firstly, this set can be used as a Poincaré surface for construction of Poincaré sections, and the trajectories then have the recurrence property. We also investigate the distribution of the intersection points. Secondly, the full classification of periodic orbits in the configuration space is performed and existence of unstable periodic orbits is demonstrated. Our general conclusion is that, although the presented model leads to several complications, like divergence of curvature invariants as a measure of sensitive dependence on initial conditions, some global results can be obtained and some additional physical insight is gained from using the conformal Jacobi metric. We also study the complex behaviour of trajectories in terms of symbolic dynamics.

Published in :

O. Hrycyna, M. Szydłowski, Chaos, Solitons and Fractals **28**, 1252 (2006), `arXiv:gr-qc/0505155`

Recently, a geometric description of chaos in Hamiltonian systems of cosmological origin has been formulated using the tools of Riemannian (or pseudo-Riemannian) geometry [95, 96]. We concentrate on the approach to dynamics of the systems with a natural Lagrangian function $\mathcal{L} = \frac{1}{2} g_{\alpha\beta}\dot{q}^{\alpha}\dot{q}^{\beta} - V(q)$. On the level of constant energy E this system can be reduced to the geodesics flow on a pseudo-Riemannian manifold with the Jacobi metric $\hat{g}_{\alpha\beta} = 2(E - V)g_{\alpha\beta}$ [97, 98, 99, 100]. The conformal metric becomes degenerate for certain values of energy E, at some points of configuration space $\{E = V\}$ for classical systems as well as for general relativistic ones. As a consequence one has the complication of matching together geodesics well defined on open sets across a singular surface and the divergence of curvature invariants characterising the property of sensitive dependence on initial conditions. One can avoid this crucial problem addressed in the context of Mixmaster models [101, 102] by formulating corresponding dynamical system as a system in the Finsler [103] or Eisenhart metric [104].

The fact that Jacobi geometry is singular suggests that this model of dynamics[1] is one of the worst possible choices when it comes to achieving characterisation of property of sensitive dependence on initial conditions it terms of curvature invariants or when it comes to achieving global results. It will be demonstrated that it is not true for the example of the behaviour of geodesics in the Jacobi metric for FRW cosmological models with conformally coupled scalar field. Of course, because of the singular nature of the Jacobi geometry, the geodesics change from time-like to space-like (sometimes several or an infinite number of times) during their evolution, but in order to "piece together the results", one is forced to try to match geodesics (which are representing periodic orbits of their original dynamics) each time the solution passes through a singular point. This leads to the full classification of periodic orbits in terms of "just piecing together" segments of geodesics. It is an example of the fact that some global theorem about geodesics can be achieved. Using this classification numerous methods based on symbolic dynamics and detection of the existence of unstable periodic orbits are proposed toward an invariant characterisation of dynamical complexity in cosmology [106].

The organisation of the chapter is the following. In section 2.1 the cosmological FRW model with conformally coupled scalar field is presented as a Hamiltonian dynamical system. This system belongs to larger class of simple indefinite dynamical systems for

[1] For interesting applications of Jacobi metric in the context of Schrödinger equation see [105]

which kinetic energy form is quadric in the momenta and has Lorentzian signature (is indefinite). In section 2.2 we consider Poincaré sections of the trajectories, with the surface formed by the boundary set of the domain classically admissible for motion, as an indicator of complex behaviour. Note that the trajectories have the property of recurrence due to multiple intersections of singular set. In this section the full classification of simple periodic orbits is performed and the largest Lyapunov exponent is calculated numerically. Section 2.2 also contains the analysis of distributions of intersection points on the singular set. The existence of a weak noise observed in the Fourier analysis of intersections seems to be a complementary indicator of chaotic behaviour.

2.1 FRW models with scalar fields as a simple indefinite dynamical systems

The dynamical systems of cosmological origin have many special features which distinguish them from those met in classical mechanics. It is in fact the origin of some problems and controversy in understanding of chaos in cosmology [107, 108].

In this section we shall study the dynamical complexity of a simple inflationary models of the Universe, regarded as Hamiltonian dynamical systems. They appeared, for example, in Linde's chaotic inflation scenario, where inflation is driven by the vacuum energy of a single slowly rolling inflaton field [2].

The dynamics of cosmological models, allowing for an inflaton field, has been studied by many authors [33]. The idea of inflation which was introduced to solve some of the underlying problems in the standard big-bang cosmology becomes strictly connected with the existence of a scalar field which generates the period of an accelerated expansion of the Universe. In this case its energy density becomes dominated by the potential energy $U(\psi)$ of the scalar field ψ (the inflaton). Although the dynamics of inflation depends on the specifics of the models, the basic mechanism lies in the equation of motion which for a homogeneous scalar field ($\psi = \psi(t)$) takes the form

$$\ddot{\psi} + 3H\dot{\psi} + U'(\psi) + \frac{1}{6}R\psi = 0, \tag{2.1}$$

where an over dot represents a derivative whit respect to the cosmological time t, and $U' = \mathrm{d}U/\mathrm{d}\psi$, R is the Ricci scalar here, and the last term vanishes for minimally coupled

scalar fields (in general the last term is $\xi R\psi$, where $\xi = 1/6$ for the case of conformally coupled scalar fields).

Here we deal with a single homogeneous and conformally coupled scalar field ψ with potential $U(\psi)$ on the FRW background. The same system was previously considered in terms of the original dynamical systems without using the conformal Jacobi metric by many authors in the context of inflation and chaos [109, 110, 111]. Our goal in this chapter is to point out different manifestations of the complex dynamics in terms of geodesics in the Jacobi metric. The motivation for such a study is to obtain an additional physical insight using the conformal metric and the behaviour of periodic orbits.

Our cosmological model assumes the FRW spatial geometry, that is, the line element is of the form

$$\mathrm{d}s^2 = a^2(\eta)\{-\mathrm{d}\eta^2 + \mathrm{d}\chi^2 + f^2(\chi)(\mathrm{d}\theta^2 + \sin^2\theta\mathrm{d}\varphi^2)\}, \tag{2.2}$$

where $0 \leq \varphi \leq 2\pi$, $0 \leq \theta \leq \pi$, $0 \leq \chi \leq \pi$ and η is the conformal time $\mathrm{d}t/a = \mathrm{d}\eta$; a – the scale factor;

$$f(\chi) = \begin{cases} \sin\chi, & 0 \leq \chi \leq \pi \quad k = +1 \\ \chi, & 0 \leq \chi \leq \infty \quad k = 0 \\ \sinh\chi, & 0 \leq \chi \leq \infty \quad k = -1 \end{cases}$$

k is the curvature index.

The gravitational dynamics is derived from the Einstein-Hilbert action

$$S_g = \frac{1}{2\kappa^2}\int \mathrm{d}^4x\sqrt{-g}(R - 2\Lambda), \tag{2.3}$$

where g is the determinant of the metric; $-g = a^4 f^2(\chi)\sin\theta$ and R is the curvature scalar for metric (2.2) given by

$$R = 6\left\{\frac{\ddot{a}}{a^3} + \frac{k}{a^2}\right\}, \tag{2.4}$$

where a dot denotes differentiation with respect to η. In so far as Robertson-Walker symmetry holds, the scalar field should be homogeneous $\psi = \psi(t)$.

The action for a conformally coupled (real) scalar field is given by

$$S_\phi = -\frac{1}{2}\int \mathrm{d}^4x\sqrt{-g}\{g^{\mu\nu}\partial_\mu\psi\partial_\nu\psi + \frac{1}{6}R\psi^2 + 2U(\psi)\} \tag{2.5}$$

where $U(\psi) = \frac{1}{2}m^2\psi^2 + \frac{\lambda}{4}\psi^4$ is the assumed form of potential for this scalar field.

After integration over the spatial variables ($\int \mathrm{d}^3x = 2\pi^2$ is the conformal volume of an spatial hypersurface of constant curvature) and discarding total derivatives in the full

action we obtain dynamical system with two degrees of freedom: a and a rescaled scalar field $\phi : \psi \to \phi = \sqrt{1/6}a\psi$ with Hamiltonian

$$\mathcal{H} = \frac{1}{2}\{-(p_a^2 + ka^2) + (p_\phi^2 + k\phi^2) + m^2a^2\phi^2 + \lambda\phi^4 + \Lambda a^4\}, \tag{2.6}$$

where m^2 is the mass of the scalar field, Λ is constant proportional by the factor of $1/3$ to the cosmological constant.

The evolution of the system should be considered on the $\mathcal{H} = 0$ energy level for vacuum cosmology or on the $\mathcal{H} = -\rho_{r,0}$ energy surface if we add a radiation component to the energy-momentum tensor whose energy density scales like $\rho_r = \rho_{r,0}a^{-4}$, where $\rho_{r,0} =$ const [112]. Let us note that system (2.6) belongs to a larger class of dynamical systems which we call simple indefinite mechanical systems.

By simple indefinite mechanical system we understand the triple $(\mathcal{M}, g, V)$, where $\mathcal{M}$ is the configuration space carrying a metric g which defines the indefinite kinetic energy form $\mathcal{K} = \frac{1}{2}g(\mathbf{u}, \mathbf{u})$, $\mathbf{u} \in T_x\mathcal{M}$, $x \in \mathcal{M}$. V is the potential function $V : \mathcal{M} \to \mathcal{R}$ which is C^∞, and g has the Lorentz signature $(-, +, +, +)$.

The "simple" in the above context means that dynamical system has the natural form of Lagrange function $\mathcal{L} = \frac{1}{2}g_{\alpha\beta}\dot{q}^\alpha\dot{q}^\beta - V(q)$, where $\alpha, \beta = 1, \ldots, N$ and q and $\dot{q}$ are generalised coordinates and velocities respectively. The Hamilton function for such a system is of the form

$$\mathcal{H}(p, q) = \frac{1}{2}g^{\alpha\beta}p_\alpha p_\beta + V(q), \qquad p_\alpha = g_{\alpha\beta}\dot{q}^\beta. \tag{2.7}$$

For the system under consideration $(q^1, q^2) = (a, \phi)$. Because of our general relativity and cosmology application $\mathcal{H} = E = \text{const} \iff g_{\alpha\beta}\dot{q}^\alpha\dot{q}^\beta = 2(E - V(q))$. Therefore trajectories of the system in the tangent space of $\mathcal{R}^{2N}$ with coordinates $(q^\alpha, \dot{q}^\alpha)$ are situated in the domain described by $\Omega = \{(q^\alpha, \dot{q}^\alpha) \in \mathcal{R}^{2N} : g_{\alpha\beta}\dot{q}^\alpha\dot{q}^\beta = \|\mathbf{u}\|^2 = 2(E - V(q))\}$.

In the tangent space $T_q(\mathcal{R}^N)$ it is natural to distinguish three classes of vectors, namely, a vector $\mathbf{u}$ is time-like if $\|\mathbf{u}\|^2 < 0$, space-like if $\|\mathbf{u}\|^2 > 0$ and null if $\|\mathbf{u}\|^2 = 0$.

In the configuration space we distinguish three subsets

$$\begin{aligned} \mathcal{D}_S &= \{q \in \mathcal{R}^N : E - V(q) < 0\}, \\ \mathcal{D}_T &= \{q \in \mathcal{R}^N : E - V(q) > 0\}, \\ \partial\mathcal{D} &= \{q \in \mathcal{R}^N : E - V(q) = 0\}. \end{aligned} \tag{2.8}$$

Note that set $\partial\mathcal{D}$ is the boundary set because in its neighbourhood we can always find points of $\mathcal{D}_S$ and $\mathcal{D}_T$

$$\partial\mathcal{D}_S = \partial\mathcal{D}_T = \partial\mathcal{D}. \tag{2.9}$$

In the three distinguished domains the character of the vector tangent to a trajectory is determined by the Hamiltonian constraint $\mathcal{H} = E$. Therefore if a trajectory changes the domain, say $\mathcal{D}_S$ to $\mathcal{D}_T$, it crosses $\partial\mathcal{D}$ and the tangent vector to that trajectory at the point $q \in \partial\mathcal{D}$ is situated on the cone determined by the kinetic form: $g_{\alpha\beta}\dot{q}^\alpha\dot{q}^\beta = E$. In Ref. [101] we can find the proof that in the case of Bianchi IX model trajectory crosses the boundary set $V = 0$. During each of oscillations that occur close to boundary set the solution is instantaneously Kasner and therefore $V = 0$ an infinite number of times.

The physical trajectories of the simple indefinite systems are geodesics on pseudo-Riemannian manifold without the boundary (on which metric is degenerate) if we define the metric

$$\hat{g}_{\alpha\beta} = 2|E - V|g_{\alpha\beta}$$

and reparameterize the time variable $\eta \to s$ [113]:

$$\frac{\mathrm{d}s}{\mathrm{d}\eta} = 2|E - V|.$$

In our further considerations, we will demonstrate the advantages of the analysis of behaviour of trajectories in a neighbourhood of the boundary set $\partial\mathcal{D}$ of the region classically admissible for motion. It is also a surface of degeneration of the Jacobi metric. This surface and points of its intersections with the trajectories of the system contain interesting information about complex behaviour. For simplicity of presentation of this idea we assume $k = +1$, i.e. the closed FRW model filled with the conformally coupled scalar field is considered. The domain (classically) admissible for motion, as well as the boundary set, are shown on the figure 2.1 ($q^1 = a$, $q^2 = \phi$).

2.2 Different evidences of chaotic behaviour

2.2.1 Poincaré sections

It is clear that if a trajectory passes trough the boundary set $\partial\mathcal{D}$, then tangent vector to the trajectory is null, i.e. it lies on the cone $g_{\alpha\beta}\dot{q}^\alpha\dot{q}^\beta = 0$. The physical trajectories of the indefinite mechanical systems for given total energy E (zero for vacuum cosmology) are geodesics if we choose metric in the form $\hat{g}_{\alpha\beta} = 2(E - V)g_{\alpha\beta}$ in both domains $\mathcal{D}_S$ and $\mathcal{D}_T$. On the boundary $E = V$ the metric is degenerate, which is a source of obstacles if we define the property of sensitive dependence on initial conditions in terms of curvature

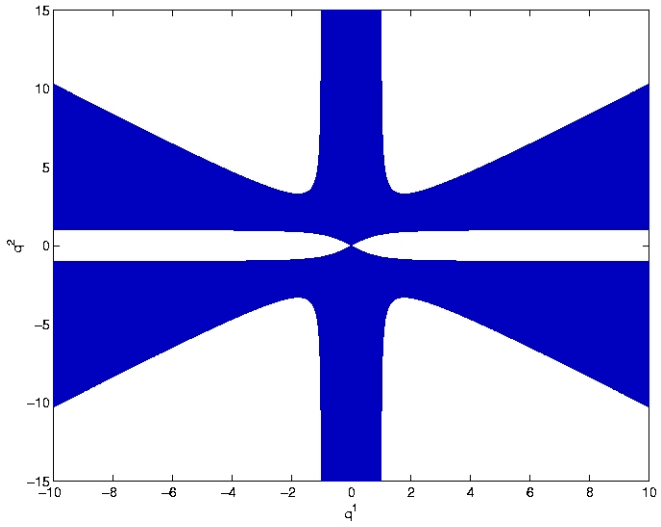

Figure 2.1: The domain admissible for motion of the FRW closed system with a conformally coupled scalar field. In the shaded area trajectories behave locally unstable $Kg(\mathbf{u},\mathbf{u}) < 0$ where K is the Gauss curvature for the Jacobi metric.

invariants (the Gauss curvature in our case). In both open regions $\mathcal{D}_S$ and $\mathcal{D}_T$ the Euler-Lagrange equation for the Lagrangian $\mathcal{L} = \frac{1}{2}g_{\alpha\beta}\dot{q}^\alpha\dot{q}^\beta - V(q)$, ($\dot{} = \frac{\mathrm{d}}{\mathrm{d}t}$) assumes the form of geodesics equation after reparameterization of the time variable [113]

$$t \to s : \frac{\mathrm{d}s}{\mathrm{d}t} = 2|E - V| \tag{2.10}$$

where s is the natural parameter defined along geodesics.

The criterion of local instability of geodesics flow can be formulated as $Kg(\mathbf{u},\mathbf{u}) < 0$, where $\mathbf{u}$ is the vector tangent to the trajectory and K is the Gauss curvature for the Jacobi metric. This domain is represented by shaded regions on the figure 2.1. Due to the representation dynamics as a geodesics flow one can imagine fictitious free falling particle in both domains $\mathcal{D}_S$ and $\mathcal{D}_T$ meeting the singularity (infinite curvature K) at the boundary set $\partial\mathcal{D}$ which play the role of a scattering surface.

The figures 2.2, 2.3, 2.4 show three trajectories in the configuration space for three different initial conditions together with Lyapunov exponents in time, calculated in the standard way. Note that in all cases Lyapunov principal exponent goes to zero as $\eta \to \infty$ which corresponds to the singularity at the conformal time. This suggests that the system under consideration has no property of sensitive dependence on initial conditions which is characteristic rather for integrable systems. Another property which distinguishes

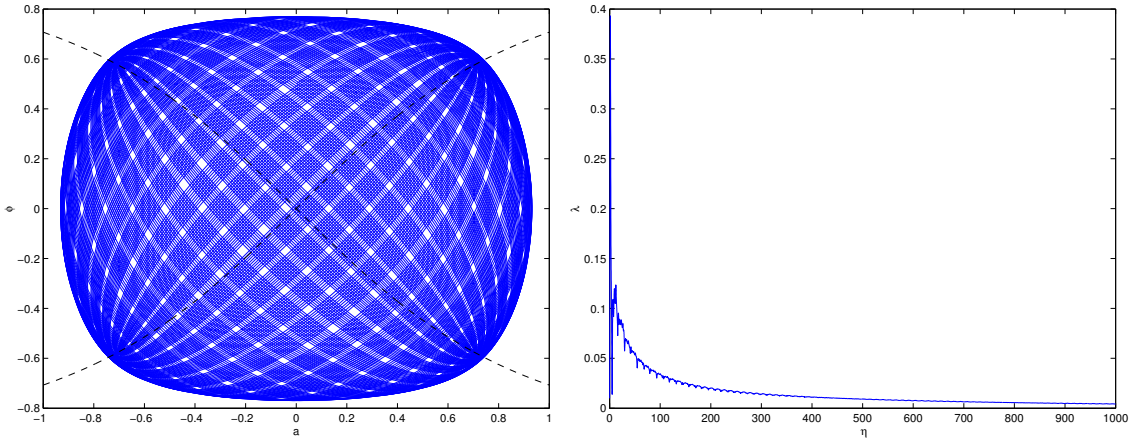

Figure 2.2: The trajectory in the configuration space for initial conditions $a_0 = 0$, $\phi_0 = \dot{\phi}_0 = 0.5$ ($\dot{a}_0$ calculated from Hamiltonian constraint) and Lyapunov principal exponent which tends to zero which may suggest that the system is regular.

the system from other systems of classical mechanics with conception of absolute time is that they do not posses property of topological transitivity which is crucial point for understanding of classical chaos conception [60].

It is useful to choose degeneration line $V(a, \phi) = 0$ as a Poincaré surface. Let us concentrate on the simplest case of $k = +1$ and $\Lambda = \lambda = 0$. Then $\phi = \pm a/\sqrt{1 + a^2}$ is an algebraic equation of the boundary set. On figure 2.5 one can see Poincaré section on the surface $V(a, \phi) = 0$ on the plane $(a, \dot{\phi})$ for different initial conditions.

While in figure 2.5 we find most trajectories as regular, there are, of course, chaotic trajectories. Some details of their concentrations in neighbourhood of saddle points and forming stochastic layers is illustrated on figure 2.6.

2.2.2 Symbolic dynamics in detection of dynamical complexity

Hadamard [114] was the first to use methods of trajectories coding in investigations of geodesics on compact space with negative curvature, which belongs now to the field of symbolic dynamics. The significance of this method in the context of closed cosmology with a scalar field was pointed out by Kamenshchik *et al.* [115]. The crucial feature of this model is the existence of points of maximal expansion ($\dot{a} = 0$, $\ddot{a} < 0$) and sometimes points of minimal contraction ($\dot{a} = 0$, $\ddot{a} > 0$) or "bounces". Then it is possible to classify all trajectories using localisation of their points of maximal expansion and calculate the

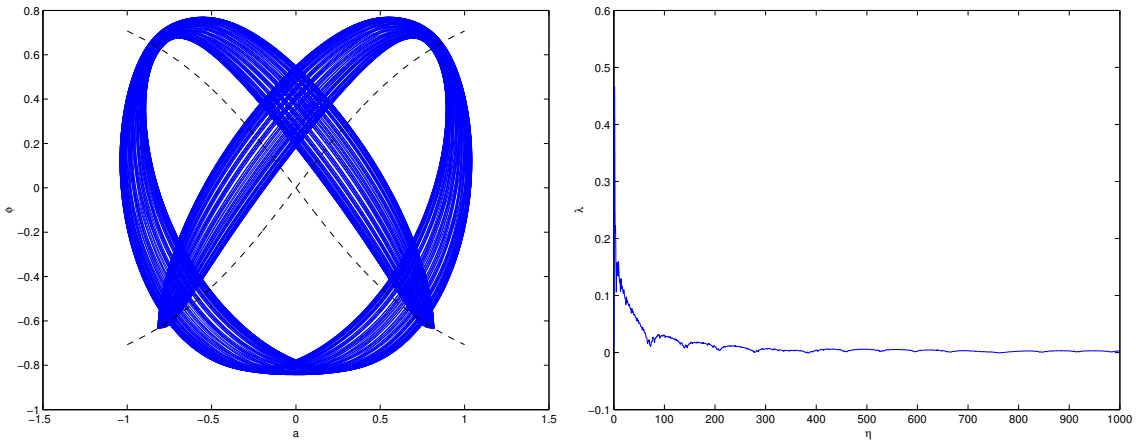

Figure 2.3: The trajectory in the configuration space for initial conditions $a_0 = 0$, $\phi_0 = \dot{\phi}_0 = 0.55$ ($\dot{a}_0$ calculated from Hamiltonian constraint) and Lyapunov principal exponent.

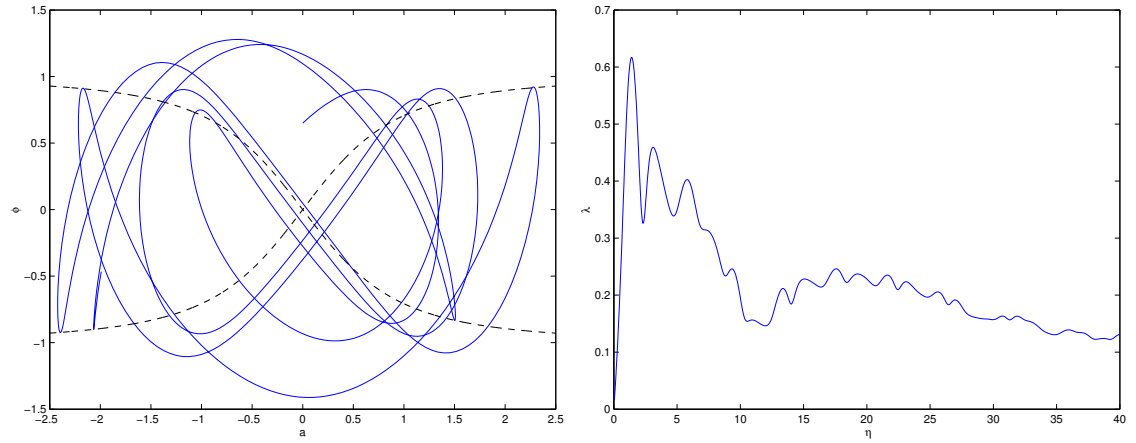

Figure 2.4: The trajectory in the configuration space for initial conditions $a_0 = 0$, $\phi_0 = \dot{\phi}_0 = 0.65$ ($\dot{a}_0$ calculated from Hamiltonian constraint) and Lyapunov principal exponent.

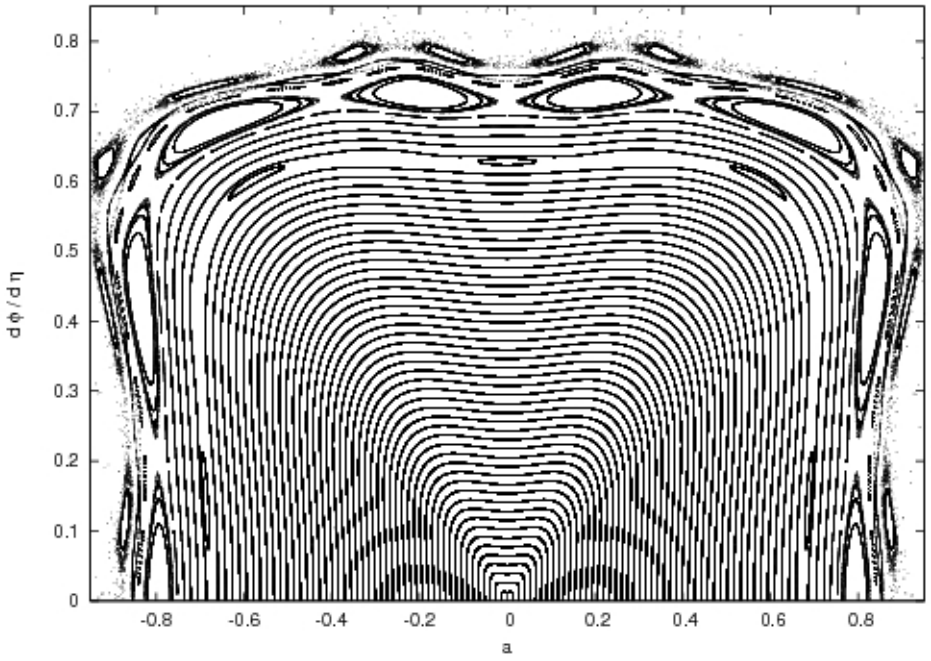

Figure 2.5: Poincaré section surface $V(a,\phi)=0$ and $\dot{a}<0$, $\dot{\phi}>0$.

topological entropy which measures the growth of the number of periodical orbits as their period increases. Hence one can quantify the length of orbit by the number of symbols A – bounce of trajectory ($\dot{a}=0$, $\ddot{a}>0$), B – crossing the line $\phi=0$. Note that $a\geq 0$ for physical reasons the extension of trajectories to $a<0$ domain means the extending the solutions beyond the big crunch which is only mathematically admissible [107].

For the model under consideration, two different coding procedures were used. In the first method we count all the intersections of trajectories with the axis $\{a=0\}$. For $\phi>0$ we put symbol (1) while in opposite case if $\phi<0$ we put symbol (0). Another method of codding trajectories rests on the analysis of intersections points with the boundary set $\partial\mathcal{D}$ defined as the surface $V(a,\phi)=0$ in the configuration space (a,ϕ). One can quantify the length of the orbit by two symbols : (1) – if $\phi>0$ at intersection point, and (0) in the opposite case if $\phi<0$. In both approaches mentioned before the trajectories are represented by a sequence of zeros and ones. The next step in our analysis is the division of all coding trajectories into blocks in the simplest way. The blocks consist of to letters (00), (01), (10) and (11) and blocks (01) and (10) are treated as a identical. Then, after counting different

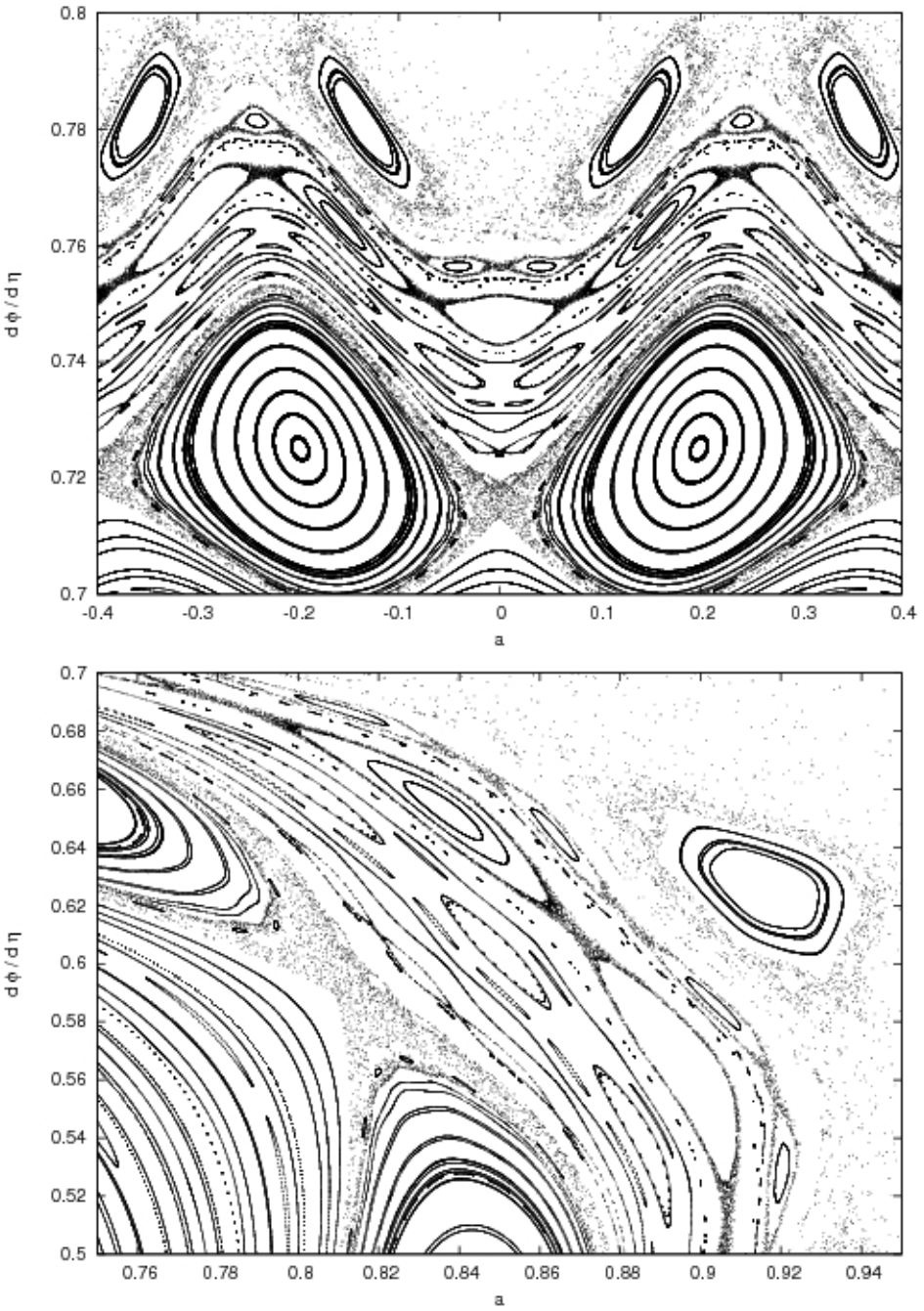

Figure 2.6: Details of Poincaré section from figure 2.5.

blocks one can calculate the Shannon informative entropy following the rule

$$H_S = \sum_{i=1}^{r} p_i \ln \frac{1}{p_i}, \tag{2.11}$$

where p_i $(i = 1, \ldots, r)$ is the probability that a given block will appear in the trajectory coding.

The informative Shannon entropy characterises the uncertainty degree of appearance of a given result. Following definition (2.11) H_S is a number which belongs to the interval $[0, \ln r]$. If for all i p_i assumes the same value equal $1/r$ then from definition (2.11) we obtain $H_S = \ln r$ which is the maximal value of H_S. From figure 2.7 one can observe that H_S is a growing function of initial conditions ϕ_0 to the limit which corresponds to purely chaotic behaviour.

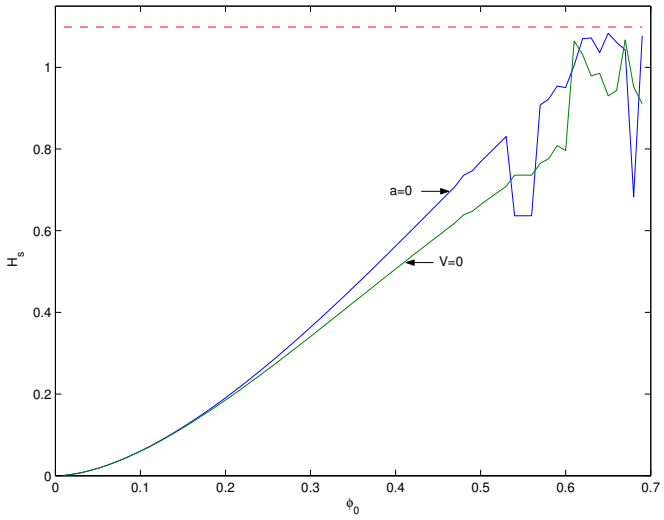

Figure 2.7: Shannon informative entropy as a function of ϕ_0 for two different codding methods. The horizontal line $H_S = \ln 3$ denotes the limit for purely random process.

2.2.3 Distribution of intersection points on the boundary set

It is interesting to check how the intersection points are distributed on the boundary line described by function $\phi = a/\sqrt{1+a^2}$. Let L be the length along that line calculated from the origin to the intersection point and N denote number of such intersections in the interval $L \pm \Delta L$. Of course N can be normalised to P and treated as a probability of finding a fictitious particle moving along a geodesic at a given point of $\partial\mathcal{D}$. The probability P as

a function of L (normalised to unity) is shown in figure 2.8. For deeper analysis of the distribution of the points Fourier analysis was performed and the results of such analysis are shown in figure 2.9. The existence of weak noise in the power spectrum can indicate chaotic distribution of the intersection points.

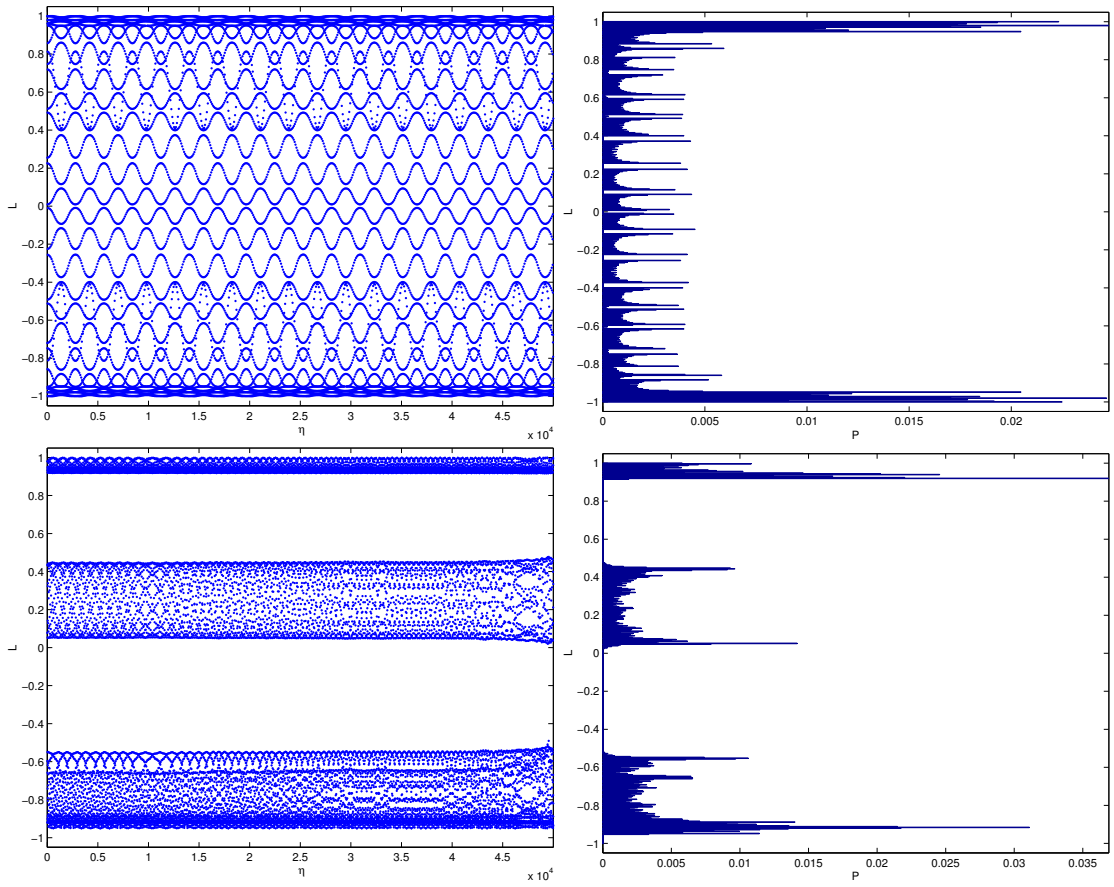

Figure 2.8: Intersection points of the boundary set $\partial\mathcal{D}$. Points of intersection of trajectory with set $\partial\mathcal{D}$ as a function of time (left) and probability of finding a particle-universe on a given subset of the set $\partial\mathcal{D}$ during evolution (right).

2.2.4 Unstable periodic orbits as an indicator of complexity of dynamics

It would by useful for classification of the periodic orbits to consider some reflection symmetries of the system. Of course, the system possesses reflection symmetry $\eta \to -\eta$ and $q^i \to -q^i$ ($q^i = a, \phi$). Therefore it is sufficient to investigate motion in one quarter, say $a > 0$ and $\phi > 0$, to reconstruct the motion in the remaining quarters.

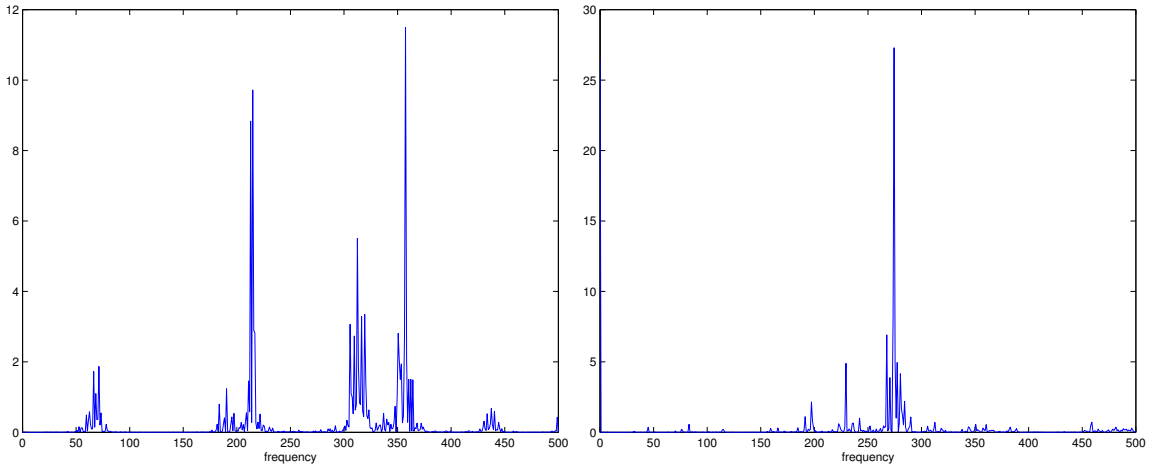

Figure 2.9: Fourier analysis of distributions from figure 2.8. Existence of weak noise in the power spectrum can indicate a chaotic distribution of intersection points.

Due to the symmetries mentioned before the simplest periodic orbits in the configuration space can be grouped in the following five classes

- trajectories of type 'I a' starting from the boundary line $V(a_0, \phi_0) = 0$ with initial conditions $(\dot{a}_0, \dot{\phi}_0) = (0, 0)$ for which after a 1/4 of period the inflection point at ϕ at $a = 0$ is reached with $(\dot{a}, \dot{\phi}) = (-\phi, 0)$ or $(+\phi, 0)$; see figure 2.10

- trajectories of type 'I b' also starting from the boundary set and reaching the singular point $(a, \phi) = (0, 0)$ for which $\dot{a} = \dot{\phi}$ or $\dot{a} = -\dot{\phi}$ after a 1/4 of the full period; see figure 2.11

- trajectories of type 'II a' starting from a point of configuration space $(a_0, 0)$ with $(\dot{a}_0, \dot{\phi}_0) = (0, a_0)$ and arriving at the inflection point of $\phi(a)$ diagram at $a = 0$ $(\dot{a}, \dot{\phi}) = (-\phi, 0)$ or $(+\phi, 0)$ after a 1/4 of full period; see figure 2.12

- trajectories of type 'II b' starting from the point $(a_0, 0)$, $(\dot{a}_0, \dot{\phi}_0) = (0, a_0)$ and reaching the singular point $(a, \phi) = (0, 0)$ and $\dot{a} = \dot{\phi}$ or $\dot{a} = -\dot{\phi}$ after a 1/4 of the full period; see figure 2.13

- trajectories of type 'III' (which are the union of all previously mentioned cases) starting from the boundary set $V(a_0, \phi_0) = 0$ with $(\dot{a}_0, \dot{\phi}_0) = (0, 0)$, after a 1/4 of the full period they reach one inflection point at scale factor a, and $\phi = 0$ with $(\dot{a}, \dot{\phi}) = (0, \pm a)$,

Type	$q_0^1 = a_0$	Period
I a	1.90228463575087	8.21179541505428
	4.07891339562106	9.68359976287486
	6.14180160301955	10.3389393707077
I b	2.63614545223571	9.49181146895361
	4.67384662462167	10.4432886891063
	6.68822113801299	10.8883259280963
II a	3.08416398565973	9.12958397138681
	5.16022385714180	10.06129848810491
	7.19459890603674	10.55370414489915
II b	1.64890985955010	8.45628399932237
	3.71764148794895	10.07328719135456
	5.72295574169836	10.69967308122208
III	2.47587020635594	17.99123630712047
	2.75437747583008	19.56534435565128
	2.94236929747301	20.15957644135879

Table 2.1: Unstable periodic trajectories.

after a 1/2 of the period they reach the symmetrical point to the initial condition with respect to ϕ–axis; see figure 2.14

Of course there are also non-symmetric periodic orbits present (see figure 2.15) but they are not a subject of our consideration. In Table 2.1 we can find the periods of typical periodic orbits which we obtain by using the modified multi shooting method [116]. To illustrate the property of sensitive dependence on initial conditions we investigate the evolution of the separation vector in the phase space in the term of "Lyapunov like" principal exponent. The principal Lyapunov exponent as well as the distance of the separation vector for initial conditions' separation $\Delta a = 10^{-12}$, are illustrated in figure 2.16. One can observe the existence of unstable periodic orbits in the model which should be treated as a strong evidence of chaos [117].

2.3 Conclusions

The complex behaviour of trajectories of FRW cosmological models with scalar field was investigated by means of geodesics of the Jacobi metric.

We pointed out the role of the singular set $\partial\mathcal{D}$ of degeneration of the Jacobi metric

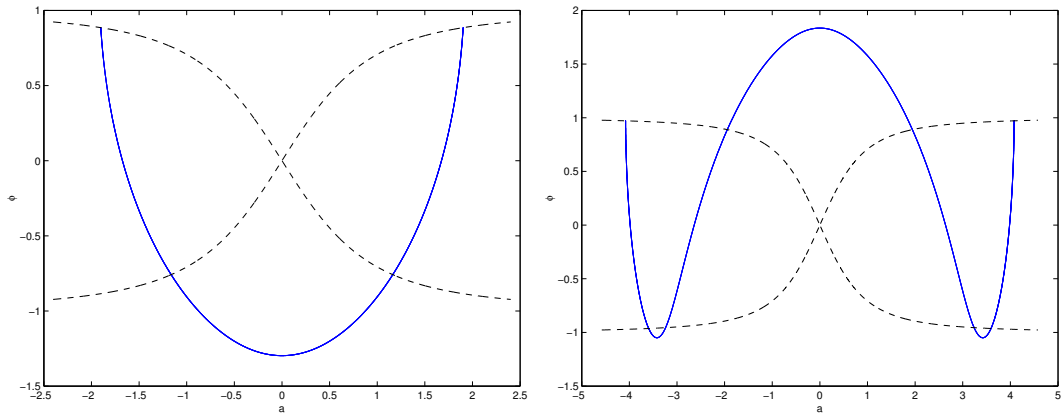

Figure 2.10: Periodic trajectories of type 'I a' in the configuration space.

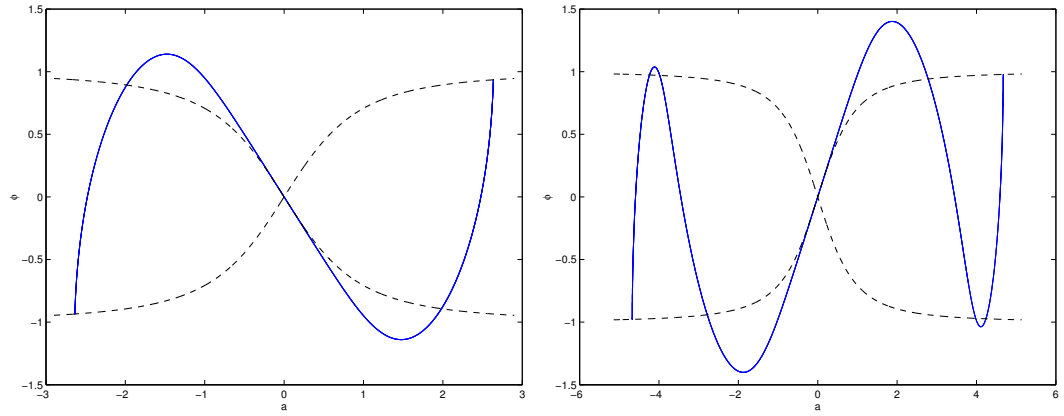

Figure 2.11: Periodic trajectories of type 'I b' in the configuration space.

in detection of complexity of dynamical behaviour. We find that this domain can be useful as a Poincaré surface. Moreover, the distribution of the intersection points as well as the existence of periodic orbits contain interesting information about the degree of complexity of its dynamics. Therefore all these investigations should be treated as a complementary description of chaotic behaviour in a geometrical way.

We have demonstrated the complexity of dynamics in the sense of (1) Poincaré sections, (2) random distribution of intersection points, (3) the existence of unstable periodic orbits and (4) chaos in trajectories coding. All this evidence has rather mathematical sense because we prolong trajectories to the nonphysical domain $a < 0$. The true sense of

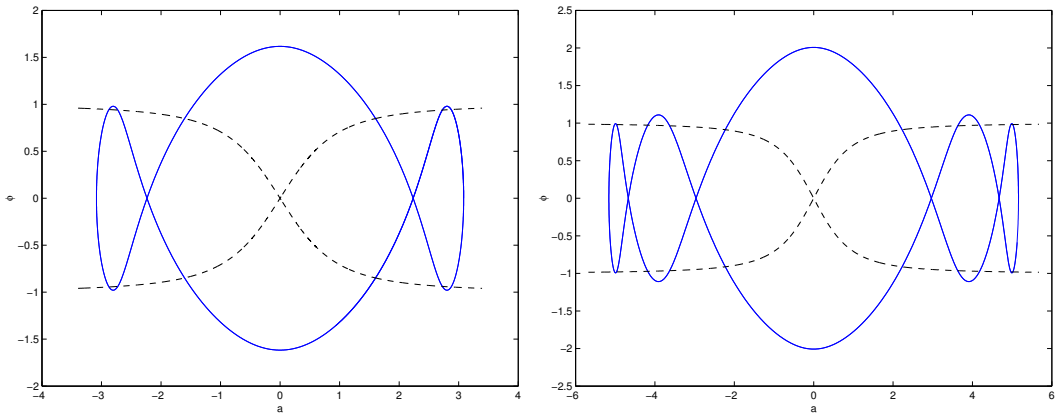

Figure 2.12: Periodic trajectories of type 'II a' in the configuration space.

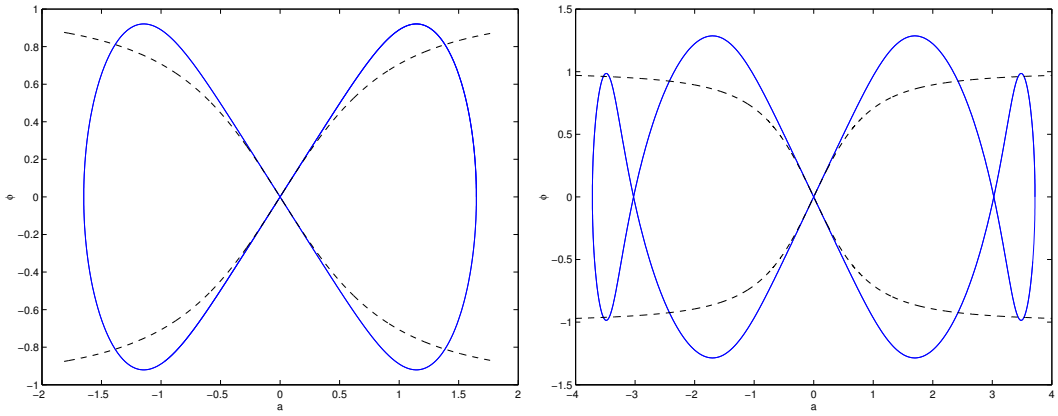

Figure 2.13: Periodic trajectories of type 'II b' in the configuration space.

complexity following Motter and Letelier [107] is in the nonintegrability of its dynamics. In Ref. [118, 119, 120] authors have investigated the model under consideration in the framework of nonintegrability and showed that they are non-integrable in the sense of nonexistence of meromorfic first integrals for the generic case of the model's parameters. To that end, the Yoshida, Ziglin, and strong methods of differential Galois group are used.

The presented approach offers some new possibilities of coding trajectories for which a well defined conception of Kolmogorov complexity can be also applied [121]. In 1963-1965 A. N. Kolmogorov proposed to consider a measure of complexity in the framework of the general theory of algorithms. Let us consider model of dynamics in the form of

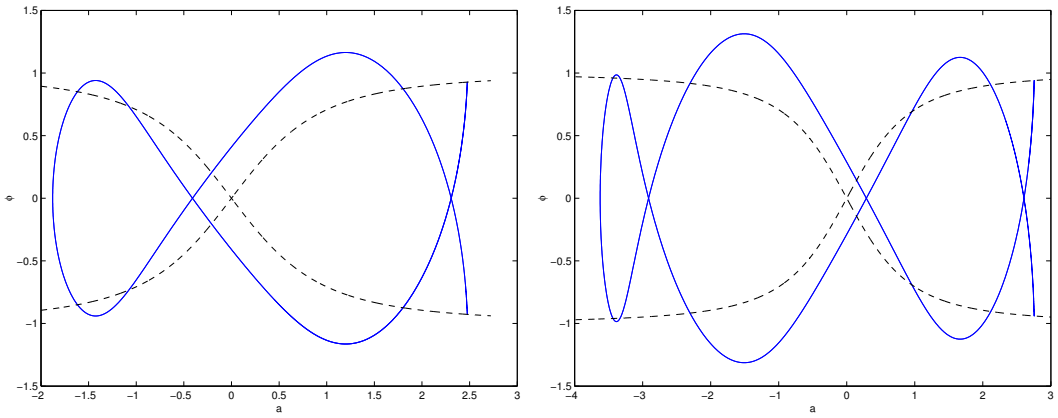

Figure 2.14: Periodic trajectories of type 'III' in the configuration space.

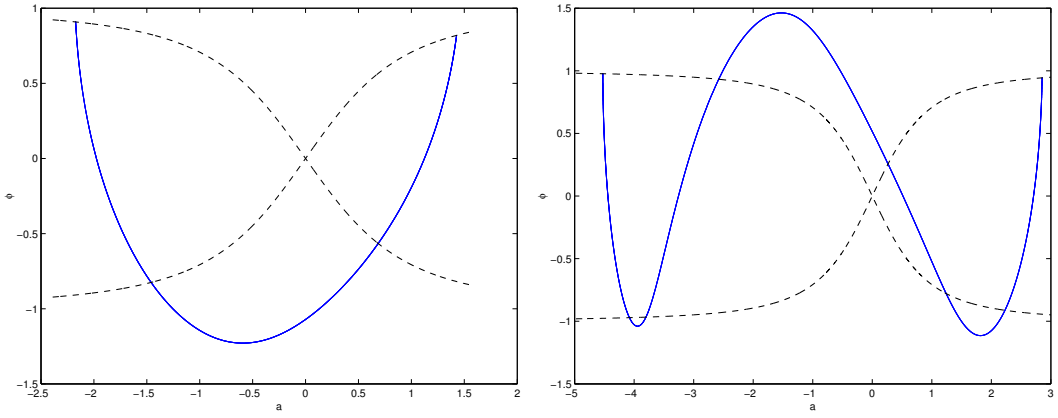

Figure 2.15: Non-symmetrical periodic trajectories in the configuration space.

mathematical object that has binary string α as its complete description. Then we can use the length of the shortest program in bits as a measure of the complexity of the object [122].

Let us now consider a cosmological model as a mathematical object that has coding dynamics in the form of binary string α as its complete description. Then for the purpose of quantifying complexity, the notion of Kolmogorov idea can be useful. The question, whether the FRW cosmological model is complex in the Kolmogorov sense, is open. In our opinion the geometrical language introduced here offers a new, interesting possibility of trajectories coding in the form of binary strings which makes answering this question easier.

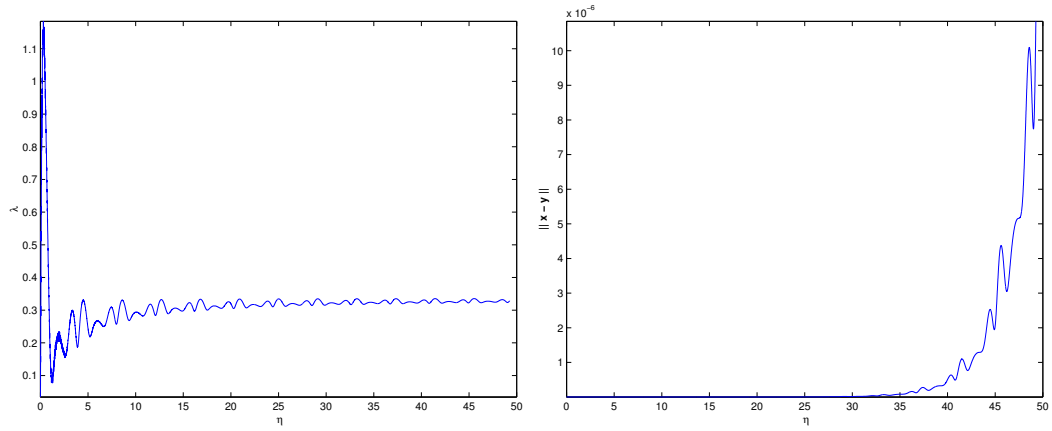

Figure 2.16: Stability analysis for the first trajectory from figure 2.10. Principal Lyapunov exponent (left) and the distance of separation vector (right) for initial conditions' separation $\Delta a = 10^{-12}$.

Chapter 3

Scattering processes in cosmological dynamics

The general chaotic features of dynamics of the phantom field modelled in terms of a single scalar field conformally coupled to gravity are studied. We demonstrate that the dynamics of the FRW model with dark energy in the form of phantom field can be regarded as a scattering process of two types: multiple chaotic and classical non-chaotic. It depends whether the spontaneous symmetry breaking takes place. In the first class of models with the spontaneous symmetry breaking the dynamics is similar to the one in Yang–Mills theory. We find the evidence of a fractal structure in the phase space of initial conditions. We observe similarities to the phenomenon of a multiple scattering process around the origin. In turn the class of models without the spontaneous symmetry breaking can be described as the classical non-chaotic scattering process and the methods of symbolic dynamic are also used in this case. We show that the phantom cosmology can be treated as a simple model with scattering of trajectories whose character depends crucially on the sign of a square of mass. We demonstrate that there is a possibility of chaotic behaviour in the flat Universe with a conformally coupled phantom field in the system considered on non-zero energy level. We obtain that the acceleration is a generic feature in the considered model without the spontaneous symmetry breaking.

Published in :

M. Szydłowski, O. Hrycyna, A. Krawiec, JCAP06(2007)010, `arXiv:hep-th/0608219`

The main goal of this chapter is to model the phantom fields in terms of scalar fields with a potential rather than in terms of the barotropic equation of state. For the latter case the dynamics is regular and can be represented on the two-dimensional phase space [123]. Usually phantom fields are modelled in terms of minimally coupled scalar fields The case of phantom field minimally coupled to gravity was analysed in the context of existence of periodic solutions [124]. The authors demonstrated that the dynamics is trivial in the sense of nonexistence of periodic solutions. Faraoni used the framework of phase space for investigating the dynamics of phantom cosmology, late-time attractors, and their existence for different shapes of potential [125]. It was showed that dynamics of the flat FRW universe can be reduced to the form of a two-dimensional dynamical system on a double sheeted phase space. It is a simple consequence of an algebraic equation for $\dot{\psi}$ which can be expressed as a function of the Hubble parameter H and ψ. In this case there is no place for chaotic behaviour of trajectories in the phase space $(H, \psi, \dot{\psi})$ [126]. The exit on the inflationary epoch and bounce was showed in the flat FRW universe with two interacting phantom scalar fields [127]. In the closed FRW cosmological model with minimally coupled scalar field there appears transient chaos which has the character of the scattering process [128]. The scattering process takes place during the bounce — a transition from a contracting to expanding universe. In this context the language of symbolic dynamics and topological entropy were used [129, 130, 115].

In this chapter we ask what kind of dynamics can be expected from the FRW model with phantom field. It is well known that the standard FRW model reveals some complex dynamics. The detailed studies gave us a deeper understanding of dynamical complexity and chaos in cosmological models and resulted in conclusion that complex behaviour depends on the choice of a time parameterisation or a lapse function in general relativity [131, 132, 111]. Castagnino et al. [133] showed that dynamics of the closed FRW models with a conformally coupled massive scalar field is not chaotic if considered in the cosmological time. The same model was analysed in the conformal time by Calzetta and Hasi [110] who presented the existence of chaotic behaviour of trajectories in the phase space. Motter and Letelier [107] explained that this contradiction in the results is obtained because the system under consideration is non-integrable. Therefore we can speak about complex dynamics in terms of nonintegrability rather than deterministic chaos. The significant feature is that nonintegrability is an invariant evidence of dynamical complexity in general relativity and cosmology [119].

We can find many analogies between models with spontaneously symmetry breaking and the Yang-Mills systems. Problems of chaotic behaviour in the Yang-Mills cosmological models have been investigated by Barrow and his collaborators. Chaos from Yang-Mills can only occur in an anisotropic universe but it occurs for some arbitrarily small anisotropy (see the study of Bianchi I [134] and other Bianchi types [135]). However, when a perfect fluid is added things change in an interesting way that contrast with the situation with a magnetic field [136].

For the FRW model with phantom it can be shown that there is a monotonous function along its trajectories and it is not possible to obtain the Lyapunov exponents or construct the Poincaré sections. Therefore it is useful to study the nonintegrability of the phantom system and set it in a much stronger form by proving that the system does not possess any additional and independent of Hamiltonian first integrals, which are in the form of analytic or meromorphic functions. Of course, it is not the evidence of sensitive dependence of solution on a small change of initial conditions. However, it is the possible evidence of complexity of dynamical behaviour formulated in an invariant way [123].

The notion of deterministic chaos is a controversial issue in the Mixmaster models. The value of the numerically computed maximal Lyapunov exponent for those systems depends on the time parameterisation used [137]. However, the existence of fractal structures in the phase space provides the coordinate independent signal of chaos in cosmology as it was shown by Cornish and Levin [111]. In particular, they found that the Bianchi IX has a form of chaotic scattering. The short scattering periods intermittent integrable motion and evolution of the system is chaotic. It is similar to a pin-ball machine.

The main goal of this chapter is to show that dynamics of phantom cosmology can be treated as a scattering process. If the spontaneous symmetry breaking is admitted this process has chaotic character. Evidences of dynamical behaviour are studied in tools of symbolic dynamics, fractal dimension, and analytically the Toda-Brumer-Duff test.

3.1 Hamiltonian dynamics of phantom cosmology

We assume the model with FRW geometry, i.e., the line element has the form

$$\mathrm{d}s^2 = -\mathrm{d}t^2 + a^2(t)[\mathrm{d}\chi^2 + f^2(\chi)(\mathrm{d}\theta^2 + \sin^2\theta\mathrm{d}\varphi^2)], \tag{3.1}$$

where

$$f(\chi) = \begin{cases} \sin\chi, & 0 \le \chi \le \pi \quad k = +1 \\ \chi, & 0 \le \chi \le \infty \quad k = 0 \\ \sinh\chi, & 0 \le \chi \le \infty \quad k = -1 \end{cases} \tag{3.2}$$

$k = 0, \pm 1$ is the curvature index, $0 \le \varphi \le 2\pi$ and $0 \le \theta \le \pi$ are comoving coordinates, t stands for the cosmological time.

It is also assumed that a source of gravity is the phantom scalar field ψ with a generic coupling to gravity. The gravitational dynamics is described by the standard Einstein-Hilbert action

$$S_g = \frac{1}{2\kappa^2} \int \mathrm{d}^4x\sqrt{-g}(R - 2\Lambda), \tag{3.3}$$

where $\kappa^2 = 8\pi G$; for simplicity and without lost of generality we assume $4\pi G/3 = 1$. The action for the matter source is

$$S_{\mathrm{ph}} = -\frac{1}{2} \int \mathrm{d}^4x\sqrt{-g}\Big\{ - g^{\mu\nu}\partial_\mu\psi\partial_\nu\psi - \xi R\psi^2 + 2U(\psi)\Big\}, \tag{3.4}$$

where $U(\psi)$ is a scalar field potential. We assume

$$U(\psi) = \frac{1}{2}m^2\psi^2 + \frac{1}{4}\lambda\psi^4 \tag{3.5}$$

and that conformal volume $\int d^3x$ over the spatial 3-hypersurface is unity. ξ is the coupling constant of the scalar field to the Ricci scalar

$$R = 6\left(\frac{\ddot{a}}{a} + \frac{\dot{a}^2}{a^2} + \frac{k}{a^2}\right) \tag{3.6}$$

where a dot means the differentiation with respect to the cosmic time t.

The dynamical equation for phantom cosmology in which the phantom field is modelled by the scalar field with an opposite sign of the kinetic term in action can be obtained from the variational principle $\delta(S_g + S_{\mathrm{ph}}) = 0$. After dropping the full derivatives with respect to time we obtain the dynamical equation for phantom cosmology from variation $\delta(S_g + S_{\mathrm{ph}})/\delta g = 0$ as well as the dynamical equation for field from variation $\delta(S_g + S_{\mathrm{ph}})/\delta\psi = 0$

$$\ddot{\psi} + 3H\dot{\psi} - \frac{\mathrm{d}U}{\mathrm{d}\psi} + \xi R\psi = 0. \tag{3.7}$$

It can be shown that for any value of ξ the phantom behaves like some perfect fluid with the effective energy ρ_ψ and the pressure p_ψ in the form which determines the equation of state factor

$$w_\psi = \frac{-\frac{1}{2}\dot{\psi}^2 - U(\psi) + \xi[2H(\psi^2)^{\cdot} + (\psi^2)^{\cdot\cdot}] + \xi\psi^2(2\dot{H} + 3H^2)}{-\frac{1}{2}\dot{\psi}^2 + U(\psi) - 3\xi H[H\psi^2 + (\psi^2)^{\cdot}]} \equiv \frac{p_\psi}{\rho_\psi}. \tag{3.8}$$

In equation (3.8) the second derivative $(\psi^2)^{\cdot\cdot}$ in the expression for the pressure can be eliminated and then we obtain

$$p_\psi = \left(-\frac{1}{2}+2\xi\right)\dot{\psi}^2 - \xi H\left(\psi^2\right)^{\cdot} - 2\xi\left(6\xi-1\right)\dot{H}\psi^2 - 3\xi\left(8\xi-1\right)H^2\psi^2 - U(\psi) + 2\xi\psi\frac{\mathrm{d}U}{\mathrm{d}\psi}. \quad (3.9)$$

Of course such perfect fluid which mimics the phantom field satisfies the conservation equation

$$\dot{\rho}_\psi + 3H(\rho_\psi + p_\psi) = 0. \quad (3.10)$$

We can see that complexity of a dynamical equation should manifest by complexity of w_ψ.

Let us consider the FRW quintessential dynamics with some effective energy density ρ_ψ given in equation (3.8). This dynamics can be reduced to the form like of a particle in a one-dimensional potential [138] and the Hamiltonian of the system is

$$\mathcal{H}(a', a) = \frac{(a')^2}{2} + V(a) \equiv 0, \qquad V(a) = -\rho_\psi a^4 \quad (3.11)$$

where a prime means the differentiation with respect to the conformal time η.

The trajectories of the system lie on the zero energy level for flat and vacuum models. Note that if we additionally postulate the presence of radiation matter for which $\rho_r \propto a^{-4}$ then it is equivalent to consider the Hamiltonian on the level $\mathcal{H} = E = \mathrm{const}$. Of course the division on kinetic and potential parts has only a conventional character and we can always translate the term containing $\dot{\psi}^2$ into a kinetic term.

The dynamics of the model is governed by the equation of motion (3.7), which is equivalent to the conservation condition (3.10) and the acceleration condition

$$\frac{\ddot{a}}{a} = -\rho_\psi(1 + 3w_\psi). \quad (3.12)$$

This equation admits the generalised Friedmann first integral which assumes the following form

$$-\frac{1}{2}\dot{\psi}^2 + U(\psi) - 3\xi H^2\psi^2 - 3\xi H(\psi^2)^{\cdot} = \frac{1}{2}H^2 - \frac{1}{6}\Lambda - \rho_r. \quad (3.13)$$

If we postulate existence of radiation in model then left hand of this equation can be negative.

3.1.1 Conformally coupled phantom fields

For conformally coupled phantom fields we put $\xi = 1/6$ and rescaled the field $\psi \to \phi = \psi a$. Then the energy function takes the following form for a simple mechanical

system with a natural Lagrangian function $\mathcal{L} = \frac{1}{2} g_{\alpha\beta}(q^\alpha)'(q^\beta)' - V(q)$

$$\mathcal{E} = \frac{1}{2}\left((a')^2 + (\phi')^2\right) - \frac{1}{2}m^2\phi^2 a^2 - \frac{\lambda}{4}\phi^4 - \frac{\Lambda}{6}a^4. \tag{3.14}$$

In contrast to the FRW model with conformally coupled scalar field the kinetic energy form is positive definite like for classical mechanical systems. The general Hamiltonian which represents the special case of a two coupled non-harmonic oscillators system is

$$\mathcal{H} = \frac{1}{2}g^{\alpha\beta}p_\alpha p_\beta + V(q) = \frac{1}{2}(p_x^2 + p_y^2) + Ax^2 + By^2 + Cx^4 + Dy^4 + Ex^2y^2, \tag{3.15}$$

where A, B, C, D, and E are constants.

In order to study the integrability of dynamical systems we use Painlevé's approach. Painlevé's analysis gives necessary conditions for the integrability of dynamical systems and it is the most popular integrability detector. The recapitulation of Painlevé's analysis for system (3.15) was done by Lakshmanan and Sahadevan [139]. They found that system (3.15) passes the Painlevé test and is integrable in the following four cases

$$\begin{aligned}
\Lambda &= \lambda & m^2 &= 3\Lambda \\
\Lambda &= \lambda & m^2 &= \Lambda \\
\Lambda &= 8\lambda & m^2 &= 3\Lambda \\
\Lambda &= 16\lambda & m^2 &= 6\Lambda.
\end{aligned}$$

This result is in full agreement with conclusions concerning integrability of the two coupled quartic non-harmonic oscillator systems. Therefore, phantom cosmology can be considered as coupled quartic non-harmonic oscillators. Of course, Painlevé analysis gives necessary conditions for the integrability of dynamical systems. However, there exist whole classes of integrable systems which do not possess the Painlevé property. It means that the Painlevé approach gives over-restrictive conditions for integrability. It is obvious that for $m^2 = 0$ the FRW phantom cosmology is integrable because of the possibility to separate of variables in the potential. Then we have two decoupled quartic non-harmonic oscillators.

The non-integrability of the non-flat FRW model with the scalar field with the potential $V(\phi) \propto \phi^2$ was investigated in an analytical way by Ziglin [140]. For a deeper analysis of integrability in the terms of differential Galois group methods developed by Ziglin and Morales-Ruiz and Ramis see [123].

It would be useful to compare Hamiltonians for the cosmological model with phantom fields and the standard cosmological model with scalar fields. Let us consider that $\Lambda = \lambda = 0$ for simplicity of presentation. Then for both models we have Hamiltonians

$$\mathcal{H}_{\rm ph} = \frac{1}{2}(-p_a^2 - p_\phi^2) + \frac{k}{2}(\phi^2 - a^2) + \frac{1}{2}m^2a^2\phi^2 \tag{3.16}$$

and

$$\mathcal{H}_{\rm FRW} = \frac{1}{2}(-p_a^2 + p_\phi^2) + \frac{k}{2}(\phi^2 - a^2) + \frac{1}{2}m^2a^2\phi^2. \tag{3.17}$$

If we add a radiation component to the energy momentum tensor, whose energy density scales like $\rho_{\rm r} = \rho_{\rm r,0}a^{-4}$ then both systems should be considered on the constant energy level $\mathcal{H} = \mathcal{E} = \rho_{\rm r,0}$ or the constant $\rho_{\rm r,0}$ can be absorbed by the new Hamiltonian $\bar{\mathcal{H}} \equiv \mathcal{H} - \rho_{\rm r,0}$ and $\bar{\mathcal{H}}$ is considered on the zero energy level.

Let us concentrate on the flat models to analyse the similarities to the Yang-Mills systems. While the standard cosmological model is described by the Hamiltonian

$$\mathcal{H}_{\rm FRW} = \frac{1}{2}(-p_a^2 + p_\phi^2) + \frac{1}{2}m^2a^2\phi^2. \tag{3.18}$$

the phantom cosmological model is

$$\mathcal{H}_{\rm ph} = \frac{1}{2}(-p_a^2 - p_\phi^2) + \frac{1}{2}m^2a^2\phi^2 \tag{3.19}$$

The crucial difference between system (3.18) and (3.19) lies in the definiteness of their kinetic energy forms. It is indefinite and has the Lorentzian signature for the standard model, and it is positive definite for the phantom model. As a consequence we obtain that the configuration space for the standard model is $\mathbb{R}^2$ whereas the condition $\rho_{\rm r,0} + \frac{1}{2}m^2\phi^2a^2 > 0$ determines the domain of the configuration space admissible for motion for the phantom model. Note that if $m^2 < 0$ (the model with the spontaneous symmetry breaking) then this domain is bounded by four hyperbolas in every quarter of the (a, ϕ) plane. The same situation can be obtained for the model without the spontaneous symmetry breaking ($m^2 > 0$) and dark radiation ($\rho_{\rm r,0} < 0$).

The flat phantom model with the spontaneous symmetry breaking is well known as the Yang-Mills systems which have been analysed since the pioneering paper by Savvidy [141]. For this system the Lyapunov exponents were found [142] and the Poincaré sections were obtained [143]. The spatially flat universes filled with the Yang-Mills fields exhibit chaotic oscillations of these fields [134, 135, 136].

This system was also investigated by using the Gaussian curvature criterion [144]. Let us apply this criterion to the non-flat phantom model. The potential function takes the following form

$$V(a,\phi) = -k(\phi^2 - a^2) - \frac{1}{2}m^2\phi^2 a^2 \tag{3.20}$$

According to this criterion the periodic and quasi-periodic orbits appear in the domains of the configuration space in which the Gaussian curvature of a diagram of the potential function is positive. The line of zero curvature separates these domains from the instability regions where the curvature is negative. If the total energy of the system E increases the system will be in a region of negative curvature for some initial conditions and the motion is chaotic.

Let us consider the dynamical system in an autonomous form in the form $(x^i)' = f^i(x^j)$ then we linearised around the special solution and we obtain equation

$$(\delta x^i)' = \frac{\partial f^i}{\partial x^k}\delta x^k$$

where $\frac{\partial f^i}{\partial x^k}$ builds the Jacobian and δx^k is the deviation vector connecting the points on two nearby trajectories corresponding the same value of parameter t. In our case $x^1 = a$, $x^2 = a'$, $x^3 = \phi$, $x^4 = \phi'$ then the local instability of nearby trajectories are determined by eigenvalues of the Jacobian matrix, i.e. the effective potential $V(a,\phi)$. The eigenvalues are

$$\mu_{1,2} = \frac{1}{2}\left(-3H \pm \sqrt{9H^2 + 4\gamma}\right) \tag{3.21}$$

$$\gamma = \gamma_{1,2} = \frac{1}{2}\left(-V_{\phi\phi} - V_{aa} \pm \sqrt{(V_{\phi\phi} + V_{aa})^2 - 4(V_{\phi\phi}V_{aa} - V_{\phi a}^2)}\right)$$

Therefore the necessary condition for local instability is that at least one of the eigenvalues is positive [145]. These positive values decide about the local instability of trajectories. Note that the negative sign of the Gaussian curvature of potential $V(a,\phi)$ is the sufficient condition of local instability [144, 146]

$$\mathrm{sgn}K = \mathrm{sgn}(V_{\phi\phi}V_{aa} - V_{\phi a}^2) < 0 \tag{3.22}$$

We can see that test (3.22) of negative curvature adopted in our case gives to $K < 0$. However it is not a sufficient condition for the chaos. It should be pointed out that this criterion has a purely local character in contrast to the Lyapunov exponent. Moreover the compactness of a region admissible for motion is required for chaos existence.

It is worthwhile to mention that the Toda criterion is only the measure of the local instability of nearby trajectories [147]. Therefore the presented analysis of the order-chaos transition should be combined with the Poincaré sections and other deeper indicators of the chaotic behaviour.

3.2 Numerical investigations of chaos in phantom cosmology

To make the numerical analysis we need to distinguish the the model without the spontaneous symmetry breaking ($m^2 > 0$) and the model with the spontaneous symmetry breaking ($m^2 < 0$). In both cases the system is considered on the some energy level.

3.2.1 The positive quadratic potential function

We would like to stress out why we use the nonintegrability criterion instead of standard measure like the Lyapunov exponents or Poincaré sections. The main reason is that in analogy to Castagnino et al.'s work [133] we can find a monotonous function along a trajectory. This excludes the property of the recurrence the trajectories or topological transitivity in the standard Wiggins chaos definition. Then $F(\phi, \dot{\phi})$ (or $F(a, \dot{a})$) is a monotonous function of the time parameter along the trajectories and trajectories escape to infinity for arbitrary initial conditions. In this case it is impossible to construct the Poincarè sections. It is obvious for any curvature and positive values of Λ, λ, and m^2. The phase space as well as the configuration space is unbounded in this case. In contrast to classical chaotic systems there is invariant compact chaotic set for this system. It does not mean the system is non-chaotic as it does not follow the Wiggins definition of chaos. The essence of this phenomenon has different nature. The system is oversensitive with respect to small change of initial conditions like in chaotic scattering processes.

The typical case of the model is a class of models without the spontaneous symmetry breaking

$$\text{class A:} \qquad A = B = C = D = 0, \quad E = -1 \ (\text{or } m^2 > 0).$$

In this case the domain admissible for motion is unbounded. For the classical mechanical systems with chaos there are chaotic sets of trajectories on a compact invariant submanifold. However it does not mean that the system with an unbounded region admissible for motion is nonchaotic because the essence of chaotic behaviour is of different nature. The system can

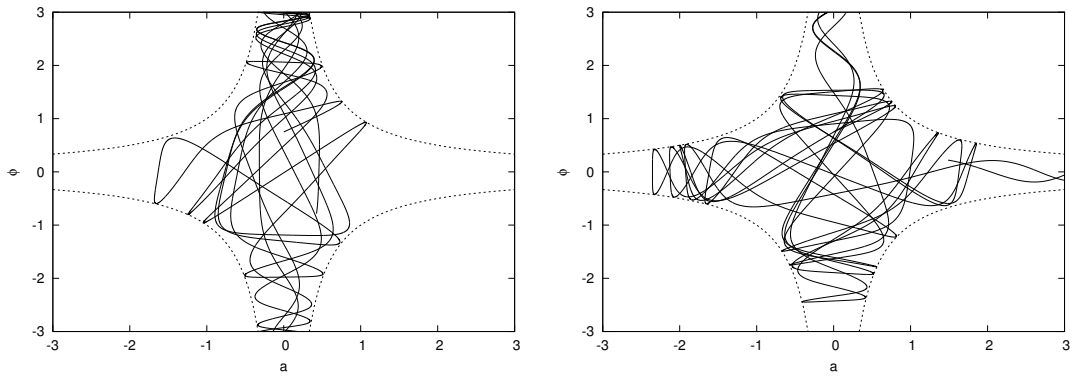

Figure 3.1: Two samples of trajectories for model class I. Initial conditions $a_0 = 0$, $\phi_0' = 0.779$, $\phi_0 = 0.75$ (left) and $\phi_0 = 0.751$ (right), $a_0' > 0$ calculated from the Hamiltonian constraint.

be oversensitive with respect to small changes of initial conditions—the key ingredient of chaos. In this respect the system is similar to chaotic scattering processes [148]. Therefore it seems to be natural to use the methods of investigation of scattering processes.

The class A model does not possess the property of sensitive dependence on initial conditions. Moreover, there are no fractal structures of basin boundaries in the phase space. Because the scattering of trajectories in the potential well is present, we deal with the nonchaotic scattering process. In more details it will be discussed in Sec. 3.3.

The different chaotic behaviour was found in the Einstein-Yang-Mills (EYM) colour field in the flat Bianchi I spacetime [134]. The authors considered the model with radiation and isotropic curvature in contrast to the Mixmaster models. It was showed that the EYM systems are also an example of chaotic scattering. Because the Lyapunov exponents are coordinate dependent they cannot be used for invariant characterisation of chaos. For this aim the methods of chaotic scattering are more suitable. They are extremely useful in this context because of noncompact phase space (also the configuration space)—the major obstacle of the standard analysis of chaos. Let us note that the case of their model with flat spacetime is analogous to our second case with the cosmological constant.

3.2.2 The negative quadratic potential function

The idea of the description of a dark energy field in terms of a Higgs field which creates inertial mass through the spontaneous symmetry breaking has been investigated

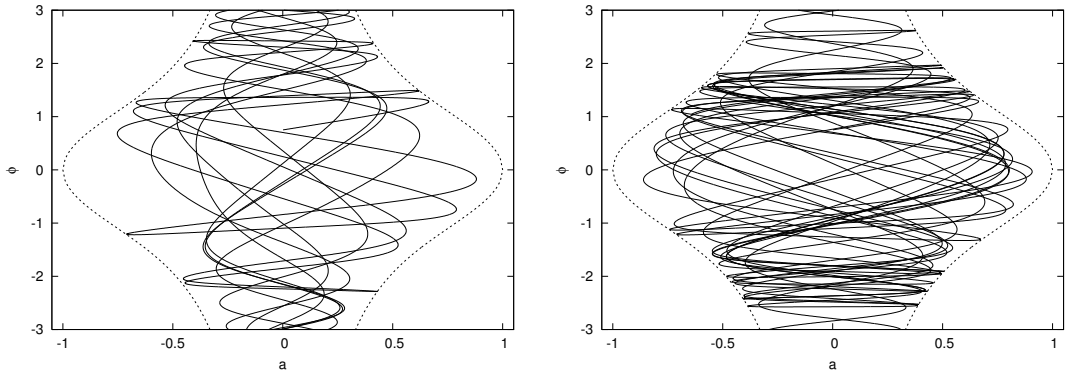

Figure 3.2: Two samples of trajectories for model class II. Initial conditions $a_0 = 0$, $\phi_0' = 0.779$, $\phi_0 = 0.75$ (left) and $\phi_0 = 0.751$ (right), $a_0' > 0$ calculated from the Hamiltonian constraint.

lately [149]. For $m^2 < 0$ we can distinguish two subclasses of the model with the spontaneous symmetry breaking for which chaotic behaviour can be detected

$$\begin{aligned} &\text{class I:} && A = B = C = D = 0, \quad E > 0 \text{ (or } m^2 < 0), \\ &\text{class II:} && A = B = D = 0, \quad C > 0 \text{ (or } \Lambda < 0), \quad E > 0 \text{ (or } m^2 < 0). \end{aligned}$$

These are flat models with conformally coupled phantom fields for which trajectories have the property of topological transitivity in contrast to the case $m^2 > 0$. In figure 3.1 and 3.2 we present sample trajectories for both models and evolution of every trajectory lasts for the same interval of time. From this simple picture we can initially conclude that the systems are sensitive on initial conditions.

The first class of models is isomorphic with the well known Yang-Mills systems with the potential function $V \propto x^2y^2$. Because the domain admissible for motion is bounded and its boundary has negative curvature, the property of recurrence of trajectories is present. We consider both classes of systems on some distinguished energy level $\mathcal{H} = \mathcal{E} \propto \rho_{\mathrm{r},0} > 0$. The Poincaré sections for both classes are represented in figures 3.3, 3.4, 3.5. The Poincarè section for the flat cosmological model with vanishing Λ, λ, and $m^2 < 0$ (class I) is shown in the figure 3.3. If we postulate additionally the existence of radiation matter in the model than we deal with the system on the constant non-zero energy level. In this case we obtain some chaotic distribution of points on the Poincarè section (a, ϕ'). Figures 3.4 and 3.5 present the flat cosmological model with the negative cosmological constant Λ and $m^2 < 0$

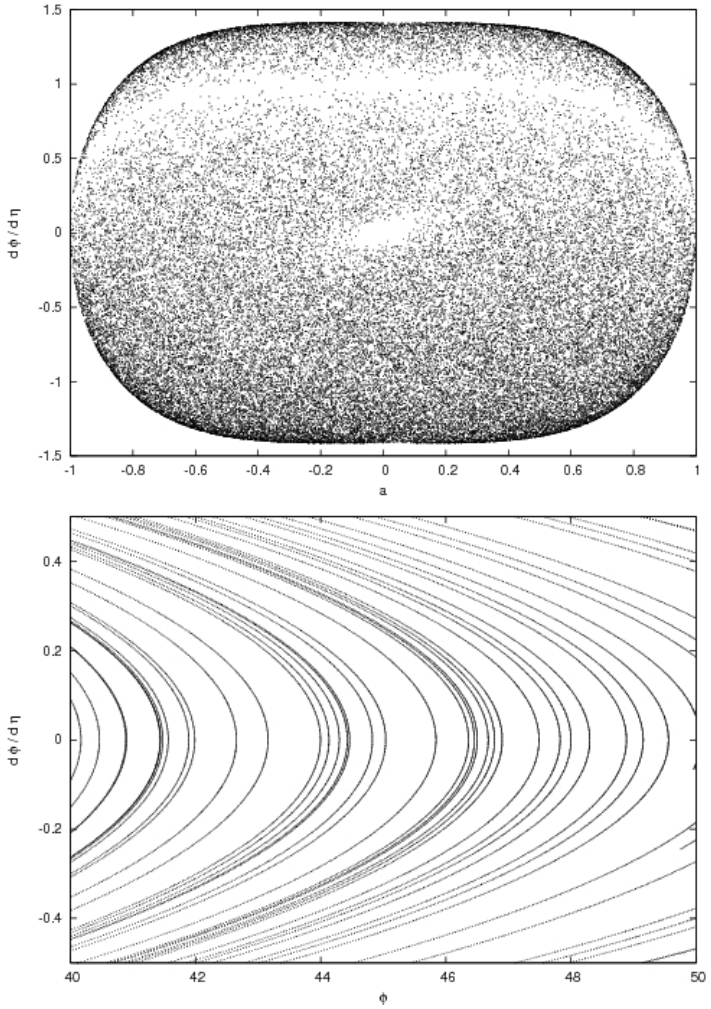

Figure 3.3: The Poincaré section for the model class I, $a = \phi$ and $a' > 0$ (upper); $a = 0$, $a' > 0$ (bottom). Motion in narrow field between two hyperbolas is completely regular. Complexity of behaviour comes from motion near the origin of the configuration space.

(class II) on the plane (a, a'). In this case we can observe islands of stability. However, the trajectories wander to the non-physical region of $a < 0$. This allows many cycles to be considered if we continue the scale factor into negative values. But what it means physically is not clear.

All these figures illustrate what we proved earlier, namely the standard chaos with recurrence of orbits and the property of sensitive dependence on initial conditions.

We cannot perform the analogous analysis for the class of models with $m^2 > 0$

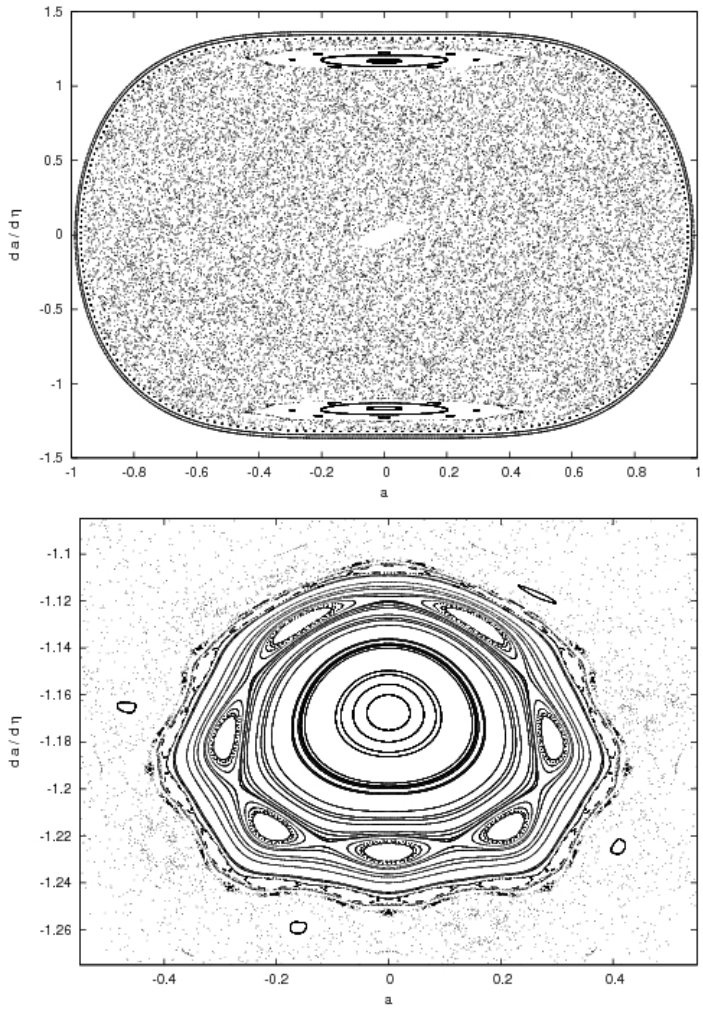

Figure 3.4: The Poincaré section for the model class II, $\phi = 0$ and $\phi' > 0$. The empty region at the upper section comes from motion of a particle-universe along the ϕ ($a = 0$) axis.

because there is no chaos in Wiggins' standard sense. However they possess the property of complex behaviour of trajectories similar to the non-chaotic scattering process. Note that the evidence of chaos in terms of fractal basins, Cantori or stochastic layers requires the recurrence of trajectories. Similarly the Poincaré sections can be constructed from many cycles for a useful picture to emerge [111].

In the case of $m^2 < 0$, trajectories of the system return to the neighbourhood of the origin time after time and we have the multiple scattering process on the potential walls (boundaries of the domain admissible for motion). We can control and count how many

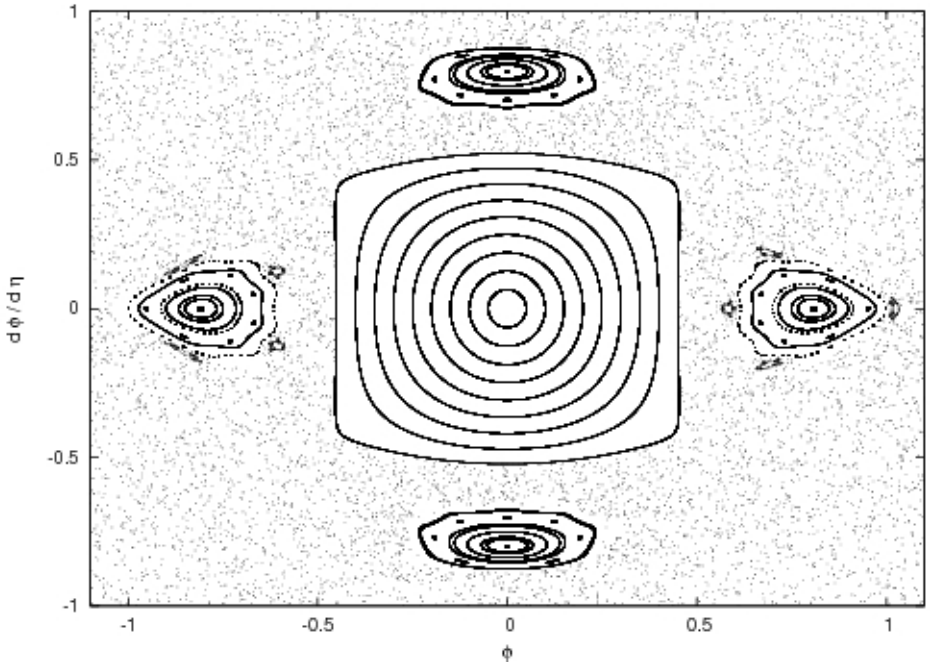

Figure 3.5: The Poincaré section for the model class II, $a = 0$ and $a' > 0$.

times the trajectory gets closer to the origin than some fixed distance from the origin. With increasing this fix distance the number of controlled scattering events increases and a more complicated fractal structure arises. Figures 3.6, 3.7 and 3.8 illustrate fractal structures of the phase space of initial conditions for trajectories reaching some values a_f and ϕ_f at some moment of time evolution. The fractal dimension calculated by counting cells which contain light and dark areas (i.e. leading to two types of the final outcome) is $a_f = \phi_f = 2$ — $D_0 = 1.676$; $a_f = \phi_f = 3$ — $D_0 = 1.888$; $a_f = \phi_f = 4$ — $D_0 = 1.953$; $a_f = \phi_f = 5$ — $D_0 = 1.971$. The chosen method of counting cell enables us to order fractals with respect to the increasing complexity, i.e. for a nearly regular system the fractal dimension is close to one, in turn for a completely chaotic system is approaching two. One can also observe that the longer the trajectories spend in the neighbourhood of the origin of the coordinate system the more complex behaviour gets, because the motion between branches of hyperbolas is regular (see figure 3.3).

Figures 3.9, 3.10, 3.11 and 3.12 present the fractal structure of phase space of initial conditions for the category II model. At small enough values of ϕ_f the system is

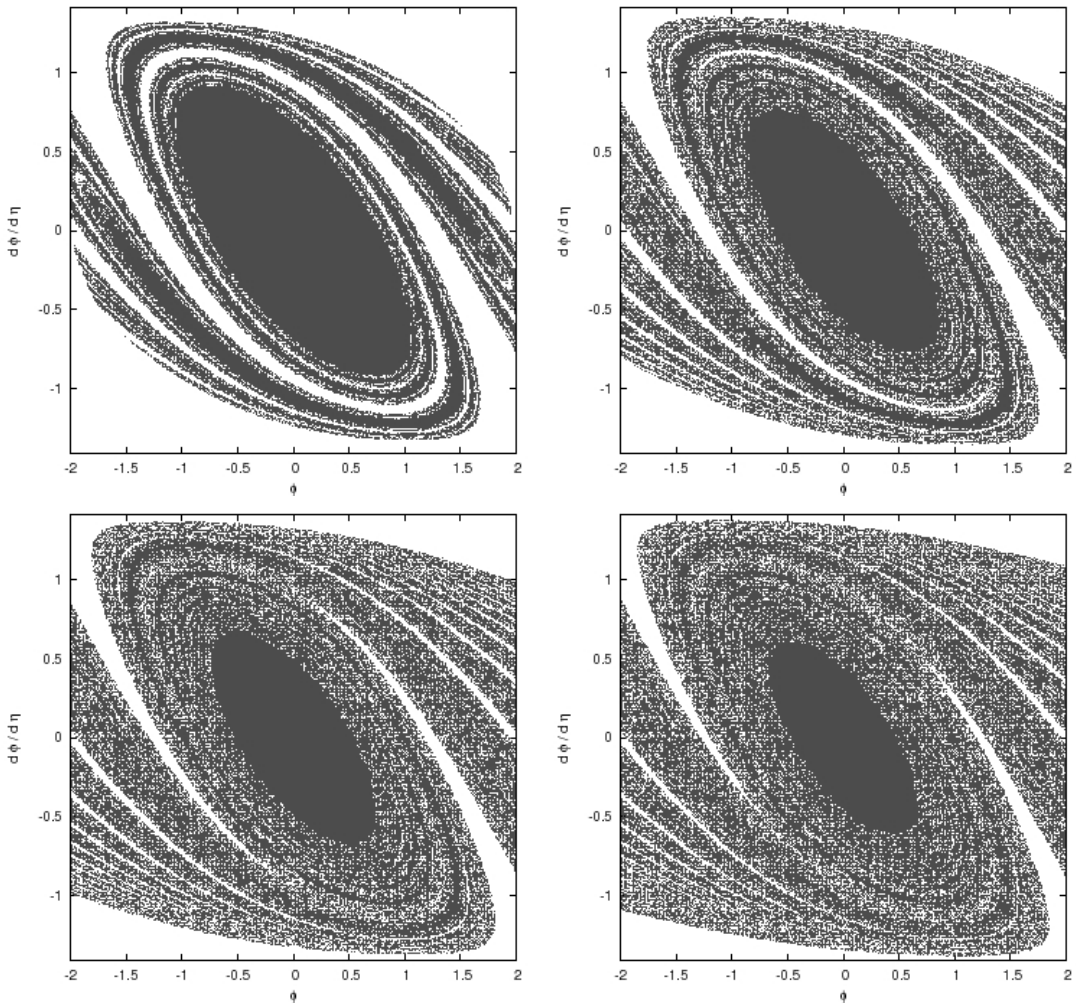

Figure 3.6: The fractal structure of the phase space of initial conditions of trajectories chosen at $a = 0$ and $a' > 0$ for class I and landing at $|a_f| = 2$, 3, 4, 5 (grey) or at $|\phi_f| = 2$, 3, 4, 5 (white), respectively. Complexity of the fractal structure increases with the final state of the trajectories which means that trajectories spend more time in the region near the point $(0, 0)$ in the configuration space. The solid areas in the center of figures come from the motion along the ϕ-axis.

regular and no chaotic behaviour is present (figure 3.9). With an increasing value of ϕ_f: $\phi_f = 2$ — $D_0 = 1.812$; $\phi_f = 3$ — $D_0 = 1.967$, we observe the transition to chaos which causes the fractal structure of the space of initial conditions to emerge (figures 3.10–3.12).

In figure 3.13 we plot the phase space of initial conditions chosen at $a = 0$ and $a' > 0$ calculated from the Hamiltonian which lead to a given property in one cycle of

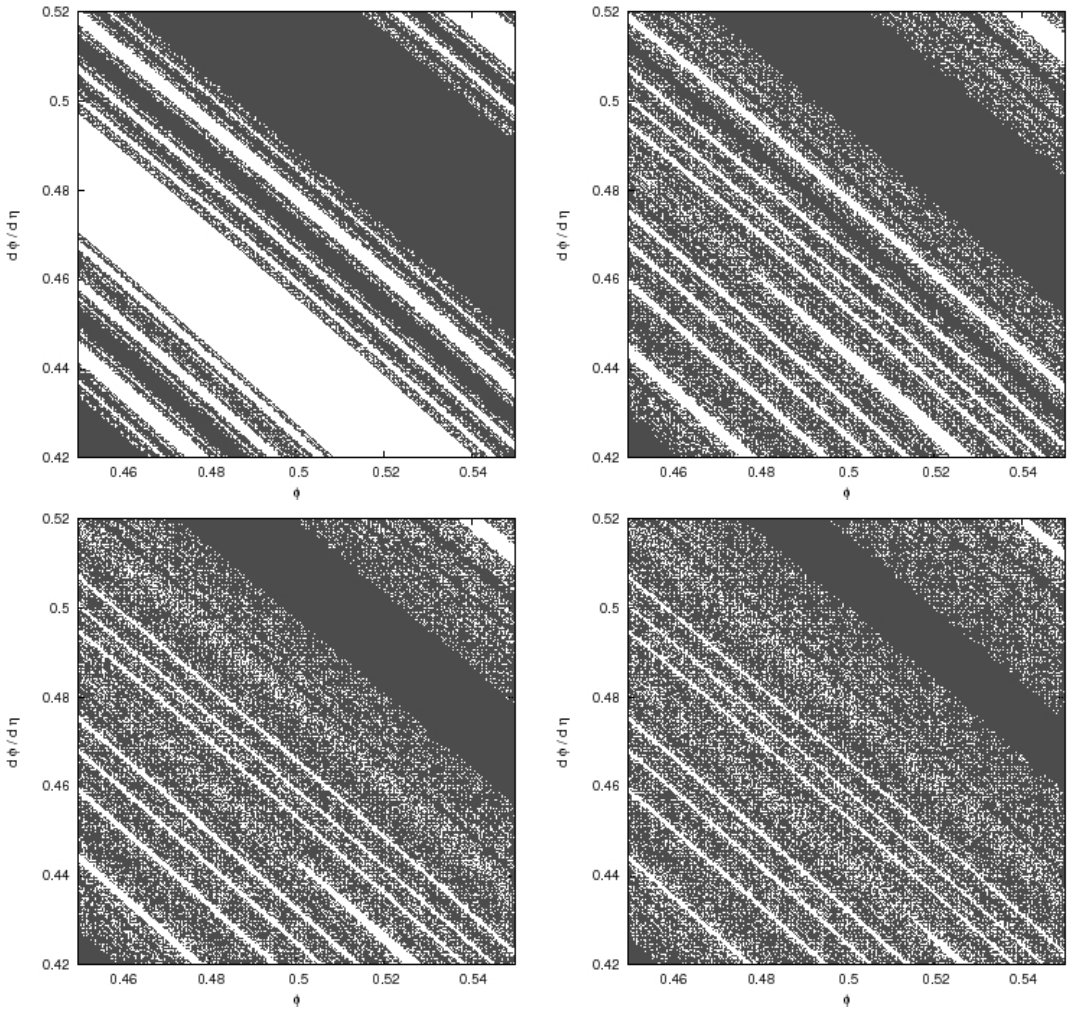

Figure 3.7: Magnification of the fractal structure of the phase space of initial conditions from figure 3.6.

evolution, i.e. to maximal expansion with a positive value of ϕ (grey) or negative value of ϕ (white) – left image, and back to a final singularity again with a positive value of ϕ (grey) or a negative value of ϕ (white) – right image. Therefore if we consider evolution in a physical domain between initial and final singularities this system cannot be chaotic. If we prolong its evolution to the non-physical domain $a < 0$ then we obtain chaos. Note that non-integrability indicators measure the true intrinsic complexity of the system in both cases [123].

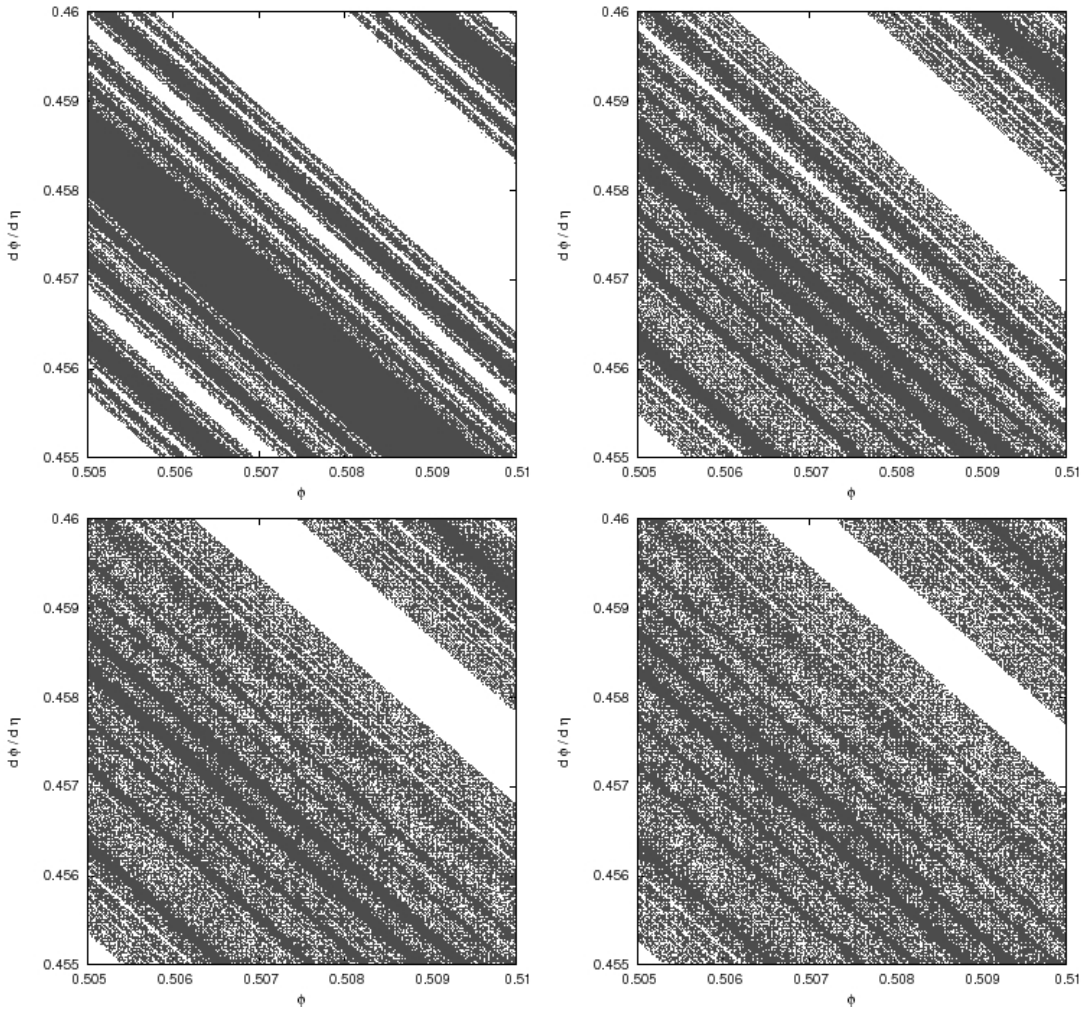

Figure 3.8: Magnification of the fractal structure of the phase space of initial conditions from figure 3.7.

3.3 Phantom cosmology as a scattering process

In this section we investigate behaviour of a model without the spontaneous symmetry breaking. This is a model with $A = B = C = D = 0$ and $E = -1$ ($m^2 = 2$) on different energy levels $\mathcal{E} > 0$, $\mathcal{E} = 0$ and $\mathcal{E} < 0$.

In the analysis of this case we explore analogy to the classical system in which appears the chaotic scattering. From the equation of motion we obtain that for any initial condition trajectories escape to infinity ($\phi \to \pm\infty$ $a \to \pm\infty$ as time goes to infinity). For energy $\mathcal{E} > 0$ the configuration space is unbounded and trajectories pass from one quadrant

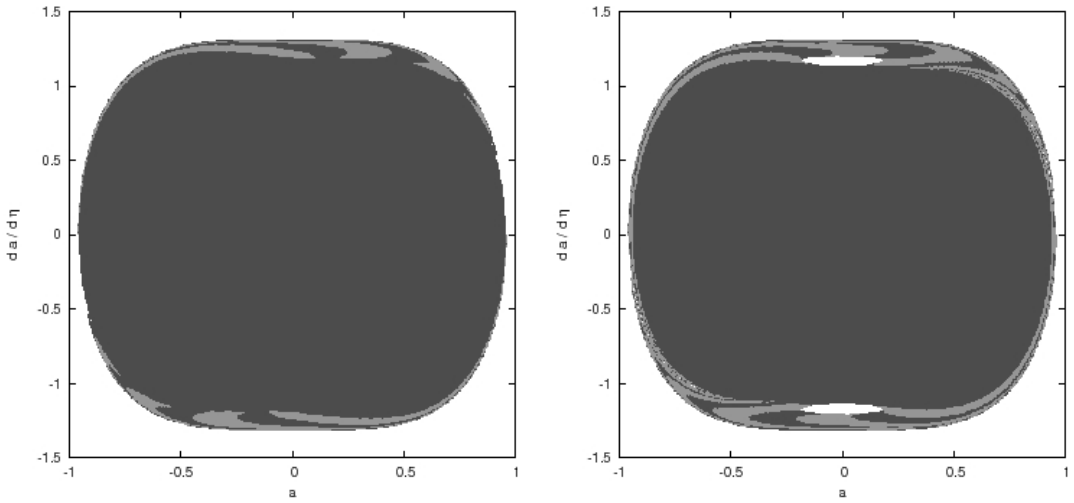

Figure 3.9: The structure of phase space of initial conditions for class II trajectories chosen at $\phi = 0$ and $\phi' > 0$ and landing at $\phi = 0.75$ (dark grey) and $\phi = -0.75$ (grey) presented in left figure and $\phi = 0.9$ (dark grey) and $\phi = -0.9$ (grey) in right figure. The white poles correspond to the centres of stability in figure 3.4.

to another. On the other hand for $\mathcal{E} \leq 0$ motion is restricted to only this quadrant of the configuration space where the initial conditions are.

In figure 3.14 we present the analysis of dependence of scattering on the energy level. For this aim the initial condition in the configuration space are chosen on the line $\phi = -a + 10$ with $a' = \phi' < 0$ under the conservation of the Hamiltonian constraint. For $\mathcal{E} \leq 0$ trajectories go toward the origin of coordinate system and after some time escape to infinity passing through a line $\phi = -a + 10$. On the x-axis we mark the initial value of a and y-axis we mark final distance from the symmetry point with coordinates $(5, 5)$ at the moment of intersection of line of initial conditions. In this figure there is no discontinuities, we do not also observe the fluctuation of distance d_f. It enable us to conclude that we deal with the scattering process although the domain of interaction is not finite [150]. So there is no chaotic scattering. The motion of the system is regular and there is no sensitivity of motion with respect to initial conditions.

For a deeper confirmation of this statement we study numerically a larger number of initial conditions (figure 3.15). In the configuration space the initial conditions are chosen as previously, i.e. $\phi = -a + 10$ and the initial conditions for velocities are parameterised in a natural way by an angle α, i.e. $a' = -V(a, \phi, \mathcal{E}) \cos\alpha$, $\phi' = -V(a, \phi, \mathcal{E}) \sin\alpha$ where

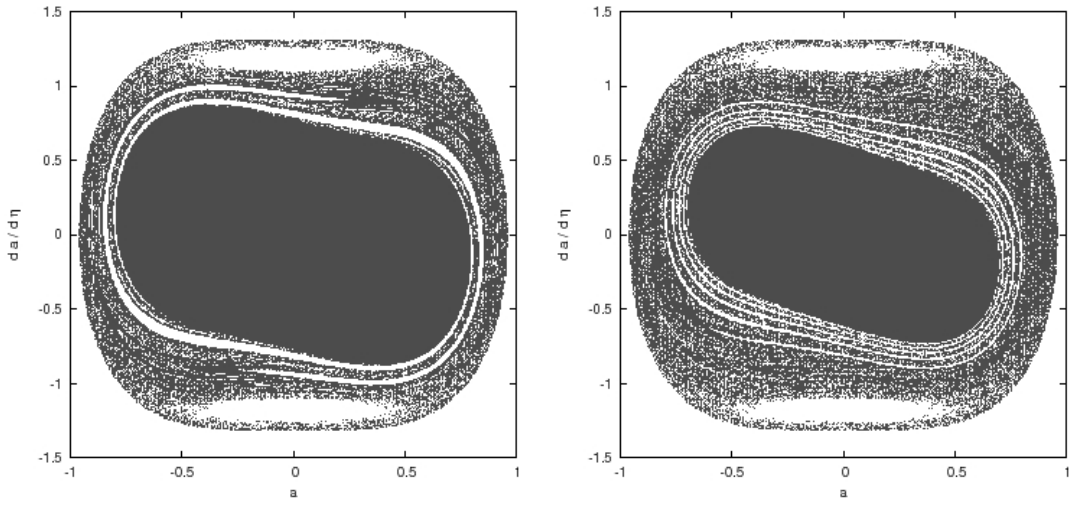

Figure 3.10: The fractal structure of phase space of initial conditions of trajectories class II landing at $\phi = 2$ (left) and $\phi = 3$ (right). Initial conditions leading to negative values of ϕ omitted for clarity.

$V(a, \phi, \mathcal{E}) = \sqrt{\mathcal{E} + m^2 a^2 \phi^2}$. In figure 3.15 (a) and (b) it is presented results of our analysis for $\mathcal{E} < 0$ and $\mathcal{E} = 0$ respectively. The grey area corresponds to initial conditions for which trajectories' pass through line $\phi = -a + 10$ with $\phi > a$. Figure 3.15 (c) illustrates domains of initial conditions for $\mathcal{E} > 0$ for which trajectories outcomes reach different quadrants : I quadrant – dark grey, II quadrant – grey, III quadrant – black, IV quadrant — medium grey. The black line presents initial conditions taken from figure 3.14. We cannot observe chaotic scattering in this case.

3.4 Acceleration in Phantom Cosmology

The current Universe is in an accelerating phase of expansion that's why we check whether the scalar fields in the FRW cosmology can explain this phenomenon. For this aim let's are consider acceleration equation which can be obtained from the Raychaudhuri equation

$$\frac{\ddot{a}}{a} = -(\rho + 3p) = -(-2\dot{\psi}^2 - 2U(\psi) + 3\xi H(\psi^2)\dot{} + 3\xi(\psi^2)\ddot{} + 6\xi\dot{H}\psi^2 + 6\xi H^2\psi^2) - 2\rho_r \quad (3.23)$$

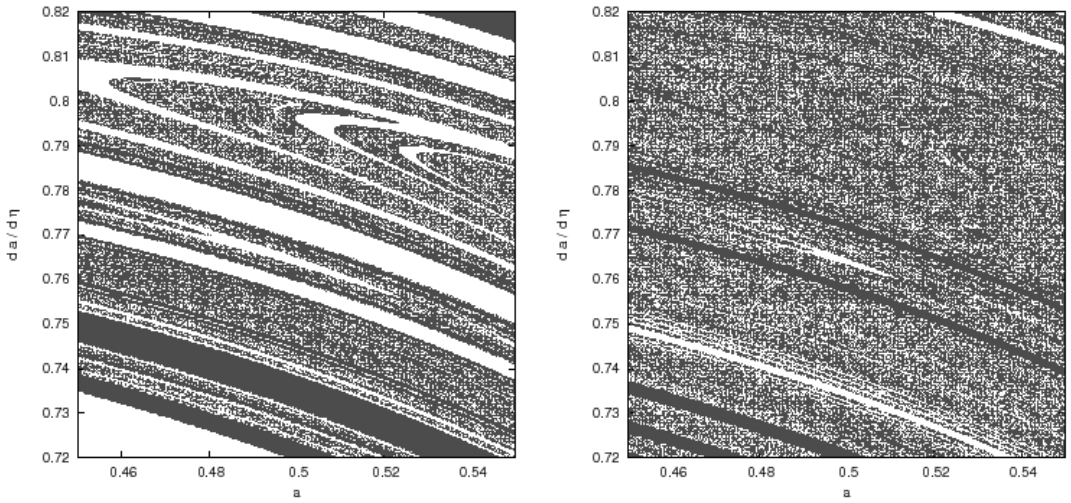

Figure 3.11: Magnification of the fractal structure of the phase space of initial conditions of trajectories class II from figure 3.10.

In the special case of the phantom field minimally coupled to gravity $\xi = 0$ and without radiation $\rho_r = 0$ we have

$$\frac{\ddot{a}}{a} = 2(\dot{\psi}^2 + U(\psi)). \tag{3.24}$$

Next, for zero energy level and $\Lambda = 0$ from (3.13) we have that

$$H^2 = 2\rho_\psi = -\dot{\psi}^2 + 2U(\psi). \tag{3.25}$$

and finally we receive the acceleration equation which is independent of the form of the potential function

$$\frac{\ddot{a}}{a} = 3\dot{\psi}^2 + H^2 \geq 0. \tag{3.26}$$

In the case of conformally coupled phantom field $\xi = 1/6$ we have

$$\frac{\ddot{a}}{a} = -(-\dot{\psi}^2 - 2U(\psi) - H^2\psi^2 - H(\psi^2)^{\cdot} + \psi\frac{\mathrm{d}U}{\mathrm{d}\psi}(\psi)) - 2\rho_r \tag{3.27}$$

and after the rescaling time and field variables: $\mathrm{d}t = a\mathrm{d}\eta$, $\phi = a\psi$ and inserting the potential function (3.5) we have

$$\frac{\ddot{a}}{a} = \frac{1}{a^4}(\phi'^2 - \frac{1}{2}\lambda\phi^4 - 2\rho_{r,0}), \tag{3.28}$$

where prime denotes differentiation with respect to the conformal time and dot with respect to the cosmological time. We can also express equation of state parameter (3.8) in these

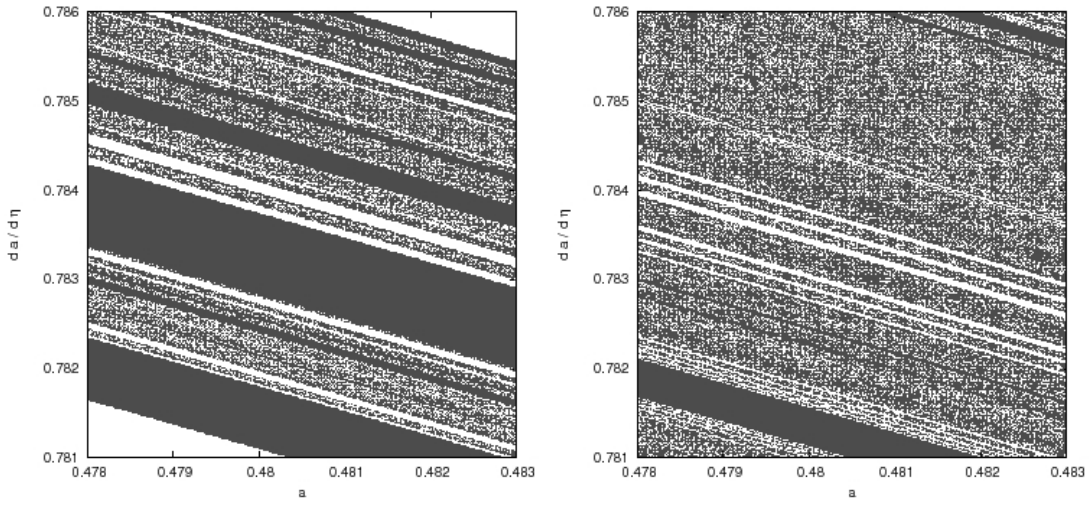

Figure 3.12: Magnification of the fractal structure of the phase space of initial conditions of trajectories class II from figure 3.11.

new variables

$$w_\phi \equiv \frac{p_\phi}{\rho_\phi} = \frac{\frac{1}{a^4}(-\frac{1}{6}\phi'^2 - \frac{1}{6}m^2a^2\phi^2 + \frac{1}{12}\lambda\phi^4)}{\frac{1}{a^4}(-\frac{1}{2}\phi'^2 + \frac{1}{2}m^2a^2\phi^2 + \frac{1}{4}\lambda\phi^4)}. \tag{3.29}$$

We clearly see that this is a good expression only if $a \neq 0$. For the physical region $a > 0$ we can express the effective equation of state parameter as

$$w_{\text{eff}} \equiv \frac{-\frac{1}{6}\phi'^2 - \frac{1}{6}m^2a^2\phi^2 + \frac{1}{3}\rho_{r,0}}{-\frac{1}{2}\phi'^2 + \frac{1}{2}m^2a^2\phi^2 + \rho_{r,0}} \tag{3.30}$$

In figure 3.16 we show the evolution of acceleration and evolution of coefficient of the equation of state w_ϕ for model class I (flat model with $m^2 < 0$) with respect to the conformal time η which is monotonous function of the cosmological time in the physical domain. Note that in the case of $m^2 < 0$ the universe is decelerating and w_ϕ stays in the interval $\langle -1/3; 1/3\rangle$, with $w_\phi = -1/3$ when $\phi' = 0$ and $w_\phi = 1/3$ when $\phi = 0$.

The analogous analysis made for the model class A without the spontaneous symmetry breaking (presented in figure 3.17) shows that the universe is always accelerating. In this case pressure p_ϕ is always negative. In the case of $\mathcal{E} > 0$ we can have positive value of w_ϕ and this means that density can be negative. Moreover, during evolution there are crossings of the line $w_\phi = -1$ and then w_{eff} goes to minus one. The amplitude of these oscillations depends on $\rho_{\text{r},0}$.

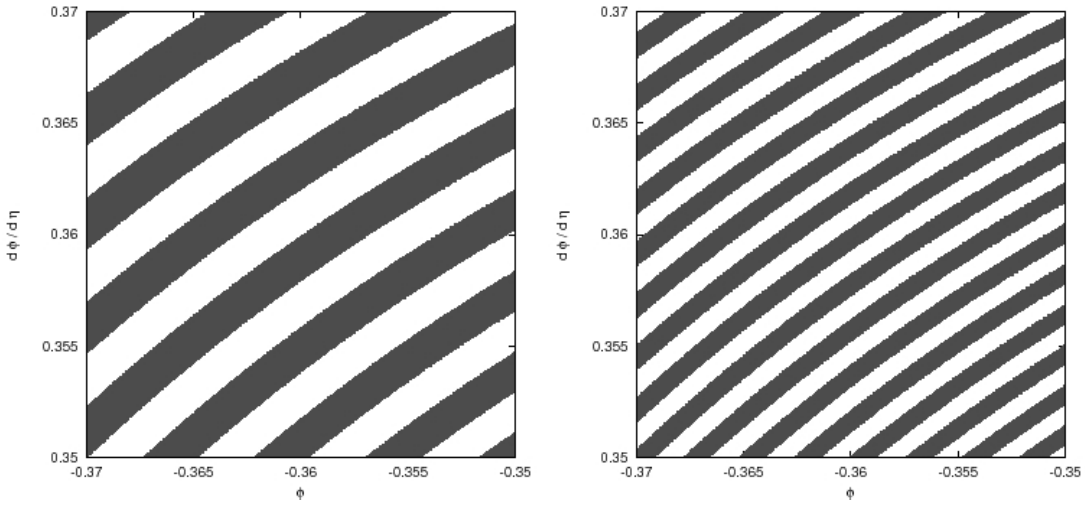

Figure 3.13: The structure of phase space of initial conditions for model class I chosen at $a = 0$ with $a' > 0$ for trajectories leading to $a' = 0$ (or equivalent $H = 0$) with $\phi > 0$ (grey) and $\phi < 0$ (white) – the left image, and initial conditions of trajectories leading to $a = 0$ with $\phi > 0$ (grey) and $\phi < 0$ (white) – the right image. There is no chaos in one cycle of evolution.

3.5 Conclusions

In cosmology the Mixmaster models are well known for their chaotic behaviour [111]. In these models chaos is caused by anisotropy of space. In this chapter we considered the phantom cosmological models which are homogeneous and isotropic where the chaos is the consequence of the nonlinearity of the potential function for the scalar field. We found chaos is a generic feature of the phantom cosmology with the spontaneous symmetry breaking. It assumes the form of the multiple chaotic scattering process. In the case of the absence of symmetry breaking we did not find the sensitivity over initial conditions and the system behaves as the standard scattering process.

There is no difference between the flat universes filled with minimal and conformally coupled scalar fields. As it was demonstrated by Faraoni et al. [151, 126] there is no chaos for the former class of models because the solution corresponding $k = 0$ are restricted to move in some two-dimensional submanifold of the phase space $(H, \phi, \dot{\phi})$. There are no enough room for chaotic motion manifestation. The analogous result is valid for the other value of the coupling constant ξ. Note that we can observe chaotic behaviour in some cases of the conformally coupled scalar field in the flat universes, when we consider the system on

non-zero energy level. Physically it means that the universe is filled with radiation matter.

The reason for which the flat universes with scalar field are non-chaotic lies in lack of invariant measure of chaotic behaviour in the general relativity [97, 106]. In general the standard chaos indicators like Lyapunov exponents or Kolmogorov-Sinai entropy depends on time parameterisation. In general relativity there is freedom of choice of the lapse function which defines reparameterization of time. The Hamiltonian is given modulo the lapse function. Therefore if we consider the Hamiltonian FRW system with scalar field on zero energy level it is possible that in the Hamiltonian constraint a i $\dot{a}$ appear only in the combination $H = \dot{a}/a$. Hence the motion of the system takes place in the 3-dimensional phase space $h(H, \phi, \dot{\phi}) = 0$ on some 2-dimensional submanifold. For any value of coupling constant and general class of potentials there is no place for chaos (even the models with the cosmological constant).

The new picture appears if the system is described on a non-zero energy level. Then the motion of the system is in the 3-dimensional submanifold of the 4-dimensional phase space. But in general case there is no possibility of choosing the lapse function in such a way that a i $\dot{a}$ contribute in the Hamiltonian constraint by the Hubble function.

Among the conformally coupled models there are in principal two types of behaviour. First, chaotic scattering process takes place for case $m^2 < 0$ (the spontaneous symmetry breaking). In this case trajectories possess the property of topological transitivity which guarantees their recurrence in the phase space and the scattering process takes place around the origin. It is similar to the chaos that appears in the Yang-Mills theory. Exploring this analogy to this system we calculate the Gaussian curvature of the potential function which measure local instability of nearby trajectories. We prove that this curvature is negative. Because the configuration space is bounded in this case the mixing of trajectories is observed.

Second, in the opposite case of $m^2 > 0$ we characterise dynamics in the system in terms of symbolic dynamics. No fractal structure in the space of initial conditions was found and conclude that the scattering process has not the chaotic character.

We also found that the universe filled with conformally coupled scalar field is accelerating without the positive cosmological constant. In principle, there are two sources of this acceleration. The acceleration is driven by negative energy density and coefficient of equation of state w_ϕ is greater than $-1/3$. Alternatively, energy density is positive and the coefficient of equation of state can be smaller than $-1/3$. The latter there is crossing

of $w_\phi = -1$. Of course, for the explanation of SNIa data apart from the acceleration of the Universe itself, the rate of acceleration is also crucial.

The system with phantom scalar field coupled conformally to gravity in the FRW universe can be treated as scattering process with chaotic and nonchaotic character. The generic feature of this class of systems with the spontaneous symmetry breaking is the chaotic scattering of trajectories.

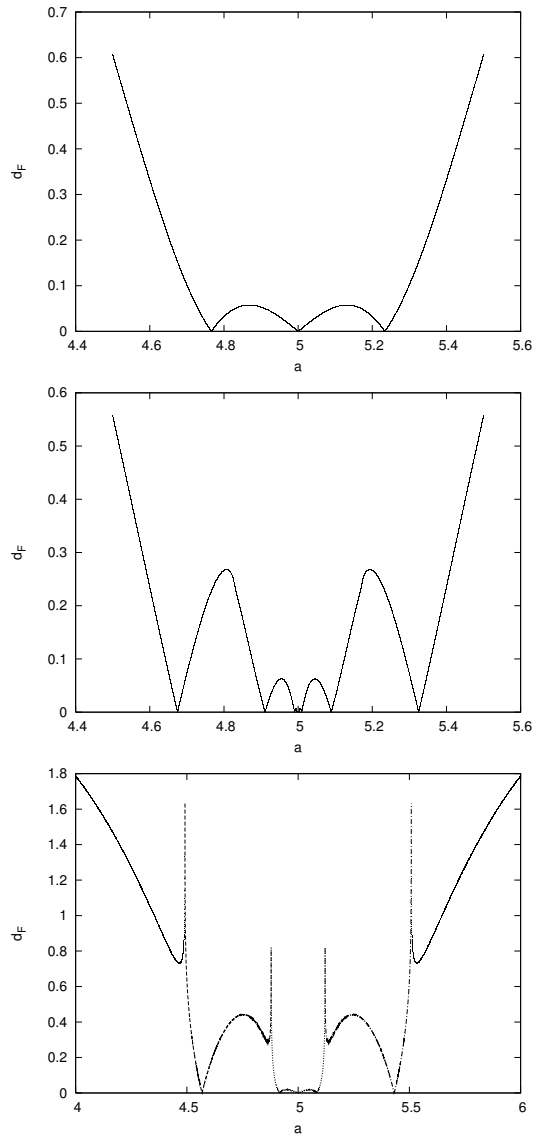

Figure 3.14: The scattering process in the class A model without the spontaneously symmetry breaking. For all trajectories initial conditions were chosen at line $\phi = -a + 10$ in configuration space and $\dot{a} = \dot{\phi} < 0$ calculated from the Hamiltonian. On the x-axis we put initial position a and on the y-axis we put a final distance from a symmetry point in the configuration space $(5, 5)$ when a trajectory is escaping to infinity. For $\mathcal{E} < 0$ (a) and $\mathcal{E} = 0$ (b) all the trajectories escape to infinity ($a \to \infty, \phi \to \infty$) without crossing $a = 0$ or $\phi = 0$. For $\mathcal{E} > 0$ (c) some trajectories change a quarter after starting from I quarter: I – solid line, II – dashed line, III – dotted line and IV – dash-dot line.

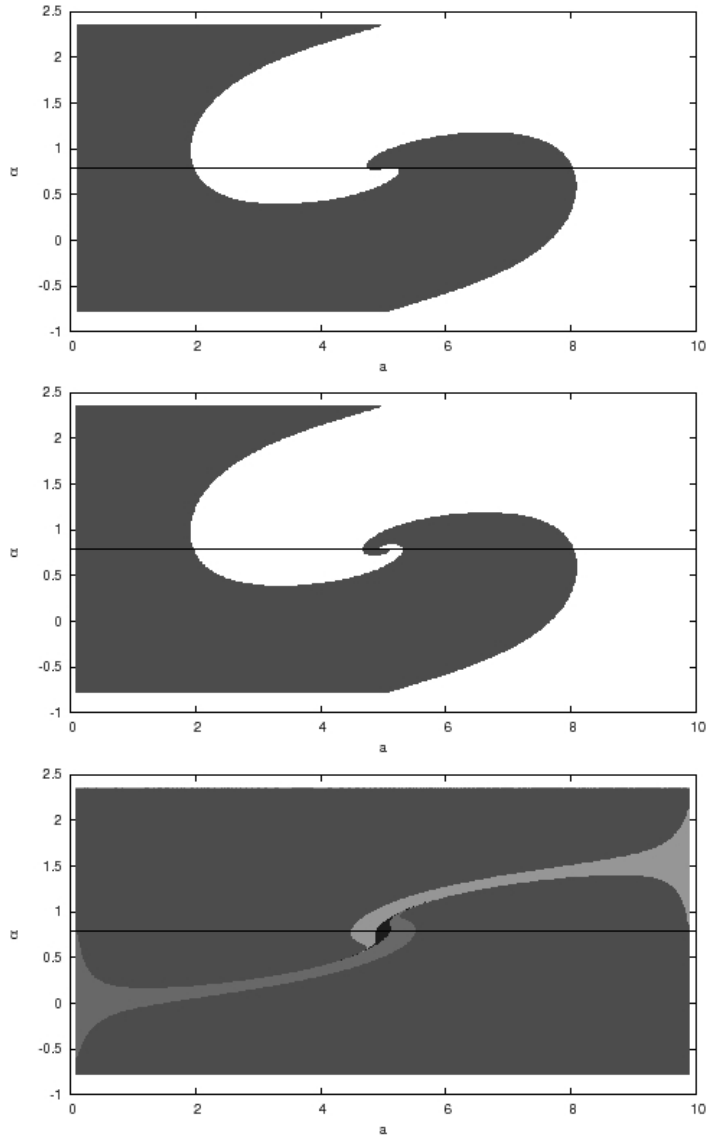

Figure 3.15: The scattering process in the class A model without the spontaneously symmetry breaking for a large number of trajectories. (See text for description). Figures (a) and (b) correspond to $\mathcal{E} < 0$ and $\mathcal{E} = 0$, respectively. The grey areas correspond to initial conditions for which trajectories pass through the line $\phi = -a + 10$ with $\phi > a$. Figure (c) corresponds $\mathcal{E} > 0$ (the configuration space is unbounded) and illustrates domains of initial conditions for which trajectories outcomes reach different quadrants: I quadrant – dark grey, II quadrant – grey, III quadrant – black, IV quadrant — medium grey. The black lines represent initial conditions from figure 3.14.

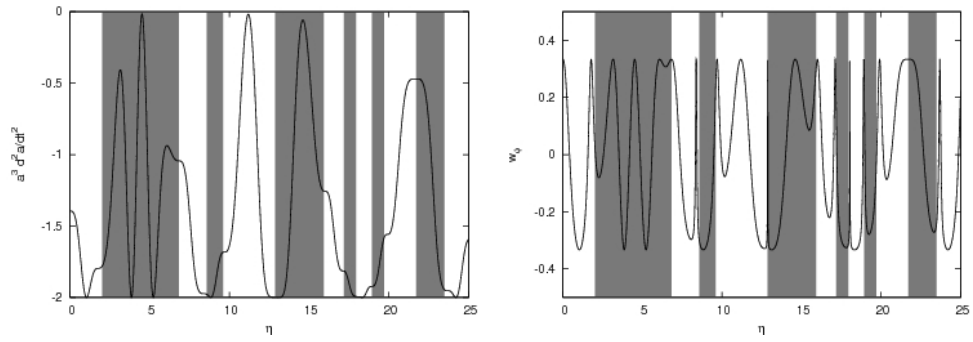

Figure 3.16: The evolution of acceleration from Eq. (3.28) with $\lambda = 0$ (left panel) and equation of state parameter w_ϕ from Eq. (3.29) (right panel) for model class I with respect to conformal time for short period of time for trajectory from left panel of figure 3.1. Shaded area denote unphysical regions of scale factor $a \leq 0$. In physical regions acceleration is always negative $\ddot{a} \leq 0$ model decelerates and equation of state parameter never crosses $w_\phi = -1$ barrier.

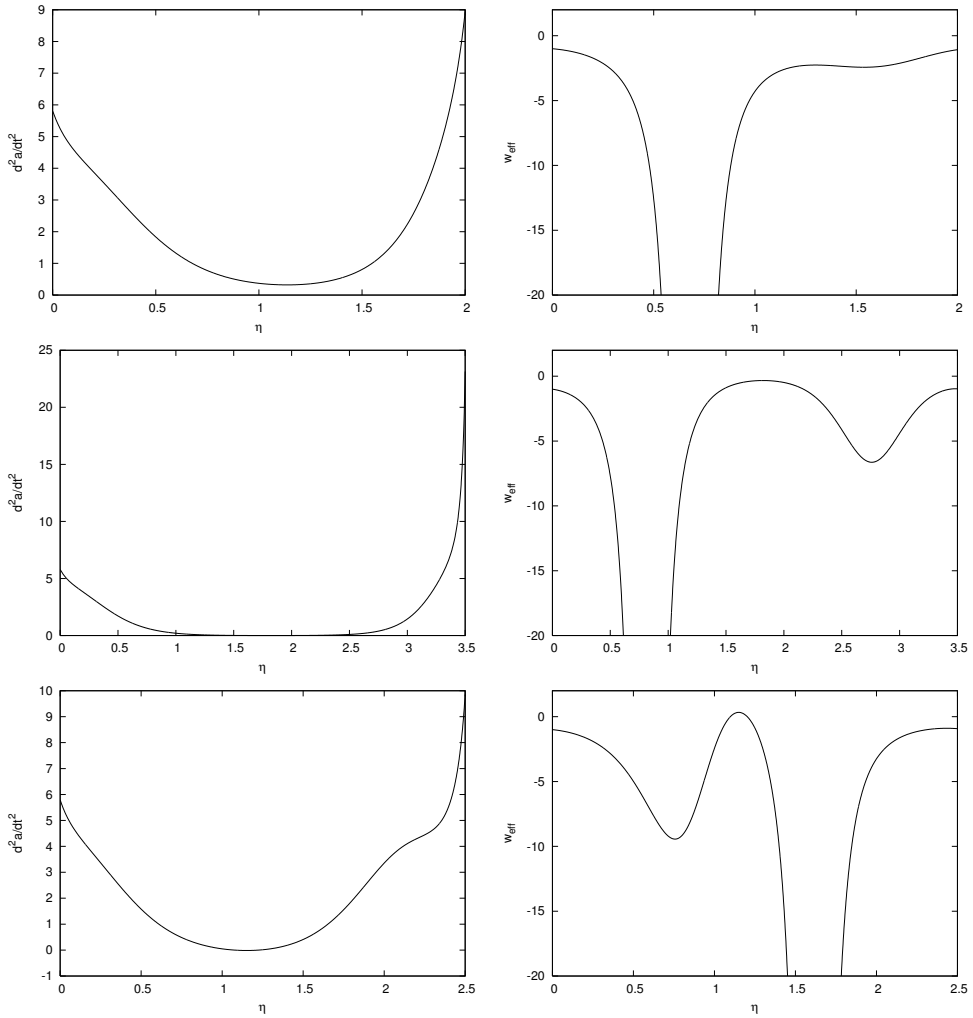

Figure 3.17: The evolution of acceleration from Eq. (3.28) (left panel) and the equation of the state parameter w_{eff} from Eq. (3.30) (right panel) for model class A without spontaneous symmetry breaking for a sample trajectory starting from the same initial conditions in the configuration space ($a_0 = 4.75$, $\phi_0 = -a_0 + 10$ and $a_0' = \phi_0' < 0$ calculated from the Hamiltonian constrain) but for different energy levels: $\mathcal{E} < 0$ (top), $\mathcal{E} = 0$ (middle) and $\mathcal{E} > 0$ (bottom). For every sample we have acceleration but the equation of the state parameter oscillates and approaches $w_{\text{eff}} = -1$.

Chapter 4

Non-minimally coupled scalar field cosmology on the phase plane

We investigate dynamics of a flat FRW cosmological model with a non-minimally coupled scalar field with the coupling term $\xi R\psi^2$ in the scalar field action. The quadratic potential function $U(\psi) \propto \psi^2$ is assumed. All the evolutional paths are visualised and classified in the phase plane, at which the parameter of non-minimal coupling ξ plays the role of a control parameter. The fragility of global dynamics with respect to changes of the coupling constant is studied in detail. We find that the future big rip singularity appearing in the phantom scalar field cosmological models can be avoided due to non-minimal coupling constant effects. We have shown the existence of a finite scale factor singular point (future or past) where the Hubble function as well as its first cosmological time derivative diverge.

Published in :

O. Hrycyna, M. Szydłowski, JCAP04(2009)026, `arXiv:0812.5096 [hep-th]`

In this chapter we present a phase space analysis of the evolution of a spatially flat Friedmann–Robertson–Walker (FRW) universe containing a scalar field non-minimally coupled to gravity, both canonical and phantom, with the simplest form of quadratic potential function. The similar analysis for the case of minimally coupled scalar field was performed in [152]. We extend this analysis on models with a non-zero coupling constant ξ which plays the role of a control parameter for an autonomous dynamical system on the phase plane. Therefore the location of fixed points (physically representing asymptotic states of the system) as well as their character depend upon the value of ξ. The values of parameter ξ for which the global dynamics changes dramatically are called bifurcation values.

The main advantage of dynamical system analysis is that we can visualise all the trajectories of the system admissible for all initial conditions. Therefore one can classify generic routes to the accelerating phase (the de Sitter attractor where $p_\psi = -\rho_\psi$). This attractor corresponds to the model with the cosmological constant.

The chapter has the following organisation: in section 4.1 we reduce dynamics to the form of an autonomous dynamical system which describes both canonical and phantom scalar field models. Section 4.2 is devoted to a detailed analysis of the phase portraits for different values of the parameter ξ. In this section we also discuss the change of evolutionary scenarios depending on the value of parameter ξ.

4.1 Non-minimally coupled scalar field cosmologies as a dynamical system

We assume the flat model with the FRW geometry and that a matter source is in the form of a scalar field ψ with a generic coupling to gravity. The gravitational dynamics is described by the standard Einstein-Hilbert action

$$S_g = \frac{1}{2\kappa^2}\int \mathrm{d}^4x\sqrt{-g}R, \tag{4.1}$$

the action for the matter source is

$$S_\psi = -\frac{1}{2}\int \mathrm{d}^4x\sqrt{-g}\left[\varepsilon\left(g^{\mu\nu}\nabla_\mu\psi\nabla_\nu\psi + \xi R\psi^2\right) + 2U(\psi)\right]. \tag{4.2}$$

where $\kappa^2 = 8\pi G$ and $R = 6(\ddot{a}/a + \dot{a}^2/a^2)$ and $\varepsilon = +1, -1$ corresponds to the scalar field and the phantom scalar field, respectively. For simplicity and without lost of generality we will assume $4\pi G/3 = 1$ which corresponds to $\kappa^2 = 6$.

After dropping the full derivatives with respect to time we obtain the dynamical equation for scalar field from variation $\delta(S_g + S_\psi)/\delta\psi = 0$

$$\ddot{\psi} + 3H\dot{\psi} + \xi R\psi + \varepsilon U'(\psi) = 0. \tag{4.3}$$

as well as the energy conservation condition from variation $\delta(S_g + S_\psi)/\delta g = 0$

$$\mathcal{E} = \varepsilon\frac{1}{2}\dot{\psi}^2 + \varepsilon 3\xi H^2\psi^2 + \varepsilon 3\xi H(\psi^2)^{\cdot} + U(\psi) - \frac{3}{\kappa^2}H^2 \tag{4.4}$$

If we include other forms of matter this condition can be expressed as

$$\frac{3}{\kappa^2}H^2 = \rho_\psi + \rho_r + \rho_m \tag{4.5}$$

where ρ_r and ρ_m are energy densities of radiation and matter, respectively. It can be shown that for any value of ξ scalar field behaves like a perfect fluid with energy density ρ_ψ and pressure p_ψ

$$\rho_\psi = \varepsilon\frac{1}{2}\dot{\psi}^2 + U(\psi) + \varepsilon\xi\big[3H(\psi^2)^{\cdot} + 3H^2\psi^2\big], \tag{4.6a}$$

$$p_\psi = \varepsilon\frac{1}{2}\dot{\psi}^2 - U(\psi) - \varepsilon\xi\big[2H(\psi^2)^{\cdot} + (\psi^2)^{\cdot\cdot} + (2\dot{H} + 3H^2)\psi^2\big]. \tag{4.6b}$$

Changing the dynamical variables according to the relation

$$\dot{\psi} = \frac{\mathrm{d}\psi}{\mathrm{d}t} = \frac{\dot{a}}{a}\frac{\mathrm{d}\psi}{\mathrm{d}\ln a} = H\psi'$$

we can express the Hubble function as

$$H^2 = 2\frac{U(\psi) + \rho_r + \rho_m}{1 - \varepsilon\big[(1-6\xi)\psi'^2 + 6\xi(\psi' + \psi)^2\big]}. \tag{4.7}$$

The denominator of (4.7) equal to zero defines a line of singularities of the Hubble function which separates the phase space in two regions one physical $H^2 > 0$, and the second one nonphysical $H^2 < 0$. It does not depend on the form of the potential function but only on a value of the coupling constant.

The Euler-Lagrange equations for the system under consideration are given in the form

$$a^2\frac{\mathrm{d}^2\psi}{\mathrm{d}\eta^2} + 6\xi a\psi\frac{\mathrm{d}^2 a}{\mathrm{d}\eta^2} = -2a\frac{\mathrm{d}a}{\mathrm{d}\eta}\frac{\mathrm{d}\psi}{\mathrm{d}\eta} - \varepsilon a^4 U'(\psi), \tag{4.8a}$$

$$\frac{\mathrm{d}^2 a}{\mathrm{d}\eta^2}(1 - \varepsilon 6\xi\psi^2) - \varepsilon 6\xi a\psi\frac{\mathrm{d}^2\psi}{\mathrm{d}\eta^2} = -\varepsilon a(1-6\xi)\Big(\frac{\mathrm{d}\psi}{\mathrm{d}\eta}\Big)^2 + \varepsilon 12\xi\psi\frac{\mathrm{d}a}{\mathrm{d}\eta}\frac{\mathrm{d}\psi}{\mathrm{d}\eta} + 4a^3U(\psi) + \rho_{m,0}. \tag{4.8b}$$

where η stands for the conformal time, $\mathrm{d}\eta = \mathrm{d}t/a$.

After the elimination of the scale factor and its derivative from system (4.8) we obtain the condition

$$\begin{aligned}\big(\psi'' + \psi'\big)\Big(1 - \varepsilon 6\xi(1-6\xi)\psi^2\Big) - \varepsilon\psi'^2(1-6\xi)\big(\psi' + 6\xi\psi\big) + \\ + \frac{1}{H^2}\Big\{\varepsilon U'(\psi)\big(1 - \varepsilon 6\xi\psi(\psi'+\psi)\big) + \big(4U(\psi) + \rho_m\big)\big(\psi' + 6\xi\psi\big)\Big\} = 0.\end{aligned} \tag{4.9}$$

where the prime denotes differentiation with respect to the natural logarithm of the scale factor.

Now we can simply present equation (4.9) in the form of the autonomous dynamical system

$$\psi' = y, \tag{4.10a}$$

$$\begin{aligned}y' = -y + \frac{\varepsilon y^2(1-6\xi)\big(y + 6\xi\psi\big)}{\Big(1 - \varepsilon 6\xi(1-6\xi)\psi^2\Big)} - \frac{1}{2}\frac{\Big(1 - \varepsilon\big[(1-6\xi)y^2 + 6\xi(y+\psi)^2\big]\Big)}{\Big(1 - \varepsilon 6\xi(1-6\xi)\psi^2\Big)\Big(U(\psi) + \rho_r + \rho_m\Big)}\times \\ \times\Big(\varepsilon U'(\psi)\big(1 - \varepsilon 6\xi\psi(y+\psi)\big) + \big(4U(\psi) + \rho_m\big)\big(y + 6\xi\psi\big)\Big).\end{aligned} \tag{4.10b}$$

In what follows we will assume a quadratic potential function $U(\psi) = \frac{1}{2}m^2\psi^2$, and that there is no other form of matter than the scalar field, i.e that $\rho_r = \rho_m = 0$. It is easy to notice that in this case the dynamics does not depend on the change of a sign of the potential $U(\psi) \to -U(\psi)$. Finally, the dynamical system is in the form

$$\alpha\frac{\mathrm{d}\psi}{\mathrm{d}\sigma} = y\psi\Big(1 - \varepsilon 6\xi(1-6\xi)\psi^2\Big), \tag{4.11a}$$

$$\begin{aligned}\alpha\frac{\mathrm{d}y}{\mathrm{d}\sigma} = -y\psi\Big(1 - \varepsilon 6\xi(1-6\xi)\psi^2\Big) + \varepsilon(1-6\xi)\psi y^2(y + 6\xi\psi) - \\ - \Big(1 - \varepsilon\big[(1-6\xi)y^2 + 6\xi(y+\psi)^2\big]\Big)\Big(\varepsilon\big(1 - \varepsilon 6\xi\psi(y+\psi)\big) + 2\psi\big(y + 6\xi\psi\big)\Big).\end{aligned} \tag{4.11b}$$

where we have made the following "time" transformation

$$\alpha\frac{\mathrm{d}}{\mathrm{d}\sigma} = \psi\Big(1 - \varepsilon 6\xi(1-6\xi)\psi^2\Big)\frac{\mathrm{d}}{\mathrm{d}\ln(a)} \tag{4.12}$$

where the parameter α

$$\alpha = +1 \iff \psi\big(1 - \varepsilon 6\xi(1-6\xi)\psi^2\big) > 0, \tag{4.13a}$$

$$\alpha = -1 \iff \psi\big(1 - \varepsilon 6\xi(1-6\xi)\psi^2\big) < 0. \tag{4.13b}$$

was introduced to preserve the orientation of the trajectories in this way that on all of the phase portraits direction of arrows indicate the direction of growth of the scale factor.

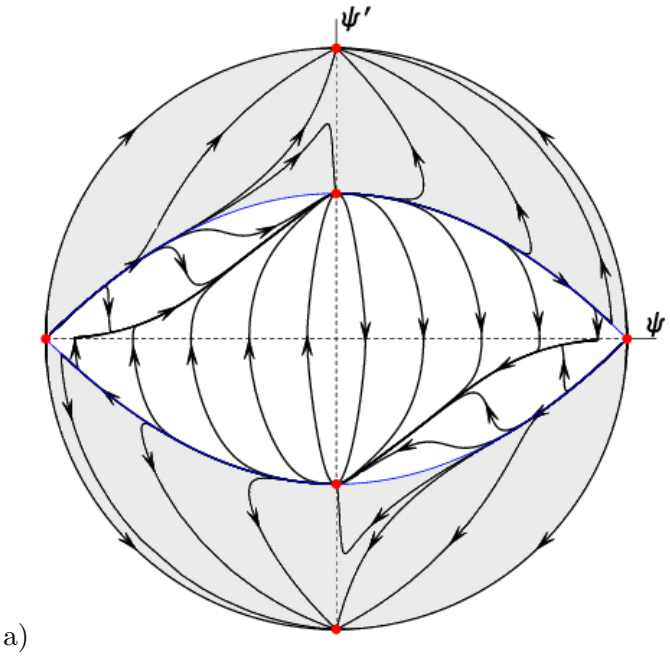

a)

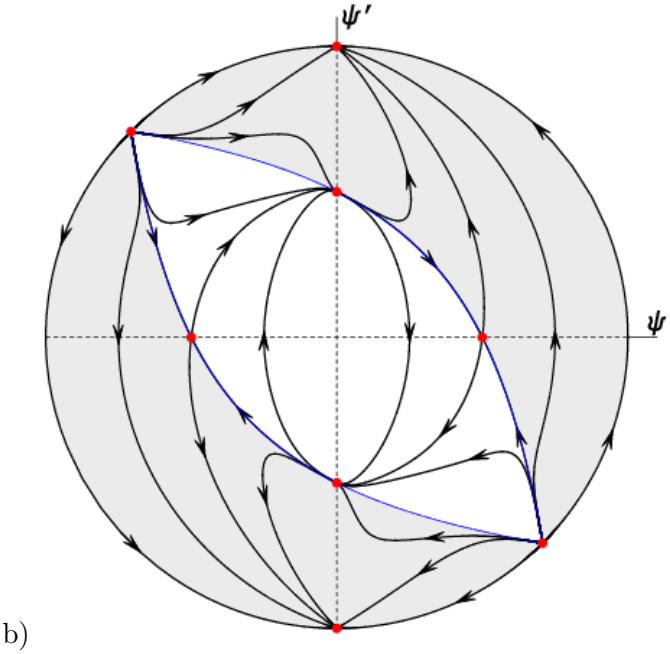

b)

Figure 4.1: The phase portraits for the canonical scalar field $\varepsilon = 1$ for: a) minimal $\xi = 0$ and b) conformal $\xi = 1/6$ coupling. The shaded region denotes nonphysical part of the phase space for the strictly positive potential function. If the potential function is strictly negative the meaning of the regions is reversed. The shape of the border between the regions does not depend on the shape of the potential function. At the border of the physical region we have two symmetric critical points at the ψ axis for both cases. The value of H^2 at that points is finite. The presence of a saddle type critical point in the case b) is the effect of non-zero ξ.

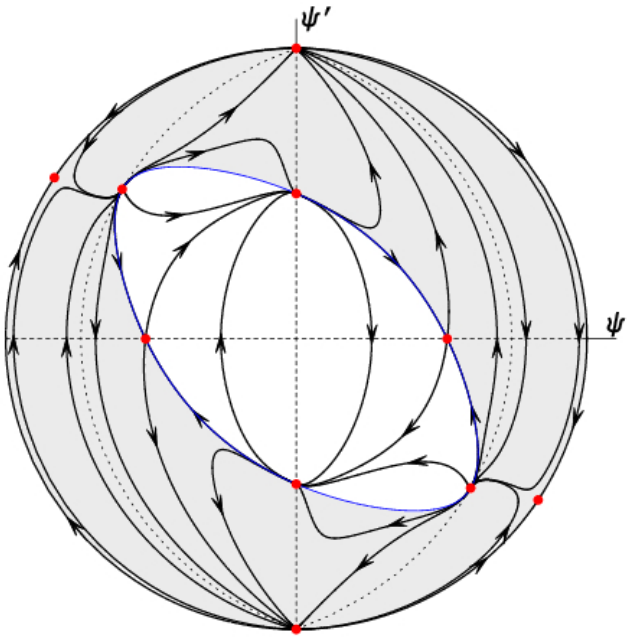

Figure 4.2: The phase portrait for the canonical scalar field $\varepsilon = 1$ and coupling constant $0 < \xi < 1/6$. The shaded region is nonphysical: $H^2 < 0$ for $U(\psi) > 0$. There are three types of critical points at the finite domain of the phase space: 1) $\psi_0 = 0$, $y_0^2 = 1$ and $H^2 = \text{const.}$ which are of a stable or unstable node type; 2) $\psi_0^2 = 1/6\xi$, $y_0 = 0$, $H^2 = \infty$ of a saddle type 3) $\psi_0 \neq 0$, $y_0 \neq 0$, $H^2 = \infty$ of unstable node type for $U(\psi) > 0$ and stable node type for $U(\psi) < 0$ (shaded region). The dashed line denotes singularity of "time" transformation (4.12). In comparison with the phase portrait from figure 4.1 for conformal coupling we can see that both phase portraits are equivalent at the physical domain.

Table 4.1: The position (ψ_0, y_0) of finite critical points and their characters.

	existence		eigenvalues
	$\varepsilon = +1$	$\varepsilon = -1$	
$\psi_0^2 = \frac{1}{\varepsilon 6\xi}$, $y_0 = 0$	$\xi > 0$	$\xi < 0$	$\lambda_1 = \frac{1}{2}(\varepsilon 3 - 5)\frac{1}{\psi_0}$, $\lambda_2 = \frac{1}{2}(\varepsilon 3 + 5)\frac{1}{\psi_0}$
$\psi_0^2 = -\frac{1}{\varepsilon 6\xi}$, $y_0 = 0$	$\xi < 0$	$\xi > 0$	$\lambda_{1,2} = -3(1-3\xi)\psi_0 \pm$ $\pm\sqrt{-\frac{\varepsilon}{2\xi}(1-3\xi)(3-25\xi)}$
$\psi_0 = 0$, $y_0^2 = \varepsilon$	$\forall \xi \in \mathbf{R}$	–	$\lambda_1 = y_0$, $\lambda_2 = 2y_0$
$\psi_0^2 = \frac{1}{\varepsilon 6\xi(1-6\xi)}$, $y_0 = -\varepsilon\frac{1}{1-6\xi}\frac{1}{\psi_0}$	$0 < \xi < \frac{1}{6}$	$\xi < 0$ or $\xi > \frac{1}{6}$	$\lambda_1 = -2y_0$, $\lambda_2 = 6\xi\psi_0$
$\psi_0^2 = \frac{1}{\varepsilon 6\xi(1-6\xi)}$, $y_0 = -4\xi\frac{1-3\xi}{1-4\xi}\psi_0 \pm \frac{2\sqrt{-\varepsilon 3\xi(1-3\xi)}}{3(1-4\xi)}$	–	$\frac{1}{6} < \xi < \frac{1}{3}$	$\lambda_1 = -2y_0$, $\lambda_2 = 2y_0$

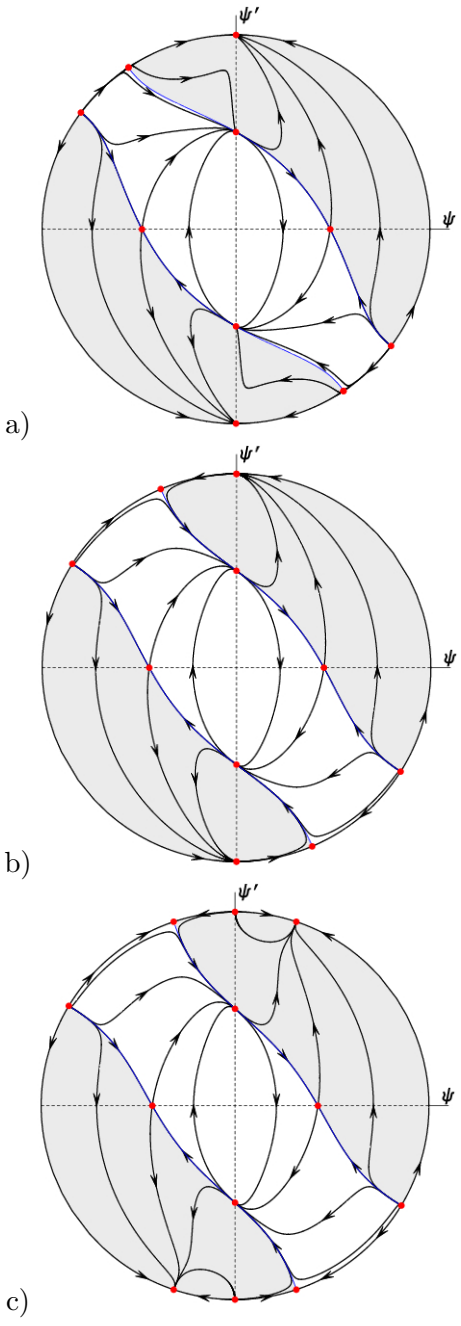

Figure 4.3: The phase portraits for the canonical scalar field $\varepsilon = 1$ and for the specific values of coupling constant: a) $\xi = 3/16$, b) $\xi = 1/4$, c) $\xi = 3/10$. In the cases a) and b) there are the critical points at infinity of a mixed type (multiple critical points). At the physical domain the phase portraits are topologically equivalent.

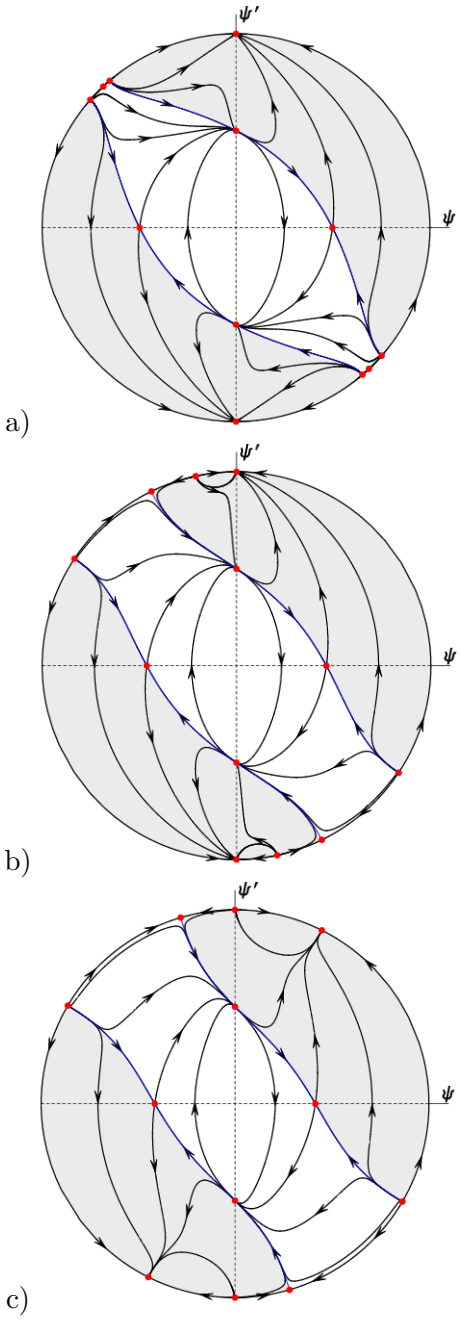

Figure 4.4: The phase portraits for the canonical scalar field $\varepsilon = 1$ and values of coupling constant: a) $1/6 < \xi < 3/16$, b) $3/16 < \xi < 1/4$, c) $\xi = 1/3$.

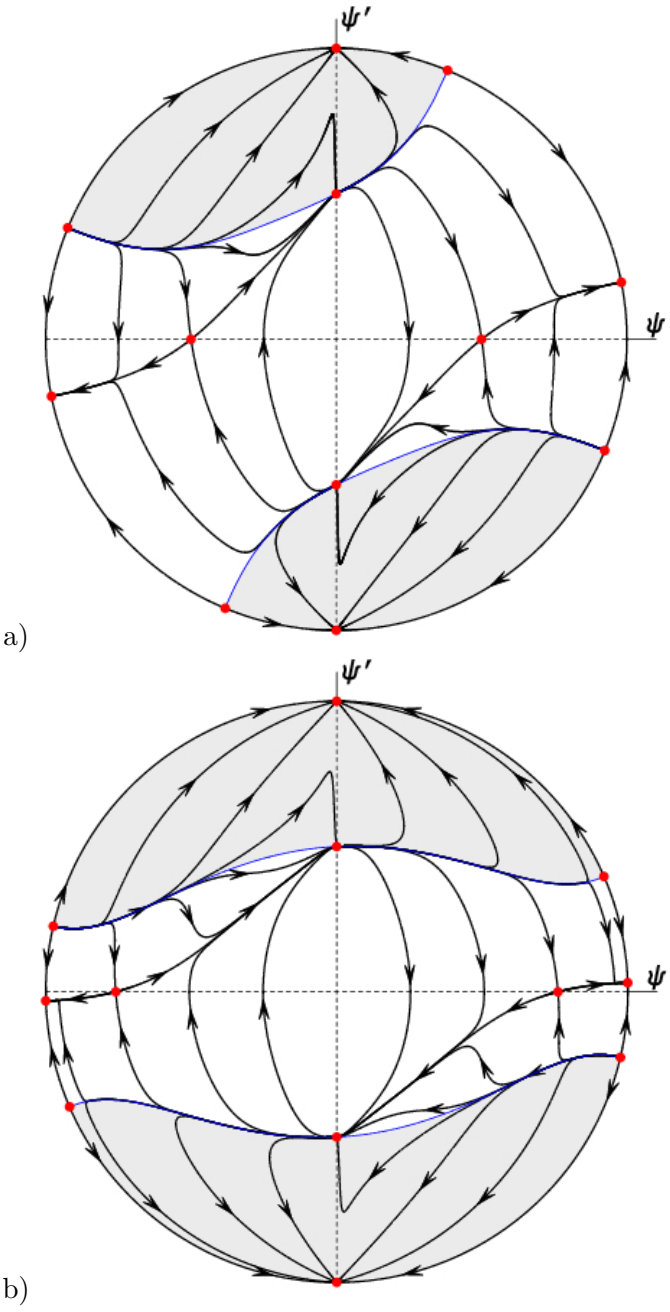

Figure 4.5: The phase portraits for the canonical scalar field $\varepsilon = 1$ and negative coupling constant $\xi < 0$: in figure b) ξ is greater, but still negative, than in figure a). In the limit $\xi \to 0^-$ we receive phase portrait in figure 4.1a.

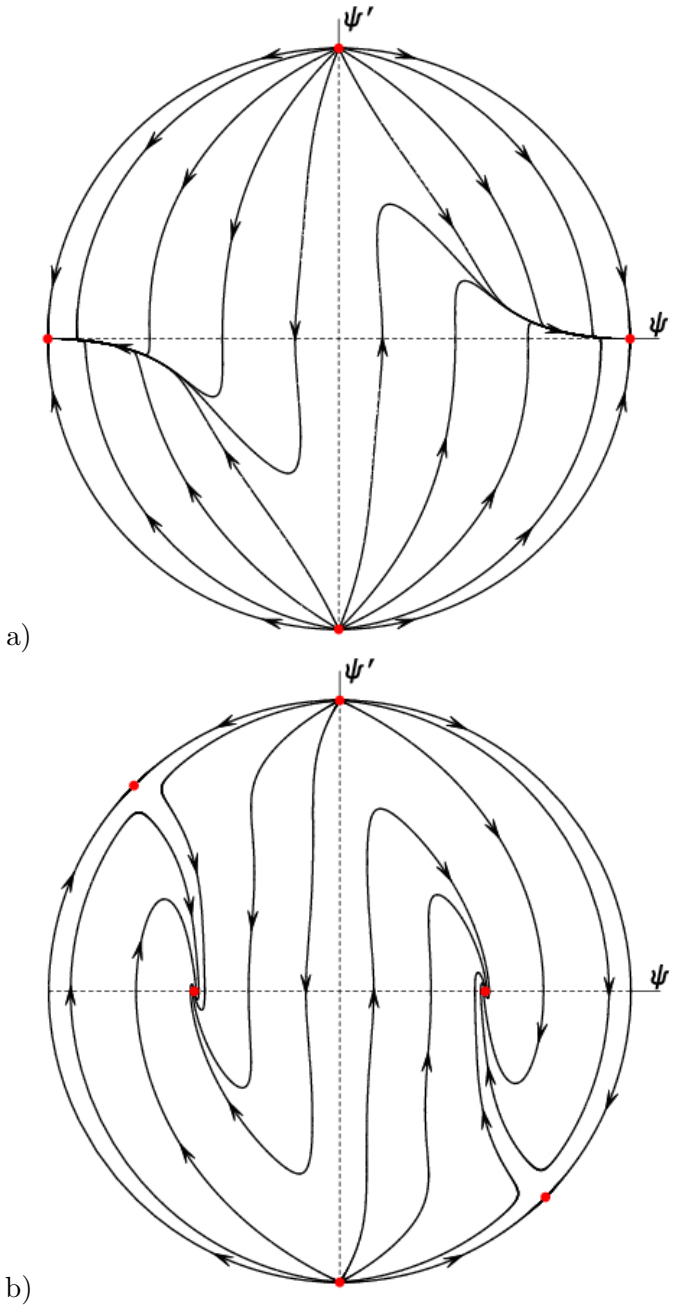

Figure 4.6: The phase portraits for the phantom scalar field $\varepsilon = -1$ and: a) minimal $\xi = 0$ and b) conformal $\xi = 1/6$ coupling. All the phase space (ψ, ψ') is admissible only for the positive potential function. We can conclude, that for negative potential functions in the case of minimally or conformally coupled phantom scalar fields, the scale factor is not a monotonic function of the cosmological time. For the case b) a global attractor represents the de Sitter state with $w_\psi = -1$. There are two types of trajectories which tend to this attractor: 1) trajectories starting from $\psi = 0$, $\psi' = \pm\infty$ state, and 2) two single trajectories representing a separatrix of saddles at infinity (not shown).

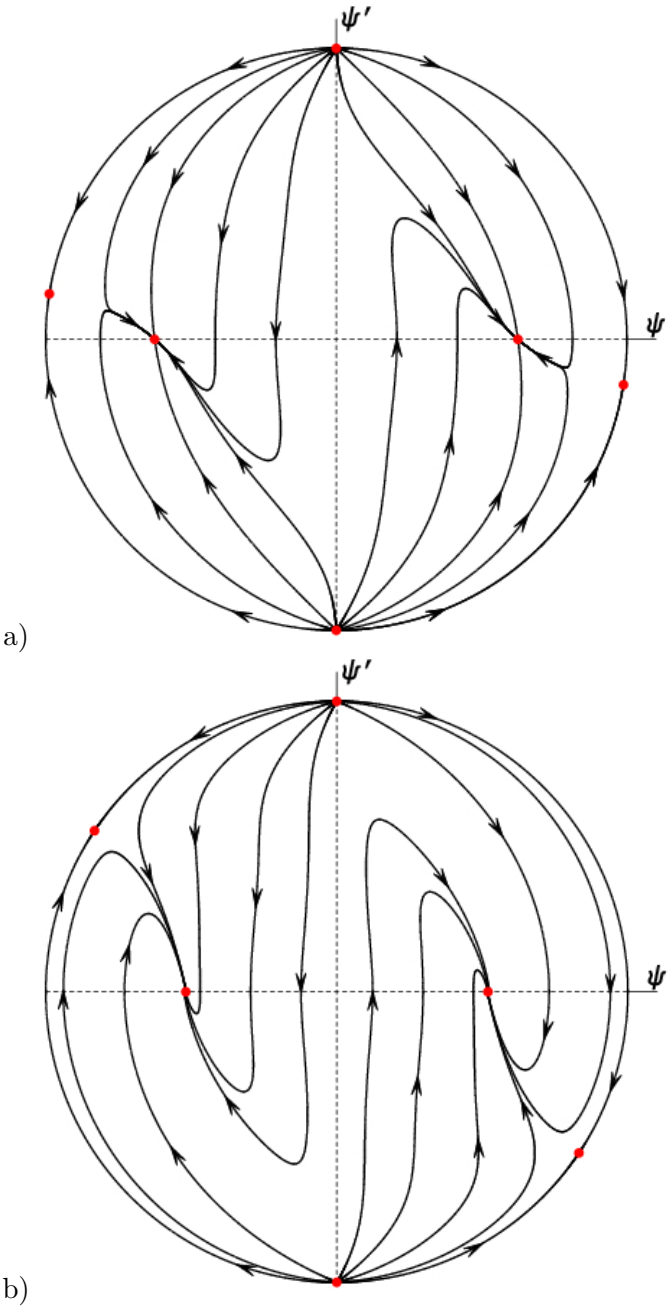

Figure 4.7: The global phase portraits for the phantom scalar field and values of coupling constant: a) $0 < \xi < 3/25$ and b) $3/25 < \xi < 1/6$. In the case a) in the finite domain the critical domain is of a stable node type and in the case b) of a focus type.

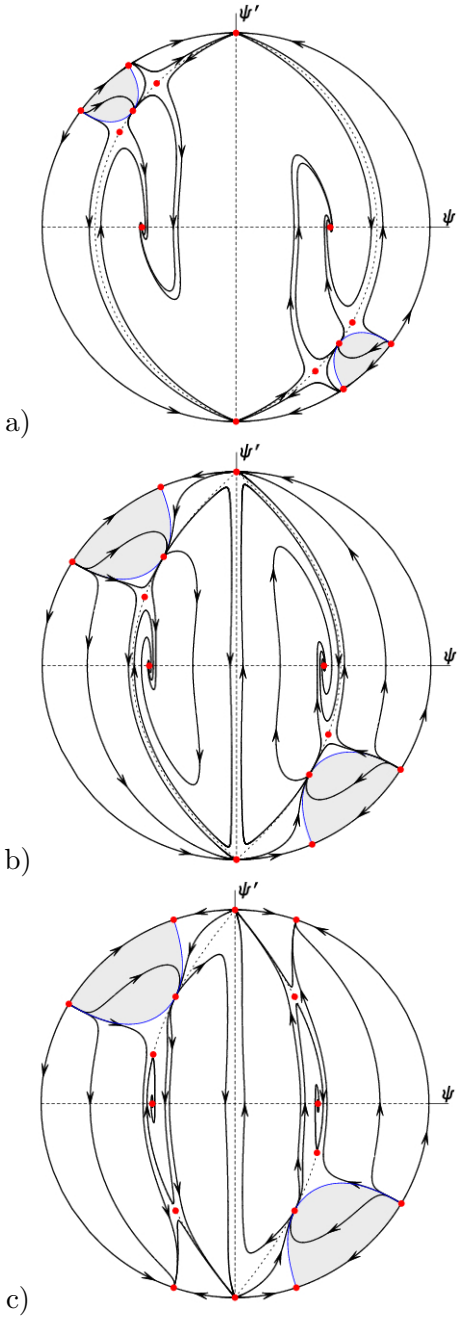

Figure 4.8: The global phase portraits for the phantom scalar field $\varepsilon = -1$ and for the specific values of coupling constant: a) $\xi = 3/16$, b) $\xi = 1/4$, c) $\xi = 3/10$. In cases a) and b) one of the critical points at infinity is of a mixed type (multiple critical points) (see figure 4.3). On all figures one can see trajectories starting from the unstable node and landing at the stable focus as a generic scenario of route to the de Sitter state.

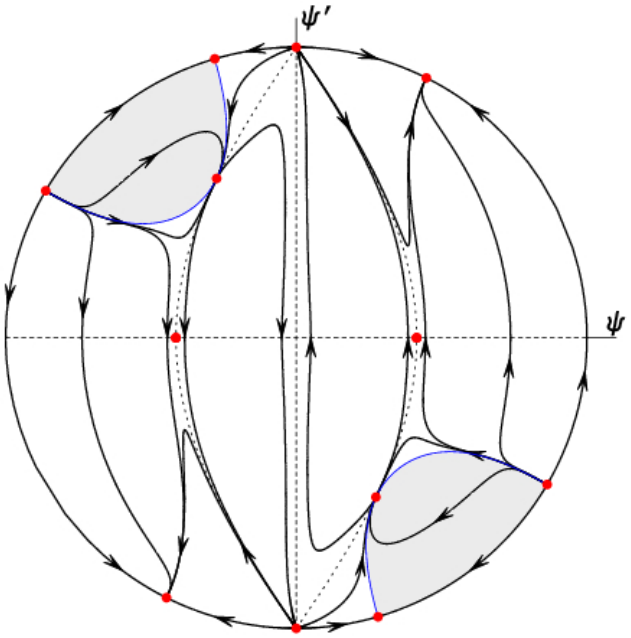

Figure 4.9: The global phase portrait for the phantom scalar field $\varepsilon = -1$ and distinguished value of coupling constant $\xi = 1/3$. In this case critical point at the finite domain of the phase space is located at the line of singularities of the time transformation (4.12).

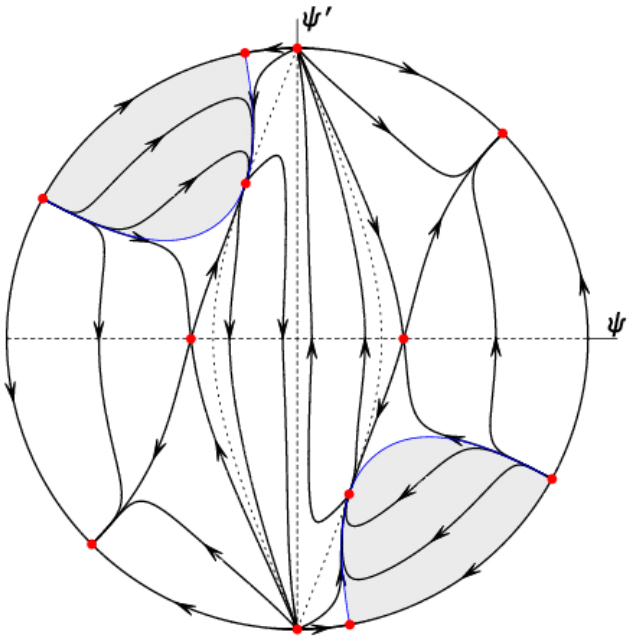

Figure 4.10: The global phase portrait for the phantom scalar field $\varepsilon = -1$ and the values of coupling constant $\xi > 1/3$. The characteristic critical point of a focus type disappeared.

4.2 Phase space analysis of dynamics

In this section we present detailed discussion of the type of critical points of the dynamical system (4.11).

If we write the evolutional equations for the non-minimally coupled scalar field in the form of the dynamical system, the first step would be the identification of the critical points of the system. Physically they represent asymptotic (or stationary) states of the system under consideration and mathematically correspond to vanishing r.h.s. of the system. The second step is a characterisation of the type of critical point which can be performed after calculation of the eigenvalues of the linearization matrix calculated of this critical point. The critical points are usually represented by physically interesting solutions and these solutions can be attractors for trajectories in its neighbourhood which evolve to it independent of the initial conditions. In the quintessence cosmology we are looking for the attractors, which give rise to solutions with desired property but we would like to know whether it is a typical (generic) solution or an exceptional (non-generic). This is a reason of our interest in the stability of the critical points.

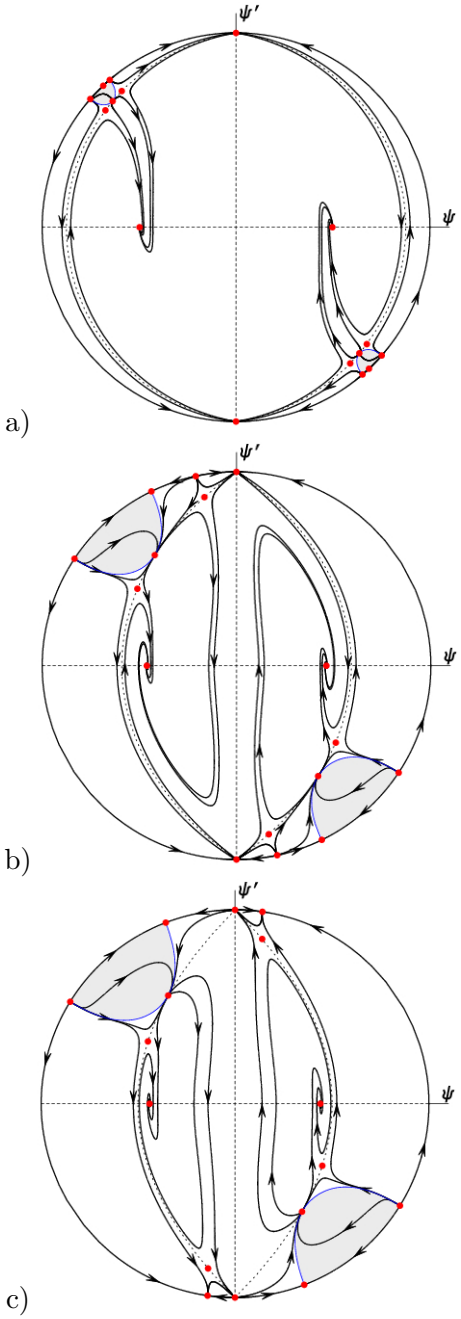

Figure 4.11: The global phase portraits for the phantom scalar field $\varepsilon = -1$ and the values of coupling constant: a) $1/6 < \xi < 3/16$, b) $3/16 < \xi < 1/4$, c) $1/4 < \xi < 3/10$. In all cases there is present scenario of reaching the global attractor (a focus type critical point) from the unstable node. Note that in the case c) not all of the trajectories starting from an unstable node are reaching the de Sitter state, in contrast to cases a) and b).

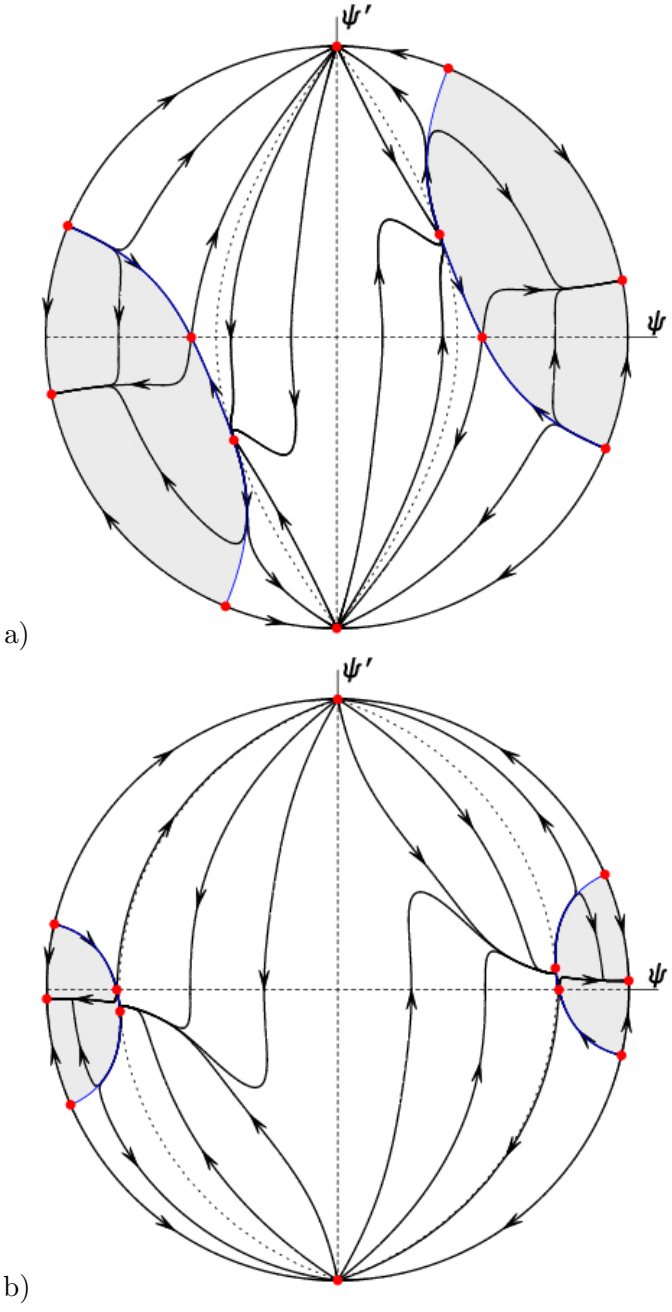

Figure 4.12: The global phase portraits for the phantom scalar field $\varepsilon = -1$ and negative coupling constant $\xi < 0$: in figure b) ξ is greater, but still negative, than in figure a). It is easy to notice that in the limit $\xi \to 0^-$ we receive phase portrait from the figure 4.6a. for the phantom scalar field with minimal coupling.

For full dynamical analysis of the behaviour of the trajectories at infinity is needed. It can be performed by construction of Poincaré sphere [59]. If we complete the phase plane by a circle at infinity which is a projection on the equator, then we obtain the global phase portrait with a circle at infinity. In our case r.h.s. contain the non-minimal coupling constant ξ as a free parameter. The global phase portraits depend on the value of this parameter but for some ranges of the values of ξ phase portraits can be equivalent (indistinguishable from the dynamical system point of view). If we fix the value of non-minimal coupling, then one can study the influence of this parameter on the global dynamics. The equivalence of the phase portraits is established by homeomorphism preserving direction of time along the trajectories.

Critical point: $\psi_0 = 0$, $y_0^2 = \varepsilon$ exists only for the canonical scalar field $\varepsilon = +1$. Direct calculation of the Hubble function (4.7) at this point gives an undefined symbol $\frac{0}{0}$. It is why we use the linearised solutions in the vicinity of this critical point to show that the Hubble function at this point is finite and depends on the initial conditions of the linearised solutions. They are in the form

$$\psi(\sigma) = \psi_{(\mathrm{i})} \exp(\alpha\lambda_1\sigma), \tag{4.14a}$$

$$y(\sigma) = y_0 - 6\xi\psi_{(\mathrm{i})} \exp(\alpha\lambda_1\sigma) + \big(6\xi\psi_{(\mathrm{i})} + (y_{(\mathrm{i})} - y_0)\big) \exp(\alpha\lambda_2\sigma), \tag{4.14b}$$

where $\lambda_1 = y_0$ and $\lambda_2 = 2y_0$ are eigenvalues of the linearization matrix calculated at this critical point, $\psi_{(\mathrm{i})}$ and $y_{(\mathrm{i})}$ are initial conditions and y_0 is a coordinate of the critical point.

Inserting those solution into the formula (4.7) we receive that the Hubble function in the vicinity of the critical point ($\psi_0 = 0$, $y_0^2 = \varepsilon$) is

$$\begin{aligned} H_{\mathrm{lin}}^2 = m^2\psi_{(\mathrm{i})}^2 \exp(2\alpha\lambda_1\sigma)\Big[&- 6\xi(1-6\xi)\psi_{(\mathrm{i})}^2 \exp(2\alpha\lambda_1\sigma) - \\ &- 2y_0\big(6\xi\psi_{(\mathrm{i})} + (y_{(\mathrm{i})} - y_0)\big) \exp(\alpha\lambda_2\sigma) - \\ &- \big(36\xi^2\psi_{(\mathrm{i})}^2 + 12\xi\psi_{(\mathrm{i})}(y_{(\mathrm{i})} - y_0) + (y_{(\mathrm{i})} - y_0)^2\big) \exp(2\alpha\lambda_2\sigma)\Big]^{-1} \end{aligned} \tag{4.15}$$

then taking the limit value of this function for $\sigma \to \pm\infty$ (depending on the critical point $y_0 = \mp 1$) we receive

$$\lim H_{\mathrm{lin}}^2 = m^2 \frac{\psi_{(\mathrm{i})}^2}{-2y_0\big(6\xi\psi_{(\mathrm{i})} + (y_{(\mathrm{i})} - y_0)\big) - 6\xi(1-6\xi)\psi_{(\mathrm{i})}^2} \tag{4.16}$$

which is always a positive quantity. For the special values of minimal $\xi = 0$ (see figure 4.1a) and conformal coupling $\xi = 1/6$ (see figure 4.1b) the values of the Hubble function are

$$H^2_{\text{lin}} = m^2 \frac{\psi^2_{(\text{i})}}{-2y_0(y_{(\text{i})} - y_0)}, \qquad \text{for} \qquad \xi = 0,$$
$$H^2_{\text{lin}} = m^2 \frac{\psi^2_{(\text{i})}}{-2y_0\big(\psi_{(\text{i})} + (y_{(\text{i})} - y_0)\big)}, \qquad \text{for} \qquad \xi = \frac{1}{6}.$$

Critical point: $\psi_0^2 = \frac{1}{\varepsilon 6\xi(1-6\xi)}$, $y_0 = -\varepsilon\frac{1}{(1-6\xi)\psi_0}$ is very interesting because the Hubble function (4.7) at this point is singular $H^2 = \infty$ and $\dot{H} = (\frac{1}{2}H^2)' = \infty$.

Linearised solutions in the vicinity of this critical points are

$$\psi(\sigma) = \psi_0 + \exp(\alpha\lambda_2\sigma)\big(\psi_{(\text{i})} - \psi_0\big), \tag{4.17a}$$
$$y(\sigma) = y_0 + \exp(\alpha\lambda_1\sigma)\Big(2(1-3\xi)\big(\psi_{(\text{i})} - \psi_0\big) + \big(y_{(\text{i})} - y_0\big)\Big) - \\ - \exp(\alpha\lambda_2\sigma)\Big(2(1-3\xi)\big(\psi_{(\text{i})} - \psi_0\big)\Big) \tag{4.17b}$$

where $\lambda_1 = -y_0$ and $\lambda_2 = -2y_0$ are eigenvalues of the linearization matrix at the critical point, $\psi_{(\text{i})}$ and $y_{(\text{i})}$ are initial conditions and ψ_0 and y_0 are coordinates of the critical point.

Using time transformation (4.12) we can calculate the scale factor growth along the trajectory

$$\Delta \ln a = \int_0^\infty \psi(\sigma)\big(1 - \varepsilon 6\xi(1-6\xi)\psi(\sigma)^2\big)\mathrm{d}\sigma, \tag{4.18}$$

and the cosmological time growth

$$\Delta t = \int_{a_i}^{a_f} \frac{1}{H}\mathrm{d}\ln a = \int_0^\infty \frac{1}{H}\psi(\sigma)\big(1 - \varepsilon 6\xi(1-6\xi)\psi(\sigma)^2\big)\mathrm{d}\sigma. \tag{4.19}$$

Linearised solutions are good approximations of the original system in the vicinity of the critical point. In what follows we assume that $\big(\psi_{(\text{i})} - \psi_0\big)^2 = \big(y_{(\text{i})} - y_0\big)^2 = \big(\psi_{(\text{i})} - \psi_0\big)\big(y_{(\text{i})} - y_0\big) = 0$, $\alpha = 1$ and $y_0 > 0$ (see figure 4.12). Then

$$\Delta \ln a = \varepsilon(1-6\xi)\big(\psi_{(\text{i})} - \psi_0\big)\psi_0 \tag{4.20}$$

and

$$\Delta t = \frac{-1}{\sqrt{m^2}}\varepsilon 12\xi(1-6\xi)\big(\psi_{(\text{i})} - \psi_0\big)\psi_0 \int_0^\infty \sqrt{A\exp(-y_0\sigma) + B\exp(-2y_0\sigma)}\exp(-2y_0\sigma)\mathrm{d}\sigma \\ = \frac{1}{\sqrt{m^2}}\varepsilon 12\xi(1-6\xi)\big(\psi_{(\text{i})} - \psi_0\big)\frac{1}{y_0 24 B^{5/2}}\Big\{\frac{3}{2}A^2\Big(\log A - 2\log\big(\sqrt{B} + \sqrt{A+B}\big)\Big) - \\ - \sqrt{B(A+B)}(-A+2B)(3A+4B)\Big\} \tag{4.21}$$

where A and B are positive constants

$$A = -\varepsilon\big(y_0 + 12\xi\psi_0\big)\big(2(1-3\xi)(\psi_{(\mathrm{i})} - \psi_0) + (y_{(\mathrm{i})} - y_0)\big)$$

$$B = \varepsilon 4(1-6\xi)(y_0 + 3\xi\psi_0)(\psi_{(\mathrm{i})} - \psi_0)$$

For every case of existence of such a critical point (see figures 4.2, 4.8, 4.9, 4.10, 4.11 for an unstable node and figure 4.12 for a stable node in the "physical region") growth of the scale factor and the cosmological time are finite.

Now we calculate the first derivative of the Hubble function (4.7) with respect to the cosmological time at this point

$$\dot{H} = \frac{1}{2}(H^2)' = \Big(\frac{U(\psi)}{1 - \varepsilon[\psi'^2 + 12\xi\psi\psi' + 6\xi\psi^2]}\Big)' \tag{4.22}$$

where a dot denotes differentiation with respect to the cosmological time and a prime with respect to the natural logarithm of the scale factor. Then after the elimination of second derivative of the field with respect to the natural logarithm of the scale factor we have

$$\dot{H} = -\frac{6\xi U'(\psi)\psi}{1 - \varepsilon 6\xi(1-6\xi)\psi^2} - \frac{\varepsilon 2U(\psi)\big((1-6\xi)\psi'^2 + (\psi' + 6\xi\psi)^2\big)}{\big(1 - \varepsilon 6\xi(1-6\xi)\psi^2\big)\big(1 - \varepsilon[\psi'^2 + 12\xi\psi\psi' + 6\xi\psi^2]\big)} \tag{4.23}$$

This expression at the critical point $\psi_0^2 = \frac{1}{\varepsilon 6\xi(1-6\xi)}$, $\psi_0' = -\varepsilon\frac{1}{1-6\xi}\frac{1}{\psi_0}$ is singular since the numerator is finite and the denominator is equal to zero.

The trajectories starting form this critical point corresponding to the singularities of finite scale factor seems to be most interesting. For such state appearing for both, canonical and phantom scalar fields we have curvature singularity because the Hubble parameter is infinite but the scale factor assumes a finite value. They are typical because the critical point is an unstable node (see figure 4.2 for an unstable node for the canonical scalar field and and figures 4.8, 4.9, 4.10 and 4.11 for an unstable node and figure 4.12 for a stable node for the phantom scalar field).

Next we can proceed to the analysis of behaviour of system (4.11) at the circle at infinity. Introducing the polar variables in order to compactify the phase space by adjoining the circle at infinity

$$\psi = \frac{r}{1-r}\cos\theta, \qquad y = \frac{r}{1-r}\sin\theta,$$

where r and θ are the polar system coordinates, we receive the following dynamical system

$$\alpha\frac{\mathrm{d}r}{\mathrm{d}\sigma}r(1-r)^3 = r(1-r)\sin\theta\Big\{r^2\cos\theta(\cos\theta-\sin\theta)\Big((1-r)^2-\varepsilon 6\xi(1-6\xi)r^2\cos^2\theta\Big)+ \\ +\varepsilon(1-6\xi)r^4\sin^2\theta\cos\theta(\sin\theta+6\xi\cos\theta)- \\ -\Big((1-r)^2-\varepsilon r^2\big((1-6\xi)\sin^2\theta+6\xi(\sin\theta+\cos\theta)^2\big)\Big) \\ \Big(\varepsilon\big((1-r)^2-\varepsilon 6\xi r^2\cos\theta(\sin\theta+\cos\theta)\big)+2r^2\cos\theta(\sin\theta+6\xi\cos\theta)\Big)\Big\}, \tag{4.24a}$$

$$\alpha\frac{\mathrm{d}\theta}{\mathrm{d}\sigma}r(1-r)^3 = \cos\theta\Big\{-r^2\sin\theta(\sin\theta+\cos\theta)\Big((1-r)^2-\varepsilon 6\xi(1-6\xi)r^2\cos^2\theta\Big)+ \\ +\varepsilon(1-6\xi)r^4\sin^2\theta\cos\theta(\sin\theta+6\xi\cos\theta)- \\ -\Big((1-r)^2-\varepsilon r^2\big((1-6\xi)\sin^2\theta+6\xi(\sin\theta+\cos\theta)^2\big)\Big) \\ \Big(\varepsilon\big((1-r)^2-\varepsilon 6\xi r^2\cos\theta(\sin\theta+\cos\theta)\big)+2r^2\cos\theta(\sin\theta+6\xi\cos\theta)\Big)\Big\}. \tag{4.24b}$$

For identification of the critical points at infinity we can calculate the polar angle θ from those equations simply by putting $r = 1$. Then we receive the following equation for the direction θ determining the localisation of the critical points

$$\varepsilon 3\cos^2\theta\big(2\xi\cos\theta+(1-4\xi)\sin\theta\big)\big(\sin^2\theta+6\xi\cos^2\theta+12\xi\sin\theta\cos\theta\big)=0. \tag{4.25}$$

We can notice that positions of the critical points at infinity do not depend on the form of scalar field assumed, i.e. critical points are the same for both canonical and phantom scalar fields. In Table 4.2 we have gathered positions and the character of these points. Note that there are specific values of the coupling constant ξ for which some critical points coincide. For example for minimal $\xi = 0$ and conformal $\xi = \frac{1}{6}$ coupling critical points 2) and 3) in Table 4.2 have the same location. This is the reason why in these cases the critical points at infinity are degenerated (i.e. the eigenvalues of linearization matrix calculated for the critical points located at infinity is identically zero). Such points are called multiple critical points. In our approach we treat the coupling constant ξ as a control parameter for which the bifurcation analysis is performed. The values of ξ different from minimal and conformal coupling split multiple critical points and remove the degeneration.

Table 4.2: The critical points at infinity and their characters.

	Critical point	existence	eigenvalues
1)	$\cos\theta = 0$	$\forall\xi \in \mathbf{R}$	$\lambda_1 = \lambda_2 = 0$
2)	$\tan\theta = -\frac{2\xi}{1-4\xi}$	$\forall\xi \in \mathbf{R} \setminus \{\frac{1}{4}\}$	$\lambda_1 = \varepsilon 6\xi(1-6\xi)\frac{3-16\xi}{1-4\xi}$, $\lambda_2 = -\varepsilon 12\xi^2\frac{1-6\xi}{1-4\xi}$
3)	$\tan\theta = -6\xi \pm \sqrt{6\xi(6\xi-1)}$	$\xi \leq 0$ or $\xi \geq \frac{1}{6}$	$\lambda_1 = -\varepsilon 12\xi(1-6\xi)\big(3(1-4\xi) \mp 2\sqrt{6\xi(6\xi-1)}\big)$, $\lambda_2 = -\varepsilon 6\xi(1-6\xi)\Big(6\xi \pm \sqrt{6\xi(6\xi-1)}\Big)$

Now we can simply calculate the value of the Hubble function (4.7) at critical points at infinity. Using the polar coordinates with compactification with circle at infinity we obtain

$$H^2|_\infty = -\varepsilon m^2 \frac{\cos^2\theta}{\sin^2\theta + 12\xi\sin\theta\cos\theta + 6\xi\cos^2\theta}. \tag{4.26}$$

Inserting the position angle of the critical points at infinity to the above expression we can conclude that at critical point 1) in Table 4.2 $H^2 = 0$, for the second point $H^2 = -\varepsilon m^2\frac{(1-4\xi)^2}{2\xi(1-6\xi)(3-16\xi)}$, and finally for the point 3) the Hubble function is singular $H^2 = \infty$. The most interesting critical point seems to be the second critical point because for the wide range of values of the parameter ξ the final state can be the de Sitter attractor with $H^2 = \text{const}$ in spite of the fact that the phase variables ψ and ψ' assume the infinite values.

4.3 Conclusions

We study the dynamics of a scalar field with a simple quadratic potential function and non-minimal coupling to the gravity via $\xi R\psi^2$ term, where R is the Ricci scalar of the Robertson-Walker spacetime. We reduce the dynamical problem to the autonomous dynamical system on the phase plane in the variables ψ and its derivative with respect to the natural logarithm of the scale factor. The constraint condition is solved in such a way that the final dynamical system is free of it and is defined on the plane. We investigate the whole dynamics at the finite domain and at infinity. All the trajectories for all admissible initial conditions are classified, and critical points representing the asymptotic states (stationary solutions) are found. We explore generic evolutionary paths to find the stable de Sitter state as a global attractor and classify typical routes to this point. We study the effects of the canonical scalar field as well as the phantom scalar field. The following conclusions, as the results of our studies, can be drawn:

1. The cosmological models with the quadratic potential function and non-minimal coupling term $\xi R\psi^2$ are represented by a 2-dimensional autonomous dynamical system which is studied in details on the (ψ, ψ') phase plane (see Table 4.1 for the critical points at the finite domain). The shape of the physical region $H^2 \geq 0$ does not depend on the form of the potential function, but only on the value of the coupling constant ξ;

2. We investigated the fixed points of the dynamical system and their stability to find the generic evolutional scenarios. We have shown the existence of a finite scale factor singular point (both future and past) where the Hubble function as well as its first cosmological time derivative diverge $H^2 = \infty$ and $\dot{H} = \infty$;

3. For the phantom scalar field $\varepsilon = -1$ we found existence of a sink type critical point (i.e. a stable node or a focus, depending on the value of the parameter ξ) which represents the de Sitter solution. Only for $\xi < 1/6$ the evolutional paths avoid a past finite scale factor singularity (see for example figures 4.6 and 4.8);

4. For the canonical scalar field $\varepsilon = 1$ we found that for $0 < \xi < 1/6$ exists the critical point which corresponds to a past finite scale factor singularity for models with $U(\psi) = \frac{1}{2}m^2\psi^2 > 0$. If $m^2 < 0$ then this point corresponds to a future finite scale factor singularity (see figure 4.2).

Chapter 5

Twister quintessence scenario

We study generic solutions in a non-minimally coupled to gravity scalar field cosmology. It is shown that dynamics for both canonical and phantoms scalar fields with the potential can be reduced to the dynamical system from which the exact forms for an equation of the state parameter can be derived. We have found the stationary solutions of the system and discussed their stability. Within the large class of admissible solutions we have found a non-degenerate critical points and we pointed out multiple attractor type of trajectory travelling in neighbourhood of three critical points at which we have the radiation dominating universe, the barotropic matter dominating state and finally the de Sitter attractor. We have demonstrated the stability of this trajectory which we call the twister solution. Discovered evolutional path is only realized if there exists a non-minimal coupling constant. We have found simple duality relations between twister solutions in phantom and canonical scalar fields in the radiation domination phase. For the twister trajectory we have found an oscillating regime of approaching the de Sitter attractor.

Published in :

O. Hrycyna, M. Szydłowski, Phys. Lett. B **694**, 191 (2010), `arXiv:0906.0335 [astro-ph.CO]`

In this contribution we investigate dynamics of the cosmological model with the scalar field non-minimally coupled to the gravity with the positive and negative kinetic energy forms (i.e., canonical and phantom scalar fields) in the background of the flat Friedmann-Robertson-Walker (FRW) geometry. We point out interesting properties of a three phase model obtained within these class of solutions. They are interesting because they are generic and interpolate three physically important phases of the evolution of the universe, namely, radiation, matter and dark energy domination in the evolution of the universe. Therefore, this solutions can be treated as a natural extension of the quartessence idea [153, 154, 155, 156]. In standard cosmology the expression "radiation dominated universe" implies a universe dominated by photons. In this chapter, the meaning is different: it means a universe with effective equation of state parameter $w_{eff} = 1/3$ dominated by non-minimally coupled scalar field. In this case the dynamics of the scale factor mimics the evolution of the radiation dominated universe.

In our investigations we apply the dynamical systems methods in exploring stationary states represented by critical points in the phase space as well as their stability [39, 157, 17, 18, 15, 16, 33, 34, 35, 36, 37, 38]. We characterise all generic scenarios appearing in the case of the constant non-minimal coupling for both canonical and phantom scalar fields. In our dynamical study we relax the choice of the potential function. The presented approach to study the dynamics with the dynamical form of the equation of the state parameter is a different form the most popular one mainly used in the confrontation of the assumed model with dynamical dark energy with the observational data [158, 159]. While the authors who estimate parameters from the observational data postulate at the very beginning the form of the parameterisation of the equation of state parameter $w(z)$ as a function of the redshift z, in the presented approach such a form is directly derived from the closed dynamics of the FRW model filled by the non-minimally coupled scalar field. Moreover, basing on the twister solution one can derive approximated forms of the effective equation of the state parameter $w(z)$ in three characteristic phases of the evolution of the universe, namely during the radiation, the barotropic matter and the dark energy domination.

In the model under consideration we assume the spatially flat FRW universe filled with the non-minimally coupled scalar field and barotropic fluid with the equation of the

state coefficient w_m. The action assumes following form

$$S = \frac{1}{2}\int \mathrm{d}^4x\sqrt{-g}\left(\frac{1}{\kappa^2}R - \varepsilon\Big(g^{\mu\nu}\partial_\mu\phi\partial_\nu\phi + \xi R\phi^2\Big) - 2U(\phi)\right) + S_m, \tag{5.1}$$

where $\kappa^2 = 8\pi G$, $\varepsilon = +1, -1$ corresponds to canonical and phantom scalar field, respectively, the metric signature is $(-,+,+,+)$, $R = 6\left(\frac{\ddot{a}}{a} + \frac{\dot{a}^2}{a^2}\right)$ is the Ricci scalar, a is the scale factor and a dot denotes differentiation with respect to the cosmological time and $U(\phi)$ is the scalar field potential function. S_m is the action for the barotropic matter part.

The dynamical equation for the scalar field we can obtain from the variation $\delta S/\delta\phi = 0$

$$\ddot{\phi} + 3H\dot{\phi} + \xi R\phi + \varepsilon U'(\phi) = 0, \tag{5.2}$$

and energy conservation condition from the variation $\delta S/\delta g^{\mu\nu} = 0$

$$\mathcal{E} = \varepsilon\frac{1}{2}\dot{\phi}^2 + \varepsilon 3\xi H^2\phi^2 + \varepsilon 3\xi H(\phi^2)\dot{} + U(\phi) + \rho_m - \frac{3}{\kappa^2}H^2. \tag{5.3}$$

Then conservation conditions read

$$\frac{3}{\kappa^2}H^2 = \rho_\phi + \rho_m, \tag{5.4a}$$

$$\dot{H} = -\frac{\kappa^2}{2}\Big[(\rho_\phi + p_\phi) + \rho_m(1 + w_m)\Big] \tag{5.4b}$$

where the energy density and the pressure of the scalar field are

$$\rho_\phi = \varepsilon\frac{1}{2}\dot{\phi}^2 + U(\phi) + \varepsilon 3\xi H^2\phi^2 + \varepsilon 3\xi H(\phi^2)\dot{}, \tag{5.5a}$$

$$p_\phi = \varepsilon\frac{1}{2}(1-4\xi)\dot{\phi}^2 - U(\phi) + \varepsilon\xi H(\phi^2)\dot{} - \varepsilon 2\xi(1-6\xi)\dot{H}\phi^2 - \varepsilon 3\xi(1-8\xi)H^2\phi^2 + \\ + 2\xi\phi U'(\phi). \tag{5.5b}$$

In what follows we introduce the energy phase space variables

$$x \equiv \frac{\kappa\dot{\phi}}{\sqrt{6}H}, \quad y \equiv \frac{\kappa\sqrt{U(\phi)}}{\sqrt{3}H}, \quad z \equiv \frac{\kappa}{\sqrt{6}}\phi, \tag{5.6}$$

which are suggested by the conservation condition

$$\frac{\kappa^2}{3H^2}\rho_\phi + \frac{\kappa^2}{3H^2}\rho_m = \Omega_\phi + \Omega_m = 1 \tag{5.7}$$

or in terms of the newly introduced variables

$$\Omega_\phi = y^2 + \varepsilon\Big[(1-6\xi)x^2 + 6\xi(x+z)^2\Big] = 1 - \Omega_m. \tag{5.8}$$

The acceleration equation can be rewritten to the form

$$\dot{H} = -\frac{\kappa^2}{2}\Big(\rho_{\rm eff} + p_{\rm eff}\Big) = -\frac{3}{2}H^2(1 + w_{\rm eff}) \tag{5.9}$$

where the effective equation of the state parameter reads

$$w_{\rm eff} = \frac{1}{1 - \varepsilon 6\xi(1-6\xi)z^2}\Big[-1 + \varepsilon(1-6\xi)(1-w_m)x^2 + \varepsilon 2\xi(1-3w_m)(x+z)^2 + \\ +(1+w_m)(1-y^2) - \varepsilon 2\xi(1-6\xi)z^2 - 2\xi\lambda y^2 z\Big] \tag{5.10}$$

where $\lambda = -\frac{\sqrt{6}}{\kappa}\frac{1}{U(\phi)}\frac{{\rm d}U(\phi)}{{\rm d}\phi}$.

The dynamical system of the model under considerations is in the form [157]

$$\begin{aligned}
x' &= -(x - \varepsilon\frac{1}{2}\lambda y^2)\Big[1 - \varepsilon 6\xi(1-6\xi)z^2\Big] + \frac{3}{2}(x + 6\xi z)\Big[-\frac{4}{3} - 2\xi\lambda y^2 z \\
&\quad +\varepsilon(1-6\xi)(1-w_m)x^2 + \varepsilon 2\xi(1-3w_m)(x+z)^2 + (1+w_m)(1-y^2)\Big], &(5.11a)\\
y' &= y\left(2 - \frac{1}{2}\lambda x\right)\Big[1 - \varepsilon 6\xi(1-6\xi)z^2\Big] + \frac{3}{2}y\Big[-\frac{4}{3} - 2\xi\lambda y^2 z \\
&\quad +\varepsilon(1-6\xi)(1-w_m)x^2 + \varepsilon 2\xi(1-3w_m)(x+z)^2 + (1+w_m)(1-y^2)\Big], &(5.11b)\\
z' &= x\Big[1 - \varepsilon 6\xi(1-6\xi)z^2\Big], &(5.11c)\\
\lambda' &= -\lambda^2(\Gamma - 1)x\Big[1 - \varepsilon 6\xi(1-6\xi)z^2\Big], &(5.11d)
\end{aligned}$$

where $\Gamma = \frac{U(\phi)_{,\phi\phi}U(\phi)}{U(\phi)_{,\phi}^2}$ and a prime denotes differentiation with respect to time τ defined as

$$\frac{\rm d}{{\rm d}\tau} = \Big[1 - \varepsilon 6\xi(1-6\xi)z^2\Big]\frac{\rm d}{{\rm d}\ln a}. \tag{5.12}$$

If λ is constant then we obtain the scaling potential $\exp(\lambda\phi)$ and the basic system reduces to the 3-dimensional autonomous dynamical system in the case of the model with the barotropic matter. In the case without the matter the dynamical system is a 2-dimensional autonomous one.

In the rest of the chapter we will assume the following form of the function $\Gamma(\lambda)$

$$\Gamma(\lambda) = 1 - \frac{\alpha}{\lambda^2} \tag{5.13}$$

where α is an arbitrary constant beside the case of $\alpha = 0$ for which $\Gamma = 1$ which corresponds to an exponential potential. For the assumed form of $\Gamma(\lambda)$ function we can simply eliminate one of the variables namely z given by the relation

$$z(\lambda) = -\int \frac{{\rm d}\lambda}{\lambda^2\big(\Gamma(\lambda) - 1\big)} = \frac{\lambda}{\alpha} + {\rm const} \tag{5.14}$$

Table 5.1: The location and eigenvalues of the critical points in twister quintessence scenario

w_{eff}	w_ϕ	Ω_ϕ	location	eigenvalues
$\frac{1}{3}$	$\frac{1}{3}$	1	$x_1^*=0, y_1^*=0, (\lambda_1^*)^2=\frac{\alpha^2}{\varepsilon 6\xi}$	$l_1=-6\xi,\ l_2=12\xi,\ l_3=6\xi(1-3w_m)$
w_m	—	0	$x_2^*=0, y_2^*=0, \lambda_2^*=0$	$l_{1,3}=-\frac{3}{4}(1-w_m)\Big(1\pm\sqrt{1-\frac{16}{3}\xi\frac{1-3w_m}{(1-w_m)^2}}\Big)$, $l_2=\frac{3}{2}(1+w_m)$
-1	-1	1	$x_{3a}^*=0, (y_{3a}^*)^2=1, \lambda_{3a}^*=0$	$l_{1,3}=-\frac{1}{2}\Big(3\pm\sqrt{9+\varepsilon 2\alpha-48\xi}\Big),\ l_2=-3(1+w_m)$
-1	-1	1	$x_{3b}^*=0, (y_{3b}^*)^2=\frac{1}{\alpha}\varepsilon 24\xi$, $(\lambda_{3b}^*)^2=\alpha\left(\frac{\alpha}{\varepsilon 6\xi}-4\right)$	$l_1=-18\xi(1+w_m)\left(1+\frac{\varepsilon}{\alpha}4(1-6\xi)\right)$ $l_{2,3}=-3\xi\left(1+\frac{\varepsilon}{\alpha}4(1-6\xi)\right)\left(3\pm\sqrt{\frac{-7+\frac{\varepsilon}{\alpha}12(3+14\xi)}{1+\frac{\varepsilon}{\alpha}4(1-6\xi)}}\right)$

where in the rest of the chapter we take the integration constant as equal to zero.

From Eq. (5.13) and the definition of the function Γ we can simply calculate the form of the potential function

$$U(\phi)=U_0\exp\left[-\frac{\kappa^2}{6}\left(\frac{\alpha}{2}\phi^2+\beta\phi\right)\right]=\tilde{U}_0\exp\left[-\alpha\frac{\kappa^2}{12}\left(\phi+\frac{\beta}{\alpha}\right)^2\right] \tag{5.15}$$

where β is the integration constant. As we can see the dynamics of the model does not depend on the value of this parameter. In such a case we are exploring the solutions in the very rich family of potential functions.

Following the Hartman-Grobman theorem [59] the system can be well approximated by the linear part of the system around a non-degenerate critical point. Then the stability of the critical point is determined by eigenvalues of a linearization matrix only. In Table 5.1 we have gathered critical points appearing in twister scenario together with the eigenvalues of the linearization matrix calculated at those points.

The critical point of a saddle type which represents the radiation dominated universe $w_{\text{eff}}=1/3$ is $(x_1^*=0, y_1^*=0, (\lambda_1^*)^2=\frac{\alpha^2}{\varepsilon 6\xi})$ and the linearised solutions in the vicinity

of this critical point are

$$\begin{aligned} x_1(\tau) &= \tfrac{1}{2-3w_m}\Big\{\Big[x_1^{(i)} - \tfrac{1}{\alpha}(1-3w_m)(\lambda_1^{(i)}-\lambda_1^*)\Big]\exp(l_1\tau) + \\ &\quad +(1-3w_m)\Big[x_1^{(i)} + \tfrac{1}{\alpha}(\lambda_1^{(i)}-\lambda_1^*)\Big]\exp(l_3\tau)\Big\}, \\ y_1(\tau) &= y_1^{(i)}\exp(l_2\tau), \\ \lambda_1(\tau) &= \lambda_1^* - \tfrac{\alpha}{2-3w_m}\Big\{\Big[x_1^{(i)} - \tfrac{1}{\alpha}(1-3w_m)(\lambda_1^{(i)}-\lambda_1^*)\Big]\exp(l_1\tau) - \\ &\quad -\Big[x_1^{(i)} + \tfrac{1}{\alpha}(\lambda_1^{(i)}-\lambda_1^*)\Big]\exp(l_3\tau)\Big\}, \end{aligned} \tag{5.16}$$

where $l_1 = -6\xi$, $l_2 = 12\xi$ and $l_3 = 6\xi(1-3w_m)$ are eigenvalues of the linearization matrix calculated at this critical point and the transformation from time τ into the scale factor can be made using relation (5.12) calculated at the critical point

$$\ln\left(\frac{a}{a_1^{(i)}}\right) = \int_0^\tau \Big[1 - \varepsilon 6\xi(1-6\xi)z(\lambda_1^*)^2\Big]\mathrm{d}\tau = 6\xi\tau,$$

where $a_1^{(i)}$ is the initial value of the scale factor at $\tau = 0$. In the case of canonical scalar field $\varepsilon = +1$ this critical point exists only if $\xi > 0$ and for the phantom scalar field $\varepsilon = -1$ if $\xi < 0$.

The matter dominated universe where $w_{\text{eff}} = w_m$ is represented by the critical point $(x_2^* = 0, y_2^* = 0, \lambda_2^* = 0)$ which character depends on the value of the parameter d

$$d = 1 - \frac{16}{3}\xi\frac{1-3w_m}{(1-w_m)^2}.$$

For $d > 0$ the critical point is of a saddle type and the linearised solutions are in the form

$$\begin{aligned} x_2(\tau) &= \tfrac{1}{2\sqrt{d}}\Big\{(1+\sqrt{d})\Big[x_2^{(i)} + \tfrac{1}{\alpha}\tfrac{3}{4}(1-w_m)(1-\sqrt{d})\lambda_2^{(i)}\Big]\exp(l_1\tau) - \\ &\quad -(1-\sqrt{d})\Big[x_2^{(i)} + \tfrac{1}{\alpha}\tfrac{3}{4}(1-w_m)(1+\sqrt{d})\lambda_2^{(i)}\Big]\exp(l_3\tau)\Big\}, \\ y_2(\tau) &= y_2^{(i)}\exp(l_2\tau), \\ \lambda_2(\tau) &= -\tfrac{2\alpha}{3(1-w_m)\sqrt{d}}\Big\{\Big[x_2^{(i)} + \tfrac{1}{\alpha}\tfrac{3}{4}(1-w_m)(1-\sqrt{d})\lambda_2^{(i)}\Big]\exp(l_1\tau) - \\ &\quad -\Big[x_2^{(i)} + \tfrac{1}{\alpha}\tfrac{3}{4}(1-w_m)(1+\sqrt{d})\lambda_2^{(i)}\Big]\exp(l_3\tau)\Big\}. \end{aligned} \tag{5.17}$$

where $l_{1,3} = -\frac{3}{4}(1-w_m)\Big(1 \pm \sqrt{1 - \frac{16}{3}\xi\frac{1-3w_m}{(1-w_m)^2}}\Big)$, $l_2 = \frac{3}{2}(1+w_m)$ are eigenvalues of the linearization matrix.

For $d<0$ the critical point is of an unstable focus type

$$\begin{aligned}
x_2(\tau) &= -\frac{\exp\left(-\frac{3}{4}(1-w_m)\tau\right)}{\sqrt{|d|}}\left\{\left[x_2^{(i)}+\tfrac{1}{\alpha}\tfrac{3}{4}(1-w_m)(1+|d|)\lambda_2^{(i)}\right]\sin\left(\tfrac{3}{4}(1-w_m)\sqrt{|d|}\tau\right)-\right.\\
&\qquad\left.-\sqrt{|d|}x_2^{(i)}\cos\left(\tfrac{3}{4}(1-w_m)\sqrt{|d|}\tau\right)\right\},\\
y_2(\tau) &= y_2^{(i)}\exp\left(\tfrac{3}{2}(1+w_m)\tau\right),\\
\lambda_2(\tau) &= \tfrac{4}{3}\frac{\alpha\exp\left(-\frac{3}{4}(1-w_m)\tau\right)}{(1-w_m)\sqrt{|d|}}\left\{\left[x_2^{(i)}+\tfrac{1}{\alpha}\tfrac{3}{4}(1-w_m)\lambda_2^{(i)}\right]\sin\left(\tfrac{3}{4}(1-w_m)\sqrt{|d|}\tau\right)+\right.\\
&\qquad\left.+\tfrac{1}{\alpha}\tfrac{3}{4}(1-w_m)\sqrt{|d|}\lambda_2^{(i)}\cos\left(\tfrac{3}{4}(1-w_m)\sqrt{|d|}\tau\right)\right\}.
\end{aligned}\tag{5.18}$$

For both cases the transformation from time τ to the scale factor in the vicinity of the critical point corresponding to matter dominated universe is the following

$$\ln\left(\frac{a}{a_2^{(i)}}\right)=\tau,$$

where $a_2^{(i)}$ is the initial value of the scale factor at $\tau=0$.

The final critical point represents the de Sitter universe with $w_{\text{eff}}=-1$ is ($x_{3a}^*=0,(y_{3a}^*)^2=1,\lambda_{3a}^*=0$) its character depends on the value of the discriminant $\Delta_{3a}=9+\varepsilon 2\alpha-48\xi$ of the characteristic equation.

For $\Delta_{3a}<0$ the critical point is of a stable focus type and the linearised solutions are

$$\begin{aligned}
x_{3a}(\tau) &= -\frac{\exp\left(-\frac{3}{2}\tau\right)}{\sqrt{|\Delta_{3a}|}}\left\{\left[3x_3^{(i)}+\tfrac{9+|\Delta_{3a}|}{2\alpha}\lambda_3^{(i)}\right]\sin\left(\frac{\sqrt{|\Delta_{3a}|}}{2}\tau\right)-\right.\\
&\qquad\left.-x_3^{(i)}\sqrt{|\Delta_{3a}|}\cos\left(\frac{\sqrt{|\Delta_{3a}|}}{2}\tau\right)\right\},\\
y_{3a}(\tau) &= y_3^*+(y_3^{(i)}-y_3^*)\exp\left(-3(1+w_m)\tau\right),\\
\lambda_{3a}(\tau) &= \frac{2\alpha\exp\left(-\frac{3}{2}\tau\right)}{\sqrt{|\Delta_{3a}|}}\left\{\left(x_3^{(i)}+\tfrac{3}{2\alpha}\lambda_3^{(i)}\right)\sin\left(\frac{\sqrt{|\Delta_{3a}|}}{2}\tau\right)+\right.\\
&\qquad\left.+\frac{\sqrt{|\Delta|}}{2\alpha}\lambda_3^{(i)}\cos\left(\frac{\sqrt{|\Delta_{3a}|}}{2}\tau\right)\right\}.
\end{aligned}\tag{5.19}$$

For $0<\Delta_{3a}<9$ the critical point is of a stable node type and when $\Delta_{3a}>9$ is of

a saddle type. The linearised solutions in the vicinity of these types of critical points are

$$\begin{aligned} x_{3a}(\tau) &= \tfrac{1}{2\sqrt{\Delta_{3a}}}\Big\{(3+\sqrt{\Delta_{3a}})\Big[x_{3a}^{(i)}+\tfrac{1}{2\alpha}(3-\sqrt{\Delta_{3a}})\lambda_{3a}^{(i)}\Big]\exp(l_1\tau)- \\ &\quad -(3-\sqrt{\Delta_{3a}})\Big[x_{3a}^{(i)}+\tfrac{1}{2\alpha}(3+\sqrt{\Delta_{3a}})\lambda_{3a}^{(i)}\Big]\exp(l_3\tau)\Big\}, \\ y_{3a}(\tau) &= y_{3a}^{*}+(y_{3a}^{(i)}-y_{3a}^{*})\exp(l_2\tau), \\ \lambda_{3a}(\tau) &= -\tfrac{\alpha}{\sqrt{\Delta_{3a}}}\Big\{\Big[x_{3a}^{(i)}+\tfrac{1}{2\alpha}(3-\sqrt{\Delta_{3a}})\lambda_{3a}^{(i)}\Big]\exp(l_1\tau)- \\ &\quad -\Big[x_{3a}^{(i)}+\tfrac{1}{2\alpha}(3+\sqrt{\Delta_{3a}})\lambda_{3a}^{(i)}\Big]\exp(l_3\tau)\Big\}. \end{aligned} \tag{5.20}$$

where $l_{1,3}=-\frac{1}{2}\big(3\pm\sqrt{9+\varepsilon 2\alpha-48\xi}\big)$ and $l_2=-3(1+w_m)$ are eigenvalues of the linearization matrix and using relation (5.12) we can write down transformation form time τ to the scale factor a

$$\ln\left(\frac{a}{a_{3a}^{(i)}}\right)=\tau,$$

where $a_{3a}^{(i)}$ is the initial value of the scale factor at $\tau=0$. The phase diagram of the system with the de Sitter state in the form of a stable focus critical point is presented in figure 5.1.

The next critical point represents also the de Sitter state with $w_{\text{eff}}=-1$ ($x_{3b}^{*}=0$, $(y_{3b}^{*})^2=\frac{1}{\alpha}\varepsilon 24\xi$, $(\lambda_{3b}^{*})^2=\alpha\big(\frac{\alpha}{\varepsilon 6\xi}-4\big)$). The linearised solution in the vicinity of this critical point can be presented in the condensed form as

$$\begin{pmatrix} x_{3b}(\tau)-x_{3b}^{*} \\ y_{3b}(\tau)-y_{3b}^{*} \\ \lambda_{3b}(\tau)-\lambda_{3b}^{*} \end{pmatrix} = P_{3b}\begin{pmatrix} \exp(l_1\tau) & 0 & 0 \\ 0 & \exp(l_2\tau) & 0 \\ 0 & 0 & \exp(l_3\tau) \end{pmatrix} P_{3b}^{-1}\begin{pmatrix} x_{3b}^{(i)}-x_{3b}^{*} \\ y_{3b}^{(i)}-y_{3b}^{*} \\ \lambda_{3b}^{(i)}-\lambda_{3b}^{*} \end{pmatrix} \tag{5.21}$$

where the matrix

$$P_{3b}=\begin{pmatrix} -\frac{3}{\alpha}(1+w_m) & -\frac{3}{2\alpha}-\frac{\sqrt{\Delta_{3b}}}{2\alpha} & -\frac{3}{2\alpha}+\frac{\sqrt{\Delta_{3b}}}{2\alpha} \\ \frac{6(1+w_m)\left(1+\frac{\varepsilon}{\alpha}6(w_m-4\xi)\right)}{(1-3w_m)y_{3b}^{*}\lambda_{3b}^{*}} & \frac{y_{3b}^{*}\lambda_{3b}^{*}}{8\alpha}+\frac{\sqrt{\Delta_{3b}}}{8\alpha} & \frac{y_{3b}^{*}\lambda_{3b}^{*}}{8\alpha}-\frac{\sqrt{\Delta_{3b}}}{8\alpha} \\ 1 & 1 & 1 \end{pmatrix}, \tag{5.22}$$

is constructed form the corresponding eigenvectors of the linearization matrix of the system under considerations calculated at this critical point. The eigenvalues are $l_1=-18\xi(1+w_m)\big(1+\frac{\varepsilon}{\alpha}4(1-6\xi)\big)$, $l_{2,3}=-3\xi\big(1+\frac{\varepsilon}{\alpha}4(1-6\xi)\big)\big(3\pm\sqrt{\Delta_{3b}}\big)$ and $\Delta_{3b}=\frac{-7+\frac{\varepsilon}{\alpha}12(3+14\xi)}{1+\frac{\varepsilon}{\alpha}4(1-6\xi)}$. The transformation from time τ to the scale factor a from (5.12) is in the following form

$$\ln\left(\frac{a}{a_{3b}^{(i)}}\right)=6\xi\Big(1+\frac{\varepsilon}{\alpha}4(1-6\xi)\Big)\tau,$$

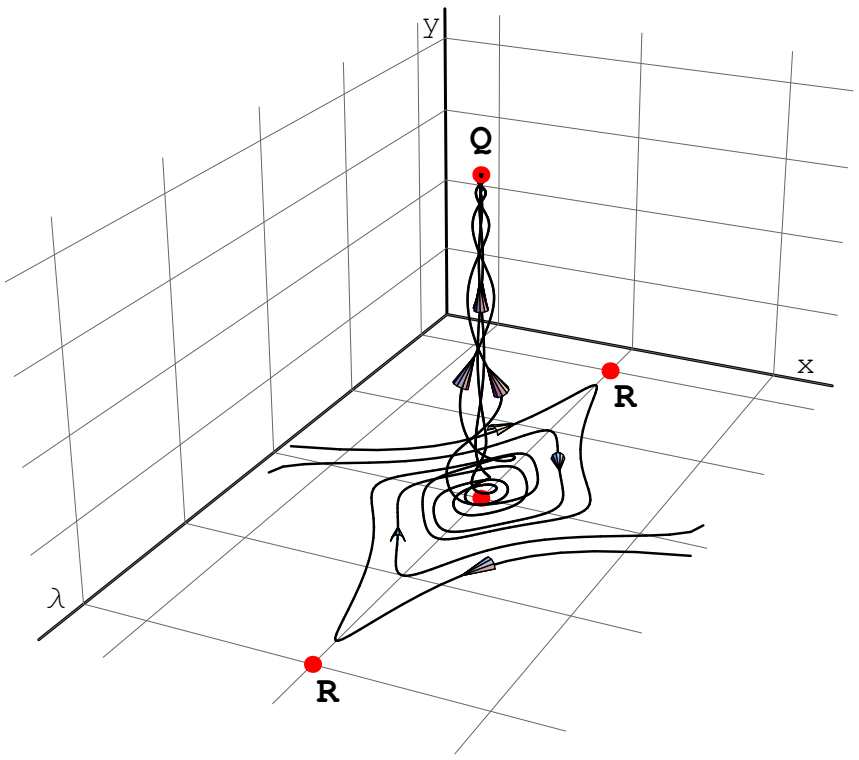

Figure 5.1: The three-dimensional phase portrait of the dynamical system under consideration for the canonical scalar field $\varepsilon = +1$, the positive coupling constant $\xi = 6$ and $\alpha = -6$. Trajectories represent a twister type solution which interpolates between the radiation dominated universe R (a saddle type critical point), the matter dominated universe (an unstable focus critical point) and the accelerating universe Q (a stable focus critical point).

where $a_{3b}^{(i)}$ is the initial value of the scale factor at $\tau = 0$. The phase space diagram for the system with one de Sitter state represented by a saddle type critical point and two stable de Sitter states is presented in figure 5.2. It is easy to check that if the critical point denoted as $3a$ is a saddle type, i.e. in the case when $\Delta_{3a} > 9$, the critical point $3b$ is a stable one.

The solutions of the linearised system in the vicinity of each critical point $x_i(a)$, $y_i(a)$ and $\lambda_i(a)$ can be used to constrain the model parameters through the cosmological data from various cosmological epochs. For example, the parameters for the solution describing the radiation dominated universe (1) can be constrained from CMB data (its effects on CMB spectrum may be different from pure photon gas [160]), and the solutions (3) describing the current accelerating expansion of the universe through the SNIa data. Therefore one can estimate the parameters of the variability with redshift of true $w(a)$ (see figure 5.3). It is possible because we have the linearization of the exact formula in different epochs.

The presented possibility of appearing of the twister type quintessence scenario is not restricted to the considered case of the $\Gamma(\lambda)$ function (5.13). One can easily show that such a scenario will be always possible if only the following functions calculated at the critical points [157]

$$f(\lambda^*) = (\lambda^*)^2\big(\Gamma(\lambda^*) - 1\big) = \text{const}, \qquad \frac{\mathrm{d}f(\lambda)}{\mathrm{d}\lambda}\Big|_{\lambda^*} = f'(\lambda^*) = \text{const}$$

are finite.

In this contribution we pointed out the presence of the new interesting solution for the non-minimally coupled scalar field cosmology which we called the twister solution (because of the shape of the corresponding trajectory in the phase space, see figures 5.1 and 5.2). This type of the solution is very interesting because in the phase space it represents the 3-dimensional trajectory which interpolates different stages of evolution of the universe, namely, the radiation dominated, dust filled and accelerating universe. We found linearised solutions around all these intermediate phases and we are able to derive approximated forms of the effective equation of the state parameter $w(a)$ in those epochs. It is interesting that the presented structure of the phase space is allowed only for a non-zero value of coupling constant, therefore it is a specific feature of the non-minimally coupled scalar field cosmology.

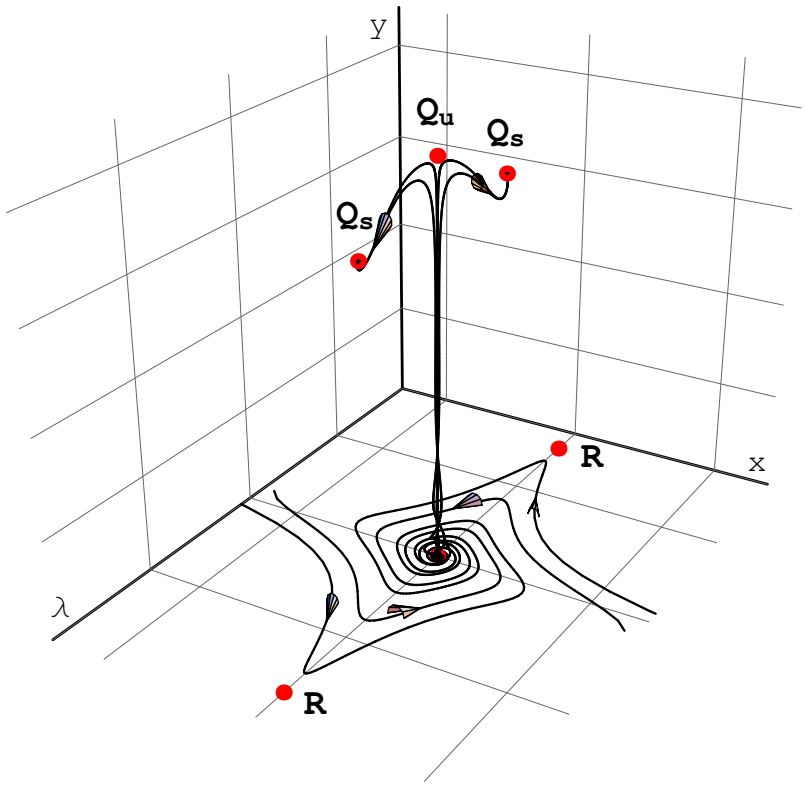

Figure 5.2: The three-dimensional phase portrait of the investigated dynamical system for the canonical scalar field $\varepsilon = +1$, the coupling constant $\xi = 6$ and $\alpha = 192$. Trajectories represent a twister typer solution interpolating between the radiation dominated universe R (a saddle type critical point), the matter dominated universe (an unstable focus critical point), the accelerating universe Q_u represented by a saddle type critical point and final de Sitter state Q_s represented by a stable focus critical point.

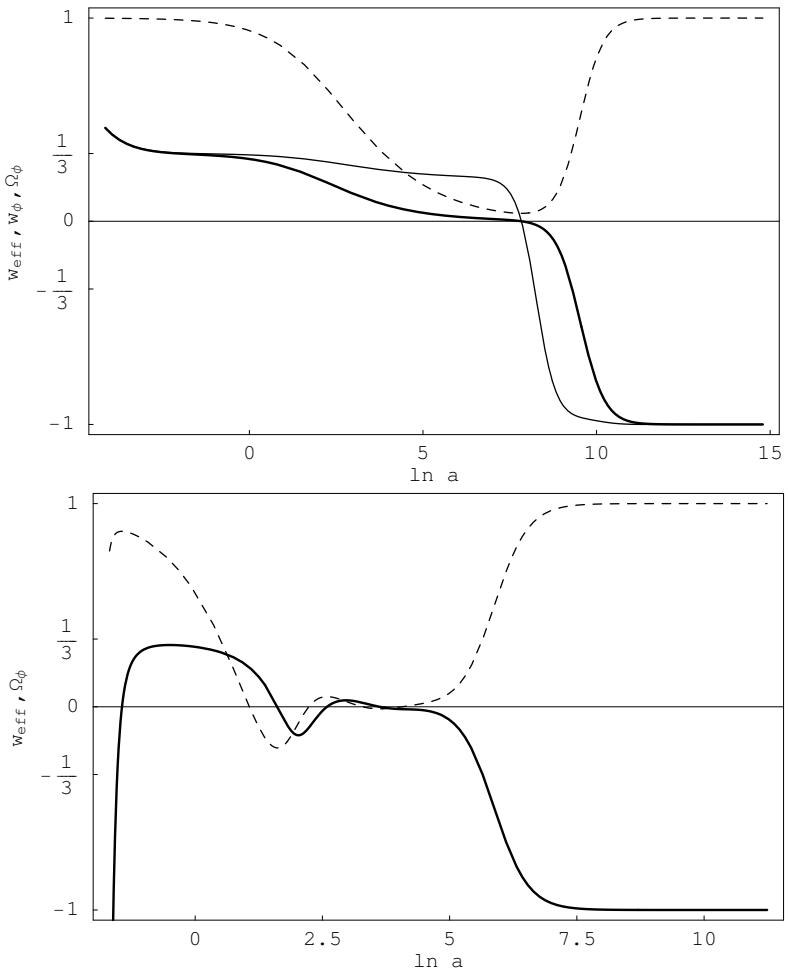

Figure 5.3: The evolution of w_{eff} given by the relation (5.10) (thick line), w_ϕ – thin line and Ω_ϕ – dashed line for the non-minimally coupled canonical scalar field $\varepsilon = +1$ and $\xi = \frac{1}{8}$, $\alpha = -6$ (left) and $\xi = 1$, $\alpha = -1$ (right). The existence of moments where $\Omega_\phi = 0$ indicate singularities in w_ϕ. The sample trajectories used to plot this relation start their evolution at $\ln a = 0$ near the saddle type critical point ($w_{\text{eff}} = 1/3$) and then approach the critical point representing the barotropic matter domination epoch $w_{\text{eff}} = w_m = 0$ and next escape to the stable de Sitter state with $w_{\text{eff}} = -1$. The existence of a short time interval during which $w_{\text{eff}} \simeq \frac{1}{3}$ is the effect of the nonzero coupling constant ξ only.

Chapter 6

Toward a unified description of cosmological evolution

We investigate dynamics of a flat FRW cosmological model with a barotropic matter and a non-minimally coupled scalar field (both canonical and phantom). In our approach we do not assume any specific form of a potential function for the scalar field and we are looking for generic scenarios of evolution. We show that the dynamics of universe can be reduced to a 3-dimensional dynamical system. We have found the set of fixed points and established their character. These critical points represent all important epochs in evolution of the universe : (a) a finite scale factor singularity, (b) an inflation (rapid-roll and slow-roll), (c) a radiation domination, (d) a matter domination and (e) a quintessence era. We have shown that the inflation, the radiation and matter domination epochs are transient ones and last for a finite amount of time. The existence of the radiation domination epoch is purely the effect of a non-minimal coupling constant. We show the existence of a twister type solution wandering between all these critical points.

Published in :

O. Hrycyna, M. Szydłowski, JCAP12(2010)016, `arXiv:1008.1432 [astro-ph.CO]`

In this chapter we investigate the dynamical evolution of scalar field cosmological models with a non-vanishing coupling constant between a scalar field and gravity. We are adopting dynamical systems methods in studying the evolution of the cosmological model and its dynamics can be visualised in the phase space which is a geometric framework for its exploration. Moreover one can investigate all evolutional paths of the system under consideration for all admissible initial conditions. Therefore one should ask whether different models with a desired property are typical (generic) in the class of all possible models. In our opinion physically interesting cosmological models should be generic in the sense that they do not depend on the special choice of initial conditions which should be determined from quantum models.

To keep generality of our considerations we do not assume any specific form of the potential function of a canonical or phantom scalar field. It will be demonstrated that the parameter of non-minimal coupling ξ plays the crucial role during the cosmological evolution. We will show the emergence of a new phase space structure organised through critical points and trajectories. For completeness we also include the model with the barotropic matter with the constant equation of state parameter w_m.

We demonstrate that, in principle, the phase space structure at a finite domain is determined by five critical points corresponding to important events during the cosmic evolution, namely, the singularity (of a finite scale factor type), inflation, radiation and matter dominated epochs and finally the accelerated expansion era. In the previous chapter we introduced the notion of the twister solutions the solutions linking the subsequent cosmological epochs [161]. In the present we generalise this notion without assuming any form of the potential function of the scalar field. The evolutional scenarios investigated in this chapter are obvious only if the non-minimal coupling is different from minimal ($\xi = 0$) and conformal ($\xi = 1/6$) coupling value. In this sense we study a unique type of evolution.

6.1 The model

In the model under consideration we assume the spatially flat FRW universe filled with the non-minimally coupled scalar field and barotropic fluid with the equation of the state coefficient w_m. The action assumes following form

$$S = \frac{1}{2}\int \mathrm{d}^4x\sqrt{-g}\left(\frac{1}{\kappa^2}R - \varepsilon\left(g^{\mu\nu}\partial_\mu\phi\partial_\nu\phi + \xi R\phi^2\right) - 2U(\phi)\right) + S_m, \tag{6.1}$$

where $\kappa^2 = 8\pi G$, $\varepsilon = +1, -1$ corresponds to canonical and phantom scalar field, respectively, the metric signature is $(-,+,+,+)$, $R = 6\left(\frac{\ddot{a}}{a} + \frac{\dot{a}^2}{a^2}\right)$ is the Ricci scalar, a is the scale factor and a dot denotes differentiation with respect to the cosmological time and $U(\phi)$ is the scalar field potential function. S_m is the action for the barotropic matter part.

The dynamical equation for the scalar field we can obtain from the variation $\delta S/\delta\phi = 0$

$$\ddot{\phi} + 3H\dot{\phi} + \xi R\phi + \varepsilon U'(\phi) = 0, \tag{6.2}$$

and energy conservation condition from the variation $\delta S/\delta g^{\mu\nu} = 0$

$$\mathcal{E} = \varepsilon\frac{1}{2}\dot{\phi}^2 + \varepsilon 3\xi H^2\phi^2 + \varepsilon 3\xi H(\phi^2)^{\cdot} + U(\phi) + \rho_m - \frac{3}{\kappa^2}H^2. \tag{6.3}$$

Then conservation conditions read

$$\frac{3}{\kappa^2}H^2 = \rho_\phi + \rho_m, \tag{6.4}$$

$$\dot{H} = -\frac{\kappa^2}{2}\Big[(\rho_\phi + p_\phi) + \rho_m(1 + w_m)\Big] \tag{6.5}$$

where the energy density and the pressure of the scalar field are

$$\rho_\phi = \varepsilon\frac{1}{2}\dot{\phi}^2 + U(\phi) + \varepsilon 3\xi H^2\phi^2 + \varepsilon 3\xi H(\phi^2)^{\cdot}, \tag{6.6}$$

$$p_\phi = \varepsilon\frac{1}{2}(1-4\xi)\dot{\phi}^2 - U(\phi) + \varepsilon\xi H(\phi^2)^{\cdot} - \varepsilon 2\xi(1-6\xi)\dot{H}\phi^2 - \varepsilon 3\xi(1-8\xi)H^2\phi^2 + 2\xi\phi U'(\phi). \tag{6.7}$$

Note that, when the non-minimal coupling is present, the energy density ρ_ϕ and the pressure p_ϕ of the scalar field can be defined in several possible inequivalent ways. This corresponds to different ways of writing the field equations. In the case adopted here the energy momentum tensor of the scalar field is covariantly conserved, which may not be true for other choices of ρ_ϕ and p_ϕ [94, 86]. For example, the redefinition of the gravitational constant $\kappa_{\text{eff}}^{-2} = \kappa^{-2} - \varepsilon\xi\phi^2$ makes it time dependent. The effective gravitational constant can diverge for a critical value of the scalar field $\phi_c = \pm(\varepsilon\kappa^2\xi)^{-1/2}$. Though the FRW model remains regular at this point, the model is unstable with respect to arbitrary small anisotropic and inhomogeneous perturbations which become infinite there. This results in the formation of a strong curvature singularity prohibiting a transition to the region $\kappa_{\text{eff}}^2 < 0$ [162].

In what follows we introduce the energy phase space variables

$$x \equiv \frac{\kappa\dot{\phi}}{\sqrt{6}H}, \quad y \equiv \frac{\kappa\sqrt{U(\phi)}}{\sqrt{3}H}, \quad z \equiv \frac{\kappa}{\sqrt{6}}\phi, \tag{6.8}$$

which are suggested by the conservation condition

$$\frac{\kappa^2}{3H^2}\rho_\phi + \frac{\kappa^2}{3H^2}\rho_m = \Omega_\phi + \Omega_m = 1 \tag{6.9}$$

or in terms of the newly introduced variables

$$\Omega_\phi = y^2 + \varepsilon\Big[(1-6\xi)x^2 + 6\xi(x+z)^2\Big] = 1 - \Omega_m. \tag{6.10}$$

The acceleration equation can be rewritten to the form

$$\dot{H} = -\frac{\kappa^2}{2}\Big(\rho_{\text{eff}} + p_{\text{eff}}\Big) = -\frac{3}{2}H^2(1 + w_{\text{eff}}) \tag{6.11}$$

where the effective equation of the state parameter reads

$$w_{\text{eff}} = \frac{1}{1-\varepsilon 6\xi(1-6\xi)z^2}\Big[-1 + \varepsilon(1-6\xi)(1-w_m)x^2 + \varepsilon 2\xi(1-3w_m)(x+z)^2 + \\ +(1+w_m)(1-y^2) - \varepsilon 2\xi(1-6\xi)z^2 - 2\xi y^2\lambda z\Big] \tag{6.12}$$

where $\lambda = -\frac{\sqrt{6}}{\kappa}\frac{1}{U(\phi)}\frac{\mathrm{d}U(\phi)}{\mathrm{d}\phi}$.

The dynamical system describing the investigated models is in the following form [157, 161]

$$\begin{aligned}
x' &= -(x - \varepsilon\frac{1}{2}\lambda y^2)\Big[1-\varepsilon 6\xi(1-6\xi)z^2\Big] + \frac{3}{2}(x+6\xi z)\Big[-\frac{4}{3} - 2\xi\lambda y^2 z + \\
&\quad +\varepsilon(1-6\xi)(1-w_m)x^2 + \varepsilon 2\xi(1-3w_m)(x+z)^2 + (1+w_m)(1-y^2)\Big], &(6.13a)\\
y' &= y\left(2 - \frac{1}{2}\lambda x\right)\Big[1-\varepsilon 6\xi(1-6\xi)z^2\Big] + \frac{3}{2}y\Big[-\frac{4}{3} - 2\xi\lambda y^2 z + \\
&\quad +\varepsilon(1-6\xi)(1-w_m)x^2 + \varepsilon 2\xi(1-3w_m)(x+z)^2 + (1+w_m)(1-y^2)\Big], &(6.13b)\\
z' &= x\Big[1-\varepsilon 6\xi(1-6\xi)z^2\Big], &(6.13c)\\
\lambda' &= -\lambda^2(\Gamma - 1)\,x\Big[1-\varepsilon 6\xi(1-6\xi)z^2\Big]. &(6.13d)
\end{aligned}$$

where a prime denotes differentiation with respect to time τ defined as

$$\frac{\mathrm{d}}{\mathrm{d}\tau} = \Big[1-\varepsilon 6\xi(1-6\xi)z^2\Big]\frac{\mathrm{d}}{\mathrm{d}\ln a} \tag{6.14}$$

Table 6.1: Different examples of potential functions for various configurations of parameters values of the assumed form of the $\Gamma(\lambda)$ function $\Gamma(\lambda) = 1 - \frac{1}{\lambda^2}\left(\alpha + \beta\lambda + \gamma\lambda^2\right)$.

parameters	$z(\lambda)$	potential function $U(\phi)$
$\alpha \neq 0,\ \beta = 0,\ \gamma = 0$	$\frac{\lambda}{\alpha} + \text{const.}$	$U_0 \exp\left(-\frac{\alpha}{2}\phi^2 + \text{const.}\phi\right)$
$\alpha = 0,\ \beta \neq 0,\ \gamma = 0$	$\frac{\ln\lambda}{\beta} + \text{const.}$	$U_0 \exp\left(\frac{\text{const.}}{\beta}\exp\left(\beta\phi\right)\right)$
$\alpha = 0,\ \beta = 0,\ \gamma \neq 0$	$-\frac{1}{\gamma\lambda} + \text{const.}$	$U_0\left(\gamma\phi - \text{const.}\right)^{\frac{1}{\gamma}}$
$\alpha \neq 0,\ \beta \neq 0,\ \gamma = 0$	$\frac{\ln(\alpha+\beta\lambda)}{\beta} + \text{const.}$	$U_0 \exp\left(\frac{1}{\beta}\left(\alpha\phi + \text{conts.}\exp\left(\beta\phi\right)\right)\right)$
$\alpha \neq 0,\ \beta = 0,\ \gamma \neq 0$	$\frac{\arctan\left(\sqrt{\frac{\gamma}{\alpha}}\lambda\right)}{\sqrt{\alpha\gamma}} + \text{const.}$	$U_0\left(\cos\left(\sqrt{\alpha\gamma}(\phi - \text{const.})\right)\right)^{\frac{1}{\gamma}}$
$\alpha = 0,\ \beta \neq 0,\ \gamma \neq 0$	$\frac{\ln\lambda - \ln(\beta+\gamma\lambda)}{\beta} + \text{const.}$	$U_0\left(\exp\left(\text{const.}\beta\right) + \gamma\exp\left(\beta\phi\right)\right)^{\frac{1}{\gamma}}$
$\alpha \neq 0,\ \beta \neq 0,\ \gamma \neq 0$	$\frac{2\arctan\left(\frac{\beta+2\gamma\lambda}{\sqrt{-\beta^2+4\alpha\gamma}}\right)}{\sqrt{-\beta^2+4\alpha\gamma}} + \text{const.}$	$U_0 \exp\left(\frac{\beta}{2\gamma}\phi\right)\left(\cos\left(\frac{1}{2}\sqrt{-\beta^2+4\alpha\gamma}(\phi - \text{const.})\right)\right)^{\frac{1}{\gamma}}$

where the expression in brackets is assumed as a positive quantity to assure that during the evolution with $\tau > 0$ the scale factor a is growing, i.e. the universe expands, and

$$\Gamma = \frac{U''(\phi)U(\phi)}{U'(\phi)^2}.$$

To investigate the dynamics of the universe described by the dynamical system (6.13) we need to define an unknown function Γ, i.e. we need to define the potential function $U(\phi)$. In the special cases of the system with the cosmological constant or exponential potential, $U = U_0 = \text{const.}$ or $U = U_0 \exp\left(-\lambda\phi\right)$, the dynamical system (6.13) can be reduced to the 3-dimensional one due to the relation $\lambda = 0$ and $\Gamma = 0$ in the former case, and $\lambda = \text{const.}$ and $\Gamma = 1$ in the latter case. Then dynamical system consists of three equations (6.13a, 6.13b, 6.13c).

There is another possibility of reduction of the system (6.13) from a 4-dimensional dynamical system to a 3-dimensional one. If we assume that $z = z(\lambda)$ and $\Gamma = \Gamma(\lambda)$, then using (6.13c) and (6.13d) we can find the function $z(\lambda)$ from the differential equation

$$\frac{\mathrm{d}z(\lambda)}{\mathrm{d}\lambda} = z'(\lambda) = -\frac{1}{\lambda^2\big(\Gamma(\lambda) - 1\big)} \tag{6.15}$$

which can be integrated for some given function $\Gamma(\lambda)$

$$z(\lambda) = -\int \frac{\mathrm{d}\lambda}{\lambda^2\big(\Gamma(\lambda) - 1\big)}. \tag{6.16}$$

Then the dynamical system describing the investigated models is in the following form

[157, 161]

$$
\begin{aligned}
x' &= -(x-\varepsilon\frac{1}{2}\lambda y^2)\Big[1-\varepsilon 6\xi(1-6\xi)z(\lambda)^2\Big]+\frac{3}{2}\left(x+6\xi z(\lambda)\right)\Big[-\frac{4}{3}-2\xi\lambda y^2 z(\lambda)+ \\
&\quad +\varepsilon(1-6\xi)(1-w_m)x^2+\varepsilon 2\xi(1-3w_m)\left(x+z(\lambda)\right)^2+(1+w_m)(1-y^2)\Big], \quad (6.17a)\\
y' &= y\left(2-\frac{1}{2}\lambda x\right)\Big[1-\varepsilon 6\xi(1-6\xi)z(\lambda)^2\Big]+\frac{3}{2}y\Big[-\frac{4}{3}-2\xi\lambda y^2 z(\lambda)+ \\
&\quad +\varepsilon(1-6\xi)(1-w_m)x^2+\varepsilon 2\xi(1-3w_m)\left(x+z(\lambda)\right)^2+(1+w_m)(1-y^2)\Big], \quad (6.17b)\\
\lambda' &= -\lambda^2\left(\Gamma(\lambda)-1\right)x\Big[1-\varepsilon 6\xi(1-6\xi)z(\lambda)^2\Big]. \quad (6.17c)
\end{aligned}
$$

where a prime denotes now differentiation with respect to time τ defined as

$$\frac{\mathrm{d}}{\mathrm{d}\tau}=\Big[1-\varepsilon 6\xi(1-6\xi)z(\lambda)^2\Big]\frac{\mathrm{d}}{\mathrm{d}\ln a} \quad (6.18)$$

and we assume that the term in bracket is positive in the phase space during the evolution.

Now we are able to express the acceleration equation (6.11) in terms of the energy phase space variables and time τ

$$\frac{\mathrm{d}\ln H^2}{\mathrm{d}\tau}=-3\Big[1-\varepsilon 6\xi(1-6\xi)z\big(\lambda(\tau)\big)^2\Big]\big(1+w_{\mathrm{eff}}\big) \quad (6.19)$$

which together with (6.12) results in

$$
\begin{aligned}
\ln\left(\frac{H}{H^{\mathrm{ini}}}\right)^2 &= -3\int_0^\tau\Big\{1+w_m+\varepsilon(1-6\xi)(1-w_m)x(\tau)^2+ \\
&\quad +\varepsilon 2\xi(1-3w_m)\Big(x(\tau)+z\big(\lambda(\tau)\big)\Big)^2- \\
&\quad -y(\tau)^2\Big(2\xi\lambda(\tau)z\big(\lambda(\tau)\big)+1+w_m\Big)- \\
&\quad -\varepsilon 8\xi(1-6\xi)z\big(\lambda(\tau)\big)^2\Big\}\mathrm{d}\tau, \quad (6.20)
\end{aligned}
$$

where H^{ini} denotes the initial value of Hubble's function at time $\tau=0$. In what follows we will be using this expression together with the linearised solutions in the vicinity of every critical point to investigate the behaviour of Hubble's function with respect to the scale factor, as well as Hubble's radius defined as

$$R_H=\frac{1}{H}.$$

For example if the function $\Gamma(\lambda)$ is assumed in the following form

$$\Gamma(\lambda)=1-\frac{1}{\lambda^2}\big(\alpha+\beta\lambda+\gamma\lambda^2\big),$$

then in Table 6.1 we have gathered forms of the functions $z(\lambda)$ and corresponding potential functions $U(\phi)$ for various configurations of values of parameters α, β and γ. As we see there are various potential functions which are the most common ones used in the literature of the subject. Of course this simple ansatz for the function $\Gamma(\lambda)$ does not manage all possible potential functions. Let us consider the following function

$$\Gamma(\lambda) = \frac{3}{4} - \frac{\sigma^2\lambda^2}{4\big(2 \pm \sqrt{4+\sigma^2\lambda^2}\big)^2}$$

as one can check from (6.16) we receive

$$z(\lambda) = -\frac{2 \pm \sqrt{4+\sigma^2\lambda^2}}{\lambda} + \text{const.}$$

and this example corresponds to the Higgs potential

$$U(\phi) = U_0\Big((\phi - \text{const.})^2 - \sigma^2\Big)^2.$$

We need to stress that the discussion presented below is not restricted to the specific potential function but is generic in the sense that it is valid for any function $\Gamma(\lambda)$ for which the integral defined in (6.16) exists.

6.2 Dynamics of universe with a potential

In our investigations of dynamics of the system given by equations (6.17) we will restrict ourselves to the finite region of the phase space, i.e. we will be interested only in the critical points in the finite domain of the phase space. The full investigations of the dynamics requires examination of critical points at infinity, i.e. compactification of the phase space with the Poincaré sphere. The procedure of transforming dynamical variables into the projective variables associated with the compactification requires that the right hand sides of the dynamical system should be polynomial. In our case this is not always true because of the form of function $z(\lambda)$ (see table 6.1). In what follows we present detailed discussion of character of critical points of the system (6.17) corresponding to different stages of cosmological evolution (table 6.2).

Table 6.2: Critical points of the system under consideration.

	x^*	y^*	λ^*	w_{eff}
1.	$x_1^* = -6\xi z(\lambda_1^*)$	$y_1^* = 0$	$\lambda_1^*\colon z(\lambda)^2 = \frac{1}{\varepsilon 6\xi(1-6\xi)}$	$\pm\infty$
2a.	$x_{2a}^* = -6\xi z(\lambda_{2a}^*)$	$(y_{2a}^*)^2 = \frac{4\xi}{2\xi\lambda_{2a}^* z(\lambda_{2a}^*)+(1+w_m)}$	$\lambda_{2a}^*\colon z(\lambda)^2 = \frac{1}{\varepsilon 6\xi(1-6\xi)}$	$w_m - 4\xi$
2b.	$x_{2b}^* = 0$	$(y_{2b}^*)^2 = \frac{2\xi(1-3w_m)}{(1-6\xi)\left(2\xi\lambda_{2b}^* z(\lambda_{2b}^*)+(1+w_m)\right)}$	$\lambda_{2b}^*\colon z(\lambda)^2 = \frac{1}{\varepsilon 6\xi(1-6\xi)}$	$\frac{w_m-2\xi}{1-6\xi}$
3a.	$x_{3a}^* : g(x) = 0$ [1]	$y_{3a}^* = 0$	$\lambda_{3a}^*\colon z(\lambda)^2 = \frac{1}{\varepsilon 6\xi(1-6\xi)}$	$\frac{1}{3}$
3b.	$x_{3b}^* = 0$	$y_{3b}^* = 0$	$\lambda_{3b}^*\colon z(\lambda)^2 = \frac{1}{\varepsilon 6\xi}$	$\frac{1}{3}$
4.	$x_4^* = 0$	$y_4^* = 0$	$\lambda_4^*\colon z(\lambda) = 0$	w_m
5.	$x_5^* = 0$	$(y_5^*)^2 = 1 - \varepsilon 6\xi z(\lambda_5^*)^2$	$\lambda_5^*\colon \lambda z(\lambda)^2 + 4z(\lambda) - \frac{\lambda}{\varepsilon 6\xi} = 0$	-1

[1] $g(x) = \varepsilon(1-4\xi-w_m)x^2 + \varepsilon 4\xi(1-3w_m)z(\lambda_{3a}^*)x + \frac{2\xi}{1-6\xi}(1-3w_m)$

6.2.1 Finite scale factor initial singularity

Our discussion of the dynamics of the model under consideration we begin with the critical point located at

$$x_1^* = -6\xi z(\lambda_1^*), \quad y_1^* = 0, \quad \lambda_1^*\colon z(\lambda)^2 = \frac{1}{\varepsilon 6\xi(1-6\xi)} \tag{6.21}$$

where the last expression means that the coordinate λ_1^* of the critical point is the solution to the equation $z(\lambda)^2 = \frac{1}{\varepsilon 6\xi(1-6\xi)}$. This critical point represents a singularity because the value of w_{eff} given by (6.12) calculated at this point is

$$w_{\text{eff}} = \pm\infty.$$

We need to stress that this critical point exists only if $\varepsilon\xi(1-6\xi) > 0$, i.e. for the canonical scalar field ($\varepsilon = +1$) for $0 < \xi < 1/6$, and for the phantom scalar field ($\varepsilon = -1$) for $\xi < 0$ or $\xi > 1/6$.

In cosmological investigations one encounters usually various types of singularities such as: initial finite scale factor singularity [163, 164], future finite scale factor singularities: the sudden future singularities [165], the Big Brake singularity [166], and the Big Boost singularity [167].

Linearised solutions in the vicinity of this critical point are

$$\begin{aligned} x_1(\tau) &= x_1^* + \left((x_1^{\text{ini}} - x_1^*) + 2(1-3\xi)z'(\lambda_1^*)(\lambda_1^{\text{ini}} - \lambda_1^*)\right)\exp(l_1\tau) - \\ &\quad -2(1-3\xi)z'(\lambda_1^*)(\lambda_1^{\text{ini}} - \lambda_1^*)\exp(l_3\tau), \qquad (6.22a) \\ y_1(\tau) &= y_1^{\text{ini}}\exp(l_2\tau), \qquad (6.22b) \\ \lambda_1(\tau) &= \lambda_1^* + (\lambda_1^{\text{ini}} - \lambda_1^*)\exp(l_3\tau). \qquad (6.22c) \end{aligned}$$

where

$$l_1 = 6\xi, \quad l_2 = 6\xi, \quad l_3 = 12\xi$$

are the eigenvalues of the linearization matrix calculated at this critical point, $x_1^{\rm ini}$, $y_1^{\rm ini}$ and $\lambda_1^{\rm ini}$ are initial conditions. For positive values of the coupling constant $\xi > 0$ this critical point represents an unstable node type critical point. For $\xi < 0$ which is possible only for the phantom scalar field ($\varepsilon = -1$) the critical point is of a stable node type.

Using the time reparameterization (6.18)

$$\mathrm{d}\ln a = \Big(1 - \varepsilon 6\xi(1-6\xi) z\big(\lambda(\tau)\big)^2\Big)\,\mathrm{d}\tau \tag{6.23}$$

and expansion into the Taylor series around the critical point coordinate λ^*

$$z(\lambda) = z(\lambda^*) + z'(\lambda^*)(\lambda - \lambda^*)$$

up to linear terms

$$z(\lambda)^2 = z(\lambda^*)^2 + 2z(\lambda^*)z'(\lambda^*)(\lambda - \lambda^*)$$

and then together with (6.22c) we have

$$z\left(\lambda(\tau)\right)^2 = z(\lambda_1^*)^2 + 2z(\lambda_1^*)z'(\lambda_1^*)(\lambda_1^{\rm ini} - \lambda_1^*)\exp\left(l_3\tau\right).$$

Inserting this expansion into the time reparameterization we receive

$$\mathrm{d}\ln a = -\varepsilon 12\xi(1-6\xi)z(\lambda_1^*)z'(\lambda_1^*)(\lambda_1^{\rm ini} - \lambda_1^*)\exp\left(l_3\tau\right)\mathrm{d}\tau$$

which can be directly integrated for $l_3 = 12\xi > 0$

$$\Delta\ln a = -\varepsilon 12\xi(1-6\xi)z(\lambda_1^*)z'(\lambda_1^*)(\lambda_1^{\rm ini} - \lambda_1^*)\int_{-\infty}^{0}\exp\left(l_3\tau\right)\mathrm{d}\tau$$

(we could take also $l_3 = 12\xi < 0$ and the integration in this expression should be taken $(0,\infty)$ because for $\xi < 0$ this critical point represents a stable node). Where the result is

$$\Delta\ln a = \ln\left(\frac{a_1^{\rm ini}}{a_s}\right) = -\varepsilon(1-6\xi)z(\lambda_1^*)z'(\lambda_1^*)(\lambda_1^{\rm ini} - \lambda_1^*)$$

Finally we receive

$$a_1^{\rm ini} = a_s\exp\left\{-\varepsilon(1-6\xi)z(\lambda_1^*)z'(\lambda_1^*)(\lambda_1^{\rm ini} - \lambda_1^*)\right\}$$

where the value in the exponent is finite, and $a_1^{\rm ini}$ is the value of the scale factor at $\tau = 0$ and a_s is the value of the scale factor at singularity. This equation gives us the scale factor

growth from singularity to the some initial point where linear approximation is still valid. From simple considerations we have that

$$z(\lambda_1^*)z'(\lambda_1^*)\big(\lambda_1^{\rm ini}-\lambda_1^*\big)<0$$

which show that the critical point under consideration represents the finite scale factor singularity. Moreover it is a past singularity for the canonical scalar field with $0<\xi<1/6$ and the phantom scalar field with $\xi>1/6$ and future singularity for the phantom scalar field with $\xi<0$.

Now, using linearised solutions (6.22), we can express (6.18) and (6.20) as parametric functions of time τ

$$\left\{\begin{array}{rcl}\ln\left(\frac{a}{a_1^{\rm ini}}\right) &=& \varepsilon(1-6\xi)z(\lambda_1^*)z'(\lambda_1^*)\big(\lambda_1^{\rm ini}-\lambda_1^*\big)\big(1-\exp\left(l_3\tau\right)\big),\\ \ln\left(\frac{H}{H_1^{\rm ini}}\right)^2 &=& 3\Big\{-4\xi\tau-\varepsilon\frac{4}{3}(1-6\xi)z(\lambda_1^*)[(x_1^{\rm ini}-x_1^*)+\\ && +2(1-3\xi)z'(\lambda_1^*)\big(\lambda_1^{\rm ini}-\lambda_1^*\big)]\big(1-\exp\left(l_1\tau\right)\big)\\ && +\varepsilon\frac{1}{3}(1-6\xi)(1-3w_m-12\xi)z(\lambda_1^*)z'(\lambda_1^*)\big(\lambda_1^{\rm ini}-\lambda_1^*\big)\big(1-\exp\left(l_3\tau\right)\big)\Big\}.\end{array}\right. \tag{6.24}$$

The linearised solutions used to obtain these relations are valid up to the Lyapunov characteristic time which is equal to the inverse of the largest eigenvalue of the linearization matrix. In our case it is $\tau_{\rm end}=\frac{1}{l_3}=\frac{1}{12\xi}$. Inserting this in to equations (6.24) we obtain maximal values of the scale factor and the Hubble's function respectively:

$$\left\{\begin{array}{rcl}\ln\left(\frac{a_1^{\rm end}}{a_1^{\rm ini}}\right) &=& \varepsilon(1-6\xi)z(\lambda_1^*)z'(\lambda_1^*)\big(\lambda_1^{\rm ini}-\lambda_1^*\big)\big(1-e\big),\\ \ln\left(\frac{H_1^{\rm end}}{H_1^{\rm ini}}\right)^2 &=& 3\Big\{-\frac{1}{3}-\varepsilon\frac{4}{3}(1-6\xi)z(\lambda_1^*)[(x_1^{\rm ini}-x_1^*)+\\ && +2(1-3\xi)z'(\lambda_1^*)\big(\lambda_1^{\rm ini}-\lambda_1^*\big)]\big(1-e\big)\\ && +\varepsilon\frac{1}{3}(1-6\xi)(1-3w_m-12\xi)z(\lambda_1^*)z'(\lambda_1^*)\big(\lambda_1^{\rm ini}-\lambda_1^*\big)\big(1-e\big)\Big\}.\end{array}\right. \tag{6.25}$$

The plot representing the evolution of these quantities together with Hubble's horizon is presented in figure 6.1. As one can simply conclude

$$\xi>0 \qquad : \qquad \lim_{\tau\to-\infty}H^2\to\infty.$$

The general conclusion is that any phantom scalar field cosmological model with the negative coupling constant $\xi<0$ and the potential function which can be represented by function $z(\lambda)$ possesses the finite scale factor future singularity with $w_{\rm eff}=\pm\infty$.

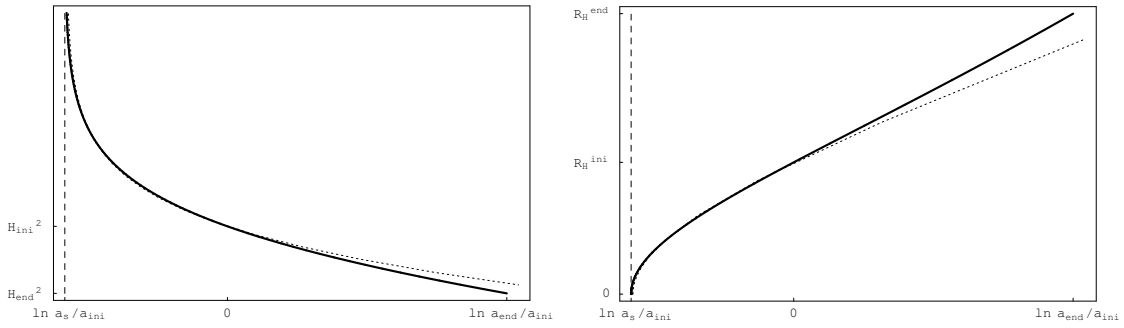

Figure 6.1: Evolution of $\ln H^2$ (left panel) and R_H (right panel) as a function of a natural logarithm of the scale factor $\ln a$ for a sample trajectory with $\varepsilon = +1$, $\xi = \frac{1}{8}$, $z'(\lambda_1^*) = \frac{1}{\alpha} = 100$ in the vicinity of the critical point corresponding to the finite scale factor singularity. The solid black line represents the linearised solution (6.24) and the dotted line corresponds to the numerical solution of the system (6.17).

6.2.2 Inflation with the non-minimal coupling and arbitrary potential

Now we proceed to the very important phase of the evolution of the universe, namely the inflation.

Fast-roll inflation

The critical point located at

$$x_{2a}^* = -6\xi z(\lambda_{2a}^*), \quad (y_{2a}^*)^2 = \frac{4\xi}{2\xi\lambda_{2a}^* z(\lambda_{2a}^*) + (1+w_m)}, \quad \lambda_{2a}^* : z(\lambda)^2 = \frac{1}{\varepsilon 6\xi(1-6\xi)} \tag{6.26}$$

with

$$w_{\text{eff}} = w_m - 4\xi$$

we identify as a fast-roll inflation (or rapid-roll) [168, 169, 170]. The first reason is that w_{eff} calculated at this critical point can be made close to -1 especially for the phantom scalar field, and the second one is that the first coordinate of this point, using transformations (6.8) can be put in the following form

$$\dot{\phi} = -6\xi H\phi$$

which for the conformal coupling $\xi = 1/6$, reduces to condition for the rapid-roll inflation given by Kofman and Mukohyama in [169]. That is we identify this critical point as a generalisation to the non-minimally coupled case (both for the canonical and phantom

scalar fields) with additional presence of the barotropic matter with the equation of state parameter w_m.

The linearization matrix for this critical point is the following

$$A_{2a} = \begin{pmatrix} 0 & 0 & \frac{\partial x'}{\partial \lambda}\big|_{2a} \\ \frac{\partial y'}{\partial x}\big|_{2a} & -12\xi & \frac{\partial y'}{\partial \lambda}\big|_{2a} \\ 0 & 0 & 12\xi \end{pmatrix}, \tag{6.27}$$

where

$$\begin{aligned} \frac{\partial x'}{\partial \lambda}\big|_{2a} &= -3(y^*_{2a})^2\Big(1 + w_m + 4\xi(1-3\xi)\lambda^*_{2a} z(\lambda^*_{2a})\Big) z'(\lambda^*_{2a}), \\ \frac{\partial y'}{\partial x}\big|_{2a} &= -\varepsilon 12\xi(1-6\xi) y^*_{2a} z(\lambda^*_{2a}), \\ \frac{\partial y'}{\partial \lambda}\big|_{2a} &= -3\xi y^*_{2a}\Big[(y^*_{2a})^2 z(\lambda^*_{2a}) + \Big(\varepsilon 6(1-6\xi)(1+w_m) z(\lambda^*_{2a}) + (2+(y^*_{2a})^2)\lambda^*_{2a}\Big) z'(\lambda^*_{2a})\Big] \end{aligned}$$

The eigenvalues of the linearization matrix are obviously $l_1 = 0$, $l_2 = 12\xi$ and $l_3 = -12\xi$. Thus the fixed point is a non-hyperbolic and we cannot make any conclusions concerning its stability based on linearization and the Hartman-Grobman theorem is not applicable [59, 60]. The answer to the question of stability or instability lies in the center manifold theory (see appendix C).

We apply following procedure: first, we expand the right hand side of the dynamical system (6.17) into the Taylor series around the critical point (6.26) up to second order, and second, we make following change of dynamical variables

$$\begin{pmatrix} u \\ v \\ w \end{pmatrix} = P^{-1}_{2a} \begin{pmatrix} x - x^*_{2a} \\ y - y^*_{2a} \\ \lambda - \lambda^*_{2a} \end{pmatrix},$$

where the matrix P_{2a} is constructed from eigenvectors of the linearization matrix (6.27) calculated for corresponding eigenvalues and its inverse is

$$P^{-1}_{2a} = \begin{pmatrix} 1 & 0 & -\frac{1}{12\xi}\frac{\partial x'}{\partial \lambda}\big|_{2a} \\ -\frac{1}{12\xi}\frac{\partial y'}{\partial x}\big|_{2a} & 1 & -\frac{1}{24\xi}\left(-\frac{1}{12\xi}\frac{\partial x'}{\partial \lambda}\big|_{2a}\frac{\partial y'}{\partial x}\big|_{2a} + \frac{\partial y'}{\partial \lambda}\big|_{2a}\right) \\ 0 & 0 & 1 \end{pmatrix}.$$

Then dynamical system in the vicinity of the critical point representing the fast-roll inflation

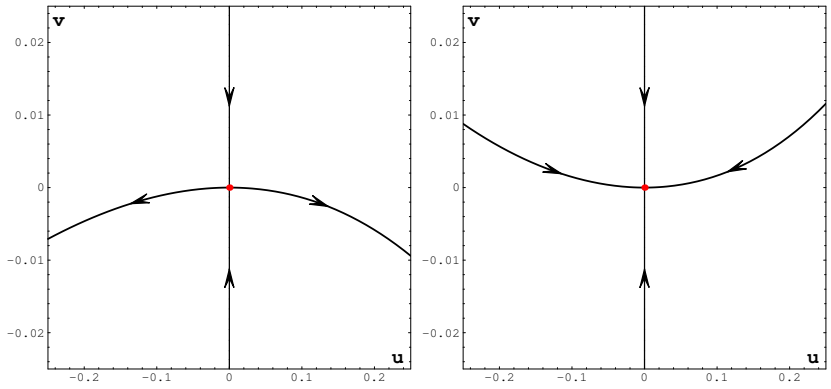

Figure 6.2: The phase portrait for the system (6.29) on the invariant submanifold in the vicinity of the critical point corresponding to the rapid-roll inflation. The bold line represents the center manifold for the problem. On the left diagram we present an unstable case for $\varepsilon(1-3w_m) < 0$ and the right diagram for a stable case for $\varepsilon(1-3w_m) > 0$. The example is given for $z(\lambda) = \frac{\lambda}{\alpha}$ and $\alpha = 1$, $w_m = 0$ left for $\varepsilon = -1$ and $\xi = 1/4$, right for $\varepsilon = 1$ and $\xi = 1/8$.

is in the following form

$$\begin{aligned} u' &= -3y^*_{2a}\Big(2\xi\lambda^*_{2a}z(\lambda^*_{2a}) + 1 + w_m\Big)uv + A_u w^2 + B_u vw + C_u uw, && \text{(6.28a)}\\ v' &= -12\xi v + \varepsilon\frac{1}{2}(1-3w_m)y^*_{2a}u^2 - \frac{9}{2}\Big(2\xi\lambda^*_{2a}z(\lambda^*_{2a}) + 1 + w_m\Big)y^*_{2a}v^2 \\ &\quad +\varepsilon 12\xi(1-6\xi)z(\lambda^*_{2a})uv + A_v w^2 + B_v vw + C_v uw, && \text{(6.28b)}\\ w' &= 12\xi w + A_w w^2 + B_w uw, && \text{(6.28c)} \end{aligned}$$

where A_i, B_i and C_i are coefficients consisting of second derivatives of right-hand sides of dynamical system (6.17) calculated at the critical point under considerations. We can note that this dynamical system admits the invariant submanifold $w = 0$, and the dynamics can be well approximated on this submanifold. Then

$$\begin{aligned} u' &= -3y^*_{2a}\Big(2\xi\lambda^*_{2a}z(\lambda^*_{2a}) + 1 + w_m\Big)uv, && \text{(6.29a)}\\ v' &= -12\xi v + \varepsilon\frac{1}{2}(1-3w_m)y^*_{2a}u^2 - \frac{9}{2}\Big(2\xi\lambda^*_{2a}z(\lambda^*_{2a}) + 1 + w_m\Big)y^*_{2a}v^2 \\ &\quad +\varepsilon 12\xi(1-6\xi)z(\lambda^*_{2a})uv, && \text{(6.29b)} \end{aligned}$$

on the invariant submanifold $w = 0$.

From the center manifold theorem (appendix C) we have

$$v = h(u) = \varepsilon\frac{1}{24\xi}(1-3w_m)y^*_{2a}u^2 + \frac{1-6\xi}{24\xi}(1-3w_m)z(\lambda^*_{2a})y^*_{2a}u^3 + O(u^4)$$

and inserting this approximation into (6.29a) we receive that the vector field restricted to the center manifold is given by

$$\eta' = -\varepsilon\frac{1}{2}(1-3w_m)\eta^3 + O(\eta^4),$$

which indicates that for $\varepsilon(1-3w_m) < 0$ it is an unstable and for $\varepsilon(1-3w_m) > 0$ it is a stable critical point on the invariant submanifold $w = 0$ (see figure 6.2 example for $z(\lambda) = \frac{\lambda}{\alpha}$). This equation can be simply integrated resulting in

$$\eta(\tau)^2 = \frac{(\eta^{\rm ini})^2}{(\eta^{\rm ini})^2\varepsilon(1-3w_m)\tau + 1}.$$

Above equation describes behaviour of the system on the center manifold which constitutes the invariant submanifold. This solution can be used in construction of exact solution of the system (6.29) in the vicinity of the critical point representing the fast-roll inflation epoch.

Using the solution from the center manifold theorem and keeping linear term in w only

$$u(\tau)v(\tau) \propto u(\tau)^3 \approx 0, \quad v(\tau)w(\tau) \propto u(\tau)^2 w(\tau) \approx 0, \quad v(\tau)^2 \propto u(\tau)^4 \approx 0,$$
$$w(\tau)^2 \approx 0, \quad u(\tau)w(\tau) \approx 0$$

from (6.18) and (6.20) we get the parametric equations for the evolution of the scale factor and Hubble's function

$$\begin{cases} \ln\left(\frac{a}{a_{2a}^{\rm ini}}\right) &= -\varepsilon(1-6\xi)z(\lambda_{2a}^*)z'(\lambda_{2a}^*)w^{\rm ini}\Big(\exp(12\xi\tau)-1\Big), \\ \ln\left(\frac{H}{H_{2a}^{\rm ini}}\right)^2 &= -\frac{1}{4\xi}Aw^{\rm ini}\Big(\exp(12\xi\tau)-1\Big), \end{cases} \tag{6.30}$$

which can be easy combine resulting in

$$\ln\left(\frac{H}{H_{2a}^{\rm ini}}\right)^2 = -\frac{A}{\varepsilon 4\xi(1-6\xi)z(\lambda_{2a}^*)z'(\lambda_{2a}^*)}\ln\left(\frac{a}{a_{2a}^{\rm ini}}\right) \tag{6.31}$$

where

$$A = \frac{1}{72\Big(2\xi\lambda_{2a}^* z(\lambda_{2a}^*)+(1+w_m)\Big)}\Big\{\big[\ -\varepsilon 144\xi(1-6\xi)(1+w_m)(1+3w_m)z(\lambda_{2a}^*)+$$
$$+96\xi(2-9\xi)\lambda_{2a}^* + 288\xi^2(\lambda_{2a}^*)^2 z(\lambda_{2a}^*)\big]z'(\lambda_{2a}^*)-$$
$$-288\xi^2 z(\lambda_{2a}^*)\Big\}.$$

One can conclude that $|A| \ll 1$ is needed in order to achieve $H^2 \approx$ const. during the evolution. The linearised solution in w direction is valid up to the Lyapunov time $\tau_{end} =$

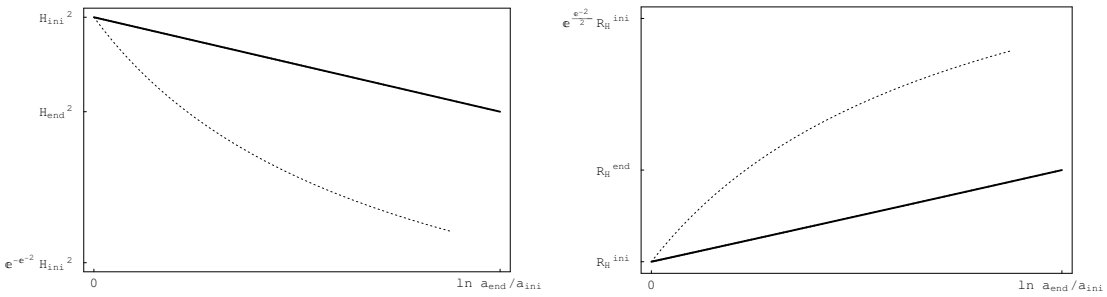

Figure 6.3: Evolution of $\ln H^2$ (left panel) and R_H (right panel) as a function of natural logarithm of the scale factor $\ln a$ for a sample trajectory with $\varepsilon = -1$, $\xi = \frac{1}{4}$, $z'(\lambda_1^*) = \frac{1}{\alpha} = 10$ in the vicinity of the critical point corresponding to the fast-roll inflation. The solid black line represents the linearised solution (6.30) and the dotted line represents the numerical solution of the system (6.17).

$\frac{1}{12\xi}$, using this we obtain maximal values of the scale factor and the Hubble's function respectively:

$$\begin{cases} \ln\left(\frac{a_{2a}^{\text{end}}}{a_{2a}^{\text{ini}}}\right) &= -\varepsilon(1-6\xi)z(\lambda_{2a}^*)z'(\lambda_{2a}^*)w^{\text{ini}}\Big(e-1\Big), \\ \ln\left(\frac{H_{2a}^{\text{end}}}{H_{2a}^{\text{ini}}}\right)^2 &= -\frac{1}{4\xi}Aw^{\text{ini}}\Big(e-1\Big), \end{cases} \tag{6.32}$$

In figure 6.3 we present the evolution of Hubble's function and Hubble's horizon in the vicinity of this critical point.

Slow-roll inflation

The critical point located at

$$x_{2b}^* = 0, \quad (y_{2b}^*)^2 = \frac{2\xi(1-3w_m)}{(1-6\xi)\big(2\xi\lambda_{2b}^* z(\lambda_{2b}^*) + (1+w_m)\big)}, \quad \lambda_{2b}^*\colon z(\lambda)^2 = \frac{1}{\varepsilon 6\xi(1-6\xi)} \tag{6.33}$$

with

$$w_{\text{eff}} = \frac{w_m - 2\xi}{1-6\xi}$$

we identify as representing the phase of a slow-roll inflation due to $x \propto \dot{\phi}$ so the dynamics in the vicinity of this point corresponds to the slow-roll condition $\dot{\phi} \approx 0$.

The linearization matrix is in the form

$$A_{2b} = \begin{pmatrix} \frac{\partial x'}{\partial x}\big|_{2b} & \frac{\partial x'}{\partial y}\big|_{2b} & \frac{\partial x'}{\partial \lambda}\big|_{2b} \\ \frac{\partial y'}{\partial x}\big|_{2b} & \frac{\partial y'}{\partial y}\big|_{2b} & \frac{\partial y'}{\partial \lambda}\big|_{2b} \\ 0 & 0 & 0 \end{pmatrix}, \tag{6.34}$$

where nonzero elements are

$$\begin{aligned}
\tfrac{\partial x'}{\partial x}\big|_{2b} &= \tfrac{6\xi}{1-6\xi}(1-3w_m),\\
\tfrac{\partial x'}{\partial y}\big|_{2b} &= -18\xi\Big(2\xi\lambda^*_{2b}z(\lambda^*_{2b})+(1+w_m)\Big)y^*_{2b}z(\lambda^*_{2b}),\\
\tfrac{\partial x'}{\partial \lambda}\big|_{2b} &= \tfrac{3}{1-6\xi}(y^*_{2b})^2\Big(-\varepsilon\xi+(1-6\xi)z'(\lambda^*_{2b})\big(6\xi^2\lambda^*_{2b}z(\lambda^*_{2b})+(1+w_m)\big)\Big),\\
\tfrac{\partial y'}{\partial x}\big|_{2b} &= \varepsilon 6\xi(1-3w_m)y^*_{2b}z(\lambda^*_{2b}),\\
\tfrac{\partial y'}{\partial y}\big|_{2b} &= -\tfrac{6\xi}{1-6\xi}(1-3w_m),\\
\tfrac{\partial y'}{\partial \lambda}\big|_{2b} &= -3\xi y^*_{2b}\Big((y^*_{2b})^2z(\lambda^*_{2b})+z'(\lambda^*_{2b})\big((y^*_{2b})^2\lambda^*_{2b}+\varepsilon 6z(\lambda^*_{2b})(1+w_m-8\xi)\big)\Big),
\end{aligned}$$

and additionally we have the following relation

$$\frac{\partial x'}{\partial x}\Big|_{2b}\frac{\partial y'}{\partial y}\Big|_{2b} = -\left(\frac{6\xi}{1-6\xi}\right)^2(1-3w_m)^2.$$

The characteristic equation for the linearization matrix gives us vanishing eigenvalues $l_1 = l_2 = l_3 = 0$, so the critical point is degenerated. In this case we cannot use standard procedures, following the Hartman-Grobman theorem [59, 60] of determining qualitative behaviour of the investigated system in the vicinity of this critical point. Instead we can notice that the linearization matrix A_{2b} calculated at this critical point is nilpotent of order 3, i.e. $(A_{2b})^3 = 0$. Then solution of the linearised problem can be presented in the following form

$$\mathbf{x}(\tau) = \Big[1 + A_{2b}\tau + \frac{1}{2}(A_{2b})^2\tau^2\Big]\mathbf{x}_0$$

Finally solutions in the vicinity of this degenerated critical point up to linear terms are

$$\begin{aligned}
x(\tau) &= x^{\rm ini}_{2b} + \left(\tfrac{\partial x'}{\partial x}\Big|_{2b}(x^{\rm ini}_{2b}-x^*_{2b}) + \tfrac{\partial x'}{\partial y}\Big|_{2b}(y^{\rm ini}_{2b}-y^*_{2b}) + \tfrac{\partial x'}{\partial \lambda}\Big|_{2b}(\lambda^{\rm ini}_{2b}-\lambda^*_{2b})\right)\tau\\
&\quad + \tfrac{1}{2}\left(\tfrac{\partial x'}{\partial x}\Big|_{2b}\tfrac{\partial x'}{\partial \lambda}\Big|_{2b} + \tfrac{\partial x'}{\partial y}\Big|_{2b}\tfrac{\partial y'}{\partial \lambda}\Big|_{2b}\right)(\lambda^{\rm ini}_{2b}-\lambda^*_{2b})\tau^2,\\
y(\tau) &= y^{\rm ini}_{2b} + \left(\tfrac{\partial y'}{\partial x}\Big|_{2b}(x^{\rm ini}_{2b}-x^*_{2b}) + \tfrac{\partial y'}{\partial y}\Big|_{2b}(y^{\rm ini}_{2b}-y^*_{2b}) + \tfrac{\partial y'}{\partial \lambda}\Big|_{2b}(\lambda^{\rm ini}_{2b}-\lambda^*_{2b})\right)\tau\\
&\quad + \tfrac{1}{2}\left(\tfrac{\partial y'}{\partial y}\Big|_{2b}\tfrac{\partial y'}{\partial \lambda}\Big|_{2b} + \tfrac{\partial y'}{\partial x}\Big|_{2b}\tfrac{\partial x'}{\partial \lambda}\Big|_{2b}\right)(\lambda^{\rm ini}_{2b}-\lambda^*_{2b})\tau^2,\\
\lambda(\tau) &= \lambda^{\rm ini}_{2b}.
\end{aligned} \tag{6.35}$$

where

$$\begin{aligned}
\tfrac{\partial x'}{\partial x}\big|_{2b}\tfrac{\partial x'}{\partial \lambda}\big|_{2b} + \tfrac{\partial x'}{\partial y}\big|_{2b}\tfrac{\partial y'}{\partial \lambda}\big|_{2b} &= 36\xi(1+w_m)\big(2+3\xi\lambda^*_{2b}z(\lambda^*_{2b})\big)(y^*_{2b})^2z'(\lambda^*_{2b}),\\
\tfrac{\partial y'}{\partial y}\big|_{2b}\tfrac{\partial y'}{\partial \lambda}\big|_{2b} + \tfrac{\partial y'}{\partial x}\big|_{2b}\tfrac{\partial x'}{\partial \lambda}\big|_{2b} &= 18\xi(1+w_m)\big(\lambda^*_{2b}+\varepsilon 4(1-6\xi)z(\lambda^*_{2b})\big)(y^*_{2b})^3z'(\lambda^*_{2b}).
\end{aligned}$$

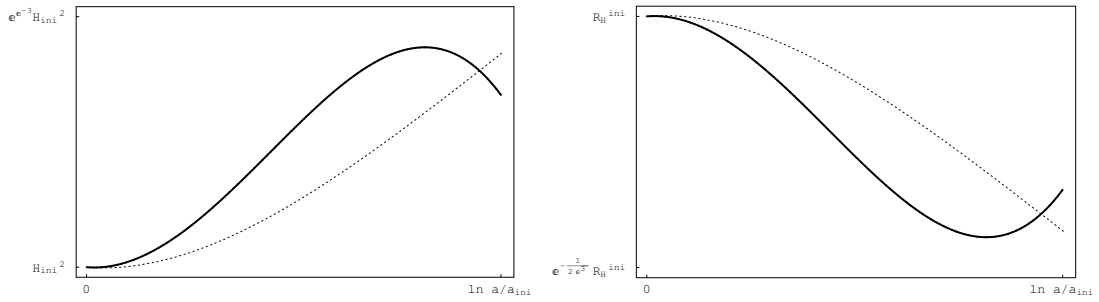

Figure 6.4: Evolution of $\ln H^2$ (left panel) and R_H (right panel) as a function of the natural logarithm of the scale factor $\ln a$ for a sample trajectory with $\varepsilon = +1$, $\xi = \frac{1}{8}$, $z'(\lambda_1^*) = \frac{1}{\alpha} = 100$ in the vicinity of the critical point corresponding to the slow-roll inflation. The solid black line represents the linearised solution (6.35) and the dotted line represents the numerical solution of the system (6.17).

These linearised solutions are valid up to a maximal value of the time parameter $\tau = \tau_{\max}$ which can be used to calculate the scale factor growth during the slow roll inflation

$$\ln \frac{a_{si}^{\text{end}}}{a_{si}^{\text{start}}} = -\varepsilon 24\xi(1-6\xi)z(\lambda_{2b}^*)z'(\lambda_{2b}^*)\big(\lambda_{2b}^{\text{ini}} - \lambda_{2b}^*\big)\tau_{\max}.$$

The direct application of the linearised solutions (6.35) to (6.18) and (6.20) gives us the approximated evolution of Hubble's function in the vicinity of the critical point representing the slow-roll inflation (figure 6.4).

6.2.3 Radiation domination epoch generated by non-minimal coupling

The following critical point located at

$$x_{3a}^*\colon g(x) = 0, \quad y_{3a}^* = 0, \quad \lambda_{3a}^*\colon z(\lambda)^2 = \frac{1}{\varepsilon 6\xi(1-6\xi)} \tag{6.36}$$

where $g(x) = \varepsilon(1-4\xi-w_m)x^2 + \varepsilon 4\xi(1-3w_m)z(\lambda_{3a}^*)x + \frac{2\xi}{1-6\xi}(1-3w_m)$ and at this point value of the effective equation of the state parameter is

$$w_{\text{eff}} = \frac{1}{3}$$

represents the radiation dominated universe. With solutions to $g(x) = 0$ equation in th form

$$x_{1,2} = \frac{1}{\varepsilon 2(1-4\xi-w_m)}\left\{-\varepsilon 4\xi(1-3w_m)z(\lambda_{3a}^*) \pm \sqrt{-\varepsilon\frac{16}{3}\xi(1-3w_m)}\right\}$$

which is real only if the expression in square root is positive and for the barotropic matter with $w_m < \frac{1}{3}$ it is possible only if $\varepsilon\xi < 0$. We are interested only in evolution with $\xi > 0$ because of the discussion of the critical point representing the finite scale factor singularity, and this is the reason we identify this critical point as representing a radiation dominated epoch only for the phantom scalar field.

The linearization matrix calculated at this point is in the following form

$$A_{3a} = \begin{pmatrix} \frac{\partial x'}{\partial x}\big|_{3a} & 0 & \frac{\partial x'}{\partial \lambda}\big|_{3a} \\ 0 & 0 & 0 \\ 0 & 0 & \frac{\partial \lambda'}{\partial \lambda}\big|_{3a} \end{pmatrix}, \tag{6.37}$$

where

$$\begin{aligned} \tfrac{\partial x'}{\partial x}\big|_{3a} &= \varepsilon 12\xi(1-6\xi)z(\lambda^*_{3a})x^*_{3a}, \\ \tfrac{\partial x'}{\partial \lambda}\big|_{3a} &= \varepsilon 6\xi z'(\lambda^*_{3a})\Big[2(1-6\xi)z(\lambda^*_{3a})x^*_{3a} + (1-3w_m)\big(x^*_{3a}+6\xi z(\lambda^*_{3a})\big)\big(x^*_{3a}+z(\lambda^*_{3a})\big)\Big], \\ \tfrac{\partial \lambda'}{\partial \lambda}\big|_{3a} &= -\varepsilon 12\xi(1-6\xi)z(\lambda^*_{3a})x^*_{3a}. \end{aligned}$$

Eigenvalues of the linearization matrix are $l_1 = -\varepsilon 12\xi(1-6\xi)z(\lambda^*_{3a})x^*_{3a}$, $l_2 = 0$, $l_3 = \varepsilon 12\xi(1-6\xi)z(\lambda^*_{3a})x^*_{3a}$. This indicates that the critical point is non-hyperbolic one and the standard linearization procedure will be inefficient and we need to proceed with the center manifold theorem (see appendix C) and the procedure described during the discussion of the critical point representing fast-roll inflation. We make following change of dynamical variables

$$\begin{pmatrix} u \\ v \\ w \end{pmatrix} = P^{-1}_{3a} \begin{pmatrix} x - x^*_{3a} \\ y - y^*_{3a} \\ \lambda - \lambda^*_{3a} \end{pmatrix},$$

where matrix P_{3a} is constructed from eigenvectors of the linearization matrix (6.37) and its inverse is

$$P^{-1}_{3a} = \begin{pmatrix} 0 & 0 & 1 \\ 0 & 1 & 0 \\ 1 & 0 & \chi \end{pmatrix}, \qquad \text{and} \qquad \chi = \frac{\frac{\partial x'}{\partial \lambda}\big|_{3a}}{\frac{\partial x'}{\partial x}\big|_{3a} - \frac{\partial \lambda'}{\partial \lambda}\big|_{3a}}.$$

Then dynamical system can be presented in the following form

$$\begin{aligned} u' &= -\varepsilon 12\xi(1-6\xi)z(\lambda^*_{3a})x^*_{3a}u + A_u u^2 + B_u uw, \\ v' &= A_v uv + B_v vw, \\ w' &= \varepsilon 12\xi(1-6\xi)z(\lambda^*_{3a})x^*_{3a}w + A_w u^2 + B_w v^2 + C_w w^2 + D_w uw, \end{aligned} \tag{6.38}$$

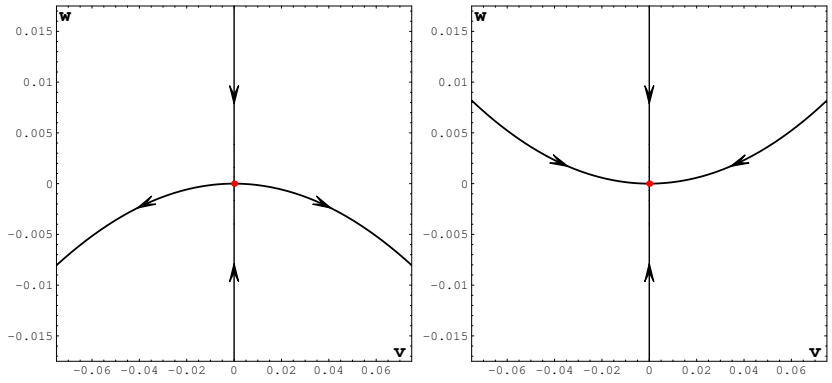

Figure 6.5: The phase portrait for the system (6.41) on the invariant submanifold $u = 0$ in the vicinity of the critical point corresponding to the radiation dominated universe with $w_{\text{eff}} = \frac{1}{3}$. The bold parabola shaped line represents the center submanifold for the problem. On the left diagram we present an unstable case and on the right diagram for a stable case. The example is given for $z(\lambda) = \frac{\lambda}{\alpha}$, $\varepsilon = -1$, $w_m = 0$, $\xi = 1/4$ and $\alpha = 1$ (left) and $\alpha = -4$ (right).

where A_i, B_i, C_i and D_i are coefficients consisting of second derivatives of the right hand sides of dynamical system (6.17) calculated at the critical point (6.36).

One can note that above dynamical system admits two invariant submanifolds namely $v = 0$ and $u = 0$.

On the first invariant submanifold the system can be simply reduced to

$$\begin{aligned} u' &= -\varepsilon 12\xi(1-6\xi)z(\lambda^*_{3a})x^*_{3a}u \\ w' &= \varepsilon 12\xi(1-6\xi)z(\lambda^*_{3a})x^*_{3a}w, \end{aligned} \tag{6.39}$$

resulting in the solution representing a saddle type critical point in the form

$$\begin{aligned} u(\tau) &= u^{\text{ini}} \exp\big(-\varepsilon 12\xi(1-6\xi)z(\lambda^*_{3a})x^*_{3a}\tau\big), \\ w(\tau) &= w^{\text{ini}} \exp\big(\varepsilon 12\xi(1-6\xi)z(\lambda^*_{3a})x^*_{3a}\tau\big). \end{aligned} \tag{6.40}$$

On the other hand we can also restrict our system to the invariant submanifold defined by $u = 0$, then

$$\begin{aligned} v' &= B_v vw, \\ w' &= \frac{\partial x'}{\partial x}\Big|_{3a} w + B_w v^2 + C_w w^2, \end{aligned} \tag{6.41}$$

and from the center manifold theorem (see appendix C) we have

$$w = h(v) = -\frac{B_w}{\frac{\partial x'}{\partial x}|_{3a}}v^2 + \frac{B_w^2}{(\frac{\partial x'}{\partial x}|_{3a})^3}(2B_v - C_w)v^4 + O(v^5)$$

and inserting this approximation into first equation of the system (6.41) we receive that the vector field restricted to the center manifold is given by

$$\eta' = -\frac{B_v B_w}{\frac{\partial x'}{\partial x}|_{3a}}\eta^3 + O(\eta^4)$$

where

$$\frac{B_v B_w}{\frac{\partial x'}{\partial x}|_{3a}} = -\varepsilon\frac{\lambda^*_{3a}}{2(1-6\xi)z(\lambda^*_{3a})} - \frac{3}{2}(1+w_m)$$

and this indicates that for $\frac{B_v B_w}{\frac{\partial x'}{\partial x}|_{3a}} < 0$ it is an unstable and for $\frac{B_v B_w}{\frac{\partial x'}{\partial x}|_{3a}} > 0$ it is a stable critical point on the invariant submanifold $u = 0$ (see figure 6.5 for an example for $z(\lambda) = \frac{\lambda}{\alpha}$).

Now we are ready to present the evolution of Hubble's function in the vicinity of this critical point. First, we use approximated solutions (6.40) on the invariant submanifold $v = 0$. We have

$$\begin{cases} \ln\left(\frac{a}{a^{\rm ini}_{3a}}\right) &= \frac{z'(\lambda^*_{3a})}{x^*_{3a}}u^{\rm ini}\Big(\exp\big(-\varepsilon 12\xi(1-6\xi)z(\lambda^*_{3a})x^*_{3a}\tau\big)-1\Big), \\ \ln\left(\frac{H}{H^{\rm ini}_{3a}}\right)^2 &= \frac{1-3w_m}{1-6\xi}\frac{x^*_{3a}+6\xi z(\lambda^*_{3a})}{(x^*_{3a})^2}w^{\rm ini}\Big(\exp\big(\varepsilon 12\xi(1-6\xi)z(\lambda^*_{3a})x^*_{3a}\tau\big)-1\Big)- \\ & \quad -\Big(4+\frac{1-w_m}{4\xi}\frac{x^*_{3a}}{z(\lambda^*_{3a})}\Big)\frac{z'(\lambda^*_{3a})}{x^*_{3a}}u^{\rm ini}\Big(\exp\big(-\varepsilon 12\xi(1-6\xi)z(\lambda^*_{3a})x^*_{3a}\tau\big)-1\Big) \end{cases} \tag{6.42}$$

On the other hand, using the solution from a center manifold and keeping only linear terms in u

$$w(\tau)^2 \propto v(\tau)^4 \approx 0, \quad u(\tau)w(\tau) \propto u(\tau)v(\tau)^2 \approx 0, \quad u(\tau)^2 \approx 0$$

we obtain

$$\begin{cases} \ln\left(\frac{a}{a^{\rm ini}_{3a}}\right) &= \frac{z'(\lambda^*_{3a})}{x^*_{3a}}u^{\rm ini}\Big(\exp\big(-\varepsilon 12\xi(1-6\xi)z(\lambda^*_{3a})x^*_{3a}\tau\big)-1\Big), \\ \ln\left(\frac{H}{H^{\rm ini}_{3a}}\right)^2 &= -\Big(4+\frac{1-w_m}{4\xi}\frac{x^*_{3a}}{z(\lambda^*_{3a})}\Big)\frac{z'(\lambda^*_{3a})}{x^*_{3a}}u^{\rm ini}\Big(\exp\big(-\varepsilon 12\xi(1-6\xi)z(\lambda^*_{3a})x^*_{3a}\tau\big)-1\Big) \end{cases} \tag{6.43}$$

which can easily be combined as

$$\ln\left(\frac{H}{H^{\rm ini}_{3a}}\right)^2 = -\Big(4+\frac{1-w_m}{4\xi}\frac{x^*_{3a}}{z(\lambda^*_{3a})}\Big)\ln\left(\frac{a}{a^{\rm ini}_{3a}}\right). \tag{6.44}$$

One can notice that this expression resembles the behaviour of the Hubble's function during the pure radiation domination epoch, but with contribution coming from non-minimal coupling. The linearised solutions are valid up to the Lyapunov time $\tau_{\rm end} = \frac{1}{-\varepsilon 12\xi(1-6\xi)z(\lambda^*_{3a})x^*_{3a}} > 0$, then inserting this in to the latter equations we receive maximal

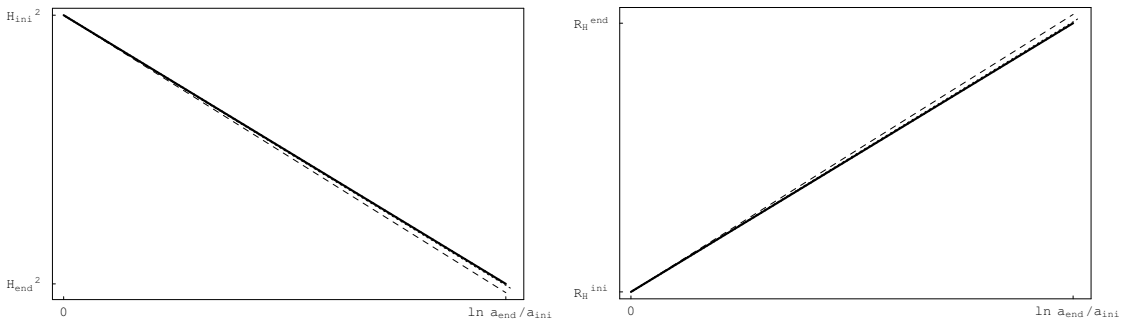

Figure 6.6: Evolution of $\ln H^2$ (left panel) and R_H (right panel) for a sample trajectory with $\varepsilon = -1$, $\xi = 10$, $z'(\lambda^*_{3a}) = \frac{1}{\alpha} = \frac{1}{10}$ in the vicinity of the critical point corresponding to the radiation dominated epoch for the phantom scalar field. The solid black line corresponds to the linearised solution (6.43), the dashed line corresponds to exact radiation dominated expansion of the universe $\ln H^2 \propto -4 \ln a$ and the dotted line corresponds to the numerical solution of the system (6.17).

values of the scale factor and Hubble's function valid in the center manifold approximation

$$\begin{cases} \ln\left(\frac{a^{\rm end}_{3a}}{a^{\rm ini}_{3a}}\right) &= \frac{z'(\lambda^*_{3a})}{x^*_{3a}} u^{\rm ini}\Big(e-1\Big), \\ \ln\left(\frac{H^{\rm end}_{3a}}{H^{\rm ini}_{3a}}\right)^2 &= -\Big(4 + \frac{1-w_m}{4\xi}\frac{x^*_{3a}}{z(\lambda^*_{3a})}\Big)\frac{z'(\lambda^*_{3a})}{x^*_{3a}} u^{\rm ini}\Big(e-1\Big) \end{cases} \tag{6.45}$$

In figure 6.6 we present evolution of $\ln H^2$ and R_H as a functions of $\ln a$ in the vicinity of the critical point representing radiation domination epoch for the phantom scalar field.

There is another critical point which represents the radiation dominated universe located at

$$x^*_{3b} = 0, \quad y^*_{3b} = 0, \quad \lambda^*_{3b}\colon z(\lambda)^2 = \frac{1}{\varepsilon 6\xi} \tag{6.46}$$

with the effective equation of the state parameter

$$w_{\rm eff} = \frac{1}{3}$$

We need to stress that this critical point exists only if $w_m \neq \frac{1}{3}$. Linearised solutions in the

vicinity of this critical point are

$$\begin{aligned} x_{3b}(\tau) &= \frac{1-3w_m}{2-3w_m}\Big(x_{3b}^{\rm ini}+z'(\lambda_{3b}^*)\big(\lambda_{3b}^{\rm ini}-\lambda_{3b}^*\big)\Big)\exp\left(l_1\tau\right)+ \\ &\quad +\frac{1}{2-3w_m}\Big(x_{3b}^{\rm ini}-(1-3w_m)z'(\lambda_{3b}^*)\big(\lambda_{3b}^{\rm ini}-\lambda_{3b}^*\big)\Big)\exp\left(l_3\tau\right), \qquad (6.47a) \\ y_{3b}(\tau) &= y_{3b}^{\rm ini}\exp\left(l_2\tau\right), \qquad (6.47b) \\ \lambda_{3b}(\tau) &= \lambda_{3b}^*+\frac{1}{2-3w_m}\frac{1}{z'(\lambda_{3b}^*)}\Big(x_{3b}^{\rm ini}+z'(\lambda_{3b}^*)\big(\lambda_{3b}^{\rm ini}-\lambda_{3b}^*\big)\Big)\exp\left(l_1\tau\right)- \\ &\quad -\frac{1}{2-3w_m}\frac{1}{z'(\lambda_{3b}^*)}\Big(x_{3b}^{\rm ini}-(1-3w_m)z'(\lambda_{3b}^*)\big(\lambda_{3b}^{\rm ini}-\lambda_{3b}^*\big)\Big)\exp\left(l_3\tau\right). \qquad (6.47c) \end{aligned}$$

where

$$l_1=6\xi(1-3w_m), \quad l_2=12\xi, \quad l_3=-6\xi$$

are the eigenvalues of the linearization matrix calculated at this critical point. Simple inspection of this eigenvalues gives us further constraint on the value of the barotropic matter equation of state parameter w_m, namely l_1 should be positive resulting in $w_m<\frac{1}{3}$ to assure that in the (x,λ) plane the dynamics in the vicinity of this critical point would correspond to a saddle type critical point. This will guarantee that the evolution proceeds towards the next critical point representing matter dominated universe.

Using linearised solutions (6.47) we are able to express (6.18) and (6.20) as a parametric functions of time τ

$$\begin{cases} \ln\left(\frac{a}{a_{3b}^{\rm ini}}\right) &= 6\xi\tau-\varepsilon 2\frac{1-6\xi}{(1-3w_m)(2-3w_m)}z(\lambda_{3b}^*)\Big(x_{3b}^{\rm ini}+z'(\lambda_{3b}^*)\big(\lambda_{3b}^{\rm ini}-\lambda_{3b}^*\big)\Big)\big(\exp\left(l_1\tau\right)-1\big)- \\ &\quad -\varepsilon 2\frac{1-6\xi}{2-3w_m}z(\lambda_{3b}^*)\Big(x_{3b}^{\rm ini}-(1-3w_m)z'(\lambda_{3b})\big(\lambda_{3b}^{\rm ini}-\lambda_{3b}^*\big)\Big)\big(\exp\left(l_3\tau\right)-1\big), \\ \ln\left(\frac{H}{H_{3b}^{\rm ini}}\right)^2 &= -24\xi\tau-\varepsilon 2\left(1-\frac{4(1-6\xi)}{(1-3w_m)(2-3w_m)}\right)z(\lambda_{3b}^*)\Big(x_{3b}^{\rm ini}+z'(\lambda_{3b}^*)\big(\lambda_{3b}^{\rm ini}-\lambda_{3b}^*\big)\Big)\big(\exp\left(l_1\tau\right)-1\big)- \\ &\quad +\varepsilon 8\frac{1-6\xi}{2-3w_m}z(\lambda_{3b}^*)\Big(x_{3b}^{\rm ini}-(1-3w_m)z'(\lambda_{3b}^*)\big(\lambda_{3b}^{\rm ini}-\lambda_{3b}^*\big)\Big)\big(\exp\left(l_3\tau\right)-1\big) \end{cases} \qquad (6.48)$$

The linearised solutions (6.47) are valid up to the Lyapunov characteristic time $\tau_{\rm end}=\frac{1}{l_2}=\frac{1}{12\xi}$ and inserting it in the latter equations we can obtain maximal values of the scale factor and the Hubble's function valid in the linear approximation.

The zero-order approximation ($x_{3b}^{\rm ini}=0$, $\lambda_{3b}^{\rm ini}=\lambda_{3b}^*$, $y_{3b}^{\rm ini}\neq 0$ but $(y_{3b}^{\rm ini})^2\approx 0$) is

$$\begin{cases} \ln\left(\frac{a}{a_{3b}^{\rm ini}}\right) &= 6\xi\tau, \\ \ln\left(\frac{H}{H_{3b}^{\rm ini}}\right)^2 &= -24\xi\tau \end{cases} \qquad (6.49)$$

and it can be combined to

$$H^2=(H_{3b}^{\rm ini})^2\left(\frac{a}{a_{3b}^{\rm ini}}\right)^{-4},$$

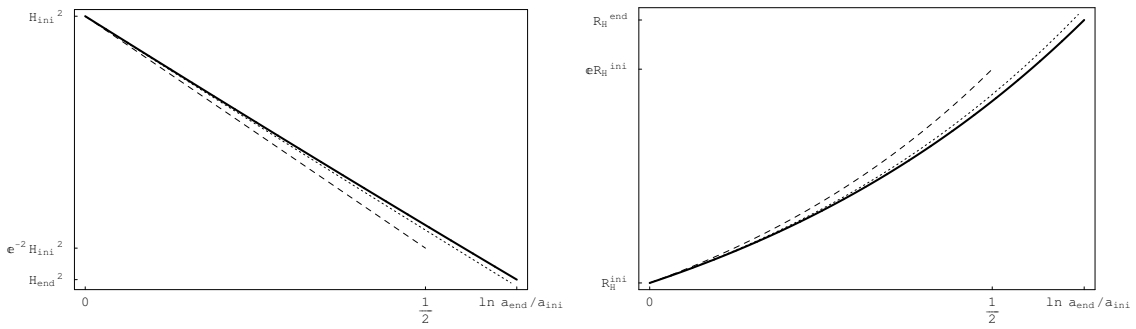

Figure 6.7: Evolution of $\ln H^2$ (left panel) and R_H (right panel) for a sample trajectory with $\varepsilon = +1$, $\xi = \frac{1}{16}$, $z'(\lambda^*_{3b}) = \frac{1}{\alpha} = 100$ in the vicinity of the critical point representing the radiation dominated epoch for the canonical scalar field. The solid black line corresponds to the linearised solution (6.48), the dashed line corresponds to exact radiation dominated expansion $\ln H^2 \propto -4 \ln a$ and the dotted line corresponds to the numerical solution of the system (6.17).

which is the exact behaviour of Hubble's function during the radiation domination era. This approximation is also valid up to $\tau_{\text{end}} = \frac{1}{12\xi}$ so one can calculate that during radiation domination epoch the scale factor grows at least

$$a_{3b}^{\text{end}} = a_{3b}^{\text{ini}} \sqrt{e}.$$

In figure 6.7 we present evolution of $\ln H^2$ and R_H as a function of $\ln a$ in the vicinity of the critical point representing the radiation domination era.

6.2.4 Matter domination

The next critical point is located at

$$x_4^* = 0, \quad y_4^* = 0, \quad \lambda_4^* \colon z(\lambda) = 0 \tag{6.50}$$

and w_{eff} given by (6.12) calculated at this point is

$$w_{\text{eff}} = w_m.$$

We identify this critical point as representing the universe whose dynamics is dominated by the barotropic matter included in the model with the equation of state parameter w_m.

The linearised solutions in the vicinity of this critical point are in the form

$$\begin{aligned} x_4(\tau) &= \tfrac{l_1}{l_1-l_3}\Big(x_4^{\rm ini} - z'(\lambda_4^*)l_3\big(\lambda_4^{\rm ini}-\lambda_4^*\big)\Big)\exp(l_1\tau) - \\ &\quad -\tfrac{l_3}{l_1-l_3}\Big(x_4^{\rm ini} - z'(\lambda_4^*)l_1\big(\lambda_4^{\rm ini}-\lambda_4^*\big)\Big)\exp(l_3\tau), \\ y_4(\tau) &= y_4^{\rm ini}\exp(l_2\tau), \\ \lambda_4(\tau) &= \lambda_4^* + \tfrac{1}{z'(\lambda_4^*)\big(l_1-l_3\big)}\Big(x_4^{\rm ini} - z'(\lambda_4^*)l_3\big(\lambda_4^{\rm ini}-\lambda_4^*\big)\Big)\exp(l_1\tau) - \\ &\quad -\tfrac{1}{z'(\lambda_4^*)\big(l_1-l_3\big)}\Big(x_4^{\rm ini} - z'(\lambda_4^*)l_1\big(\lambda_4^{\rm ini}-\lambda_4^*\big)\Big)\exp(l_3\tau). \end{aligned} \tag{6.51}$$

where

$$\begin{aligned} l_1 &= -\frac{3}{4}\left((1-w_m)+\sqrt{(1-w_m)^2-\frac{16}{3}\xi(1-3w_m)}\right), \\ l_2 &= \frac{3}{2}(1+w_m), \\ l_3 &= -\frac{3}{4}\left((1-w_m)-\sqrt{(1-w_m)^2-\frac{16}{3}\xi(1-3w_m)}\right). \end{aligned}$$

We need to note that this critical point can became degenerate for two specific values of w_m, namely, for $w_m=-1$ the second eigenvalue vanishes and for $w_m=\frac{1}{3}$ the third eigenvalue vanish, for any value of the coupling constant ξ, which makes the system in the vicinity of this critical point degenerated.

From linearised solution (6.51) we have

$$x_4(\tau)^2\approx 0, \quad y_4(\tau)^2\approx 0, \quad z\big(\lambda_4(\tau)\big)^2\approx 0$$

and from (6.18) and (6.20) parametric equations for evolution of the scale factor and Hubble's function are

$$\begin{cases} \ln\left(\frac{a}{a_4^{\rm ini}}\right) &= \tau, \\ \ln\left(\frac{H}{H_4^{\rm ini}}\right)^2 &= -3(1+w_m)\tau. \end{cases} \tag{6.52}$$

Combining these two expressions we get the Hubble's function as function of the scale factor during the barotropic matter domination epoch

$$H^2 = (H_4^{\rm ini})^2\left(\frac{a}{a_4^{\rm ini}}\right)^{-3(1+w_m)}.$$

The linearised solutions (6.51) are valid up to the Lyapunov time $\tau_{\rm end}=\frac{1}{l_2}=\frac{2}{3(1+w_m)}$,

$$\begin{cases} \ln\left(\frac{a_4^{\rm end}}{a_4^{\rm ini}}\right) &= \frac{2}{3(1+w_m)}, \\ \ln\left(\frac{H_4^{\rm end}}{H_4^{\rm ini}}\right)^2 &= -2. \end{cases} \tag{6.53}$$

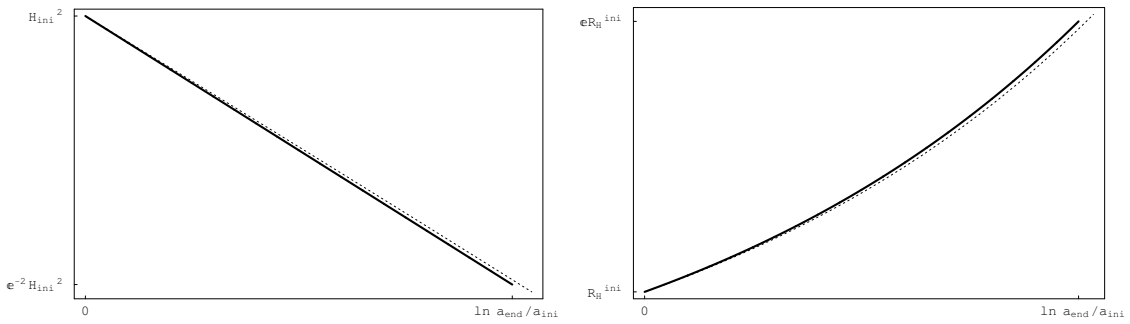

Figure 6.8: Evolution of $\ln H^2$ (left panel) and R_H (right panel) for a sample trajectory with $\varepsilon = -1$, $\xi = \frac{1}{2}$, $z'(\lambda_1^*) = \frac{1}{\alpha} = 100$ in the vicinity of the critical point corresponding to the barotropic matter dominated universe. The solid black line represents the linear approximation (6.52) and the dotted line represents the numerical solution of the system (6.17).

One can notice that for dust matter $w_m = 0$ during the matter domination epoch the scale factor grows at least $\frac{a_4^{\text{end}}}{a_4^{\text{ini}}} = e^{\frac{2}{3}} \approx 1.948$ times.

In figure 6.8 we present evolution of the scale factor and Hubble's function in the vicinity of the critical point representing the barotropic matter domination epoch.

6.2.5 The present accelerated expansion epoch

Finally we proceed to the last critical points located at

$$x_5^* = 0, \quad (y_5^*)^2 = 1 - \varepsilon 6\xi z(\lambda_5^*)^2, \quad \lambda_5^* \colon \lambda z(\lambda)^2 + 4z(\lambda) - \frac{\lambda}{\varepsilon 6\xi} = 0 \tag{6.54}$$

with

$$w_{\text{eff}} = -1.$$

There can be more than one such critical points because of the third equation in (6.54) which can have more than one solution. In what follows we will show that at least one of them represents a stable critical point.

In this case the characteristic equation for eigenvalues of the linearization matrix calculated at this critical point is in the form

$$l^3 + pl^2 + ql + r = 0$$

where

$$\begin{aligned} p &= 3(2+w_m)\big(1-\varepsilon 6\xi(1-6\xi)z(\lambda_5^*)^2\big), \\ q &= \big(1-\varepsilon 6\xi(1-6\xi)z(\lambda_5^*)^2\big)\Big[-\varepsilon\tfrac{1}{2}\tfrac{(y_5^*)^4}{z'(\lambda_5^*)}+12\xi(1+\varepsilon 6\xi z(\lambda_5^*)^2) \\ &\qquad +9(1+w_m)\big(1-\varepsilon 6\xi(1-6\xi)z(\lambda_5^*)^2\big)\Big], \\ r &= 3(1+w_m)\big(1-\varepsilon 6\xi(1-6\xi)z(\lambda_5^*)^2\big)^2\Big[-\varepsilon\tfrac{1}{2}\tfrac{(y_5^*)^4}{z'(\lambda_5^*)}+12\xi\big(1+\varepsilon 6\xi z(\lambda_5^*)^2\big)\Big]. \end{aligned}$$

In the most general case without assuming any specific form of the potential function we are unable to solve this equation. In spite of this we are able to formulate general conditions for stability of this critical point. This requires that the real parts of the eigenvalues must be negative. From the Routh-Hurwitz test [60] we have that the following conditions should be fulfilled to assure stability of this critical point

$$p>0 \qquad \text{and} \qquad r>0 \qquad \text{and} \qquad q-\frac{r}{p}>0$$

Simple inspection of these conditions gives us that, for any matter with $w_m > -2$, p is always positive because of $\big(1-\varepsilon 6\xi(1-6\xi)z(\lambda_5^*)^2\big)>0$ due to time transformation and that if r is a positive quantity it follows that $q-\frac{r}{p}$ is positive too. We conclude that if the following condition is fulfilled at the critical point

$$Re[l_{1,2,3}]<0 \iff -\varepsilon\frac{1}{2}\frac{(y_5^*)^4}{z'(\lambda_5^*)}+12\xi\big(1+\varepsilon 6\xi z(\lambda_5^*)^2\big)>0 \tag{6.55}$$

it represents a stable critical point with the negative real parts of the eigenvalues.

In order to simplify this condition let us introduce the following function

$$h(\lambda)=\lambda z(\lambda)^2+4z(\lambda)-\frac{\lambda}{\varepsilon 6\xi}, \tag{6.56}$$

where location of the critical point is the solution to the equation $h(\lambda)=0$, and obviously $h(\lambda_5^*)=0$.

Let us assume that $\lambda_5^*\neq 0$ it follows from (6.56) that also $z(\lambda_5^*)\neq 0$ but $h(\lambda_5^*)=0$. Differentiation of Eq. (6.56) gives

$$h'(\lambda_5^*)=z(\lambda_5^*)^2-\frac{1}{\varepsilon 6\xi}+2z'(\lambda_5^*)\big(\lambda_5^* z(\lambda_5^*)+2\big)$$

which, after a little of algebra, can be transformed in to the following form

$$h'(\lambda_5^*)=-\frac{(y_5^*)^2}{\varepsilon 6\xi}+4\frac{z'(\lambda_5^*)}{(y_5^*)^2}\Big(1+\varepsilon 6\xi z(\lambda_5^*)^2\Big)$$

and finally we arrive to the reformulated stability condition (6.55) in the form

$$Re[l_{1,2,3}] < 0 \iff 3\xi\frac{h'(\lambda_5^*)}{z'(\lambda_5^*)}(y_5^*)^2 > 0 \tag{6.57}$$

We have reduced analysis of stability of the critical point representing accelerated expansion to the simple analysis of the sign of the quantity given by relation (6.57). If we assume that the function $z(\lambda)$ is a monotonic one, i.e. it is a growing or decreasing function in the interesting region of the phase space then it follows that if we have at least two critical points given by (6.54) one of them is definitely a stable critical point.

To present the evolution of Hubble's function in the vicinity of this critical point, as an example, we choose the simple form of the function $z(\lambda) = \frac{\lambda}{\alpha}$, and values of the parameters ξ and α in range for which there exists only one critical point corresponding the present accelerated expansion of the universe [161]. The linearised solutions in the vicinity of the critical point located at $x_5^* = 0$, $(y_5^*)^2 = 1$, $\lambda_5^* = 0$ are

$$\begin{aligned}
x_5(\tau) &= \tfrac{1}{2\sqrt{\Delta_5}}\Big\{(3+\sqrt{\Delta_5})\Big[x_5^{\rm ini} + \tfrac{1}{2\alpha}(3-\sqrt{\Delta_5})\lambda_5^{\rm ini}\Big]\exp(l_1\tau) - \\
&\qquad -(3-\sqrt{\Delta_5})\Big[x_5^{\rm ini} + \tfrac{1}{2\alpha}(3+\sqrt{\Delta_5})\lambda_5^{\rm ini}\Big]\exp(l_3\tau)\Big\}, \\
y_5(\tau) &= y_5^* + (y_5^{\rm ini} - y_5^*)\exp(l_2\tau), \\
\lambda_5(\tau) &= -\tfrac{\alpha}{\sqrt{\Delta_5}}\Big\{\Big[x_5^{\rm ini} + \tfrac{1}{2\alpha}(3-\sqrt{\Delta_5})\lambda_5^{\rm ini}\Big]\exp(l_1\tau) - \\
&\qquad -\Big[x_5^{\rm ini} + \tfrac{1}{2\alpha}(3+\sqrt{\Delta_5})\lambda_5^{\rm ini}\Big]\exp(l_3\tau)\Big\},
\end{aligned} \tag{6.58}$$

where $l_{1,3} = -\frac{1}{2}\big(3 \pm \sqrt{9 + \varepsilon 2\alpha - 48\xi}\big)$ and $l_2 = -3(1+w_m)$ are eigenvalues of the linearization matrix and $\Delta_5 = 9 + \varepsilon 2\alpha - 48\xi$.

Then keeping only linear terms in initial conditions

$$x_5(\tau)^2 \approx 0, \quad z\big(\lambda_5(\tau)\big)^2 \approx 0, \quad \lambda_5(\tau) z\big(\lambda_5(\tau)\big) \approx 0,$$

$$y_5(\tau)^2 \approx (y_5^*)^2 + 2y_5^*\big(y_5^{\rm ini} - y_5^*\big)\exp(l_2\tau),$$

from (6.18) and (6.20) we receive the parametric equations of evolution of the scale factor and Hubble's function

$$\begin{cases}
\ln\left(\frac{a}{a_5^{\rm ini}}\right) &= \tau, \\
\ln\left(\frac{H}{H_5^{\rm ini}}\right)^2 &= 2y_5^*\big(y_5^{\rm ini} - y_5^*\big)\Big(1 - \exp\big(-3(1+w_m)\tau\big)\Big)
\end{cases} \tag{6.59}$$

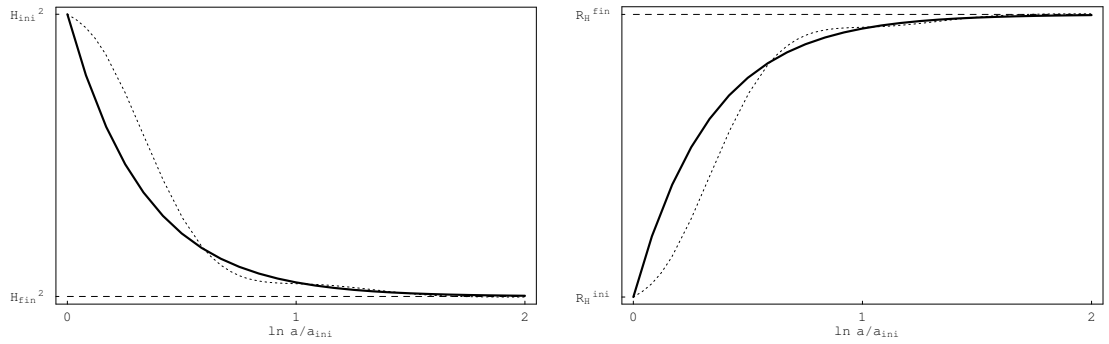

Figure 6.9: Evolution of $\ln H^2$ (left panel) and R_H (right panel) as a function of the natural logarithm of the scale factor $\ln a$ for a sample trajectory with $\varepsilon = -1$, $\xi = 1$, $z'(\lambda_5^*) = \frac{1}{\alpha} = 20$, $y_5^{\mathrm{ini}} - y_5^* = -\frac{1}{100}$ in the vicinity of the critical point representing the present accelerated expansion of the universe. The solid black line represents the linear approximation (6.59) and the dotted line corresponds to numerical solution of the dynamical system (6.17).

Combining these two expressions we get Hubble's function as a function of the scale factor in the vicinity of the critical point corresponding to the present accelerated expansion of the universe

$$H^2 = (H_5^{\mathrm{ini}})^2 \exp\left\{2y_5^*\left(y_5^{\mathrm{ini}} - y_5^*\right)\left(1 - \left(\frac{a}{a_5^{\mathrm{ini}}}\right)^{-3(1+w_m)}\right)\right\}.$$

One can notice that taking the following limit

$$H_{\mathrm{fin}}^2 = \lim_{\tau\to\infty} H^2 = \lim_{a\to\infty} H^2 = (H_5^{\mathrm{ini}})^2 \exp\left\{2y_5^*\left(y_5^{\mathrm{ini}} - y_5^*\right)\right\} \approx (H_5^{\mathrm{ini}})^2\left(1 + 2y_5^*\left(y_5^{\mathrm{ini}} - y_5^*\right)\right)$$

we get the asymptotic de Sitter expansion.

In figure 6.9 we present the evolution of $\ln H^2$ and R_H as a function of $\ln a$ in the vicinity of this critical point.

6.3 Conclusions

In this chapter we have shown that all the important epochs in the evolution of the universe can be represented by the critical points of the dynamical system arising from the non-minimally coupled scalar field cosmology in spite of not assuming a form of the potential function. We have shown that for the positive coupling constant there exists a past finite scale factor singularity for both types of the scalar fields. Additionally all the intermediate states are transient ones, i.e. they are represented by unstable critical points

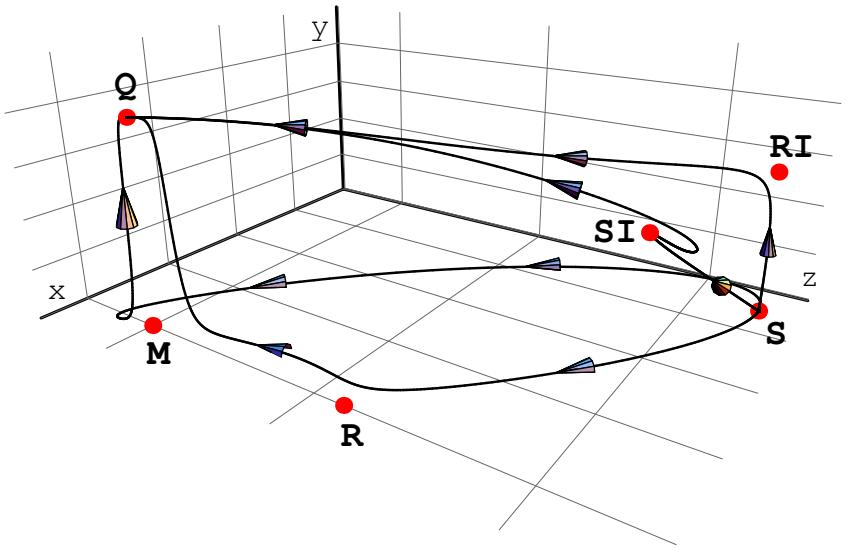

Figure 6.10: The phase space portrait for the model with the cosmological constant and the canonical scalar field ($\varepsilon = +1$) with $\xi = 1/8$ and the dust matter $w_m = 0$. The critical points are: S – the finite scale factor singularity, RI – the rapid-roll inflation, SI – the slow-roll inflation, R – the radiation dominated era, M – the barotropic matter dominated era and Q – the quintessence era. Note that the critical points representing the finite scale factor singularity, the rapid-roll inflation and the slow-roll inflation have the same value of coordinate z.

in the phase space and the evolution in the vicinity of those points last for an finite amount of time. The existence of the radiation dominated era is purely the result of the evolution of the non-minimally coupled scalar field.

For the canonical scalar field $\varepsilon = +1$ and $0 < \xi < 1/6$ we can construct the unique evolutional path represented by the trajectory in the phase space which travels in the vicinity of the following critical points (figure 6.10)

$$1 \mapsto 2b \mapsto 3b \mapsto 4 \mapsto 5$$

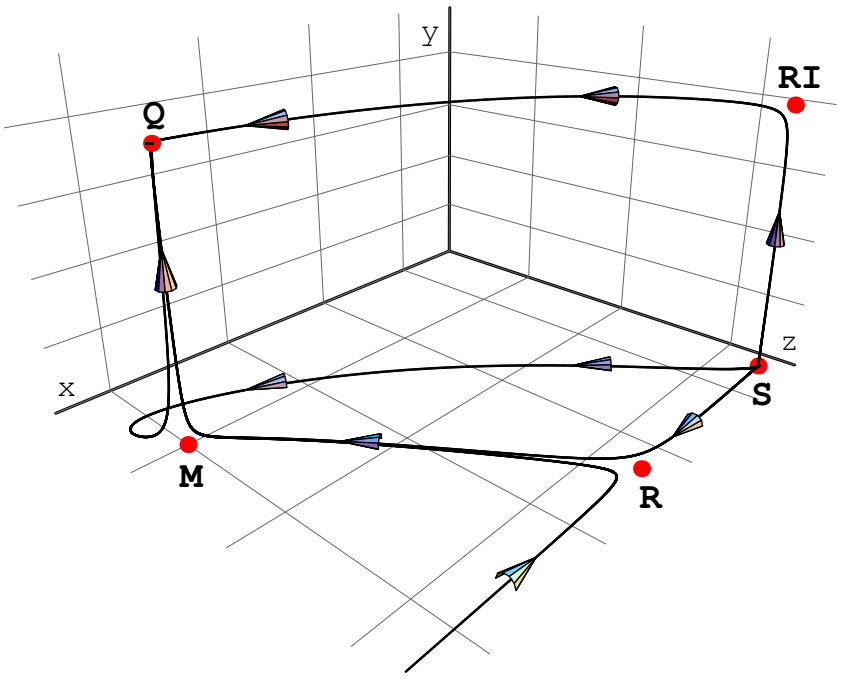

Figure 6.11: The phase space portrait for the model with the cosmological constant and the phantom scalar field ($\varepsilon = -1$) with $\xi = 1/4$ and the dust matter $w_m = 0$. The critical points are: S – the finite scale factor singularity, RI – the rapid-roll inflation, R – the radiation dominated era, M – the barotropic matter dominated era and Q – the quintessence era. In the case of the phantom scalar field the critical point representing slow-roll inflation is not present. The critical pints denoted as S, RI and R have the same value of coordinate z.

and for the phantom scalar field $\varepsilon = -1$ and $\xi > 1/6$ (figure 6.11)

$$1 \mapsto 2a \mapsto 3a \mapsto 4 \mapsto 5$$

Within one framework of non-minimally coupled scalar field cosmology we were able to unify all the major epochs in the history of the universe (see figure 6.12 for twister type behaviour where trajectories interpolate between radiation era, matter domination era and quintessence epoch).

From the analysis presented in this chapter one can draw the general conclusion that if the non-minimal coupling constant is present and is different from the conformal coupling $\xi \neq 1/6$ then new evolutional types emerge forming the structure of the phase

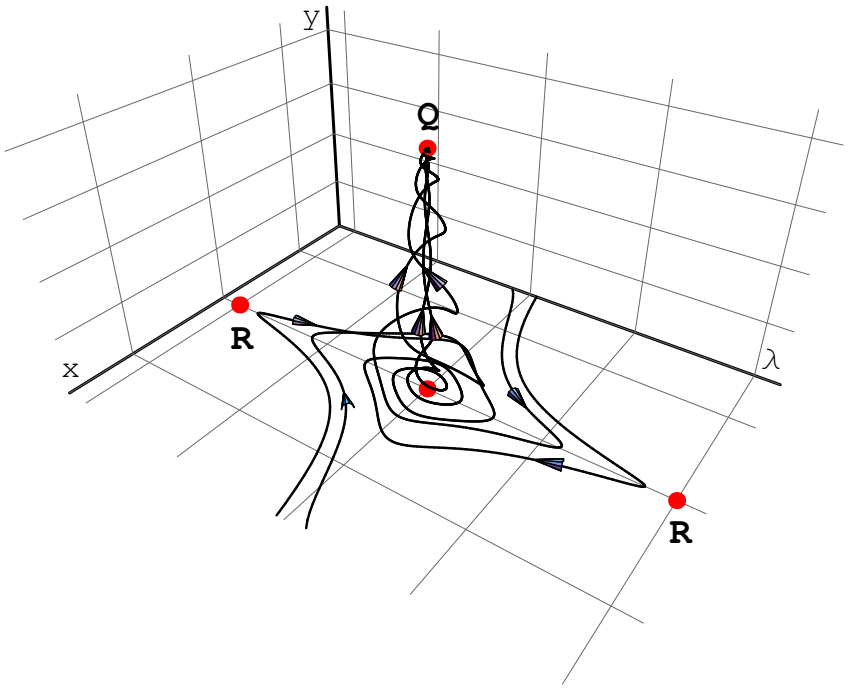

Figure 6.12: The phase space portrait representing twister type behaviour. Trajectories in this type solution interpolate between three major epochs in the history of universe: R – the radiation dominated universe with $w_{\text{eff}} = \frac{1}{3}$, the matter domination epoch (an unstable focus type critical point) and Q – the quintessence domination epoch with $w_{\text{eff}} = -1$. This type of evolution does not depend on the form of assumed function $z(\lambda)$ (i.e. the form of the scalar field potential) and is generic for the canonical scalar field cosmologies ($\varepsilon = +1$) with $\xi > 0$ and the barotropic matter with equation of state parameter $-1 < w_m < 1/3$.

space nontrivial and richer. Moreover the coupling constant gives us the effect of continuation (glues the evolution) between different cosmological epochs which is very attractive in cosmology, serving as a potential explanation of the global properties of the universe.

Chapter 7

Summary and Conclusions

Modern cosmology becomes very similar to the particle physics. Both theories have parameters and characteristic energetic cut-offs. They are effective description of more fundamental physics which is currently unknown. The values of these parameters should be obtained from fundamental theories or from observations. In cosmology (ΛCDM model is often called the Standard Cosmological Model) the role of such parameter is played by the cosmological constant. Our proposition was to extend this paradigm, in which matter content in the model is described in terms of barotropic perfect fluid, by introduction of additional scalar field non-minimally coupled to gravity.

This dissertation was devoted to investigations of dynamical evolution of cosmological models with a scalar field with a potential function and non-minimally coupled to the gravity via $\xi R\,\phi^2$ term, where R is the Ricci scalar of the Roberson–Walker spacetime.

The conclusions of the work can be stated as follows:

The closed FRW cosmological model with the conformally coupled scalar field was investigated by means of geodesics of the Jacobi metric. We showed that the singular set $\partial\mathcal{D}$ of degeneration of the Jacobi metric can serve as a Poincaré surface in detection of complexity of dynamical behaviour. The distribution of the intersection points and the existence of unstable periodic orbits contain interesting information concerning the degree of complexity of dynamics of the model. We were able to demonstrate the complex behaviour in the sense of Poincaré sections, random distribution of intersection points of trajectories with the singular set $\partial\mathcal{D}$, chaotic trajectories coding and most important the existence of the unstable periodic orbits. This last property should be treated as a very strong indication of the existence of chaos in the investigated model [117]. The flat FRW cosmological model

with the conformally coupled phantom scalar field and the quadratic potential function can be treated as a scattering system of two types: multiple chaotic or standard scattering process. We found that chaotic behaviour is a generic feature of the phantom cosmology with the spontaneously symmetry breaking while in the case of absence of symmetry braking we did not find the sensitivity dependence on the initial conditions and the system behaves as the standard scattering process. We also found that in the second case the universe filled with the conformally coupled scalar field is accelerating without the positive cosmological constant.

The dynamics of expanding flat FRW cosmological models with non-minimally coupled scalar fields, both canonical and phantom, can be reduced to two dimensional autonomous dynamical system. The constraint condition is solved in such a way that the final dynamical system is free from the constraint and is defined on the phase plane (ϕ, ϕ') where prime denotes the differentiation with respect to the natural logarithm of the scale factor. For a quadratic potential function the global dynamics of the system was studied where the method of compactification of the phase space with the circle at infinity was used. We were able to show that the shape of the physical region $H^2 \geq 0$ on the phase plane does not depend on the form of the potential function, but only on the value of the coupling constant ξ. We have shown the existence of the finite scale factor singularity, both future and past. For a wide range of the values of the coupling constant ξ we found a critical point of the sink type for the phantom scalar field which represents the de Sitter solution, which represents the present accelerated expansion of the universe.

We have shown that all important epochs in the evolution of the universe can be represented by the critical points of the dynamical system arising from the non-minimally coupled scalar field cosmology with barotropic matter content. This result is generic for a very large class of potential functions of the scalar field. We discover new evolutional paths which open new perspectives of description of the cosmological evolution in a unified way. Within one framework of non-minimally coupled scalar field cosmology all the major epochs in the history of the universe emerge in the natural way as critical points of the corresponding dynamical system (a finite scale factor singularity, an inflation epoch (slow-roll or fast-roll), a radiation era, a matter domination era and finally a quintessence epoch). Moreover, this new type of evolution is realised only if non-minimal coupling constant is present and different form the conformal coupling value $\xi \neq 1/6$.

The main general results are:

- The coexistence of chaotic and regular behaviour in the conformally coupled scalar field cosmology, together with different manifestations of dynamical complexity was demonstrated. In the case of the phantom scalar field the process of a chaotic scattering was detected.

- The fragility of cosmological evolution with respect to changes of coupling constant ξ was presented. The inclusion of the non-zero coupling constant leads to a richer dynamics of the cosmological models.

- It was shown that only inclusion of both types of matter, namely the standard barotropic matter and a non-minimally coupled scalar field leads to new, rich and interesting dynamics in the phase space. It was demonstrated that due to the non-zero coupling constant it is possible to link different cosmological epochs (from the big bang to the quintessence era).

- In the standard cosmology the matter content is usually described in the terms of a perfect fluid with energy density and pressure depending on the cosmological time. In contrast, in inflationary cosmology different approach is proposed. In this context the matter in the form of a scalar field seems to be more adequate. The generalisation of both paradigms and consideration of two components model of non interacting matter was proposed. As a result we receive all cosmological epoch squeezed in one evolutional scenario, from the big bang, through the inflation era, the radiation and the barotropic matter domination epoch to the quintessence era, with all intermediate states as transient ones.

Prospects for future work

We have to admit that our understanding of dynamics of non-minimally coupled cosmological models is far from complete. The work presented in this dissertation is just the beginning of the larger program which we will undertake in the near future.

From the conclusions presented above, natural questions emerge: What comes next? What can and what should be done in description of dynamics of non-minimally coupled cosmology? Our future projects will proceed essentially in two directions.

First, let us point out the issues concerning the complexity of dynamics. The dynamical systems of cosmological origin have many special features which distinguish them from those met in the classical mechanics. It is in fact the source of some problems and controversies in understanding of chaos in cosmology. The main aim of our upcoming projects will be dynamical investigations of the models with the topological transitivity property. The unstable periodic orbits are indicators of chaotic behaviour in any system. Those orbits are connected with the quantisation scheme proposed by Gutzwiller [117, 171] (e.g. quantisation of the helium atom starting form the chaotic classical dynamics). In this procedure the semi-classical approximation to the wave function of the quantum system is acquired from the summation of the series of contributions resulting from the unstable periodic orbits of the classical system. We think that this procedure can be very useful in the models of cosmological origin which dynamical behaviour is complex. We will establish a connection between summation rules for classical dynamics of cosmological models with indefinite kinetic energy forms. The semi-classical approximation of the wave functions of cosmological models can be constructed from studying dynamical complexity of chaotic cosmologies.

Second, let us touch the issues concerning the regular evolution of the models. We will try to answer the following questions: How will the inclusion of curvature of the FRW metric influence the twister quintessence scenario? Will perturbations destroy or improve this evolutional scenario? We are aware that a toy model of evolution of universe presented in this dissertation needs improvements to be close to reality.

Even more fundamental question about current status of the scalar–tensor cosmology. What is the precise definition of the energy-momentum tensor for a non-minimally coupled cosmology? Is it possible to distinguish between various mathematically correct, but physically inequivalent, definitions of this tensor (see Chapter 1) via observational astronomical data?

Appendix A

Einstein equations and energy–momentum tensor

We derive in a pedagogical manner the Einstein field equations in the presence of non-minimal coupling. Consider the Einstein–Hilbert action for the gravitational field

$$S_g = \frac{1}{2\kappa^2}\int \mathrm{d}^4x\sqrt{-g}\big(R - 2\Lambda\big) \tag{A.1}$$

and for non-minimally coupled scalar field

$$S_\phi = -\frac{1}{2}\int \mathrm{d}^4x\sqrt{-g}\Big\{\varepsilon\Big(g^{\mu\nu}\nabla_\mu\phi\nabla_\nu\phi + \xi R\,\phi^2\Big) + 2U(\phi)\Big\} \tag{A.2}$$

where $\kappa^2 = 8\pi G$, $\varepsilon = \pm 1$ correspond to the canonical and phantom scalar field, respectively, and $U(\phi)$ is the scalar field potential function. A dimensionless parameter ξ describes coupling between the scalar and the gravitational field. Two special values of the coupling constant ξ have exceptional importance : minimal coupling with $\xi = 0$ and conformal coupling $\xi = 1/6$ (in 4 spacetime dimensions, see Appendix B) the value that makes the Klein–Gordon equation conformally invariant if $U = 0$ or $U = \lambda\phi^4$.

Variation of the full action with respect to $g^{\mu\nu}$

$$\delta(S_g + S_\phi) = 0$$

gives the Einstein field equation for the problem.

We begin with derivation of variation of the gravitational part (see books by Wald [172] or Landau and Lifshitz [173])

$$\delta S_g = \frac{1}{2\kappa^2}\int \mathrm{d}^4x\Big\{\delta\sqrt{-g}(R - 2\Lambda) + \sqrt{-g}\delta R\Big\}$$

then using the following formula

$$\delta\sqrt{-g} = -\frac{1}{2\sqrt{-g}}\delta g = -\frac{1}{2}\sqrt{-g}g_{\mu\nu}\delta g^{\mu\nu}$$

we obtain

$$\begin{aligned}\delta S_g &= \frac{1}{2\kappa^2}\int \mathrm{d}^4x\Big\{-\frac{1}{2}\sqrt{-g}g_{\mu\nu}\delta g^{\mu\nu}(R-2\Lambda)+\sqrt{-g}\delta g^{\mu\nu}R_{\mu\nu}+\sqrt{-g}g^{\mu\nu}\delta R_{\mu\nu}\Big\}\\ &= \frac{1}{2\kappa^2}\int \mathrm{d}^4x\sqrt{-g}\Big\{R_{\mu\nu}-\frac{1}{2}g_{\mu\nu}R+\Lambda g_{\mu\nu}\Big\}\delta g^{\mu\nu}+\frac{1}{2\kappa^2}\int \mathrm{d}^4x\sqrt{-g}g^{\mu\nu}\delta R_{\mu\nu} \quad \text{(A.3)}\end{aligned}$$

Now we will show that the second term in this expression vanishes. Let us use a locally geodesic system of coordinates. Then at a given point all the $\Gamma^{\alpha}_{\mu\nu}=0$ and we can write the variation of the Ricci tensor in the following form (remembering that also $g_{\mu\nu,\alpha}=0$)

$$\begin{aligned}g^{\mu\nu}\delta R_{\mu\nu} &= g^{\mu\nu}\Big(\big(\delta\Gamma^{\alpha}_{\mu\nu}\big)_{,\alpha}-\big(\delta\Gamma^{\alpha}_{\mu\alpha}\big)_{,\nu}\Big)\\ &= g^{\mu\nu}\big(\delta\Gamma^{\alpha}_{\mu\nu}\big)_{,\alpha}-g^{\mu\alpha}\big(\delta\Gamma^{\nu}_{\mu\nu}\big)_{,\alpha}\\ &= \omega^{\alpha}{}_{,\alpha} \quad \text{(A.4)}\end{aligned}$$

where

$$\omega^{\alpha} = g^{\mu\nu}\delta\Gamma^{\alpha}_{\mu\nu}-g^{\mu\alpha}\delta\Gamma^{\nu}_{\mu\nu}.$$

This expression is a vector and then the relation (A.4) in an arbitrary coordinate system can be written as

$$g^{\mu\nu}\delta R_{\mu\nu} = \omega^{\alpha}{}_{;\alpha} = \frac{1}{\sqrt{-g}}\,\partial_{\alpha}\big(\sqrt{-g}\,\omega^{\alpha}\big).$$

Then the second integral in (A.3) is equal to

$$\frac{1}{2\kappa^2}\int \mathrm{d}^4x\sqrt{-g}g^{\mu\nu}\delta R_{\mu\nu} = \frac{1}{2\kappa^2}\int \mathrm{d}^4x\left(\sqrt{-g}\,\omega^{\alpha}\right)_{,\alpha}$$

and by Gauss' theorem can be transformed into an integral of ω^{α} over the hypersurface surrounding the whole four-volume. Since the variations of the field are zero at the integration limits, this term drops out [173]. Finally, the variation δS_g is equal to

$$\delta S_g = \frac{1}{2\kappa^2}\int \mathrm{d}^4x\sqrt{-g}\Big\{R_{\mu\nu}-\frac{1}{2}g_{\mu\nu}R+\Lambda g_{\mu\nu}\Big\}\delta g^{\mu\nu}\,. \quad \text{(A.5)}$$

Now we can proceed to the calculation of the variation δS_ϕ of the matter part in the form of non-minimally coupled scalar field. We obtain

$$\begin{aligned}
\delta S_\phi &= -\frac{1}{2}\int \mathrm{d}^4x\Big\{\delta\sqrt{-g}\Big(\varepsilon g^{\mu\nu}\nabla_\mu\phi\nabla_\nu\phi+\varepsilon\xi R\phi^2+2U(\phi)\Big)\\
&\qquad +\sqrt{-g}\Big(\varepsilon\delta g^{\mu\nu}\nabla_\mu\phi\nabla_\nu\phi+\varepsilon\xi\delta g^{\mu\nu}R_{\mu\nu}\phi^2+\varepsilon\xi g^{\mu\nu}\delta R_{\mu\nu}\phi^2\Big)\Big\}\\
&= -\frac{1}{2}\int \mathrm{d}^4x\sqrt{-g}\Big\{\varepsilon\nabla_\mu\phi\nabla_\nu\phi-\varepsilon\frac{1}{2}g_{\mu\nu}\nabla^\alpha\phi\nabla_\alpha\phi-U(\phi)g_{\mu\nu}\\
&\qquad +\varepsilon\xi\big(R_{\mu\nu}-\frac{1}{2}g_{\mu\nu}R\big)\phi^2\Big\}\delta g^{\mu\nu}\\
&\quad -\varepsilon\frac{1}{2}\xi\int \mathrm{d}^4x\sqrt{-g}g^{\mu\nu}\delta R_{\mu\nu}\phi^2
\end{aligned}\tag{A.6}$$

Now we will calculate the last term in this expression. As previously, using a locally geodesic system of coordinates, at a given point $\Gamma^\alpha_{\mu\nu}=0$ and $g_{\mu\nu,\alpha}=0$ we have

$$\begin{aligned}
g^{\mu\nu}\delta R_{\mu\nu}\phi^2 &= g^{\mu\nu}\Big(\big(\delta\Gamma^\alpha_{\mu\nu}\big)_{,\alpha}\phi^2-\big(\delta\Gamma^\alpha_{\mu\alpha}\big)_{,\nu}\phi^2\Big)\\
&= g^{\mu\nu}\Big(\big(\delta\Gamma^\alpha_{\mu\nu}\phi^2\big)_{,\alpha}-\big(\delta\Gamma^\alpha_{\mu\alpha}\phi^2\big)_{,\nu}\Big)-g^{\mu\nu}\Big(\delta\Gamma^\alpha_{\mu\nu}\phi^2_{,\alpha}-\delta\Gamma^\alpha_{\mu\alpha}\phi^2_{,\nu}\Big)\\
&= g^{\mu\nu}\big(\delta\Gamma^\alpha_{\mu\nu}\phi^2\big)_{,\alpha}-g^{\mu\alpha}\big(\delta\Gamma^\nu\mu\nu\phi^2\big)_{,\alpha}-g^{\mu\nu}\delta\Gamma^\alpha_{\mu\nu}\phi^2_{,\alpha}+g^{\mu\nu}\delta\Gamma^\alpha_{\mu\alpha}\phi^2_{,\nu}\\
&= \bar\omega^\alpha{}_{,\alpha}-g^{\mu\nu}\delta\Gamma^\alpha_{\mu\nu}\phi^2_{,\alpha}+g^{\mu\nu}\delta\Gamma^\alpha_{\mu\alpha}\phi^2_{,\nu}
\end{aligned}\tag{A.7}$$

where we introduced the vector

$$\bar\omega^\alpha=\Big(g^{\mu\nu}\delta\Gamma^\alpha_{\mu\nu}-g^{\mu\alpha}\delta\Gamma^\nu_{\mu\nu}\Big)\phi^2.$$

Using the following formula

$$g^{\mu\nu}\Gamma^\alpha_{\mu\nu}=g^{\mu\nu}g^{\alpha\sigma}\left(g_{\mu\sigma,\nu}-\frac{1}{2}g_{\mu\nu,\sigma}\right)$$

the second term in (A.7) can be written as

$$\begin{aligned}
-g^{\mu\nu}\delta\Gamma^\alpha_{\mu\nu}\phi^2{}_{,\alpha} &= -g^{\mu\nu}g^{\alpha\sigma}\left(\big(\delta g_{\mu\sigma,\nu}\big)\phi^2{}_{,\alpha}-\frac{1}{2}\big(\delta g_{\mu\nu,\sigma}\big)\phi^2{}_{,\alpha}\right)\\
&= -g^{\mu\nu}g^{\alpha\sigma}\left(\big(\delta g_{\mu\sigma}\phi^2{}_{,\alpha}\big)_{,\nu}-\frac{1}{2}\big(\delta g_{\mu\nu}\phi^2{}_{,\alpha}\big)_{,\sigma}\right)\\
&\quad +g^{\mu\nu}g^{\alpha\sigma}\left(\delta g_{\mu\sigma}\phi^2{}_{,\alpha\nu}-\frac{1}{2}\delta g_{\mu\nu}\phi^2{}_{,\alpha\sigma}\right)\\
&= \widetilde\omega^\nu{}_{,\nu}-\phi^2{}_{,\mu\nu}\delta g^{\mu\nu}+\frac{1}{2}g_{\mu\nu}g^{\alpha\sigma}\phi^2{}_{,\alpha\sigma}\delta g^{\mu\nu}
\end{aligned}\tag{A.8}$$

where the vector $\widetilde\omega^\nu$ is

$$\widetilde\omega^\nu=-\left(g^{\mu\nu}g^{\alpha\sigma}-\frac{1}{2}g^{\mu\sigma}g^{\alpha\nu}\right)\phi^2{}_{,\alpha}\delta g_{\mu\sigma}\,.$$

Then using

$$\Gamma^{\alpha}_{\mu\alpha} = \frac{1}{2} g^{\alpha\beta} g_{\alpha\beta,\mu}$$

the third term in (A.7) can be written as

$$\begin{aligned} g^{\mu\nu}\delta\Gamma^{\alpha}_{\mu\alpha}\phi^2{}_{,\nu} &= \frac{1}{2} g^{\mu\nu} g^{\alpha\beta} \left(\delta g_{\alpha\beta}\right)_{,\mu} \phi^2{}_{,\nu} \\ &= \frac{1}{2} g^{\mu\nu} g^{\alpha\beta} \left(\delta g_{\alpha\beta}\phi^2{}_{,\nu}\right)_{,\mu} - \frac{1}{2} g^{\mu\nu} g^{\alpha\beta} \delta g_{\alpha\beta}\phi^2{}_{,\mu\nu} \\ &= \widehat{\omega}^{\mu}{}_{,\mu} + \frac{1}{2} g_{\mu\nu} g^{\alpha\beta} \phi^2{}_{,\alpha\beta} \delta g^{\mu\nu} \end{aligned} \tag{A.9}$$

where the vector $\widehat{\omega}^{\mu}$ is

$$\widehat{\omega}^{\mu} = \frac{1}{2} g^{\mu\nu} g^{\alpha\beta} \phi^2{}_{,\nu} \delta g_{\alpha\beta} \,.$$

In an arbitrary coordinate system we need to replace the ordinary differentiation by the covariant derivative

$$\omega^{\alpha}{}_{,\alpha} \mapsto \omega^{\alpha}{}_{;\alpha} = \frac{1}{\sqrt{-g}} \left(\sqrt{-g}\,\omega^{\alpha}\right)_{,\alpha}$$

then using (A.8) and (A.9) the formula (A.7) can be written as

$$g^{\mu\nu}\delta R_{\mu\nu}\phi^2 = \left(\bar{\omega}^{\alpha} + \widetilde{\omega}^{\alpha} + \widehat{\omega}^{\alpha}\right)_{;\alpha} + \left(g_{\mu\nu} g^{\alpha\beta} \phi^2{}_{;\alpha\beta} - \phi^2{}_{;\mu\nu}\right) \delta g^{\mu\nu}$$

Then the last integral in (A.6) is equal to

$$\begin{aligned} -\varepsilon\frac{1}{2}\xi \int \mathrm{d}^4x \sqrt{-g} g^{\mu\nu}\delta R_{\mu\nu}\phi^2 &= -\varepsilon\frac{1}{2}\xi \int \mathrm{d}^4x \left(\sqrt{-g}\left(\bar{\omega}^{\alpha} + \widetilde{\omega}^{\alpha} + \widehat{\omega}^{\alpha}\right)\right)_{,\alpha} \\ &\quad -\varepsilon\frac{1}{2}\xi \int \mathrm{d}^4x \sqrt{-g} \left(g_{\mu\nu} g^{\alpha\beta} \phi^2{}_{;\alpha\beta} - \phi^2{}_{;\mu\nu}\right) \delta g^{\mu\nu} \end{aligned}$$

and by Gauss' theorem the first term drops out

$$\int \mathrm{d}^4x \left(\sqrt{-g}\left(\bar{\omega}^{\alpha} + \widetilde{\omega}^{\alpha} + \widehat{\omega}^{\alpha}\right)\right)_{,\alpha} = 0 \,.$$

Finally, the variation δS_{ϕ} is equal to

$$\begin{aligned} \delta S_{\phi} &= -\frac{1}{2} \int \mathrm{d}^4x \sqrt{-g} \Big\{ \varepsilon \nabla_{\mu}\phi \nabla_{\nu}\phi - \varepsilon\frac{1}{2} g_{\mu\nu} \nabla^{\alpha}\phi \nabla_{\alpha}\phi - U(\phi) g_{\mu\nu} \\ &\quad + \varepsilon\xi \left(R_{\mu\nu} - \frac{1}{2} g_{\mu\nu} R\right) \phi^2 + \varepsilon\xi \left(g_{\mu\nu} g^{\alpha\beta} \nabla_{\alpha}\nabla_{\beta}\phi^2 - \nabla_{\mu}\nabla_{\nu}\phi^2\right) \Big\} \delta g^{\mu\nu}. \end{aligned} \tag{A.10}$$

Thus from the principle of least action $\delta S_g + \delta S_\phi = 0$ and in view of arbitrariness of the $\delta g^{\mu\nu}$ we find the required equations of the gravitational field

$$R_{\mu\nu} - \frac{1}{2} g_{\mu\nu} R + \Lambda g_{\mu\nu} = \kappa^2 T_{\mu\nu} \tag{A.11}$$

and energy–momentum tensor for non-minimally coupled scalar field

$$\begin{aligned} T_{\mu\nu} &= \varepsilon \nabla_\mu \phi \nabla_\nu \phi - \varepsilon \frac{1}{2} g_{\mu\nu} \nabla^\alpha \phi \nabla_\alpha \phi - U(\phi) g_{\mu\nu} \\ &\quad + \varepsilon\xi \left(R_{\mu\nu} - \frac{1}{2} g_{\mu\nu} R \right) \phi^2 + \varepsilon\xi \left(g_{\mu\nu} \Box - \nabla_\mu \nabla_\nu \right) \phi^2, \end{aligned} \tag{A.12}$$

where $\Box = g^{\alpha\beta} \nabla_\alpha \nabla_\beta$.

Appendix B

Conformal invariance

We present a pedagogical derivation of invariance of the n–dimensional Klein–Gordon equation in the presence of the non-minimal coupling under conformal transformation. Consider the action for the non-minimally coupled scalar field in n spacetime dimensions

$$S_\phi = -\frac{1}{2}\int \mathrm{d}^n x\sqrt{-g}\Big\{\varepsilon\Big(g^{\mu\nu}\nabla_\mu\phi\,\nabla_\nu\phi + \xi R\,\phi^2\Big) + 2U(\phi)\Big\} \tag{B.1}$$

then from the variation $\delta S_\phi/\delta\phi = 0$ we can obtain the dynamical equation for the scalar field, the Klein–Gordon equation

$$\Box\phi - \xi R\,\phi - \varepsilon U'(\phi) = 0. \tag{B.2}$$

Using the conformal transformation we will find the value of of the ξ parameter for which the form of the Klein–Gordon equation is conformally invariant.

Lets consider a spacetime $(M, g_{\mu\nu})$ where M is a smooth $n \geq 2$ dimensional manifold and $g_{\mu\nu}$ a Lorentzian or Riemannian metric on it, the spacetime coordinate dependent rescaling of the metric tensor

$$g_{\mu\nu} \;\to\; \widetilde{g}_{\mu\nu} = \Omega^2(\mathbf{x}) g_{\mu\nu} \tag{B.3}$$

is called a Weyl or conformal transformation. The conformal factor $\Omega(\mathbf{x})$ is a nonsingular and regular function of spacetime coordinates.

The following transformation properties of the metric tensor, the determinant of the metric tensor and the scalar field are useful:

$$\widetilde{g}_{\mu\nu} = \Omega^2 g_{\mu\nu} \quad , \qquad \widetilde{g}^{\mu\nu} = \Omega^{-2} g^{\mu\nu} \quad , \qquad \widetilde{g} = \Omega^{2n} g \quad , \quad \widetilde{\phi} = \Omega^{-\frac{n-2}{2}}\,\phi\,.$$

We begin with calculation of the transformation rules for the d'Alambert's operator $\widetilde{\Box}$ acting on the scalar field $\widetilde{\phi}$

$$\begin{aligned}
\widetilde{\Box}\widetilde{\phi} &= \widetilde{g}^{\mu\nu}\nabla_\mu\nabla_\nu\widetilde{\phi} = \frac{1}{\sqrt{-\widetilde{g}}}\,\partial_\mu\left(\sqrt{-\widetilde{g}}\;\widetilde{g}^{\mu\nu}\,\widetilde{\phi}_{,\nu}\right)\\
&= \frac{\Omega^{-n}}{\sqrt{-g}}\,\partial_\mu\left(\Omega^n\,\sqrt{-g}\,\Omega^{-2}\,g^{\mu\nu}\,\partial_\nu\left(\Omega^{-\frac{n-2}{2}}\,\phi\right)\right)\\
&= \frac{\Omega^{-n}}{\sqrt{-g}}\,\partial_\mu\left(\Omega^{\frac{n-2}{2}}\sqrt{-g}\,g^{\mu\nu}\,\phi_{,\nu} - \frac{n-2}{2}\Omega^{\frac{n-2}{2}}\,\phi\,\sqrt{-g}\,g^{\mu\nu}\,(\ln\Omega)_{,\nu}\right)\\
&= \Omega^{-\frac{n+2}{2}}\left(\Box\phi - \frac{n-2}{2}\phi\,\Box(\ln\Omega) - \left(\frac{n-2}{2}\right)^2\phi\,g^{\mu\nu}(\ln\Omega)_{,\mu}(\ln\Omega)_{,\nu}\right)\\
&= \Omega^{-\frac{n+2}{2}}\left(\Box\phi - \frac{n-2}{2}\phi\,\Box(\ln\Omega) - \left(\frac{n-2}{2}\right)^2\phi\,\nabla^\alpha(\ln\Omega)\nabla_\alpha(\ln\Omega)\right). \qquad \text{(B.4)}
\end{aligned}$$

The Ricci tensor is given by

$$\widetilde{R}_{\mu\nu} = \widetilde{\Gamma}^\alpha_{\mu\nu,\alpha} - \widetilde{\Gamma}^\alpha_{\alpha\nu,\mu} + \widetilde{\Gamma}^\alpha_{\mu\nu}\,\widetilde{\Gamma}^\beta_{\beta\alpha} - \widetilde{\Gamma}^\alpha_{\beta\nu}\,\widetilde{\Gamma}^\beta_{\alpha\mu} \qquad \text{(B.5)}$$

and to derive its transformation the following transformation properties of the Christoffel symbols will be useful:

$$\begin{aligned}
\widetilde{\Gamma}^\alpha_{\mu\nu} &= \frac{1}{2}\,\widetilde{g}^{\alpha\sigma}\big(\,\widetilde{g}_{\nu\sigma,\mu} + \widetilde{g}_{\sigma\mu,\nu} - \widetilde{g}_{\mu\nu,\sigma}\big)\\
&= \Gamma^\alpha_{\mu\nu} + \Omega^{-1}\big(\,\delta^\alpha_\mu\,\Omega_{,\nu} + \delta^\alpha_\nu\,\Omega_{,\mu} - g_{\mu\nu}\,g^{\alpha\sigma}\,\Omega_{,\sigma}\big)\\
&= \Gamma^\alpha_{\mu\nu} + \Omega^{-1}\big(\,\delta^\alpha_\mu\,\nabla_\nu\Omega + \delta^\alpha_\nu\,\nabla_\mu\Omega - g_{\mu\nu}\,\nabla^\alpha\Omega\big) \qquad \text{(B.6)}
\end{aligned}$$

$$\begin{aligned}
\widetilde{\Gamma}^\alpha_{\mu\nu,\alpha} &= \Gamma^\alpha_{\mu\nu,\alpha} + \Omega^{-1}\big(\,\delta^\alpha_\mu\,\Omega_{,\nu\alpha} + \delta^\alpha_\nu\,\Omega_{,\mu\alpha} - (g_{\mu\nu}\,g^{\alpha\sigma}\,\Omega_{,\sigma})_{,\alpha}\big)\\
&\quad -\Omega^{-2}\,\Omega_{,\alpha}\big(\,\delta^\alpha_\mu\,\Omega_{,\nu} + \delta^\alpha_\nu\,\Omega_{,\mu} - g_{\mu\nu}\,g^{\alpha\sigma}\,\Omega_{,\sigma}\big)\\
&= \Gamma^\alpha_{\mu\nu,\alpha} + \Omega^{-1}\big(\,2\,\Omega_{,\mu\nu} - (g_{\mu\nu}\,\nabla^\alpha\Omega)_{,\alpha}\big)\\
&\quad -\Omega^{-2}\big(2\,\nabla_\mu\Omega\nabla_\nu\Omega - g_{\mu\nu}\,\nabla^\alpha\Omega\nabla_\alpha\Omega\big) \qquad \text{(B.7)}
\end{aligned}$$

$$\begin{aligned}
\widetilde{\Gamma}^\alpha_{\alpha\nu} &= \frac{1}{2}\,\widetilde{g}^{\alpha\sigma}\,\widetilde{g}_{\alpha\sigma,\nu} = \frac{1}{2}\,\Omega^{-2}\,g^{\alpha\sigma}\big(\,\Omega^2\,g_{\alpha\sigma}\big)_{,\nu}\\
&= \Gamma^\alpha_{\alpha\nu} + \delta^\alpha_\alpha\,\Omega^{-1}\,\Omega_{,\nu} = \Gamma^\alpha_{\alpha\nu} + n\,\Omega^{-1}\,\nabla_\nu\Omega \qquad \text{(B.8)}
\end{aligned}$$

$$\widetilde{\Gamma}^\alpha_{\alpha\nu,\mu} = \Gamma^\alpha_{\alpha\nu,\mu} + n\,\Omega^{-1}\,\Omega_{,\mu\nu} - n\,\Omega^{-2}\,\Omega_{,\mu}\,\Omega_{,\nu} \qquad \text{(B.9)}$$

$$\begin{aligned}
\widetilde{\Gamma}^{\alpha}_{\mu\nu}\,\widetilde{\Gamma}^{\beta}_{\beta\alpha} &= \Big(\Gamma^{\alpha}_{\mu\nu} + \Omega^{-1}\big(\,\delta^{\alpha}_{\mu}\,\Omega_{,\nu} + \delta^{\alpha}_{\nu}\,\Omega_{,\mu} - g_{\mu\nu}\,g^{\alpha\sigma}\,\Omega_{,\sigma}\big)\Big)\Big(\,\Gamma^{\beta}_{\beta\alpha} + n\,\Omega^{-1}\,\Omega_{,\alpha}\Big) \\
&= \Gamma^{\alpha}_{\mu\nu}\,\Gamma^{\beta}_{\beta\alpha} + n\,\Omega^{-1}\,\Gamma^{\alpha}_{\mu\nu}\,\Omega_{,\alpha} \\
&\quad + \Omega^{-1}\Big(\,\Gamma^{\beta}_{\beta\mu}\,\Omega_{,\nu} + \Gamma^{\beta}_{\beta\nu}\,\Omega_{\,\mu} - g_{\mu\nu}\,g^{\alpha\sigma}\,\Gamma^{\beta}_{\beta\alpha}\,\Omega_{,\sigma}\Big) \\
&\quad + n\,\Omega^{-2}\Big(\,2\,\Omega_{,\mu}\,\Omega_{,\nu} - g_{\mu\nu}\,g^{\alpha\sigma}\,\Omega_{,\alpha}\,\Omega_{,\sigma}\Big) \qquad \text{(B.10)}
\end{aligned}$$

$$\begin{aligned}
\widetilde{\Gamma}^{\alpha}_{\beta\nu}\,\widetilde{\Gamma}^{\beta}_{\alpha\mu} &= \Big(\Gamma^{\alpha}_{\beta\mu} + \Omega^{-1}\big(\,\delta^{\alpha}_{\beta}\,\Omega_{,\nu} + \delta^{\alpha}_{\nu}\,\Omega_{,\beta} - g_{\beta\nu}\,g^{\alpha\sigma}\,\Omega_{,\sigma}\big)\Big) \\
&\quad \Big(\Gamma^{\beta}_{\alpha\mu} + \Omega^{-1}\big(\,\delta^{\beta}_{\alpha}\,\Omega_{,\mu} + \delta^{\beta}_{\mu}\,\Omega_{,\alpha} - g_{\alpha\mu}\,g^{\beta\gamma}\,\Omega_{,\gamma}\big)\Big) \\
&= \Gamma^{\alpha}_{\beta\nu}\,\Gamma^{\beta}_{\alpha\mu} \\
&\quad + \Omega^{-1}\Big(\,4\,\Gamma^{\alpha}_{\mu\nu}\,\Omega_{,\alpha} + \Gamma^{\alpha}_{\alpha\mu}\,\Omega_{,\nu} + \Gamma^{\alpha}_{\alpha\nu}\,\Omega_{,\mu} - g^{\alpha\sigma}\big(\,g_{\alpha\mu,\nu} + g_{\alpha\nu,\mu}\big)\Omega_{,\sigma}\Big) \\
&\quad + \Omega^{-2}\Big(\,(n+2)\,\Omega_{,\mu}\,\Omega_{,\nu} - 2\,g_{\mu\nu}\,g^{\alpha\beta}\,\Omega_{,\alpha}\,\Omega_{,\beta}\Big) \qquad \text{(B.11)}
\end{aligned}$$

where the following relation was used

$$g_{\beta\nu}\,g^{\alpha\sigma}\,\Gamma^{\beta}_{\alpha\mu} = -\Gamma^{\sigma}_{\mu\nu} + g^{\sigma\alpha}\,g_{\alpha\nu,\mu}.$$

Now, inserting equations (B.7), (B.9), (B.10), (B.11) in to equation (B.5), we have

$$\begin{aligned}
\widetilde{R}_{\mu\nu} &= \widetilde{\Gamma}^{\alpha}_{\mu\nu,\alpha} - \widetilde{\Gamma}^{\alpha}_{\alpha\nu,\mu} + \widetilde{\Gamma}^{\alpha}_{\mu\nu}\,\widetilde{\Gamma}^{\beta}_{\beta\alpha} - \widetilde{\Gamma}^{\alpha}_{\beta\nu}\,\widetilde{\Gamma}^{\beta}_{\alpha\mu} \\
&= R_{\mu\nu} \\
&\quad + \Omega^{-1}\Big(\,-(n-2)\Omega_{,\mu\nu} - g_{\mu\nu}\,g^{\alpha\beta}\,\Omega_{,\alpha\beta} + (n-2)\,\Gamma^{\alpha}_{\mu\nu}\,\Omega_{,\alpha} + g_{\mu\nu}\,g^{\alpha\beta}\,\Gamma^{\sigma}_{\alpha\beta}\,\Omega_{,\sigma}\Big) \\
&\quad + \Omega^{-2}\Big(2(n-2)\,\Omega_{,\mu}\,\Omega_{,\nu} - (n-3)g_{\mu\nu}\,g^{\alpha\beta}\,\Omega_{,\alpha}\,\Omega_{,\beta}\Big) \qquad \text{(B.12)}
\end{aligned}$$

which using the following equations

$$(\ln\Omega)_{,\mu\nu} = \partial_{\nu}\left(\frac{\Omega_{,\mu}}{\Omega}\right) = \Omega^{-1}\,\Omega_{,\mu\nu} - \Omega^{-2}\,\Omega_{,\mu}\,\Omega_{,\nu}$$

$$\nabla_{\nu}A_{\mu} = A_{\mu,\nu} - \Gamma^{\sigma}_{\mu\nu}\,A_{\sigma}$$

$$\nabla_{\mu}\nabla_{\nu}(\ln\Omega) = \nabla_{\nu}((\ln\Omega)_{,\mu}) = (\ln\Omega)_{,\mu\nu} - \Gamma^{\alpha}_{\mu\nu}\,(\ln\Omega)_{,\alpha}$$

can be presented as the final form of the transformation property of the Ricci tensor

$$\begin{aligned}
\widetilde{R}_{\mu\nu} &= R_{\mu\nu} - (n-2)\,\nabla_{\mu}\nabla_{\nu}(\ln\Omega) - g_{\mu\nu}\,\Box(\ln\Omega) \\
&\quad + (n-2)\,\nabla_{\mu}(\ln\Omega)\,\nabla_{\nu}(\ln\Omega) - (n-2)\,g^{\mu\nu}\,\nabla^{\alpha}(\ln\Omega)\,\nabla_{\alpha}(\ln\Omega)\,. \qquad \text{(B.13)}
\end{aligned}$$

The transformation property of the Ricci scalar can be presented in the following form

$$\widetilde{R} = \Omega^{-2}\Big(R - 2(n-1)\,\Box(\ln\Omega) - (n-1)(n-2)\,\nabla^{\alpha}(\ln\Omega)\,\nabla_{\alpha}(\ln\Omega)\Big). \tag{B.14}$$

Finally, we arrive to the source–free Klein–Gordon equation in the presence of non-minimal coupling

$$\widetilde{\Box}\widetilde{\phi} - \xi\widetilde{R}\,\widetilde{\phi} = 0 \tag{B.15}$$

which transformation property, using equations (B.4), (B.14), can be written as

$$\begin{aligned}
&\Omega^{-\frac{n+2}{2}}\left(\Box\phi - \frac{n-2}{2}\phi\,\Box(\ln\Omega) - \left(\frac{n-2}{2}\right)^{2}\phi\,\nabla^{\alpha}(\ln\Omega)\,\nabla_{\alpha}(\ln\Omega)\right)\\
&-\xi\,\Omega^{-2}\Big(R - 2(n-1)\,\Box(\ln\Omega) - (n-1)(n-2)\,\nabla^{\alpha}(\ln\Omega)\,\nabla_{\alpha}(\ln\Omega)\Big)\Omega^{-\frac{n-2}{2}}\,\phi\\
&=\Omega^{-\frac{n+2}{2}}\Bigg\{\Box\phi - \xi R\,\phi + \left(2(n-1)\xi - \frac{n-2}{2}\right)\phi\,\Box(\ln\Omega)\\
&\qquad + \left((n-1)(n-2)\xi - \left(\frac{n-2}{2}\right)^{2}\right)\phi\,\nabla^{\alpha}(\ln\Omega)\,\nabla_{\alpha}(\ln\Omega)\Bigg\} = 0
\end{aligned} \tag{B.16}$$

Now one can simply notice that if

$$\xi = \frac{n-2}{4(n-1)}$$

the source–free Klein–Gordon equation (B.15) is conformally invariant

$$\widetilde{\Box}\widetilde{\phi} - \frac{n-2}{4(n-1)}\widetilde{R}\,\widetilde{\phi} = \Omega^{-\frac{n+2}{2}}\left(\Box\phi - \frac{n-2}{4(n-1)}R\,\phi\right) = 0. \tag{B.17}$$

In cosmological applications a potential function $U(\phi)$ of the scalar field is introduced, yielding (B.2)

$$\Box\phi - \xi R\,\phi - \varepsilon U'(\phi) = 0 \tag{B.18}$$

where $\varepsilon = \pm 1$ corresponds to the canonical and phantom scalar field, respectively. In four spacetime dimensions this equation is conformally invariant if $\xi = 1/6$ and $U(\phi) = 0$ or $U(\phi) = \lambda\phi^4$ [22, 174, 86]. A constant potential function $U(\phi) = \text{const}$, equivalent to the inclusion of a cosmological constant, corresponds to an effective mass for the scalar breaks conformal invariance [175].

Appendix C

The Center Manifold Theorem

We present here the theorem concerning behaviour of nonlinear dynamical system in the vicinity of degenerated critical point. Expanded discussion can be found, for example, in books by Perko [59] or Wiggins [60].

Suppose we consider the following 3-dimensional nonlinear dynamical system

$$\dot{\mathbf{x}} = f(\mathbf{x}), \qquad \mathbf{x} \in \mathbb{R}^3 \tag{C.1}$$

We are interested in the nature of solution to this dynamical system near fixed point $\bar{\mathbf{x}}$ for which $f(\bar{\mathbf{x}}) = 0$.

First, we transform the fixed point $\mathbf{x} = \bar{\mathbf{x}}$ of (C.1) to the origin using the transformation $\mathbf{y} = \mathbf{x} - \bar{\mathbf{x}}$. Then the system (C.1) becomes

$$\dot{\mathbf{y}} = f(\bar{\mathbf{x}} + \mathbf{y}), \qquad \mathbf{y} \in \mathbb{R}^3 \tag{C.2}$$

then Taylor expansion of $f(\bar{\mathbf{x}} + \mathbf{y})$ about $\mathbf{x} = \bar{\mathbf{x}}$ gives

$$\dot{\mathbf{y}} = A\mathbf{y} + R(\mathbf{y}), \qquad \mathbf{y} \in \mathbb{R}^3 \tag{C.3}$$

where $A = Df(\bar{\mathbf{x}})$ ia a linearization matrix calculated at the fixed point, $R(\mathbf{y}) = \mathcal{O}(|\mathbf{y}|^n)$ and we have used $f(\bar{\mathbf{x}}) = 0$.

From now on we will assume that the linearization matrix has purely real eigenvalues and one is zero $l_1 = 0$, one positive $l_2 > 0$ and one negative $l_3 < 0$. From elementary linear algebra we can find a linear transformation P which transforms the linear part of

equation (C.3) into a diagonal form

$$\begin{pmatrix} \dot{u} \\ \dot{v} \\ \dot{w} \end{pmatrix} = \begin{pmatrix} 0 & 0 & 0 \\ 0 & l_2 & 0 \\ 0 & 0 & l_3 \end{pmatrix} \begin{pmatrix} u \\ v \\ w \end{pmatrix} \tag{C.4}$$

with a linear transformation of variables

$$P^{-1}\mathbf{y} \equiv \begin{pmatrix} u \\ v \\ w \end{pmatrix}$$

and the matrix P is constructed from the corresponding eigenvectors of the linearization matrix A. Using this same linear transformation to transform the coordinates of the nonlinear part of the system (C.3) gives the following

$$\begin{aligned} \dot{u} &= F\big(u,v,w\big), \\ \dot{v} &= l_2 v + G\big(u,v,w\big), \\ \dot{w} &= l_3 w + H\big(u,v,w\big). \end{aligned} \tag{C.5}$$

where $F(u,v,w)$, $G(u,v,w)$ and $H(u,v,w)$ are polynomial in the coordinates. The fixed point $(u,v,w) = (0,0,0)$ is unstable due to the existence of a 1-dimensional unstable manifold associated with the negative eigenvalue $l_3 < 0$.

Definition C.1 (Center Manifold) *An invariant manifold will be called a center manifold for (C.5) if it can be locally represented by*

$$W^c(0) = \Big\{(u,v,w) \in \mathbb{R}^3 \big| v = h_1(u), w = h_2(u), |u| < \delta, h_i(0) = 0, h_i'(0) = 0, i = 1,2\Big\} \tag{C.6}$$

for δ sufficiently small.

Theorem C.1 (Existence) *There exists a $\mathbf{C}^r$ center manifold for (C.5). The dynamics of (C.5) restricted to the center manifold is, for η sufficiently small, given by the following 1-dimensional vector field*

$$\dot{\eta} = F\big(\eta, h_1(\eta), h_2(\eta)\big). \tag{C.7}$$

From the fact that the center manifold is invariant under the dynamics generated by (C.5) we obtain

$$\begin{aligned} \dot{u} &= F\big(u, h_1(u), h_2(u)\big), \\ \dot{v} &= h_1'(u)\dot{u} = l_2 h_1(u) + G\big(u, h_1(u), h_2(u)\big), \\ \dot{w} &= h_2'(u)\dot{u} = l_3 h_2(u) + H\big(u, h_1(u), h_2(u)\big), \end{aligned} \tag{C.8}$$

which yields the following quasilinear differential equation for $h_1(u)$ and $h_2(u)$

$$\begin{aligned} \mathcal{N}\big(h_1(u)\big) &= h_1'(u)F\big(u, h_1(u), h_2(u)\big) - l_2 h_1(u) - G\big(u, h_1(u), h_2(u)\big) = 0, \\ \mathcal{N}\big(h_2(u)\big) &= h_2'(u)F\big(u, h_1(u), h_2(u)\big) - l_3 h_2(u) - H\big(u, h_1(u), h_2(u)\big) = 0, \end{aligned} \tag{C.9}$$

and the following theorem (see Theorem 18.1.4 in Wiggins [60, p. 248]) justify solving (C.9) approximately via power series expansion:

Theorem C.2 (Approximation) *Let $\phi\colon \mathbb{R} \to \mathbb{R}$ be a $\mathbf{C}^1$ mapping with $\phi(0) = \phi'(0) = 0$ such that $\mathcal{N}\big(\phi(u)\big) = \mathcal{O}\big(|u|^q\big)$ as $u \to 0$ for some $q > 1$. Then*

$$|h(u) - \phi(u)| = \mathcal{O}\big(|u|^q\big) \qquad \text{as} \qquad u \to 0.$$

This theorem allows us to compute the center manifold to any desired degree of accuracy by solving (C.9) to the same degree of accuracy.

Bibliography

[1] A. D. Linde, *A New Inflationary Universe Scenario: A Possible Solution of the Horizon, Flatness, Homogeneity, Isotropy and Primordial Monopole Problems*, *Phys. Lett.* **B108** (1982) 389–393.

[2] A. D. Linde, *Chaotic Inflation*, *Phys. Lett.* **B129** (1983) 177–181.

[3] **Supernova Search Team** Collaboration, A. G. Riess, A. V. Filippenko, P. Challis, A. Clocchiattia, A. Diercks, P. M. Garnavich, R. L. Gilliland, C. J. Hogan, S. Jha, R. P. Kirshner, B. Leibundgut, M. M. Phillips, D. Reiss, B. P. Schmidt, R. A. Schommer, R. C. Smith, J. Spyromilio, C. Stubbs, N. B. Suntzeff, and J. Tonry, *Observational evidence from supernovae for an accelerating universe and a cosmological constant*, *Astron. J.* **116** (1998) 1009–1038, [astro-ph/9805201].

[4] **Supernova Cosmology Project** Collaboration, S. Perlmutter, G. Aldering, G. Goldhaber, R. Knop, P. Nugent, P. Castro, S. Deustua, S. Fabbro, A. Goobar, D. Groom, I. M. Hook, A. Kim, M. Kim, J. Lee, N. Nunes, C. P. R. Pain, R. Quimby, C. Lidman, R. Ellis, M. Irwin, R. McMahon, P. Ruiz-Lapuente, N. Walton, B. Schaefer, B. Boyle, A. Filippenko, T. Matheson, A. Fruchter, N. Panagia, H. Newberg, and W. Couch, *Measurements of omega and lambda from 42 high-redshift supernovae*, *Astrophys. J.* **517** (1999) 565–586, [astro-ph/9812133].

[5] E. J. Copeland, M. Sami, and S. Tsujikawa, *Dynamics of dark energy*, *Int. J. Mod. Phys.* **D15** (2006) 1753–1936, [hep-th/0603057].

[6] B. Ratra and P. J. E. Peebles, *Cosmological consequences of a rolling homogeneous scalar field*, *Phys. Rev.* **D37** (1988) 3406.

[7] C. Wetterich, *Cosmology and the fate of dilatation symmetry*, *Nucl. Phys.* **B302** (1988) 668.

[8] A. Kurek and M. Szydlowski, *The LambdaCDM model on the lead – a Bayesian cosmological models comparison*, *Astrophys. J.* **675** (2008) 1–7, [astro-ph/0702484].

[9] A. Kurek and M. Szydlowski, *Chasing Lambda*, *Nuovo Cim.* **122B** (2008) 1359–1364, [arXiv:0710.2125].

[10] M. Szydlowski, A. Kurek, and A. Krawiec, *Top ten accelerating cosmological models*, *Phys. Lett.* **B642** (2006) 171–178, [astro-ph/0604327].

[11] S. Weinberg, *The cosmological constant problem*, *Rev. Mod. Phys.* **61** (1989) 1–23.

[12] I. Zlatev, L.-M. Wang, and P. J. Steinhardt, *Quintessence, Cosmic Coincidence, and the Cosmological Constant*, *Phys. Rev. Lett.* **82** (1999) 896–899, [astro-ph/9807002].

[13] R. R. Caldwell, M. Kamionkowski, and N. N. Weinberg, *Phantom Energy: Dark Energy with $w < -1$ Causes a Cosmic Doomsday*, *Phys. Rev. Lett.* **91** (2003) 071301, [astro-ph/0302506].

[14] M. P. Dabrowski, T. Stachowiak, and M. Szydlowski, *Phantom cosmologies*, *Phys. Rev.* **D68** (2003) 103519, [hep-th/0307128].

[15] V. Faraoni and M. N. Jensen, *Extended quintessence, inflation, and stable de Sitter spaces*, *Class. Quant. Grav.* **23** (2006) 3005–3016, [gr-qc/0602097].

[16] V. Faraoni, *A crucial ingredient of inflation*, *Int. J. Theor. Phys.* **40** (2001) 2259–2294, [hep-th/0009053].

[17] O. Hrycyna and M. Szydlowski, *Route to Lambda in conformally coupled phantom cosmology*, *Phys. Lett.* **B651** (2007) 8–14, [arXiv:0704.1651].

[18] O. Hrycyna and M. Szydlowski, *Extended Quintessence with non-minimally coupled phantom scalar field*, *Phys. Rev.* **D76** (2007) 123510, [arXiv:0707.4471].

[19] A. Ashtekar, T. Pawlowski, and P. Singh, *Quantum nature of the big bang*, *Phys. Rev. Lett.* **96** (2006) 141301, [gr-qc/0602086].

[20] **WMAP** Collaboration, E. Komatsu, J. Dunkley, M. R. Nolta, C. L. Bennett, B. Gold, G. Hinshaw, N. Jarosik, D. Larson, M. Limon, L. Page, D. N. Spergel, M. Halpern, R. S. Hill, A. Kogut, S. S. Meyer, G. S. Tucker, J. L. Weiland, E. Wollack, and E. L. Wright, *Five-Year Wilkinson Microwave Anisotropy Probe (WMAP) Observations: Cosmological Interpretation*, *Astrophys. J. Suppl.* **180** (2009) 330–376, [arXiv:0803.0547].

[21] N. A. Chernikov and E. A. Tagirov, *Quantum theory of scalar fields in de Sitter space-time*, *Annales Poincare Phys. Theor.* **A9** (1968) 109.

[22] C. G. Callan, Jr., S. R. Coleman, and R. Jackiw, *A New improved energy-momentum tensor*, *Ann. Phys.* **59** (1970) 42–73.

[23] N. D. Birrell and P. C. W. Davies, *Conformal-symmetry breaking and cosmological particle creation in $\lambda\phi^4$ theory*, *Phys. Rev.* **D22** (1980) 322.

[24] M.-X. Luo and Q.-P. Su, *Fitting Non-Minimally Coupled Scalar Models to Gold SnIa Dataset*, *Phys. Lett.* **B626** (2005) 7–14, [astro-ph/0506093].

[25] M. Jankiewicz and T. W. Kephart, *Long-wavelength modes of cosmological scalar fields*, *Phys. Rev.* **D73** (2006) 123514, [hep-ph/0510009].

[26] M. Szydlowski, O. Hrycyna, and A. Kurek, *Coupling constant constraints in a nonminimally coupled phantom cosmology*, *Phys. Rev.* **D77** (2008) 027302, [arXiv:0710.0366].

[27] N. D. Birrell and P. C. W. Davies, *Quantum Fields in Curved Space*. Cambridge University Press, Cambridge, 1984.

[28] E. Komatsu, K. M. Smith, J. Dunkley, C. L. Bennett, B. Gold, G. Hinshaw, N. Jarosik, D. Larson, M. R. Nolta, L. Page, D. N. Spergel, M. Halpern, R. S. Hill, A. Kogut, M. Limon, S. S. Meyer, N. Odegard, G. S. Tucker, J. L. Weiland, E. Wollack, and E. L. Wright, *Seven-Year Wilkinson Microwave Anisotropy Probe (WMAP) Observations: Cosmological Interpretation*, arXiv:1001.4538.

[29] S. C. Park and S. Yamaguchi, *Inflation by non-minimal coupling*, *JCAP* **08** (2008) 009, [arXiv:0801.1722].

[30] B. L. Spokoiny, *Inflation and generation of perturbations in broken-symmetric theory of gravity*, *Phys. Lett.* **B147** (1984) 39–43.

[31] D. S. Salopek, J. R. Bond, and J. M. Bardeen, *Designing Density Fluctuation Spectra in Inflation*, *Phys. Rev.* **D40** (1989) 1753.

[32] R. Fakir, S. Habib, and W. Unruh, *Cosmological density perturbations with modified gravity*, *Astrophys. J.* **394** (1992) 396.

[33] V. A. Belinsky, I. M. Khalatnikov, L. P. Grishchuk, and Y. B. Zeldovich, *Inflationary stages in cosmological models with a scalar field*, *Phys. Lett.* **B155** (1985) 232–236.

[34] A. O. Barvinsky and A. Y. Kamenshchik, *Quantum scale of inflation and particle physics of the early universe*, *Phys. Lett.* **B332** (1994) 270–276, [gr-qc/9404062].

[35] A. O. Barvinsky and A. Y. Kamenshchik, *Effective equations of motion and initial conditions for inflation in quantum cosmology*, *Nucl. Phys.* **B532** (1998) 339–360, [hep-th/9803052].

[36] A. O. Barvinsky, A. Y. Kamenshchik, and A. A. Starobinsky, *Inflation scenario via the Standard Model Higgs boson and LHC*, *JCAP* **11** (2008) 021, [arXiv:0809.2104].

[37] M. R. Setare and E. N. Saridakis, *Braneworld models with a non-minimally coupled phantom bulk field: a simple way to obtain the -1-crossing at late times*, *JCAP* **03** (2009) 002, [arXiv:0811.4253].

[38] M. R. Setare and E. N. Saridakis, *Non-minimally coupled canonical, phantom and quintom models of holographic dark energy*, *Phys. Lett.* **B671** (2009) 331–338, [arXiv:0810.0645].

[39] O. Hrycyna and M. Szydlowski, *Non-minimally coupled scalar field cosmology on the phase plane*, *JCAP* **04** (2009) 026, [arXiv:0812.5096].

[40] J.-P. Uzan, *Cosmological scaling solutions of non-minimally coupled scalar fields*, *Phys. Rev.* **D59** (1999) 123510, [gr-qc/9903004].

[41] T. Chiba, *Quintessence, the gravitational constant, and gravity*, *Phys. Rev.* **D60** (1999) 083508, [gr-qc/9903094].

[42] L. Amendola, *Scaling solutions in general non-minimal coupling theories*, *Phys. Rev.* **D60** (1999) 043501, [astro-ph/9904120].

[43] F. Perrotta, C. Baccigalupi, and S. Matarrese, *Extended quintessence*, *Phys. Rev.* **D61** (2000) 023507, [astro-ph/9906066].

[44] D. J. Holden and D. Wands, *Self-similar cosmological solutions with a non-minimally coupled scalar field*, *Phys. Rev.* **D61** (2000) 043506, [gr-qc/9908026].

[45] N. Bartolo and M. Pietroni, *Scalar-Tensor Gravity and Quintessence*, *Phys. Rev.* **D61** (2000) 023518, [hep-ph/9908521].

[46] B. Boisseau, G. Esposito-Farese, D. Polarski, and A. A. Starobinsky, *Reconstruction of a scalar-tensor theory of gravity in an accelerating universe*, *Phys. Rev. Lett.* **85** (2000) 2236, [gr-qc/0001066].

[47] R. Gannouji, D. Polarski, A. Ranquet, and A. A. Starobinsky, *Scalar-tensor models of normal and phantom dark energy*, *JCAP* **09** (2006) 016, [astro-ph/0606287].

[48] S. Carloni, S. Capozziello, J. A. Leach, and P. K. S. Dunsby, *Cosmological dynamics of scalar-tensor gravity*, *Class. Quant. Grav.* **25** (2008) 035008, [gr-qc/0701009].

[49] F. L. Bezrukov and M. Shaposhnikov, *The Standard Model Higgs boson as the inflaton*, *Phys. Lett.* **B659** (2008) 703–706, [arXiv:0710.3755].

[50] K. Nozari and S. D. Sadatian, *Non-Minimal Inflation after WMAP3*, *Mod. Phys. Lett.* **A23** (2008) 2933–2945, [arXiv:0710.0058].

[51] A. Y. Kamenshchik, I. M. Khalatnikov, and A. V. Toporensky, *Nonminimally coupled complex scalar field in classical and quantum cosmology*, *Phys. Lett.* **B357** (1995) 36–42, [gr-qc/9508034].

[52] A. De Simone, M. P. Hertzberg, and F. Wilczek, *Running Inflation in the Standard Model*, *Phys. Lett.* **B678** (2009) 1–8, [arXiv:0812.4946].

[53] F. L. Bezrukov, A. Magnin, and M. Shaposhnikov, *Standard Model Higgs boson mass from inflation*, *Phys. Lett.* **B675** (2009) 88–92, [arXiv:0812.4950].

[54] A. O. Barvinsky, A. Y. Kamenshchik, C. Kiefer, A. A. Starobinsky, and C. Steinwachs, *Asymptotic freedom in inflationary cosmology with a non-minimally coupled Higgs field*, *JCAP* **12** (2009) 003, [arXiv:0904.1698].

[55] T. E. Clark, B. Liu, S. T. Love, and T. ter Veldhuis, *The Standard Model Higgs Boson-Inflaton and Dark Matter*, *Phys. Rev.* **D80** (2009) 075019, [arXiv:0906.5595].

[56] S. Ferrara, R. Kallosh, A. Linde, A. Marrani, and A. Van Proeyen, *Jordan Frame Supergravity and Inflation in NMSSM*, *Phys. Rev.* **D82** (2010) 045003, [arXiv:1004.0712].

[57] S. Ferrara, R. Kallosh, A. Linde, A. Marrani, and A. Van Proeyen, *Superconformal Symmetry, NMSSM, and Inflation*, *Phys. Rev.* **D83** (2011) 025008, [arXiv:1008.2942].

[58] A. Linde, M. Noorbala, and A. Westphal, *Observational consequences of chaotic inflation with nonminimal coupling to gravity*, arXiv:1101.2652.

[59] L. Perko, *Differential Equations and Dynamical Systems*. Texts in Applied Mathematics. Springer-Verlag, New York, 3rd ed., 2001.

[60] S. Wiggins, *Introduction to Applied Nonlinear Dynamical Systems and Chaos*. Texts in Applied Mathematics. Springer-Verlag, New York, 2nd ed., 2003.

[61] J. Wainwright and G. F. R. Ellis, eds., *Dynamical Systems in Cosmology*, (Cambridge), Cambridge University Press, 1997.

[62] R. R. Caldwell, *A phantom menace? Cosmological consequences of a dark energy component with super-negative equation of state*, *Phys. Lett.* **B545** (2002) 23–29, [astro-ph/9908168].

[63] S. M. Carroll, M. Hoffman, and M. Trodden, *Can the dark energy equation-of-state parameter w be less than -1?*, *Phys. Rev.* **D68** (2003) 023509, [astro-ph/0301273].

[64] L. Mersini-Houghton, M. Bastero-Gil, and P. Kanti, *Relic dark energy from trans-Planckian regime*, *Phys. Rev.* **D64** (2001) 043508, [hep-ph/0101210].

[65] M. Bastero-Gil, P. H. Frampton, and L. Mersini-Houghton, *Dark energy from closed strings in toroidal cosmology*, *Phys. Rev.* **D65** (2002) 106002, [hep-th/0110167].

[66] P. H. Frampton, *How to test stringy dark energy*, *Phys. Lett.* **B555** (2003) 139–143, [astro-ph/0209037].

[67] J. D. Barrow, *String-Driven Inflationary and Deflationary Cosmological Models*, *Nucl. Phys.* **B310** (1988) 743–763.

[68] M. Visser, S. Kar, and N. Dadhich, *Traversable wormholes with arbitrarily small energy condition violations*, *Phys. Rev. Lett.* **90** (2003) 201102, [gr-qc/0301003].

[69] L. Parker and A. Raval, *Non-perturbative effects of vacuum energy on the recent expansion of the universe*, *Phys. Rev.* **D60** (1999) 063512, [gr-qc/9905031].

[70] A. E. Schulz and M. J. White, *The tensor to scalar ratio of phantom dark energy models*, *Phys. Rev.* **D64** (2001) 043514, [astro-ph/0104112].

[71] V. Faraoni, *Superquintessence*, *Int. J. Mod. Phys.* **D11** (2002) 471–482, [astro-ph/0110067].

[72] V. K. Onemli and R. P. Woodard, *Super-acceleration from massless, minimally coupled phi**4*, *Class. Quant. Grav.* **19** (2002) 4607, [gr-qc/0204065].

[73] S. Hannestad and E. Mortsell, *Probing the dark side: Constraints on the dark energy equation of state from CMB, large scale structure and Type Ia supernovae*, *Phys. Rev.* **D66** (2002) 063508, [astro-ph/0205096].

[74] A. Melchiorri, L. Mersini-Houghton, C. J. Odman, and M. Trodden, *The State of the Dark Energy Equation of State*, *Phys. Rev.* **D68** (2003) 043509, [astro-ph/0211522].

[75] J.-g. Hao and X.-z. Li, *An attractor solution of phantom field*, *Phys. Rev.* **D67** (2003) 107303, [gr-qc/0302100].

[76] J. A. S. Lima, J. V. Cunha, and J. S. Alcaniz, *Constraining the dark energy with galaxy clusters X-ray data*, *Phys. Rev.* **D68** (2003) 023510, [astro-ph/0303388].

[77] P. Singh, M. Sami, and N. Dadhich, *Cosmological dynamics of phantom field*, *Phys. Rev.* **D68** (2003) 023522, [hep-th/0305110].

[78] J.-G. Hao and X.-z. Li, *Phantom Cosmic Dynamics: Tracking Attractor and Cosmic Doomsday*, *Phys. Rev.* **D70** (2004) 043529, [astro-ph/0309746].

[79] V. B. Johri, *Phantom cosmologies*, *Phys. Rev.* **D70** (2004) 041303, [astro-ph/0311293].

[80] Y.-S. Piao and E. Zhou, *Nearly scale-invariant spectrum of adiabatic fluctuations may be from a very slowly expanding phase of the universe*, *Phys. Rev.* **D68** (2003) 083515, [hep-th/0308080].

[81] U. Alam, V. Sahni, T. D. Saini, and A. A. Starobinsky, *Is there Supernova Evidence for Dark Energy Metamorphosis ?*, *Mon. Not. Roy. Astron. Soc.* **354** (2004) 275, [astro-ph/0311364].

[82] S. Nojiri and S. D. Odintsov, *Quantum deSitter cosmology and phantom matter*, *Phys. Lett.* **B562** (2003) 147–152, [hep-th/0303117].

[83] E. Elizalde, S. Nojiri, and S. D. Odintsov, *Late-time cosmology in (phantom) scalar-tensor theory: Dark energy and the cosmic speed-up*, *Phys. Rev.* **D70** (2004) 043539, [hep-th/0405034].

[84] M. Sami and A. Toporensky, *Phantom Field and the Fate of Universe*, *Mod. Phys. Lett.* **A19** (2004) 1509, [gr-qc/0312009].

[85] M. P. Dabrowski, C. Kiefer, and B. Sandhofer, *Quantum phantom cosmology*, *Phys. Rev.* **D74** (2006) 044022, [hep-th/0605229].

[86] V. Faraoni, *Cosmology in Scalar–Tensor Gravity*, vol. 139 of *Fundamental Theories of Phsics*. Kluwer Academic Publishers, Dordrecht/Boston/London, 2004.

[87] C. Brans and R. Dicke, *Mach's principle and a relativistic theory of gravitation*, *Phys.Rev.* **124** (1961) 925–935.

[88] C. M. Will, *The confrontation between general relativity and experiment: A 1998 update*, in *Proceedings of the Summer Instityte on Particle Physics* (L. Dixon, ed.), 2001. gr-qc/9811036.

[89] Y. Fujii and K.-i. Maeda, *The Scalar–Tensor Theory of Gravitation*. Cambridge Monographs on Mathematical Physics. Cambridge University Press, Cambridge, 2003.

[90] J. M. Overduin and P. S. Wesson, *Kaluza-Klein gravity*, *Phys. Rept.* **283** (1997) 303–380, [gr-qc/9805018].

[91] M. B. Green, J. Schwarz, and E. Witten, *SUPERSTRING THEORY: Volume 1 Introduction*. Cambridge University Press, Cambdidge, 1987.

[92] S. J. Kolitch and D. M. Eardley, *Behavior of Friedmann-Robertson-Walker cosmological models in scalar - tensor gravity*, *Ann. Phys.* **241** (1995) 128–151, [gr-qc/9405016].

[93] V. Faraoni and E. Gunzig, *Einstein frame or Jordan frame?*, *Int.J.Theor.Phys.* **38** (1999) 217–225, [astro-ph/9910176].

[94] V. Faraoni, *Inflation and quintessence with nonminimal coupling*, *Phys. Rev.* **D62** (2000) 023504, [gr-qc/0002091].

[95] M. Pettini, *Geometrical hints for a nonperturbative approach to Hamintonian dynamics*, *Phys. Rev.* **E47** (1993) 828–850.

[96] L. Casetti, M. Pettini, and E. G. D. Cohen, *Geometric approach to Hamiltonian dynamics and statistical mechanics*, *Phys. Rep* **337** (2000) 237–341, [cond-mat/9912092].

[97] M. Szydlowski and A. Krawiec, *Description of chaos in simple relativistic systems*, *Phys. Rev.* **D53** (1996) 6893–6901.

[98] M. Szydlowski, *Toward an invariant measure of chaotic behaviour in general relativity*, *Phys. Lett.* **A176** (1993) 22–32.

[99] M. Szydlowski and A. Krawiec, *Average rate of separation of trajectories near the singularity in mixmaster models*, *Phys. Rev.* **D47** (1993) 5323–5328.

[100] M. Szydlowski and A. Lapeta, *Pseudo-Riemannian manifold of mixmaster dynamical systems*, *Phys. Lett.* **A148** (1990) 239–245.

[101] A. Burd and R. Tavakol, *Invariant Lyapunov exponents and chaos in cosmology*, *Phys. Rev.* **D47** (1993) 5336–5341.

[102] A. E. Motter and P. S. Letelier, *Mixmaster chaos*, *Phys. Lett.* **A285** (2001) 127–131, [gr-qc/0011001].

[103] P. Cipriani and M. Di Bari, *Finsler Geometric Local Indicator of Chaos for Single Orbits in the Henon-Heiles Hamiltonian*, *Phys. Rev. Lett.* **81** (1998) 5532–5535.

[104] K. Ramasubramanian and M. S. Sriram, *Global geometric indicator of chaos and Lyapunov exponents in Hamiltonian systems*, *Phys. Rev.* **E64** (2001) 046207.

[105] V. Faraoni and D. M. Faraoni, *Elimination of the Potential from the Schr´odinger and Klein-Gordon Equations by Means of Conformal Transformations*, *Found. Phys.* **32** (2002) 773–788.

[106] A. E. Motter, *Relativistic chaos is coordinate invariant*, *Phys. Rev. Lett.* **91** (2003) 231101, [gr-qc/0305020].

[107] A. E. Motter and P. S. Letelier, *FRW cosmologies between chaos and integrability*, *Phys. Rev.* **D65** (2002) 068502, [gr-qc/0202083].

[108] M. A. Castagnino, H. Giacomini, and L. Lara, *Qualitative dynamical properties of a spatially closed FRW universe conformally coupled to a scalar field*, *Phys. Rev.* **D63** (2001) 044003.

[109] S. Blanco, A. Costa, and O. Rosso, *Chaos in classical cosmology (II)*, *Gen. Rel. Grav.* **27** (1995) 1295–1307.

[110] E. Calzetta and C. El Hasi, *Chaotic Friedmann-Robertson-Walker Cosmology*, *Class. Quant. Grav.* **10** (1993) 1825–1842, [gr-qc/9211027].

[111] N. J. Cornish and J. J. Levin, *Chaos, fractals, and inflation*, *Phys. Rev.* **D53** (1996) 3022–3032, [astro-ph/9510010].

[112] S. E. Joras and T. J. Stuchi, *Chaos in closed FRW: An imaginary approach*, *Phys. Rev.* **D68** (2003) 123525, [gr-qc/0307044].

[113] M. Szydłowski, M. Heller, and W. Sasin, *Geometry of spaces with the Jacobi metric*, *J. Math. Phys.* **37** (1996) 346–360.

[114] J. Hadamard, *Les surfaces á courbures opposées et leurs lignes géodésiques*, *J. Math. Pures Appl.* **4** (1898) 27–74.

[115] A. Y. Kamenshchik, I. M. Khalatnikov, S. V. Savchenko, and A. V. Toporensky, *Topological entropy for some isotropic cosmological models*, *Phys. Rev.* **D59** (1999) 123516, [gr-qc/9809048].

[116] E. Reithmeier, *Periodic Solutions of Nonlinear Dynamical Systems*, vol. 1483 of *Lecture Notes in Mathematics*. Springer-Verlag, Berlin Heidelberg, 1991.

[117] P. Cvitanović, R. Artuso, R. Mainieri, G. Tanner, and G. Vattay, *Chaos: Classical and Quantum*. Niels Bohr Institute, Copenhagen, 2010. ChaosBook.org.

[118] A. J. Maciejewski, M. Przybylska, and M. Szydlowski, *Living in the Non-Integrable Universe*, *Grav. Cosmol. Suppl. II* **8** (2002) 93–99.

[119] A. J. Maciejewski and M. Szydlowski, *Towards a description of complexity of the simplest cosmological systems*, *J. Phys. A: Math. Gen.* **33** (2000) 9241.

[120] A. J. Maciejewski and M. Szydlowski, *Integrability and Non-Integrability of Planar Hamiltonian Systems of Cosmological Origin*, *J. Nonlin. Math. Phys.* **8** (2001) 200–206.

[121] A. N. Kolmogorov, *Three Approaches to the Quantitative Definition of Information*, *Probl. Inform. Transmis.* **1** (1965) 1–7.

[122] M. Li and P. Vitányi, *An Introduction to Kolmogorov Complexity and Its Applications*. Texts in Computer Science. Springer-Verlag, New York, 3rd ed., 2008.

[123] M. Szydlowski, A. Krawiec, and C. Wojciech, *Phantom cosmology as a simple model with dynamical complexity*, *Phys. Rev.* **E72** (2005) 036221, [astro-ph/0401293].

[124] H. Giacomini and L. Lara, *Qualitative dynamical properties of a phantom field with an arbitrary potential*, *Gen. Rel. Grav.* **38** (2006) 137–144.

[125] V. Faraoni, *Phantom cosmology with general potentials*, *Class. Quant. Grav.* **22** (2005) 3235–3246, [gr-qc/0506095].

[126] V. Faraoni, M. N. Jensen, and S. A. Theuerkauf, *Non-chaotic dynamics in general-relativistic and scalar-tensor cosmology*, *Class. Quant. Grav.* **23** (2006) 4215–4230, [gr-qc/0605050].

[127] V. Dzhunushaliev, V. Folomeev, K. Myrzakulov, and R. Myrzakulov, *Phantom fields: bounce solutions in the early Universe and S-branes*, *Int. J. Mod. Phys.* **D17** (2008) 2351–2358, [gr-qc/0608025].

[128] A. V. Toporensky, *Regular and chaotic regimes in scalar field cosmology*, *SIGMA* **2** (2006) 037, [gr-qc/0603083].

[129] N. J. Cornish and E. P. S. Shellard, *Chaos in quantum cosmology*, *Phys. Rev. Lett.* **81** (1998) 3571–3574, [gr-qc/9708046].

[130] D. N. Page, *A Fractal Set of Perpetually Bouncing Universes?*, *Class. Quant. Grav.* **1** (1984) 417–427.

[131] C. W. Misner, *Mixmaster universe*, *Phys. Rev. Lett.* **22** (1969) 1071–1074.

[132] V. A. Belinsky, I. M. Khalatnikov, and E. M. Lifshitz, *Oscillatory approach to a singular point in the relativistic cosmology*, *Adv. Phys.* **19** (1970) 525–573.

[133] M. A. Castagnino, H. Giacomini, and L. Lara, *Dynamical properties of the conformally coupled flat FRW model*, *Phys. Rev.* **D61** (2000) 107302, [gr-qc/9912008].

[134] J. D. Barrow and J. J. Levin, *Chaos in the Einstein-Yang-Mills equations*, *Phys. Rev. Lett.* **80** (1998) 656–659, [gr-qc/9706065].

[135] Y. Jin and K.-i. Maeda, *Chaos of Yang-Mills field in class A Bianchi spacetimes*, *Phys. Rev.* **D71** (2005) 064007, [gr-qc/0412060].

[136] J. D. Barrow, Y. Jin, and K.-i. Maeda, *Cosmological co-evolution of Yang-Mills fields and perfect fluids*, *Phys. Rev.* **D72** (2005) 103512, [gr-qc/0509097].

[137] S. E. Rugh and B. J. T. Jones, *Chaotic behavior and oscillating three volumes in Bianchi IX universes*, *Phys. Lett.* **A147** (1990) 353–359.

[138] M. Szydlowski and W. Czaja, *Particle-like description in quintessential cosmology*, *Phys. Rev.* **D69** (2004) 083518, [gr-qc/0305033].

[139] M. Lakshmanan and R. Sahadevan, *Painlevé analysis, Lie symmetries, and integrability of coupled nonlinear oscillators of polynomial type*, *Phys. Rep.* **224** (1993) 1–93.

[140] S. L. Ziglin, *On the nonintegrability of a dynamical system of the General Relativity*, *Regul. Chaotic Dyn.* **5** (2000) 225–226.

[141] G. K. Savvidy, *Classical and quantum mechanics of non-abelian gauge fields*, *Nucl. Phys.* **B246** (1984) 302.

[142] T. Kawabe and S. Ohta, *Order to chaos transition in SU(2) Yang-Mills Higgs theory*, *Phys. Rev.* **D44** (1991) 1274–1279.

[143] B. G., R. Brambilla, and L. Galgani, *A comment on the reliability of the Toda criterion for the existence of a stochastic transition*, *Physica* **A87** (1977) 381 – 390.

[144] M. Toda, *Instability of trajectories of the lattice with cubic nonlinearity*, *Phys. Lett.* **A48** (1974) 335 – 336.

[145] Y. Jin and S. Tsujikawa, *Chaotic dynamics in preheating after inflation*, *Class. Quant. Grav.* **23** (2006) 353–372, [hep-ph/0411164].

[146] P. Brumer and J. W. Duff, *A variational equations approach to the onset of statistical intramolecular energy transfer*, *J. Chem. Phys.* **65** (1976) 3566–3574.

[147] H. Nakazato, M. Namiki, and S. Pascazio, *Temporal behavior of quantum mechanical systems*, quant-ph/9509016.

[148] C. P. Dettmann, N. E. Frankel, and N. J. Cornish, *Fractal basins and chaotic trajectories in multi - black hole space-times*, *Phys. Rev.* **D50** (1994) 618–621, [gr-qc/9402027].

[149] R. J. Nemiroff and B. Patla, *Decaying Higgs fields and cosmological dark energy*, astro-ph/0409649.

[150] E. Ott, *Chaos in Dynamical Systems*. Cambridge University Press, Cambridge, 1993.

[151] E. Gunzig, V. Faraoni, A. Figueiredo, T. M. Rocha Filho, and L. Brenig, *The dynamical system approach to scalar field cosmology*, *Class. Quant. Grav.* **17** (2000) 1783–1814.

[152] L. A. Urena-Lopez and M. J. Reyes-Ibarra, *On the dynamics of a quadratic scalar field potential*, *Int. J. Mod. Phys.* **D18** (2009) 621–634, [arXiv:0709.3996].

[153] A. Y. Kamenshchik, U. Moschella, and V. Pasquier, *An alternative to quintessence*, *Phys. Lett.* **B511** (2001) 265–268, [gr-qc/0103004].

[154] N. Bilic, G. B. Tupper, and R. D. Viollier, *Unification of dark matter and dark energy: The inhomogeneous Chaplygin gas*, *Phys. Lett.* **B535** (2002) 17–21, [astro-ph/0111325].

[155] M. Makler, S. Quinet de Oliveira, and I. Waga, *Constraints on the generalized Chaplygin gas from supernovae observations*, *Phys. Lett.* **B555** (2003) 1, [astro-ph/0209486].

[156] M. C. Bento, O. Bertolami, and A. A. Sen, *Generalized Chaplygin gas, accelerated expansion and dark energy-matter unification*, *Phys. Rev.* **D66** (2002) 043507, [gr-qc/0202064].

[157] M. Szydlowski and O. Hrycyna, *Scalar field cosmology in the energy phase-space – unified description of dynamics*, *JCAP* **01** (2009) 039, [arXiv:0811.1493].

[158] M. Chevallier and D. Polarski, *Accelerating universes with scaling dark matter*, *Int. J. Mod. Phys.* **D10** (2001) 213–224, [gr-qc/0009008].

[159] E. V. Linder, *Probing gravitation, dark energy, and acceleration*, *Phys. Rev.* **D70** (2004) 023511, [astro-ph/0402503].

[160] W. Hu and S. Dodelson, *Cosmic Microwave Background Anisotropies*, *Ann. Rev. Astron. Astrophys.* **40** (2002) 171–216, [astro-ph/0110414].

[161] O. Hrycyna and M. Szydlowski, *Twister quintessence scenario*, *Phys. Lett.* **B694** (2010) 191–197, [arXiv:0906.0335].

[162] A. A. Starobinsky, *Can the effective gravitational constant become negative*, *Sov. Astron. Lett.* **7** (1981) 36–38.

[163] J. D. Barrow and P. Saich, *The Behavior of intermediate inflationary universes*, *Phys. Lett.* **B249** (1990) 406–410.

[164] F. Cannata, A. Y. Kamenshchik, and D. Regoli, *Scalar field cosmological models with finite scale factor singularities*, *Phys. Lett.* **B670** (2009) 241–245, [arXiv:0801.2348].

[165] J. D. Barrow, *Sudden Future Singularities*, *Class. Quant. Grav.* **21** (2004) L79–L82, [gr-qc/0403084].

[166] V. Gorini, A. Y. Kamenshchik, U. Moschella, and V. Pasquier, *Tachyons, scalar fields and cosmology*, *Phys. Rev.* **D69** (2004) 123512, [hep-th/0311111].

[167] A. O. Barvinsky, C. Deffayet, and A. Y. Kamenshchik, *Anomaly Driven Cosmology: Big Boost Scenario and AdS/CFT Correspondence*, *JCAP* **05** (2008) 020, [arXiv:0801.2063].

[168] A. D. Linde, *Fast-Roll Inflation*, *JHEP* **11** (2001) 052, [hep-th/0110195].

[169] L. Kofman and S. Mukohyama, *Rapid roll Inflation with Conformal Coupling*, *Phys. Rev.* **D77** (2008) 043519, [arXiv:0709.1952].

[170] T. Chiba and M. Yamaguchi, *Extended Slow-Roll Conditions and Rapid-Roll Conditions*, *JCAP* **10** (2008) 021, [arXiv:0807.4965].

[171] M. C. Gutzwiller, *Chaos in Classical and Quantum Mechanics*, vol. 1 of *Interdisciplinary Applied Mathematics*. Springer-Verlag, New York, 1st ed., 1990.

[172] R. M. Wald, *General Relativity*. The University of Chicago Press, Chicago and London, 1984.

[173] L. D. Landau and E. M. Lifshitz, *The Classical Theory of Fields*, vol. 2 of *Course of Theoretical Physics*. Butterworth-Heinemann, Oxford, 4th ed., 2000.

[174] R. Penrose, *Conformal treatment of infinity*, in *Relativity, Groups and Topology* (C. M. DeWitt and B. S. DeWitt, eds.), (New York, U.S.A.), Gordon and Breach, 1964.

[175] M. Madsen, *Conformally coupled scalar field solutions and the cosmological constant*, *Gen.Rel.Grav.* **25** (1993) 855–860.

Research publications

1. Orest Hrycyna, Marek Szydłowski, *Uniting cosmological epochs through the twister solution in cosmology with non-minimal coupling*,
JCAP12(2010)016, arXiv:1008.1432 [astro-ph.CO]

2. Orest Hrycyna, Jakub Mielczarek, Marek Szydłowski, *Asymmetric cyclic evolution in polymerised cosmology*,
JCAP12(2009)023, arXiv:0910.4837 [gr-qc]

3. Jakub Mielczarek, Orest Hrycyna, Marek Szydłowski, *Effective dynamics of the closed loop quantum cosmology*,
JCAP11(2009)014, arXiv:0906.2503 [gr-qc]

4. Orest Hrycyna, Marek Szydłowski, *Twister quintessence scenario*,
Phys. Lett. B **694**, 191 (2010), arXiv:0906.0335 [astro-ph.CO]

5. Orest Hrycyna, Marek Szydłowski, *Non-minimally coupled scalar field cosmology on the phase plane*,
JCAP04(2009)026, arXiv:0812.5096 [hep-th]

6. Marek Szydłowski, Orest Hrycyna, *Scalar field cosmology in the energy phase-space – unified description of dynamics*,
JCAP01(2009)039, arXiv:0811.1493 [astro-ph]

7. Aleksandra Kurek, Orest Hrycyna, Marek Szydłowski, *From model dynamics to oscillating dark energy parameterisation*,
Phys. Lett. B **690**, 337 (2010), arXiv:0805.4005 [astro-ph]

8. Orest Hrycyna, Jakub Mielczarek, Marek Szydłowski, *Effects of the quantisation ambiguities on the Big Bounce dynamics*,
Gen. Relativ. Grav. **41**, 1024 (2009), arXiv:0804.2778 [gr-qc]

9. Marek Szydłowski, Orest Hrycyna, Aleksandra Kurek, *Coupling constant constraints in a nonminimally coupled phantom cosmology*,
Phys. Rev. D **77**, 027302 (2008), arXiv:0710.0366 [astro-ph]

10. Orest Hrycyna, Marek Szydłowski, *Extended Quintessence with non-minimally coupled phantom scalar field*,
Phys. Rev. D **76**, 123510 (2007), arXiv:0707.4471 [hep-th]

11. Aleksandra Kurek, Orest Hrycyna, Marek Szydłowski, *Constraints on oscillating dark energy models*,
Phys. Lett. B **659**, 14 (2008), arXiv:0707.0292 [astro-ph]

12. Orest Hrycyna, Marek Szydłowski, *Route to Lambda in conformally coupled phantom cosmology*,
Phys. Lett. B **651**, 8 (2007), arXiv:0704.1651 [hep-th]

13. Marek Szydłowski, Orest Hrycyna, *Paths of Friedmann-Robertson-Walker brane models*,
J. Math. Phys. **49**, 072703 (2008), arXiv:gr-qc/0612172

14. Marek Szydłowski, Orest Hrycyna, Adam Krawiec, *Phantom cosmology as a scattering process*,
JCAP06(2007)010, arXiv:hep-th/0608219

15. Marek Szydłowski, Orest Hrycyna, *Dissipative or Conservative cosmology with dark energy ?*,
Annals Phys. **322**, 2745 (2007), arXiv:astro-ph/0602118

16. Orest Hrycyna, Marek Szydłowski, *Different faces of chaos in FRW models with scalar fields – geometrical point of view*,
Chaos, Solitons and Fractals **28**, 1252 (2006), arXiv:gr-qc/0505155

17. Marek Szydłowski, Orest Hrycyna, *Dynamical dark energy models – dynamical system approach*,
Gen. Relativ. Grav. **38**, 121 (2006), arXiv:gr-qc/0505126

Conference papers

1. Orest Hrycyna, Marek Szydłowski, Adam Krawiec, *Scalar field cosmology – toward description of dynamic complexity of cosmological evolution*,
arXiv:1012.0172 [astro-ph.CO],
22nd Rencontres de Blois on Particle Physics and Cosmology, Blois, Loire Valley, France, 15-20 Jul 2010

2. Orest Hrycyna, Marek Szydłowski, *Three steps to accelerated expansion*,
Annalen Phys. **19**, 320 (2010), arXiv:0911.2208 [astro-ph.CO],
Grassmannian Conference in Fundamental Cosmology (Grasscosmofun'09),
Szczecin, Poland, 14-19 Sep 2009